

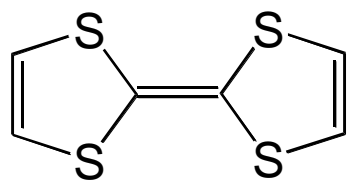
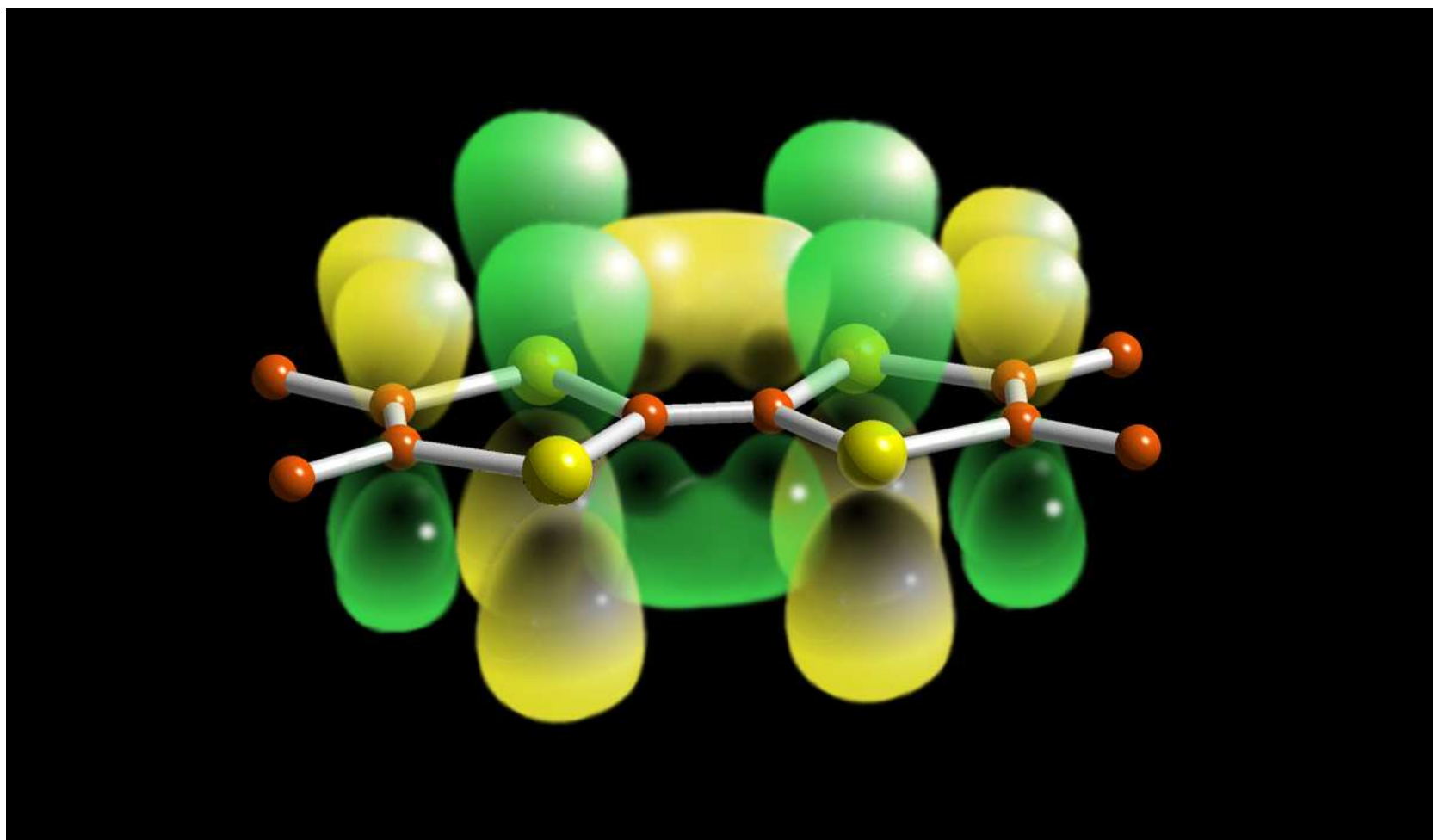
chemistry and physics of low dimensional molecular conductors

Patrick Batail
UMR CNRS 6200 MOLTECH
Angers
patrick.batail@univ-angers.fr

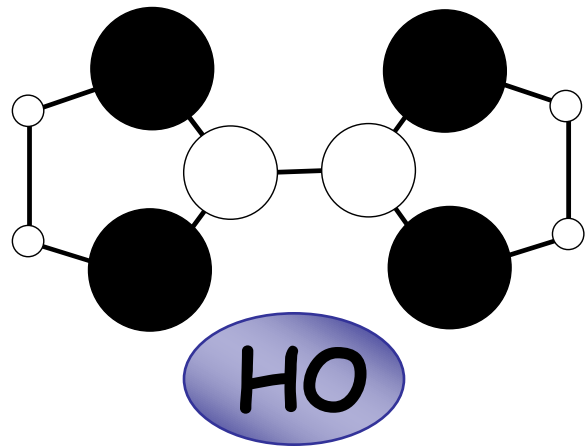
Ecole du GDR MICO
5-11 juin 2010
AUSSOIS



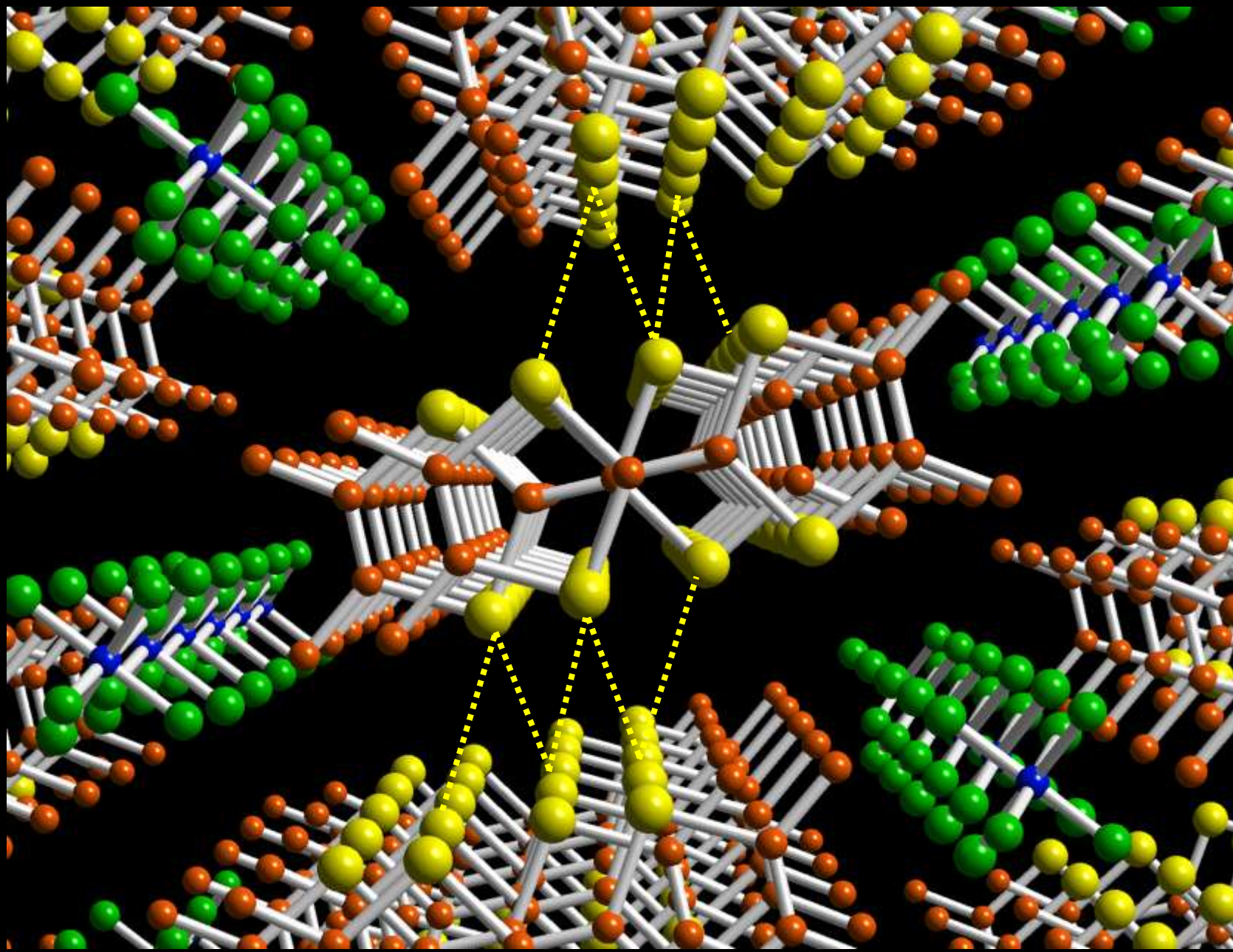
cristaux et photo Cécile Mézière



TTF



TMTTF
TMTSF



a typical molecular metal: $(\text{TMTSF})_2^{\bullet+}\text{PF}_6^-$

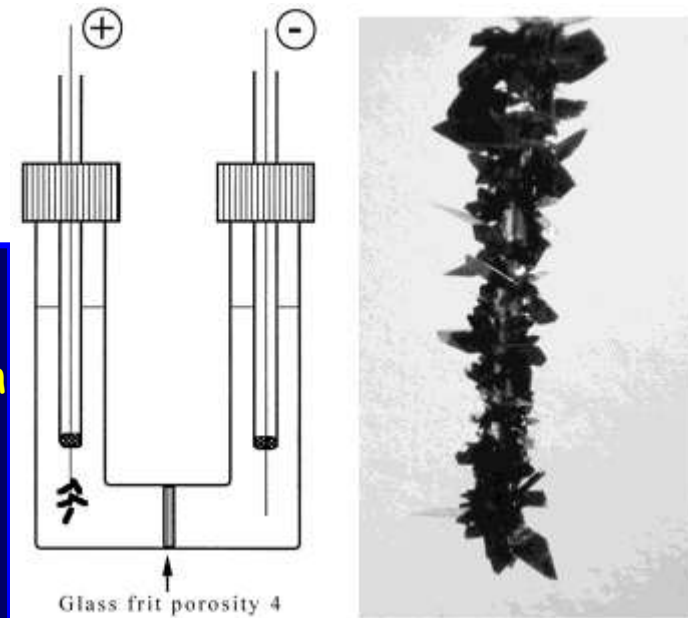
electrocrySTALLIZATION

an invaluable tool for the construction of electroactive molecular solids

one single, day-to-weeks experiment

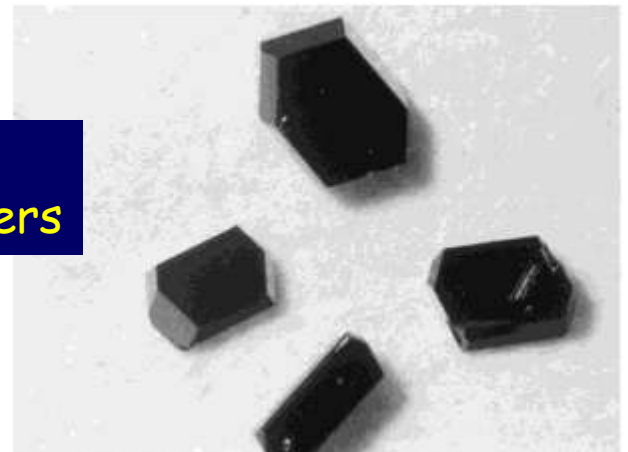
achieves:

- carriers generation
- carriers stabilization by delocalization/localization within stacks / slabs (intermolecular conjugation)
- electrostatic self-assembly / auto-templating into bi-continuous O-I hybrid frameworks



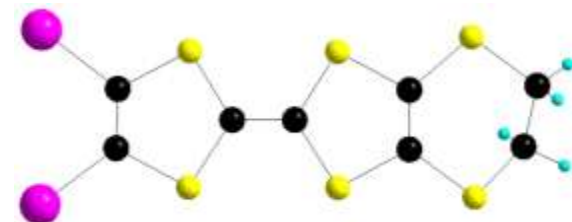
allows:

- halogen-bonded co-assembly into ternary systems upon engaging neutral functional π -conjugated spacers



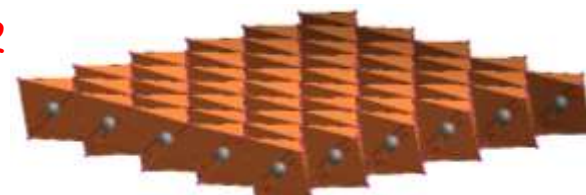
$I_{\text{org}} \cdots I_{\text{inorg}}$ halogen bonding interactions

associate in CH_3CN :



with either:

- the corner-sharing, perovskite-layer-like 2D polymer $(\text{BuNH}_3^+)_2(\text{PbI}_4^{2-})$
- or
- the edge-sharing 2D polymer PbI_2



in the presence of NaI

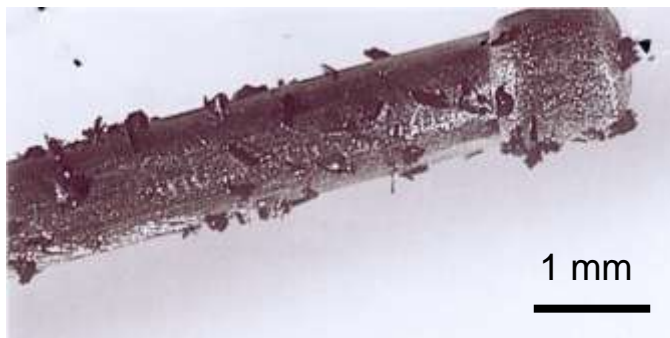
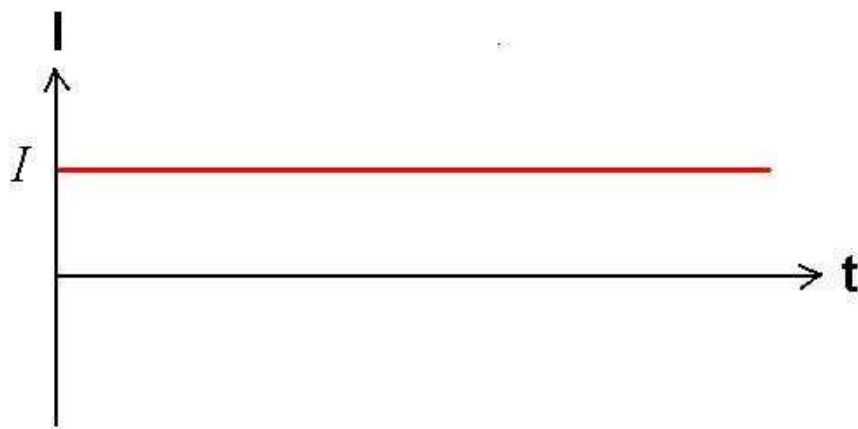
Best crystals typically under controlled rhythmic reversal of the current flow in the e-cell (0.7 s in oxidation coupled to 0.3 s in reduction),

see Hünig et al. *Eur. J. Inorg. Chem.* 1999, 899.

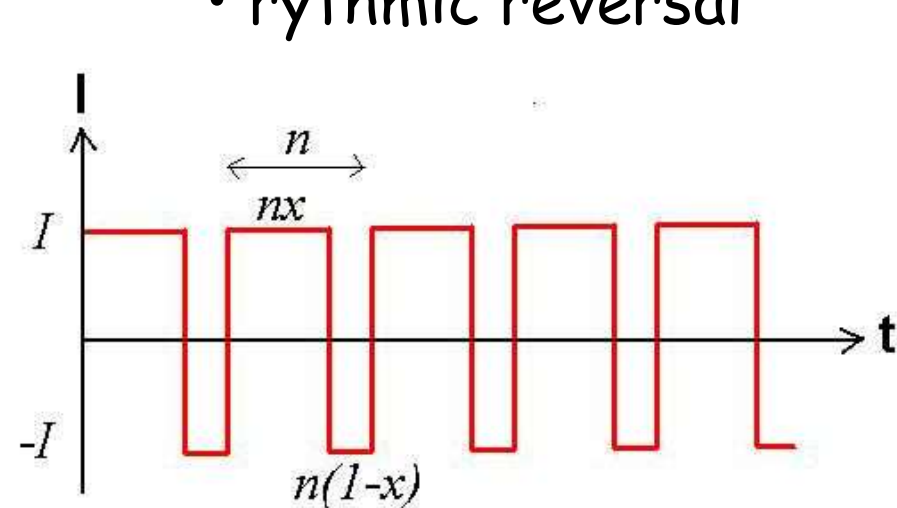
Thomas Devic

e-crystallization upon controlled rhythmic reversal of dc current flow

- poor crystal quality at constant current



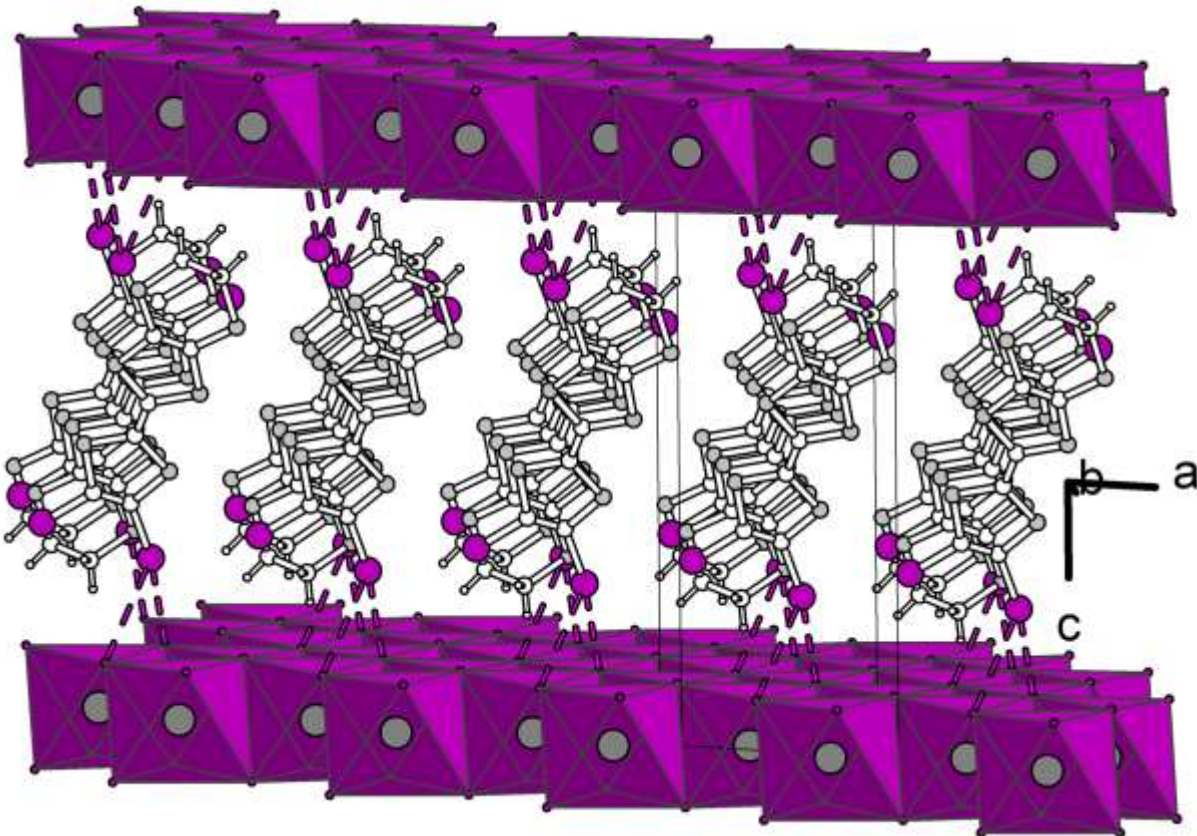
- rhythmic reversal



T. DEVIC, M. ÉVAIN, Y. MOËLO, E. CANADELL, P. AUBAN-SENZIER, M. FOURMIGUÉ, P. BATAIL
J. Am. Chem. Soc. 125, 3295 (2003)

early example, see Hünig et al., *Eur. J. Inorg. Chem.* 1999, 899

$\beta\text{-(I}_2\text{-EDT-TTF)}^{\cdot+}\text{[}(\text{Pb}_{5/6}\square_{1/6}\text{I}_2)^{1/3-}\text{]}_3$



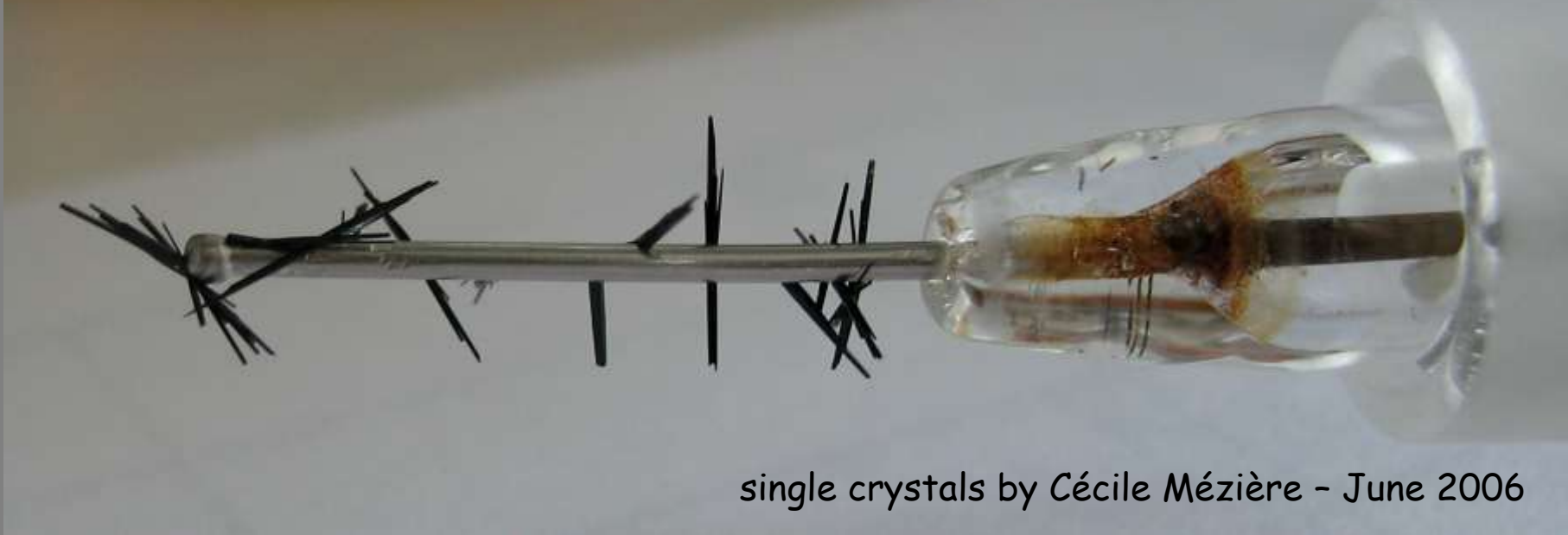
Single crystals!!

- a bi-continuous hybrid composite

T. Devic

- pseudo-intercalation of β -slab into lacunar, edge-sharing (CdI_2 -type), $[\text{Pb}_{(1-x)}\text{I}_2]^{(-2x)}$ hexagonal single layers
- interfacial Halogen-bonding : $C\text{-I}\cdots\text{I} = 3.81$ and 4.09 \AA
- charge balance from lead site occupancy

electrocrySTALLIZATION laboratory



single crystals by Cécile Mézière - June 2006

δ -(EDT-TTF-CONMe₂)₂AsF₆ et δ -(EDT-TTF-CONMe₂)₂Br

β -(EDT-TTF-I₂)₂^{..+}[(Pb_{5/6}□_{1/6}I₂)^{1/3-}]₃

β -(EDT-TTF-I₂)₂^{..+}[(Pb_{2/3+x}Ag_{1/3-2x}I₂)^{1/3-}]₃ x ≈ 0.05

β' -(EDT-TTF-I₂)₂PbI₃·H₂O

Kagome-(EDT-TTF-CONH₂)₆[Re₆Se₈(CN)₆]

β -(EDT-TTF-I₂)₂[HO₂C-CH=CH-CO₂⁻]_{1-x}[O₂C-CH=CH-CO₂⁻]_x

[(rac), (R) et (S)-(EDT-TTF-Me-Oxazoline)]₂X (X = AsF₆, PF₆, Au(CN)₂)

chemistry and physics of intermolecular interactions act in unison

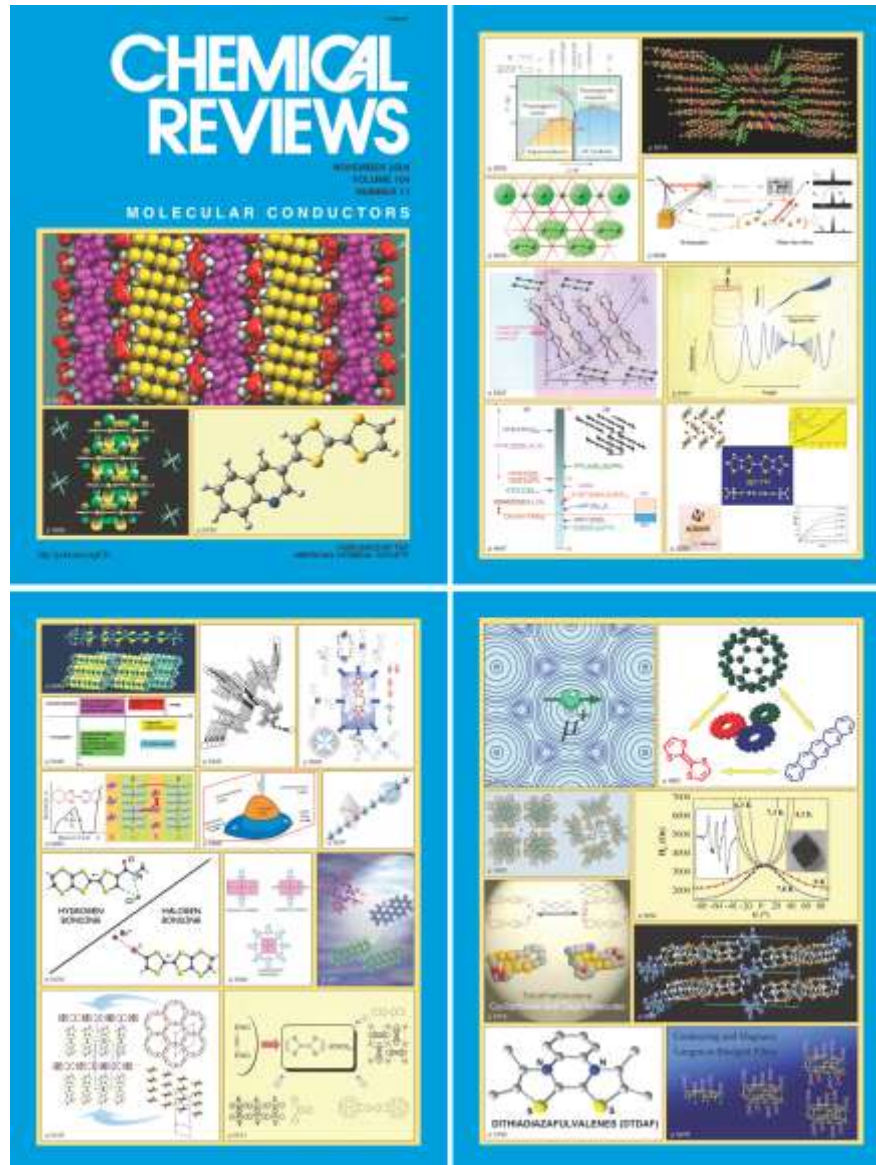
objectif cet après-midi :

- crystal engineering of π -conjugated systems:
getting familiar with redox chemistry and intermolecular interactions
- how to reveal a hidden structural detail relevant to pertinent features of
a complex electronic structure and lying behind a beautiful low dim physics

OUTLINE

1. electrocrystallization
2. redox chemistry
3. intermolecular interactions, and their redox activation, direct the structure
4. orbitals and bands (in one dimension)
5. decipher BS of TTF-TCNQ, Bechgaard salts
6. modify / control electronic structure
 - 6.1 tune stoichiometry
 - 6.2 tune anion charge
 - 6.3 ternary phases by halogen bonding
 - 6.4 $[H^+]/[\text{hole}]$ mixed valence
 - 6.5 chemical pressure

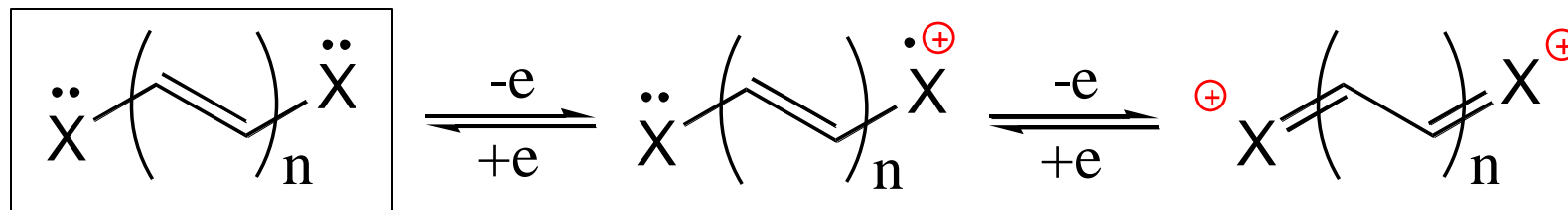
November 2004
Volume 104
Number 11



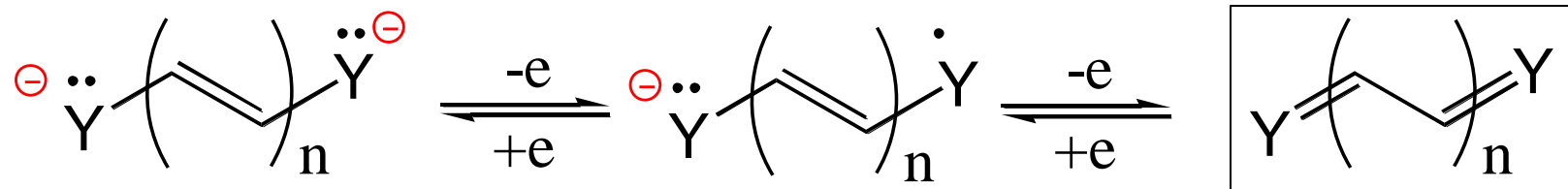
OUTLINE

1. electrocrystallization
2. redox chemistry

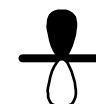
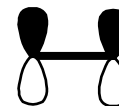
Reversible 2-Steps Redox Systems of the Violene Type

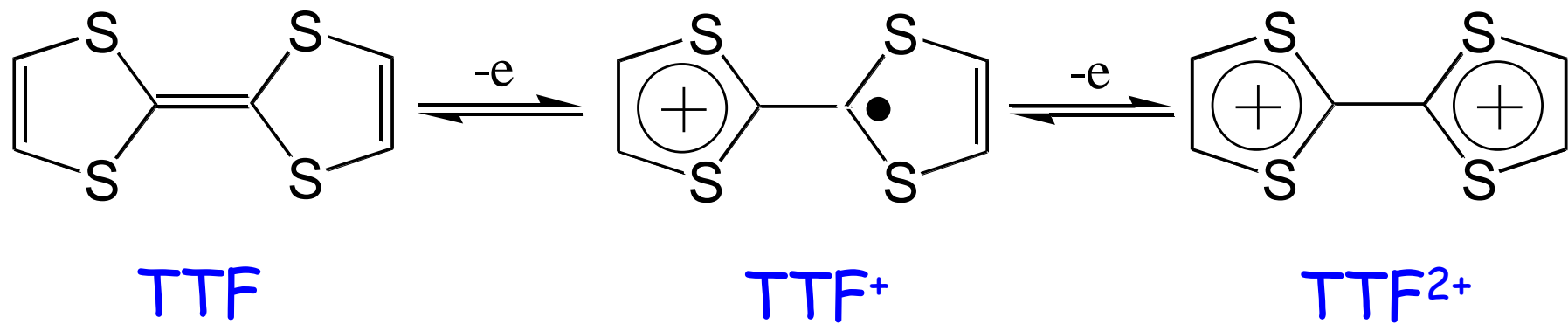
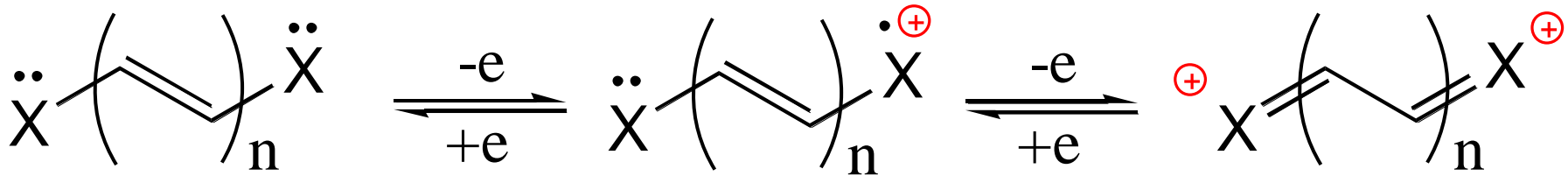


resonance / conjugation



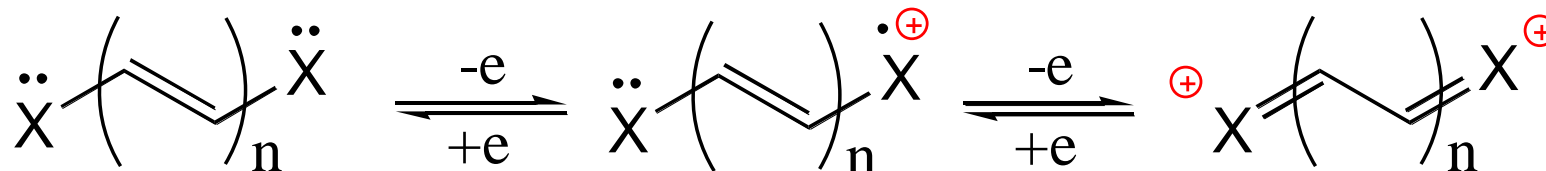
Hückel formalism: treat heteroatom/group as a perturbation



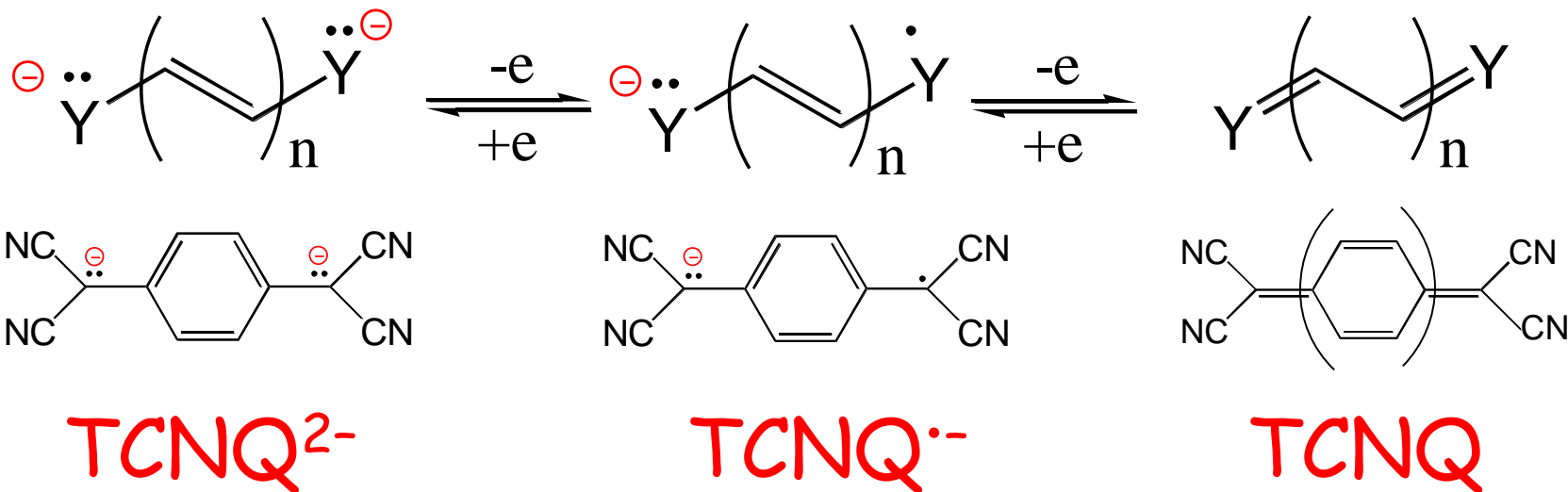


tetrathiafulvalene

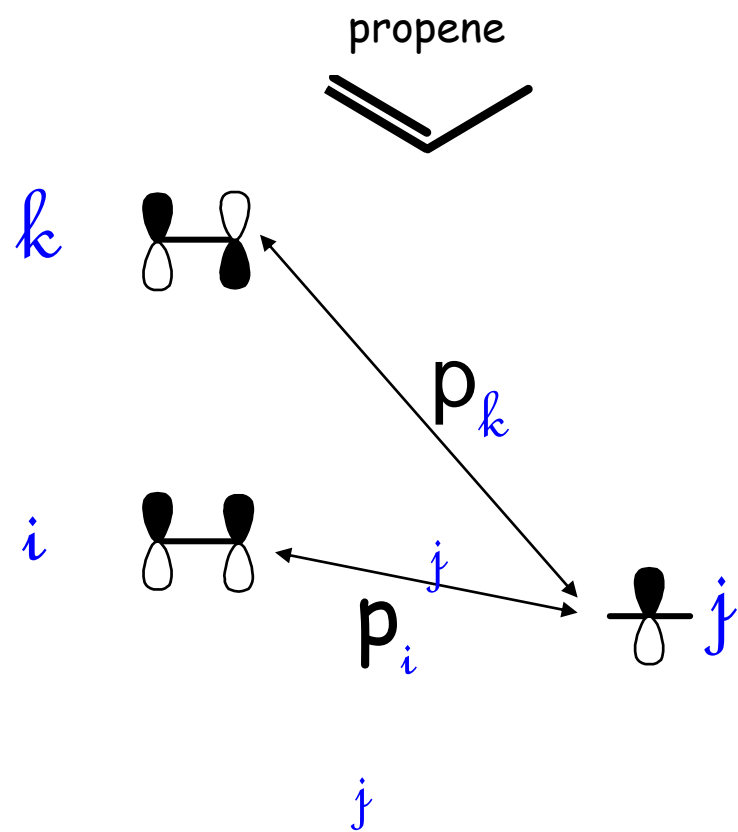
Reversible Two-Steps Redox Systems of the Violene Type



resonance / conjugation

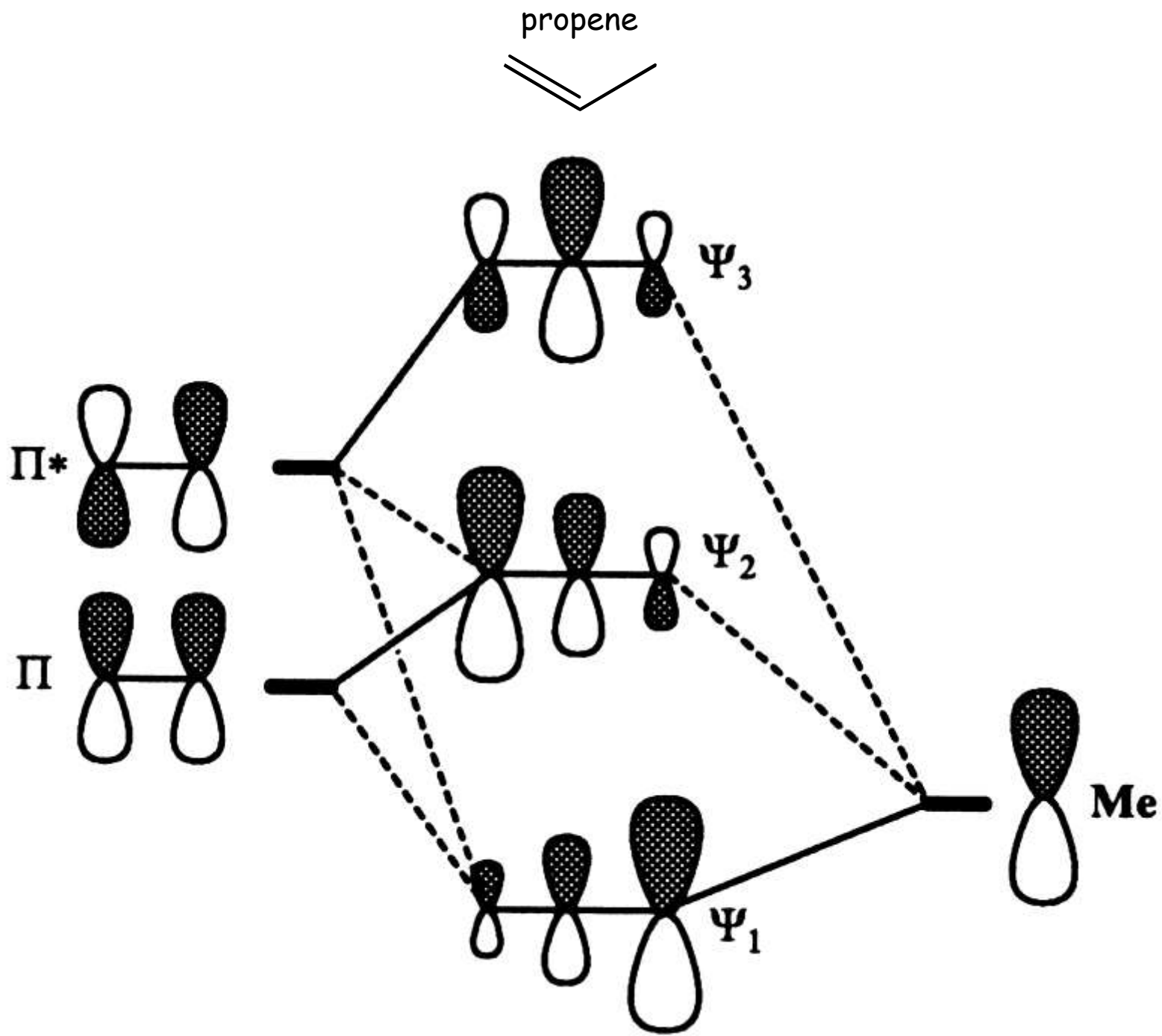


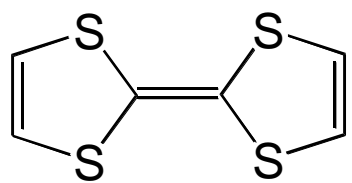
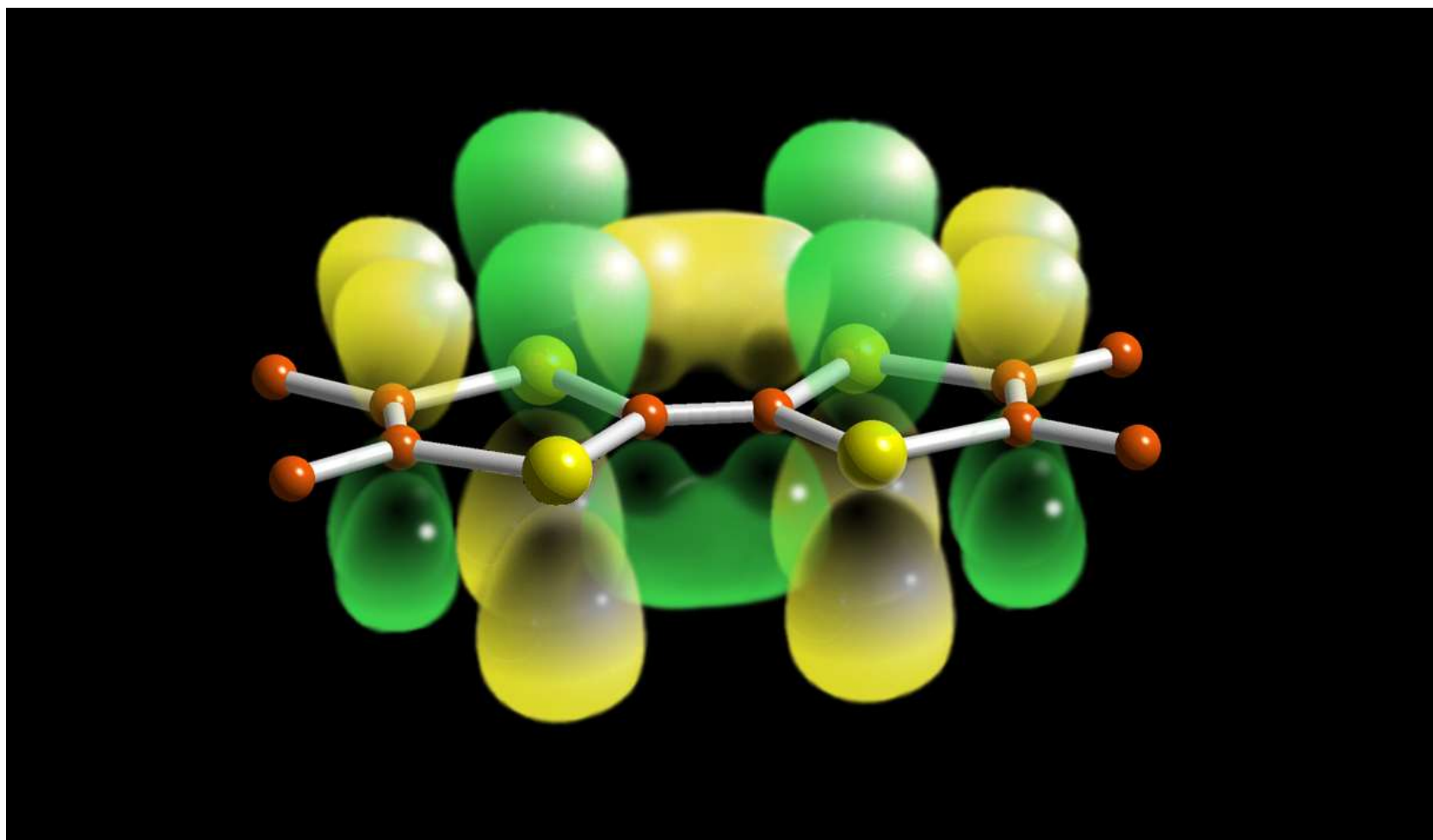
Hückel formalism: treat heteroatom/group as a perturbation



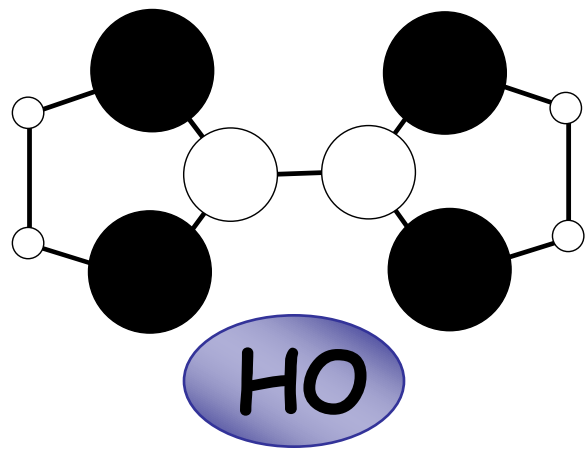
$$|\Psi_i\rangle = |\psi_i^{\circ}\rangle + \sum_{j \neq i} \frac{P_{ij}}{E_i^{\circ} - E_j^{\circ}} |\psi_j^{\circ}\rangle + \frac{P_{ij} P_{kj}}{(E_i^{\circ} - E_j^{\circ})(E_i^{\circ} - E_k^{\circ})} |\psi_k^{\circ}\rangle$$

$$\psi_{\text{propene}}^{\text{HOMO}} = \psi_{\text{ethylene}}^{\text{HOMO}} + \frac{P_{\text{HOMO, methyl}}}{E_{\text{HOMO}} - E_{\text{methyl}}} \psi_{\text{methyl}} + \dots$$





TTF

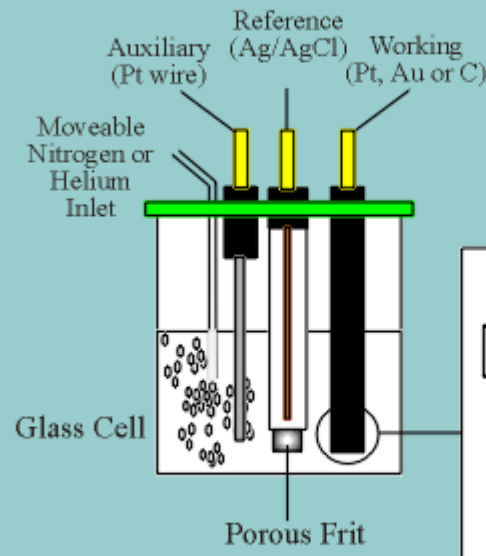


TMTTF
TMTSF

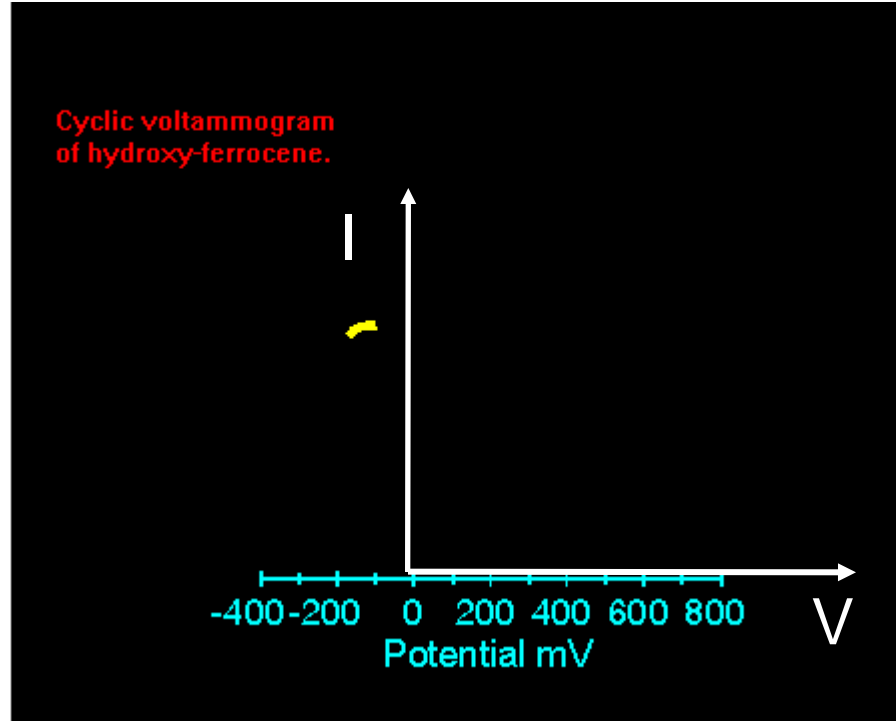
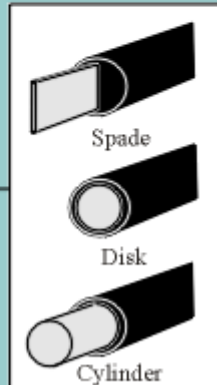
characterization of redox properties: cyclic voltammetry experiments



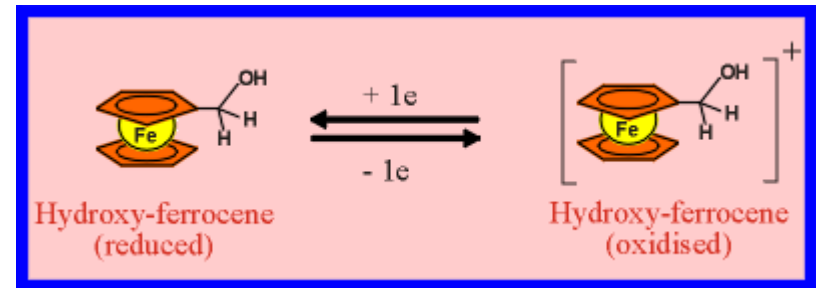
Electrodes



Electrode Geometries Used

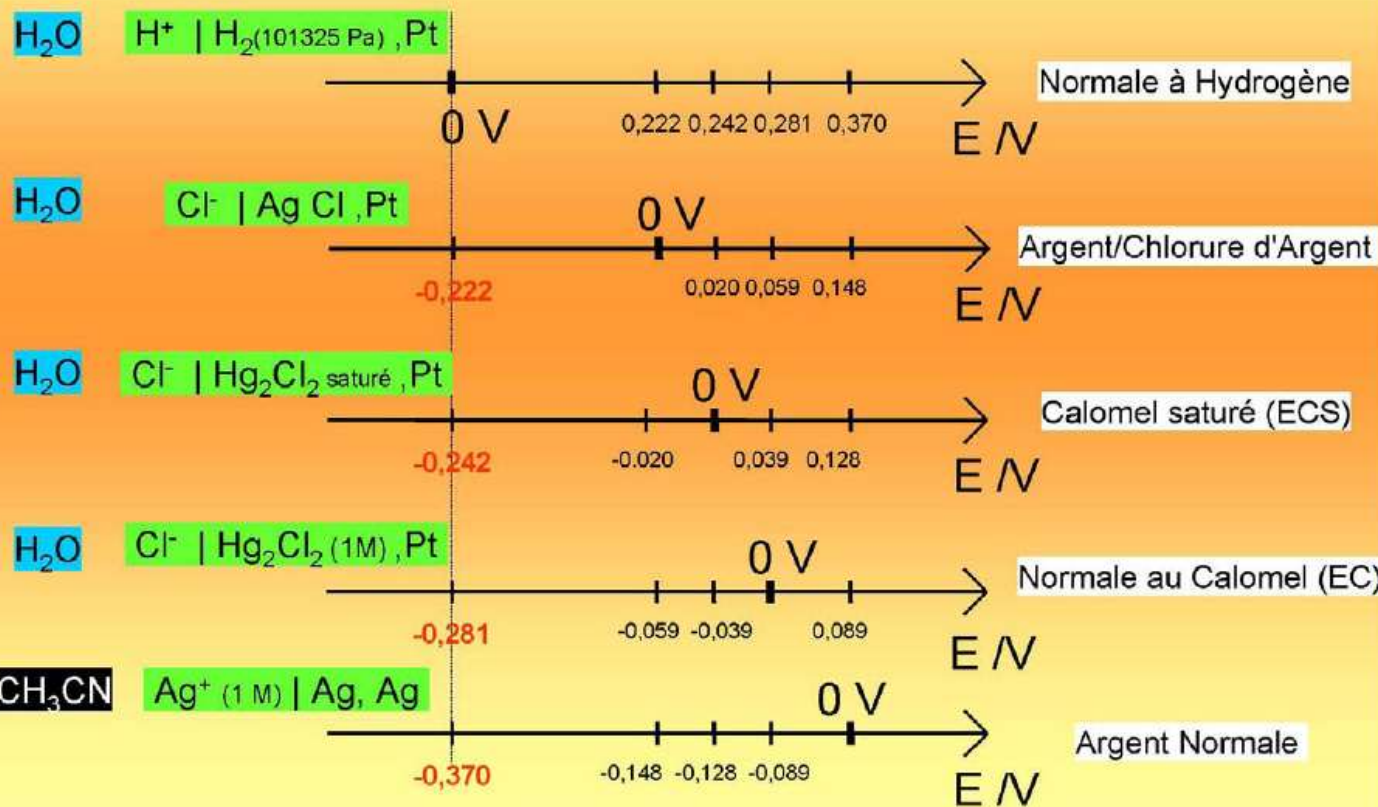


Glass Cell



Systèmes rédox de référence

Solvant: Système rédox ,Electrode: Echelle à 298 K: Nom:

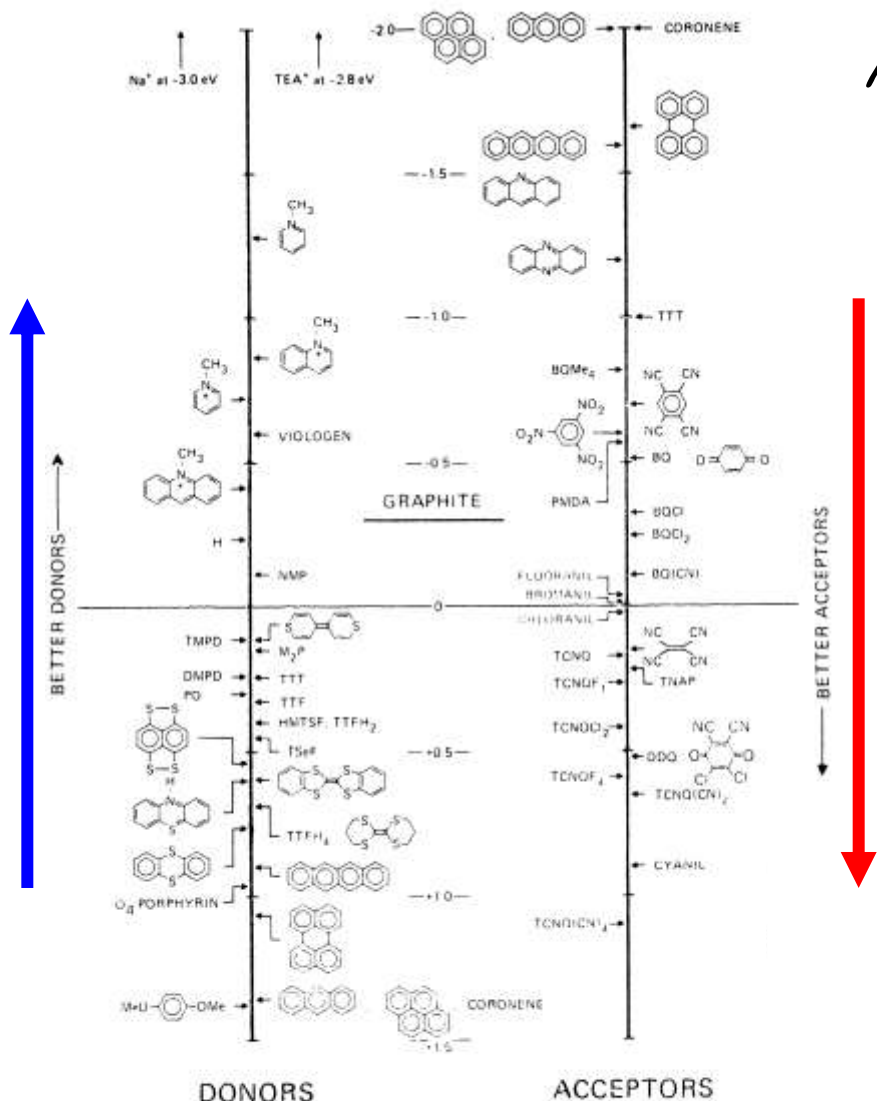


Dans 0.1 M TBAHP/ CH_2Cl_2 :

$$\text{E}(\text{Fc}^+/\text{Fc}) = +0.405 \text{ V } vs. \text{ SCE} = +0.425 \text{ V } vs. \text{ Ag/AgCl}$$

$$\text{E}(\text{Dichloronaphthoquinone}) = -0.87 \text{ V } vs. \text{ Fc}^+/\text{Fc} = -0.465 \text{ V } vs. \text{ SCE} = -0.445 \text{ vs. Ag/AgCl}$$

Torrance
Mol. Cryst. Liq. Cryst. 1985, 126, 5567



π-donor

VS

π-acceptors

FIGURE 1. Values of the oxidation potential for a wide variety of donors (on left) and the reduction potential for a number of acceptors (on right) in Volts. (For meaning of symbols, see References.)

OUTLINE

1. electrocrystallization
2. redox chemistry
3. intermolecular interactions, and their redox activation, direct the structure

intermolecular interactions

- p_{π} - p_{π} overlap, π - π , vdW, H- and Hal-bonding
- direct the structure
- weak

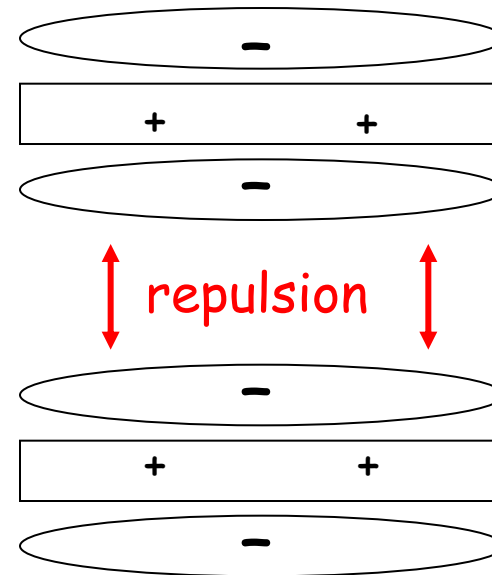
“Directing the Structures and Collective Electronic Properties of Organic Metals:
the Interplay of Overlap Interactions and Hydrogen Bonds”
K. HEUZÉ, M. FOURMIGUÉ, P. BATAIL, E. CANADELL, P. AUBAN-SENZIER
Chem. Eur. J. **5(9)**, 2971-2976 (1999)

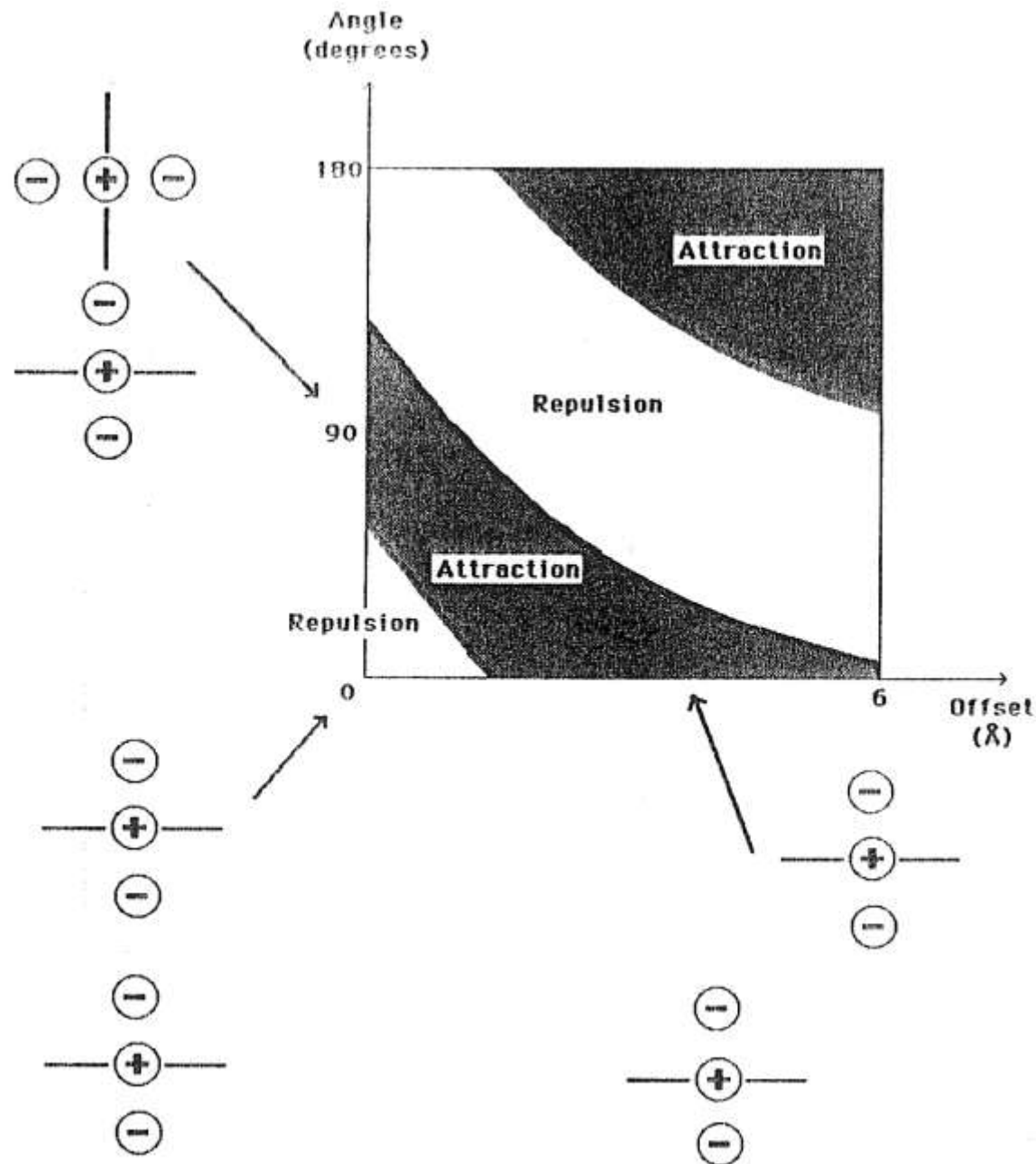
“Activation of Hydrogen and Halogen Bonding Interactions in Crystalline Molecular
Conductors”
M. FOURMIGUE, P. BATAIL
Chem. Rev. **104**, 5379-5418 (2004)

π - π interactions

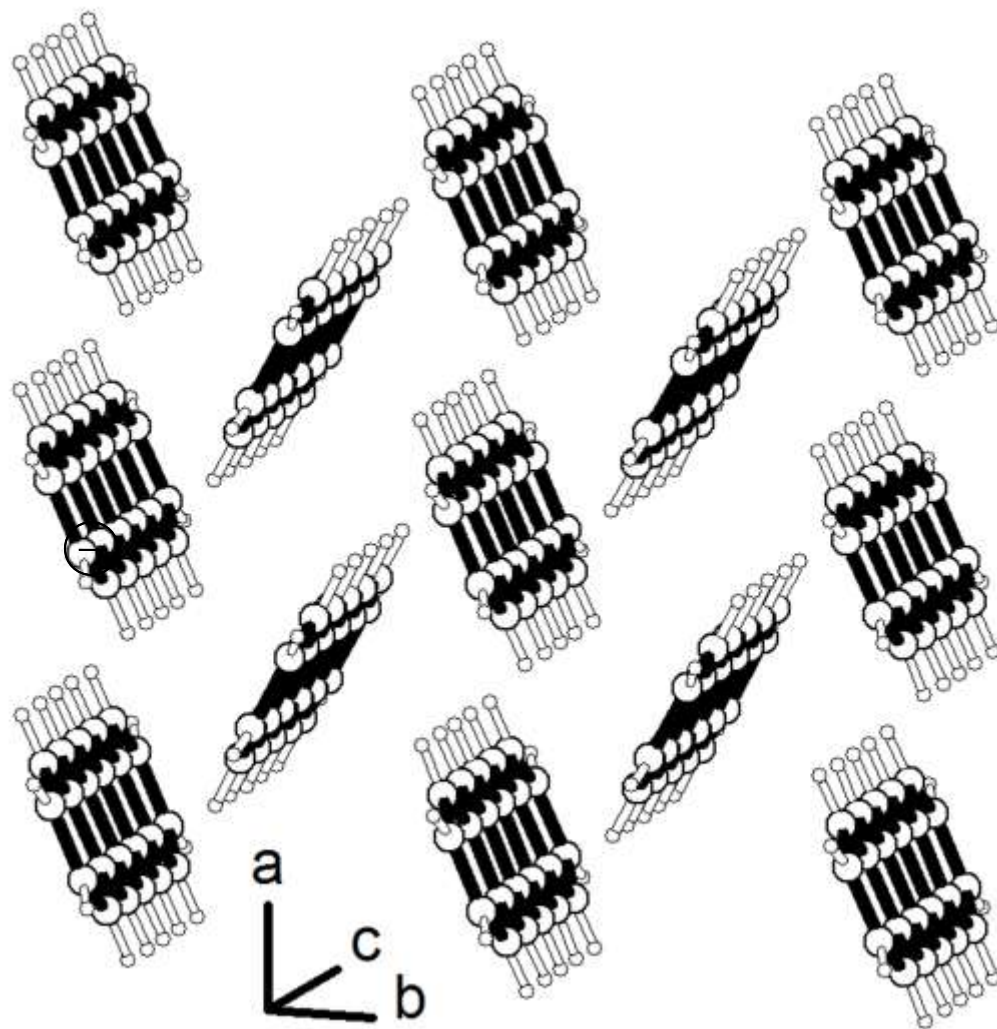
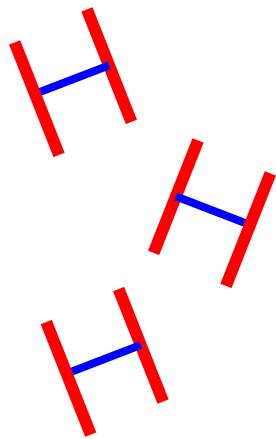
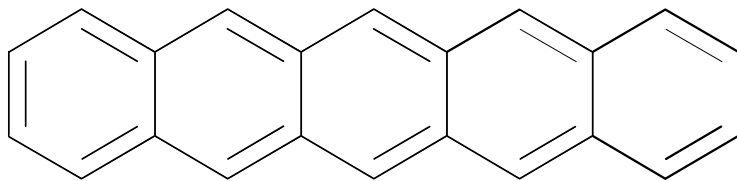
interactions between π -conjugated closed shell molecules

quadrupoles - quadrupoles interactions





pentacene, a paradigm for π - π interactions / stacking



herring-bone pattern of intermolecular interactions

hydrogen bonds

1) normal hydrogen bonds

2) weak hydrogen bonds: $C_{sp}^3\text{-H}\cdots X$ and $C_{sp}^2\text{-H}\cdots X$



- electrostatic, between an H-bond donor and an H-bond acceptor
- directional
- vanishes very slowly with distance

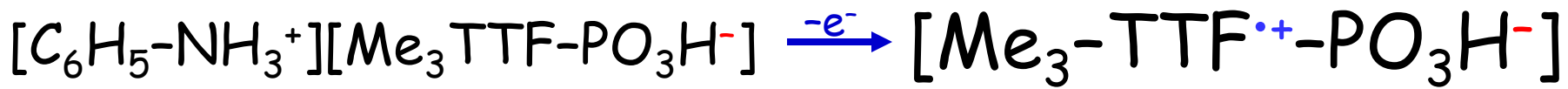
O-H \cdots O et N-H \cdots O: normal hydrogen bonds

$\text{NH}_4^+ \cdots \text{OH}_2$	19 kcal mole $^{-1}$	0.8 eV
$\text{HO}-\text{H} \cdots \text{Cl}^-$	13.5 kcal mole $^{-1}$	0.6 eV
$\text{HO}-\text{H} \cdots \text{OH}_2$	5 kcal mole $^{-1}$	0.2 eV

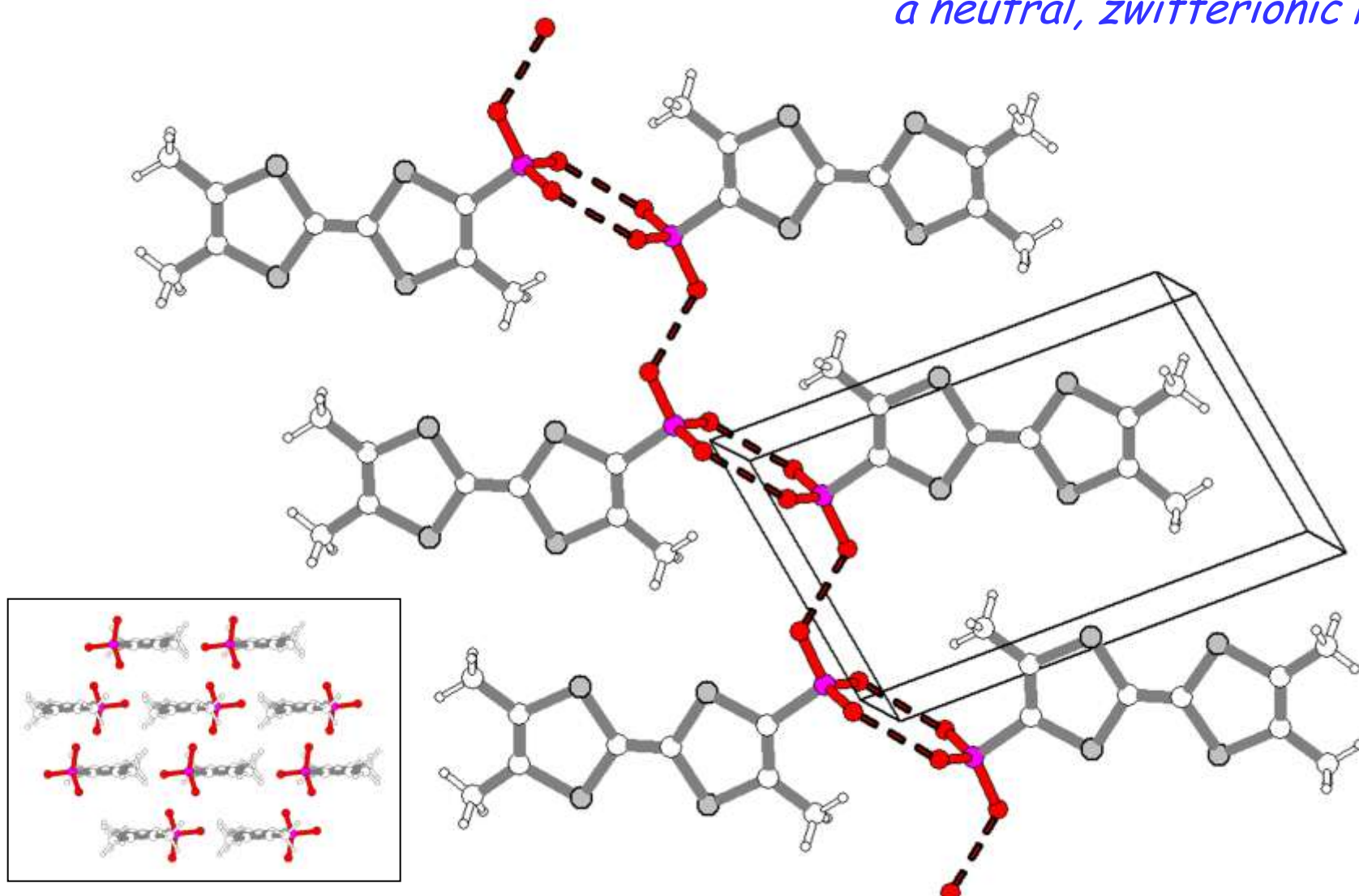
CH \cdots X: weaker hydrogen bonds

$\text{HC}\equiv\text{C}-\text{H} \cdots \text{OH}_2$	2.2 kcal mole $^{-1}$	0.1 eV
$\text{H}_2\text{C}=\text{C}-\text{H} \cdots \text{OH}_2$	1 kcal mole $^{-1}$	0.04 eV

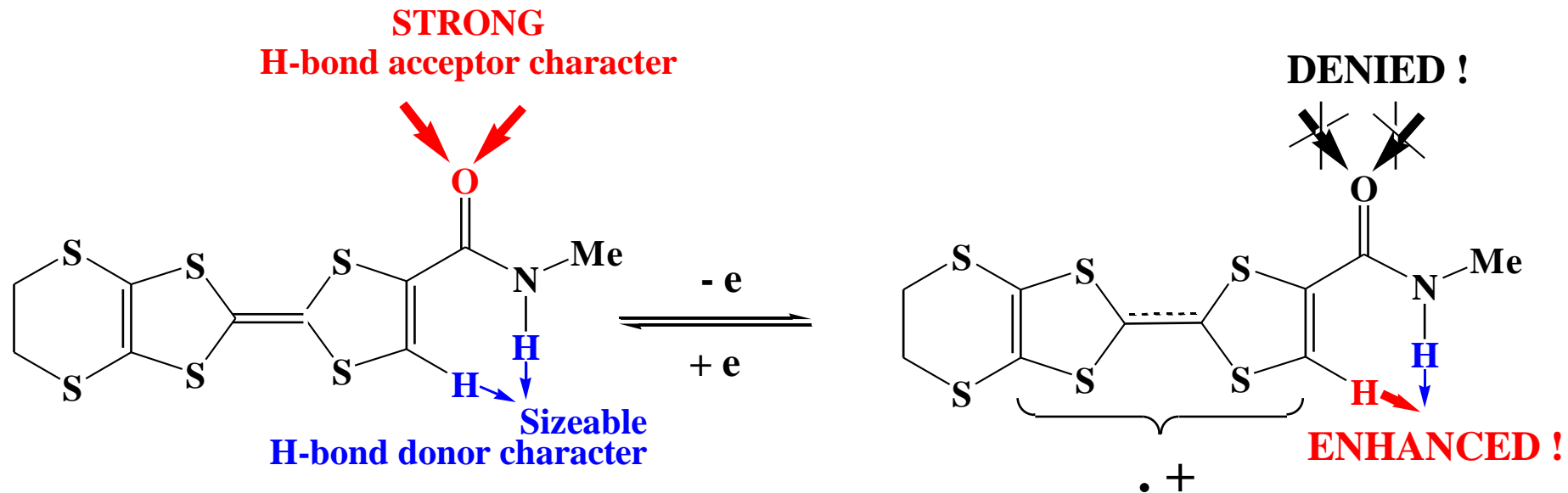
$$1 \text{ kcal mole}^{-1} = 4.33641146 \times 10^{-2} \text{ eV}$$



a neutral, zwitterionic radical

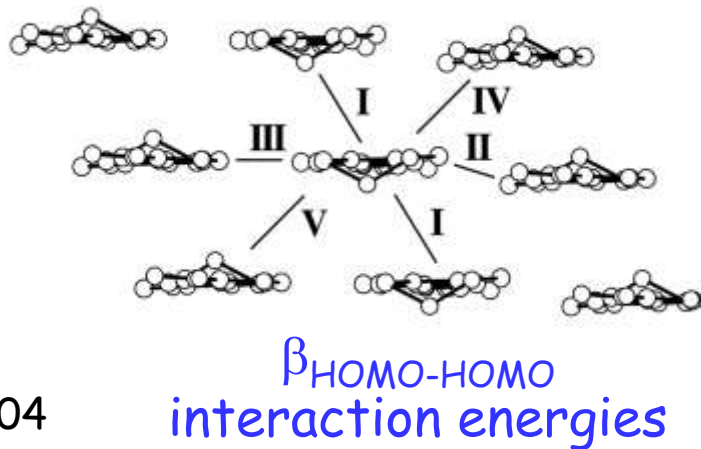
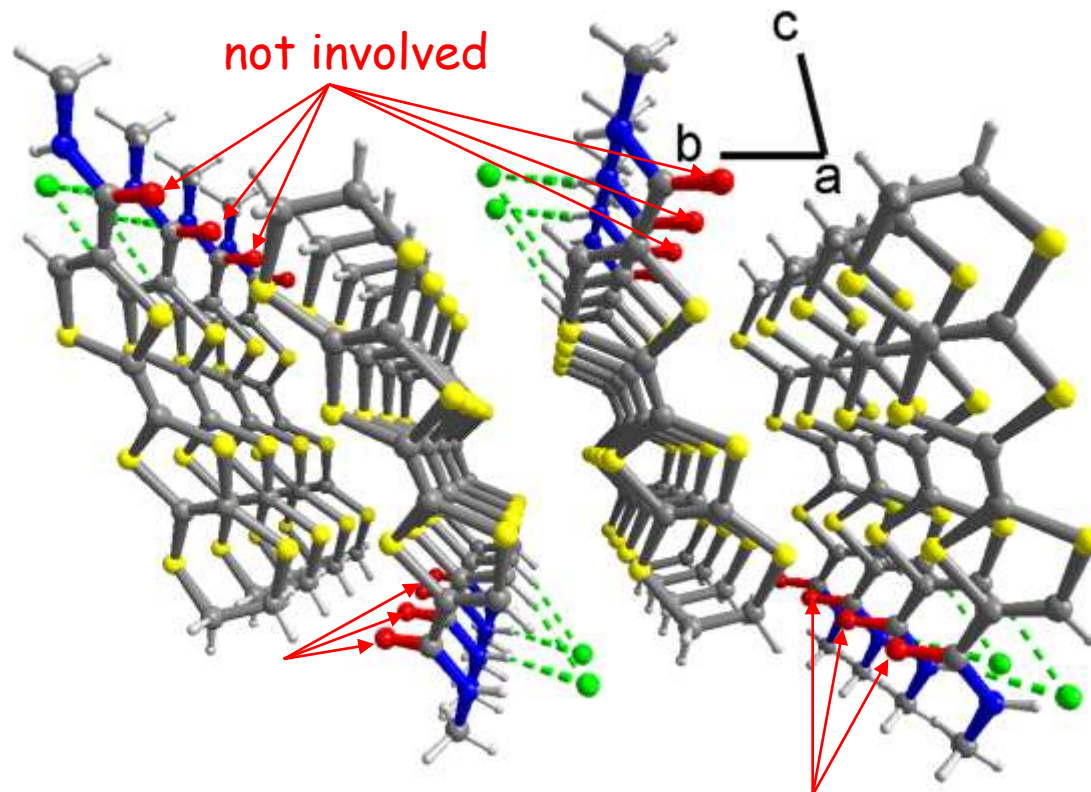
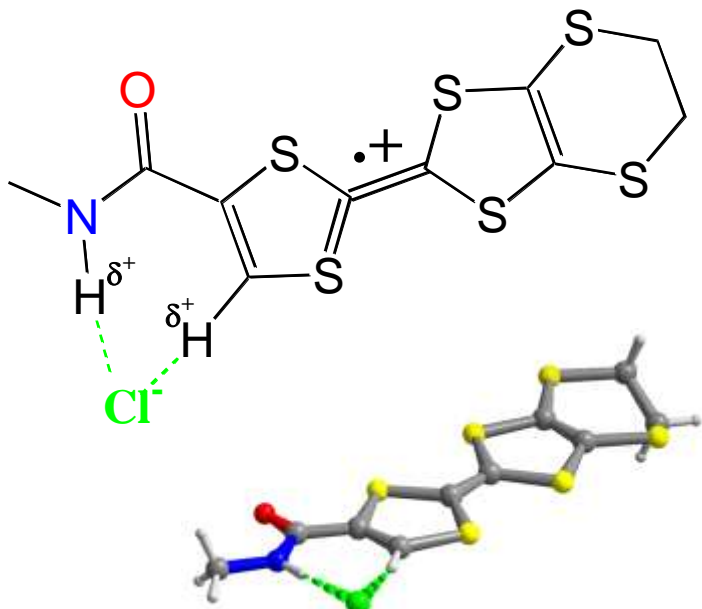


REDOX ACTIVATION



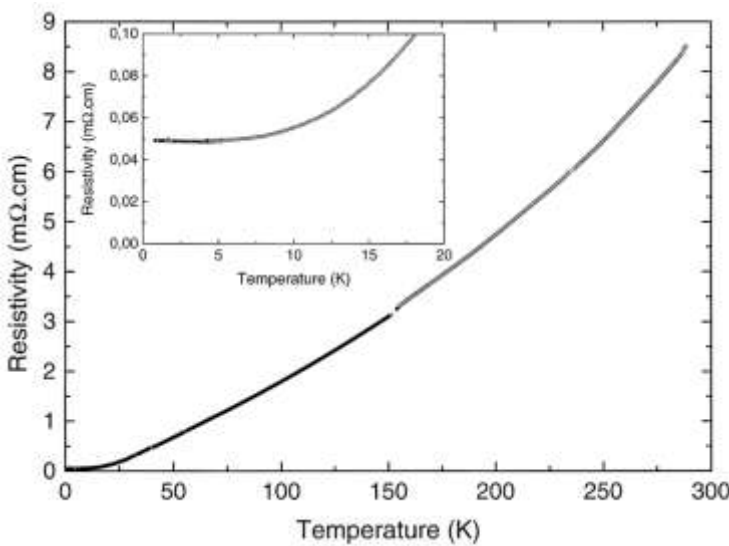
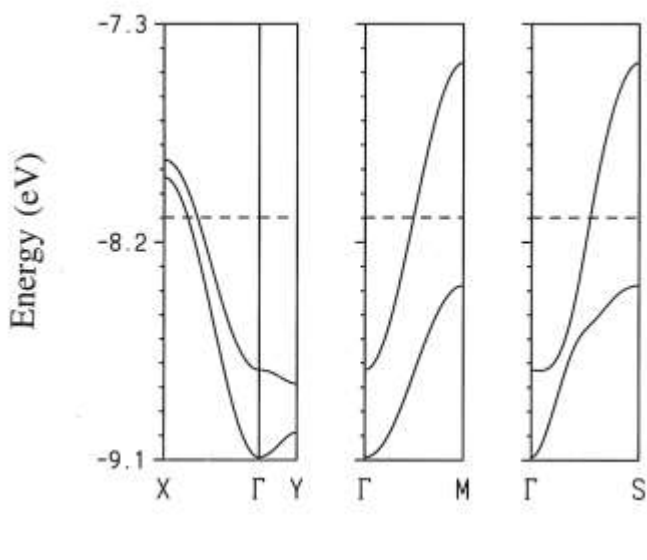
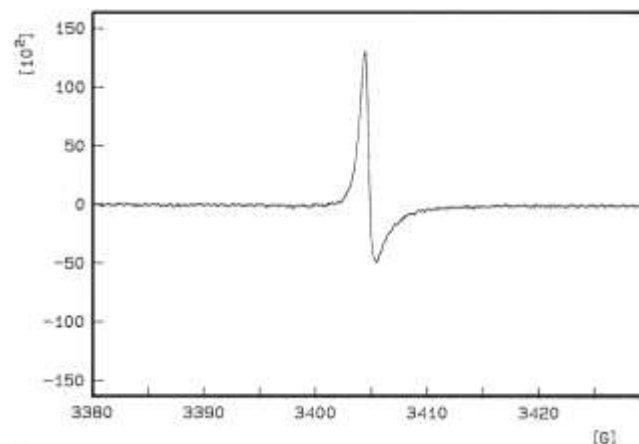
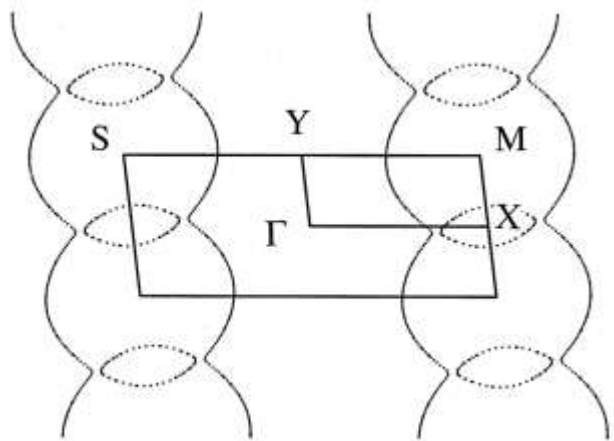
- Redox state (off/on)
- Intermolecular interactions
- Molecular recognition (binding strength)
- Competition : charges and spins localization (magnetism)
vs delocalization (transport)

$\beta''\text{-(EDT-TTF-CONHMe)}_2[\text{Cl}^-\cdot\text{H}_2\text{O}]$



I	0.3974 eV
II	0.1171
III	0.2259
IV	0.2550
V	0.2216

$\beta''\text{-(EDT-TTF-CONHMe)}_2[\text{Cl}^- \cdot \text{H}_2\text{O}]$



OUTLINE

1. electrocrystallization
2. redox chemistry
3. intermolecular interactions, and their redox activation, direct the structure
4. orbitals and band (in one dimension)

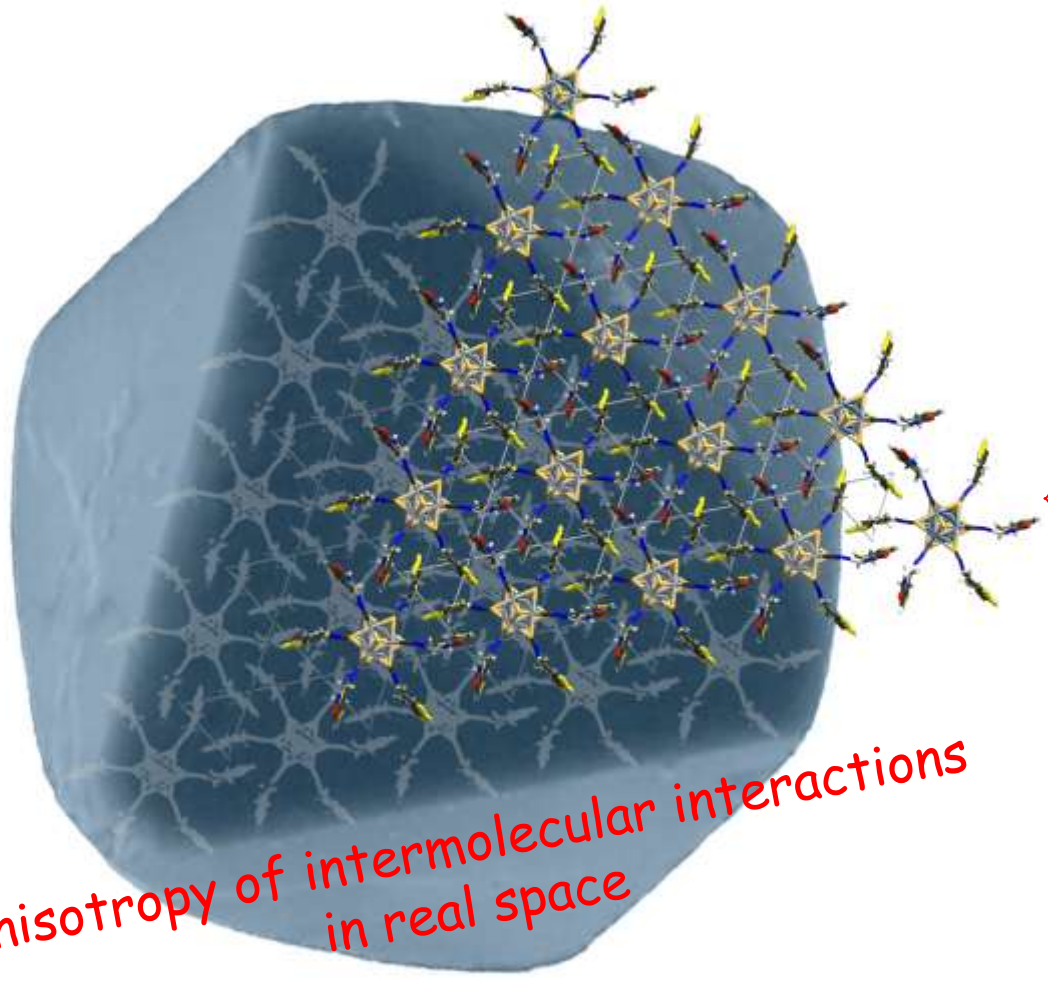
low dimensional *molecular* solids

intermolecular interactions (those which direct the structure: p_{π} - p_{π} overlap, vdW, H- and Hal-bonding) are weak

understanding crystal and electronic structure correlation:
easier (back of the envelop arguments) in materials with stronger, covalent
and/or ionic interactions

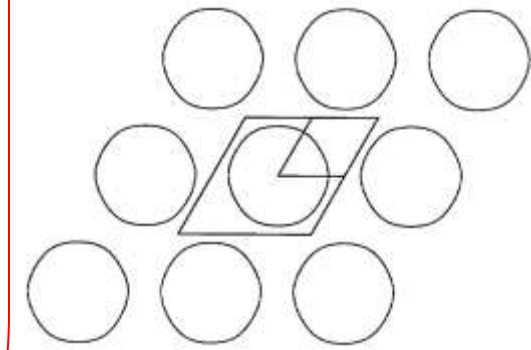
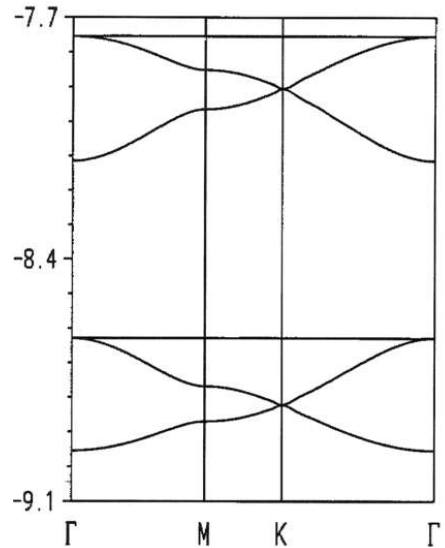
it is a much more delicate task to look for such correlations for systems with
weak interactions because we lack the kind of feeling and control of the relative
weight of the different interactions, all of which are weak

anisotropy of intermolecular interactions
in real space



extended-Hückel tight-binding band structure
calculations

Grant
Whangbo
Hoffmann
Burdett
Mori
Canadell

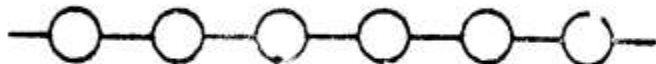


anisotropy of the system
in the momentum space

Purpose: how to reveal a hidden, apparently innocuous structural detail relevant to pertinent features of their electronic structures and lying behind a beautiful physics ?

basic concepts: orbitals and bands in one-dimension

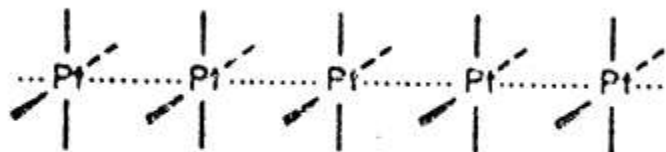
working with small, simple things:



1



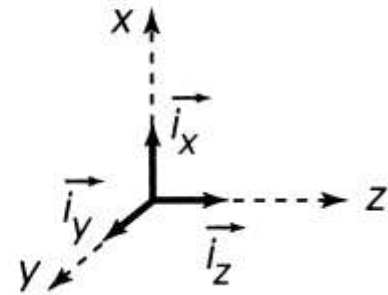
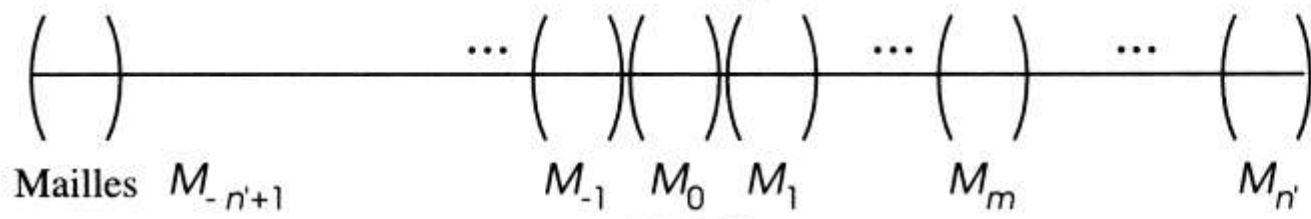
2



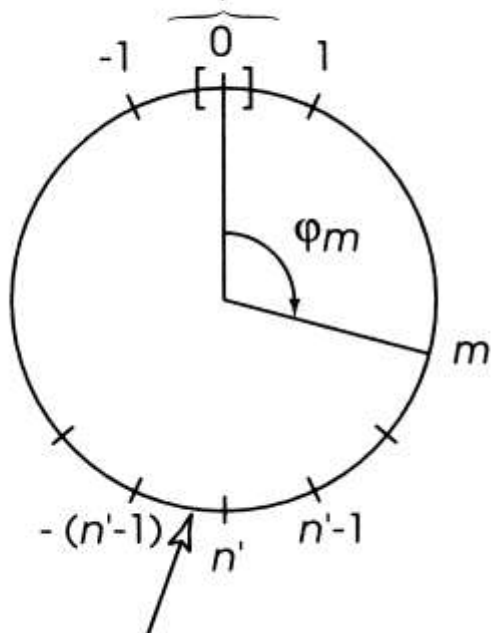
3

$$\vec{r}_m = m\vec{a} = ma \vec{i}_z$$

$$\vec{a} = a \vec{i}_z$$



Maille de référence M_0



Emplacement
de la maille M_m

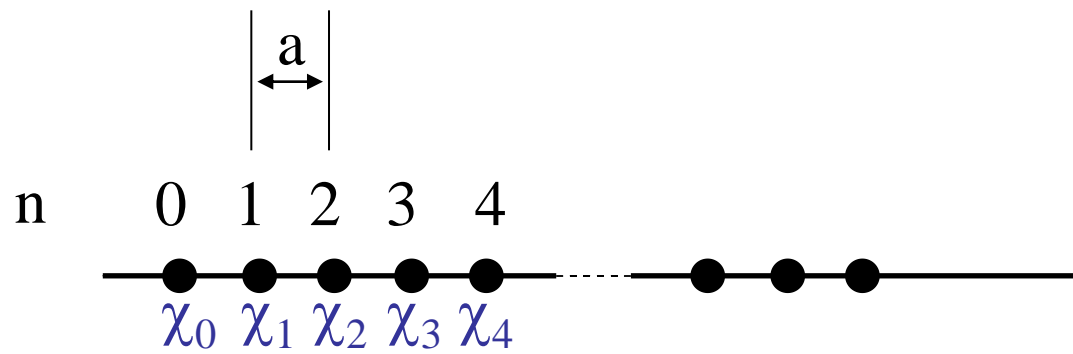
La maille $M_{n'}$ a été reliée à la maille $M_{-n'+1}$

Tableau 3.1 Table de caractères du groupe C_n (n pair). C_n^m représente la rotation d'angle $\frac{2\pi m}{n}$. Les opérations E et C_2 correspondent respectivement aux valeurs $m=0$ et $m=n'=n/2$. La dernière ligne reproduit les caractères de la représentation $\Gamma_{\phi_j} = \{(\phi_j)_{-n'+1}, \dots, (\phi_j)_0, \dots, (\phi_j)_{n'}\}$ vis-à-vis des différentes rotations.

C_n	E	C_2	C_n	C_n^{-1}	...
$\Gamma_\ell, \ell = 0, \pm 1, \dots, \pm(n'-1), n'$	1	$(-1)^\ell$	$\exp\left(\frac{-2i\pi\ell}{n}\right)$	$\exp\left(\frac{2i\pi\ell}{n}\right)$...
Γ_{ϕ_j}	n	0	0	0	...

C_n^m	C_n^{-m}	...	$C_n^{n'-1}$	$C_n^{-n'+1}$
$\exp\left(\frac{-2mi\pi\ell}{n}\right)$	$\exp\left(\frac{2mi\pi\ell}{n}\right)$...	$\exp\left(\frac{2(1-n')i\pi\ell}{n}\right)$	$\exp\left(\frac{2(n'-1)i\pi\ell}{n}\right)$
0	0	...	0	0

$$(\Psi_j)_\ell = \frac{1}{\sqrt{n}} \sum_{m=-n'+1}^{n'} \exp\left(i\frac{2\pi m\ell}{n}\right) (\phi_j)_m$$



$$\Psi_{\mathbf{k}} = \sum_{\mathbf{n}} e^{i \mathbf{k} \cdot \mathbf{n} a} \chi_{\mathbf{n}}$$

Roald Hoffmann *Angew. Chem. Int. Ed.* **1987**, *26*, 846-878

k varie par intervalles de $2\pi/a$

$k=0$

$$\Psi_0 = \sum_n e^0 \chi_n = \sum_n \chi_n = \chi_0 + \chi_1 + \chi_2 + \chi_3 + \dots$$



$k=\pi/a$

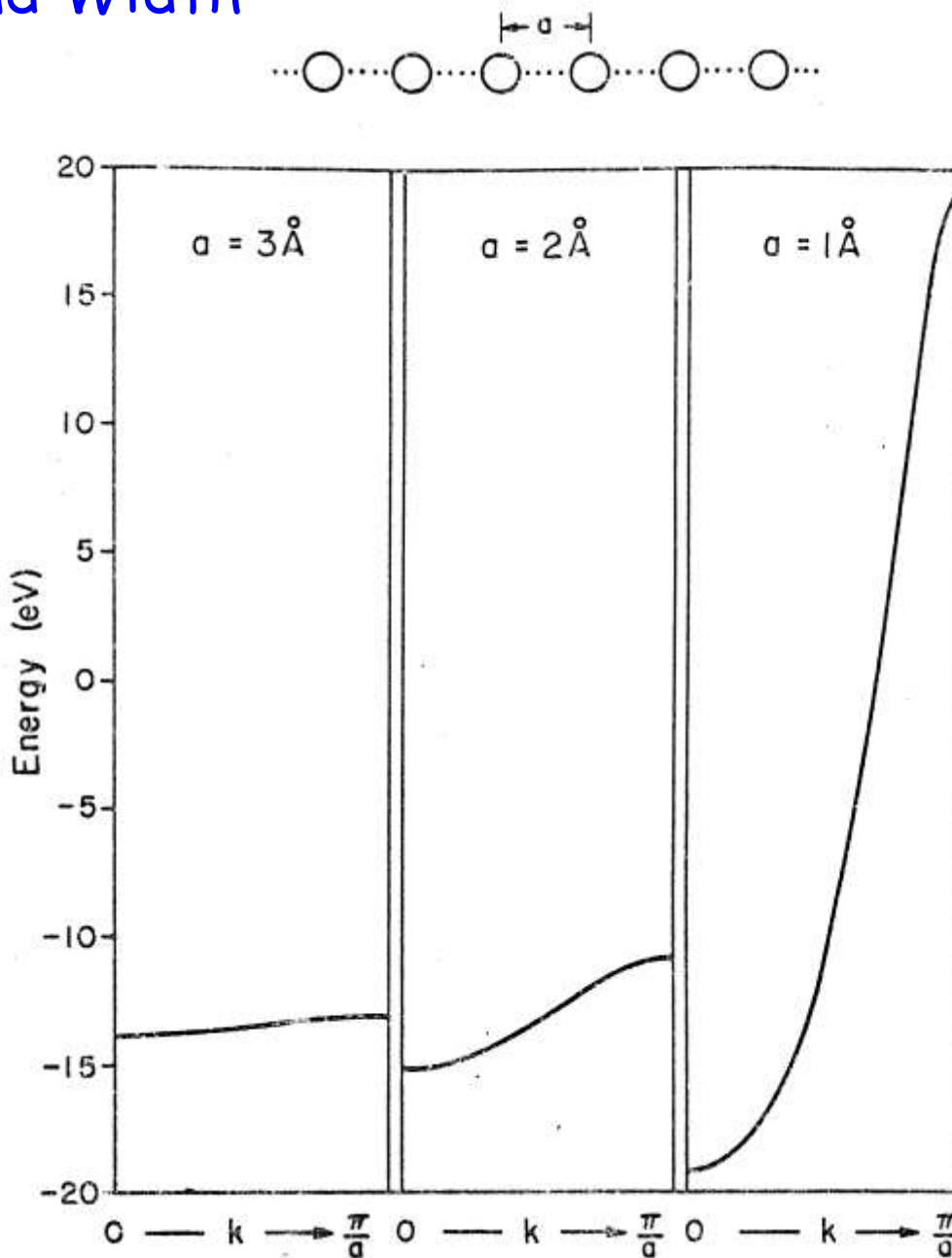
$$\begin{aligned}\Psi_{\pi/a} &= \sum_n e^{\pi i n} \chi_n = \sum_n (-1)^n \chi_n \\ &= \chi_0 - \chi_1 + \chi_2 - \chi_3 + \dots\end{aligned}$$



$k=-\pi/a$



Band Width



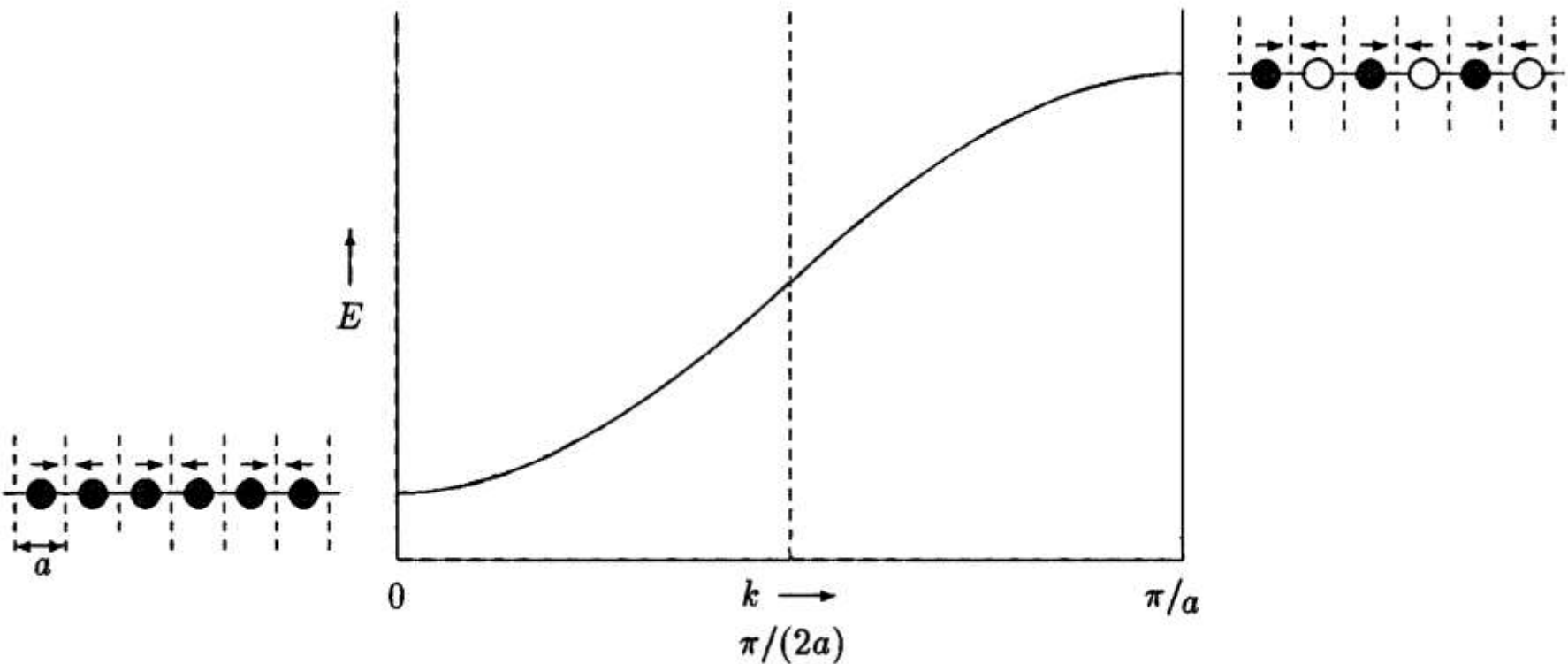
- that the bands extend unsymmetrically around their "origin" (energy of a free H atom at -13.6 eV) is a consequence of the inclusion of overlap:

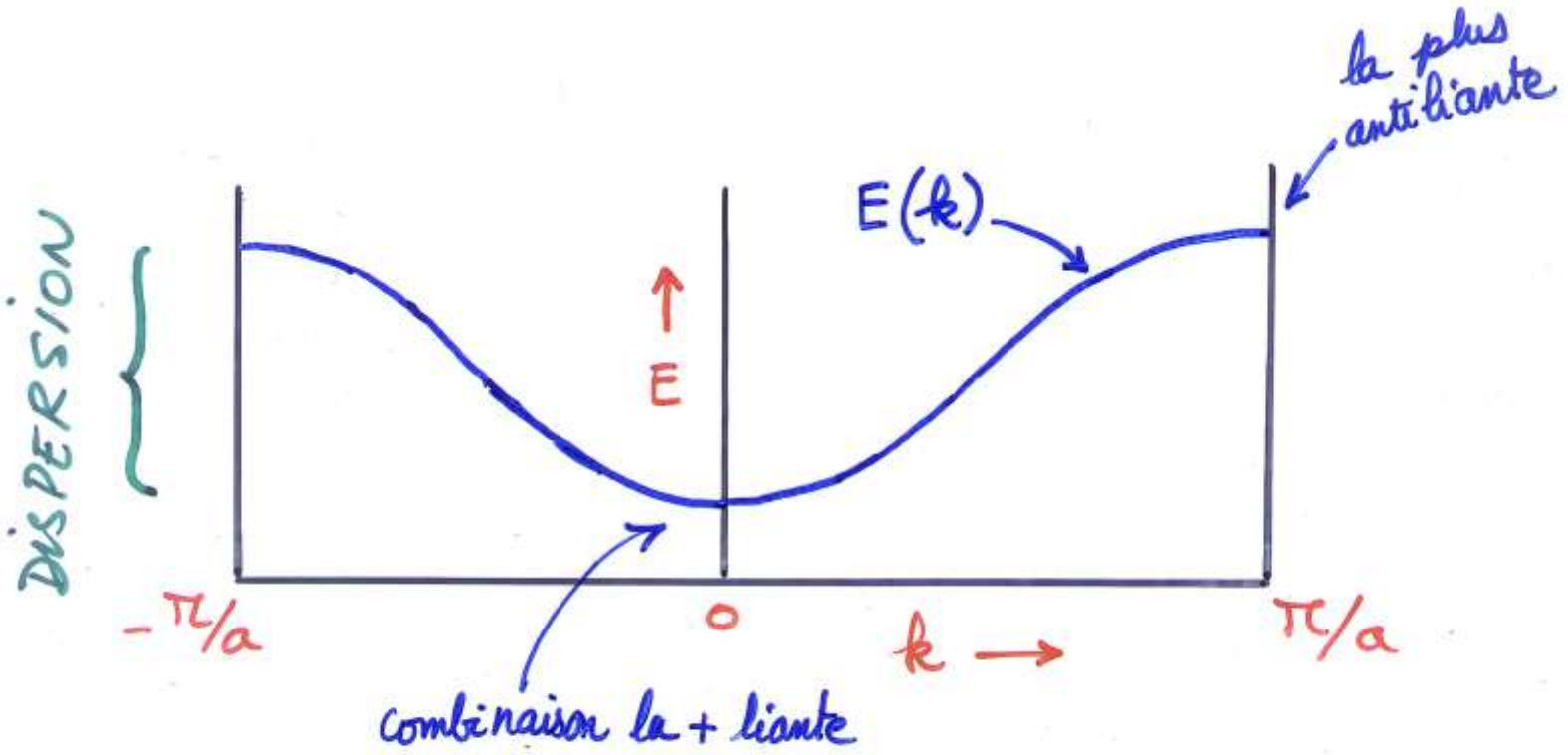
- for two levels, a dimer:

$$E_{\pm} = \frac{H_{AA} \pm H_{AB}}{1 \pm S_{AB}}$$

the bonding E_+ combination is less stabilized than the antibonding one E_- is destabilized

orbitals and bands in one dimension





$E(k)$ est une fonction périodique, de période 2π
 k , valeurs discrètes, espacées régulièrement

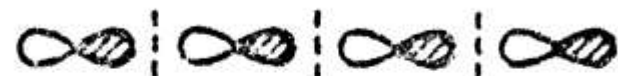
see how they run:

$$\Psi_{\mathbf{k}} = \sum e^{i\mathbf{k}\cdot\mathbf{r}_n} \chi_n$$

p_x along x :



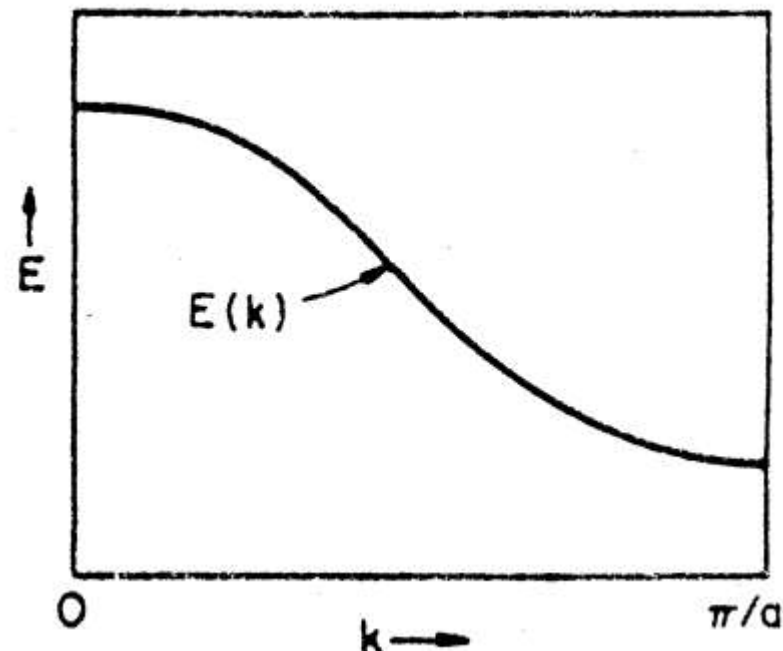
$$\Psi_0 = \chi_0 + \chi_1 + \chi_2 + \chi_3 + \dots$$



$$\Psi_{\frac{\pi}{a}} = \chi_0 - \chi_1 + \chi_2 - \chi_3 + \dots$$

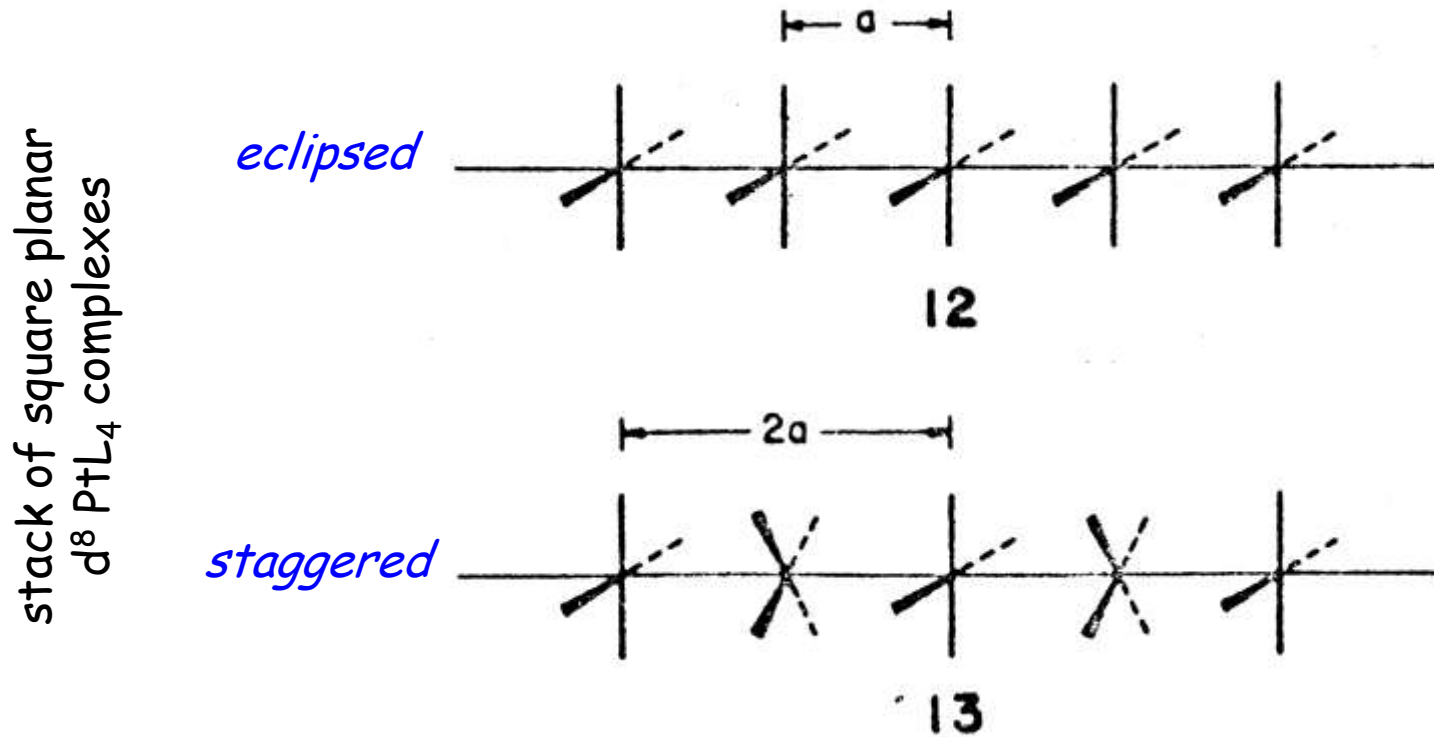


9



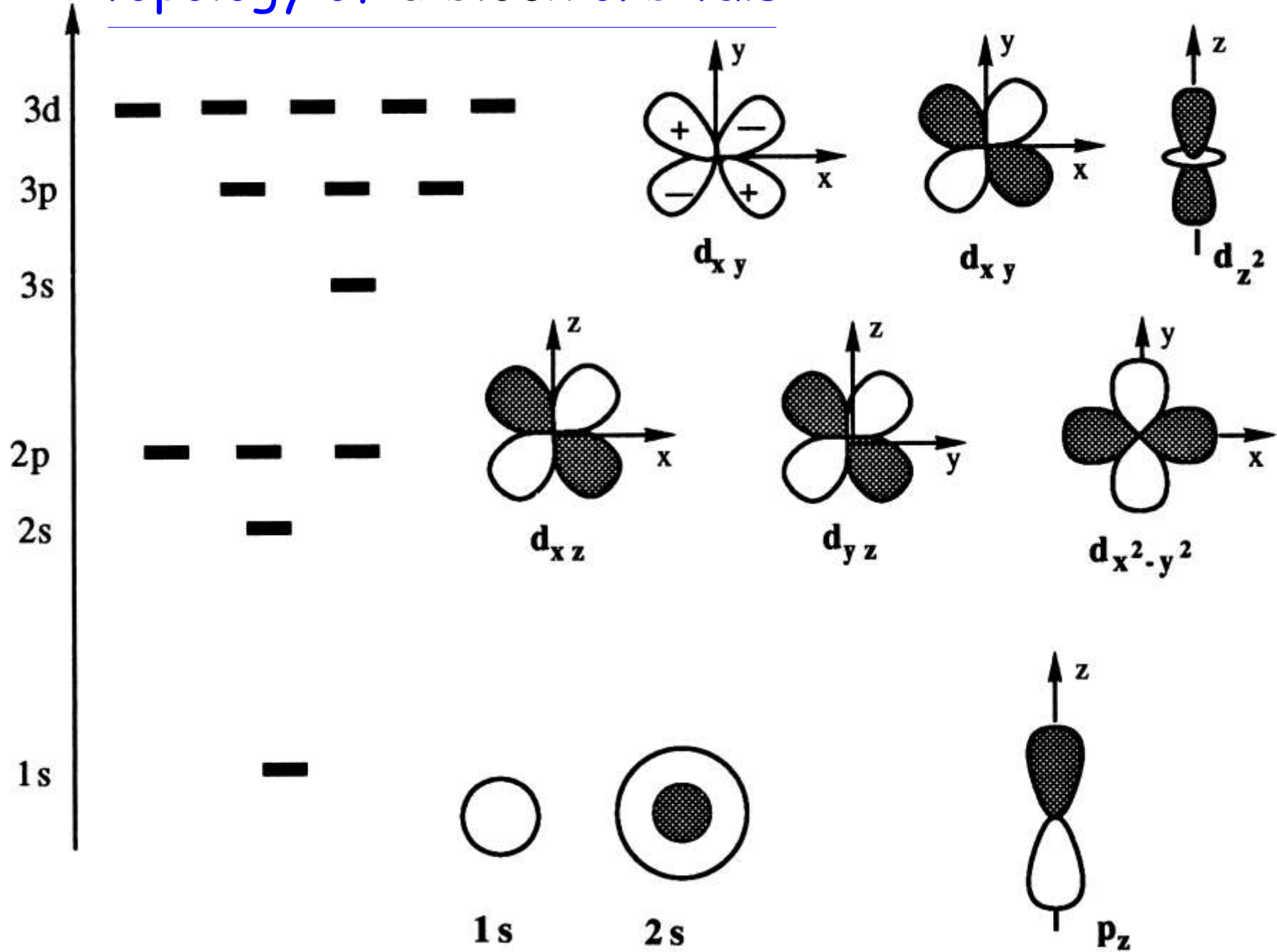
the band of p orbitals runs down from zone center to zone edge

try predict the approximate band structure of
 $K_2Pt(CN)_4$ and $K_2Pt(CN)_4Br_{0.3}$
without calculation



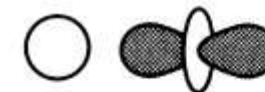
the Pt-Pt distance has been shown to be inversely related
to the degree of oxidation of the materials

topology of d block orbitals

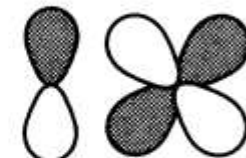
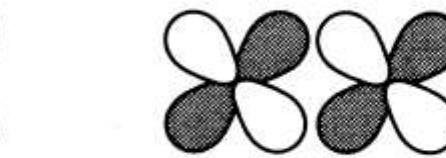
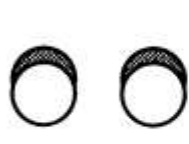


types of overlap

σ



π



δ



- type σ : **strong**, axis of rotation
- type π : **medium**, lateral, co-planar
- type δ : **weak**, face-to-face

inventory of all possible modes of overlap
within pairs of orbitals s, p or d along z

z

overlap type

only between orbitals

σ

s, p or d_z^2

π

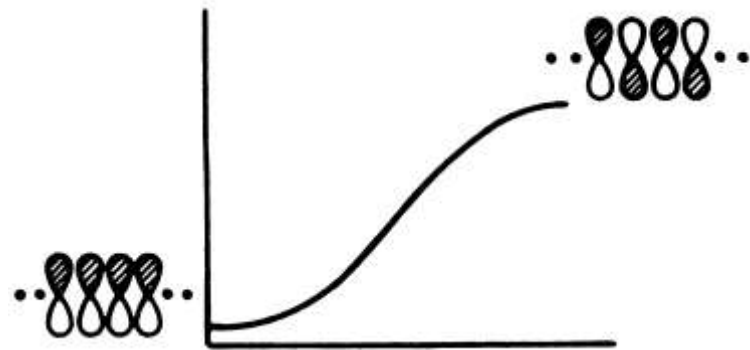
p_x, p_y, d_{xz} or d_{yz}

δ

$d_{x^2-y^2}$ or d_{xy}

try and see how they run (along z)?

- a π band out of N p orbitals:



runs up, moderate yet sizeable dispersion

- a π band out of d_{xz} 's:

runs down, moderate yet sizeable dispersion

- a σ band out of d_z^2 's:

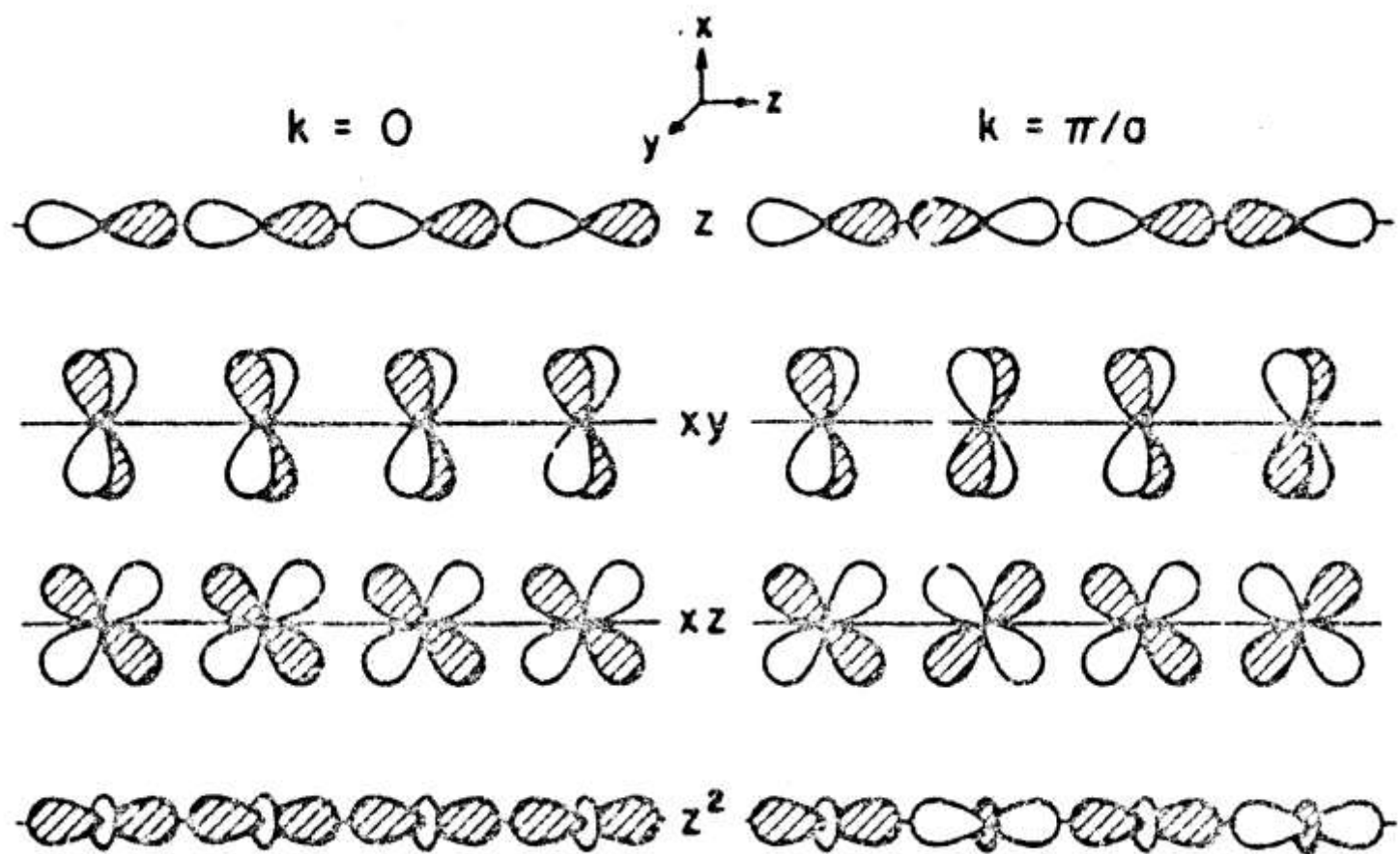


runs up, dispersion is large

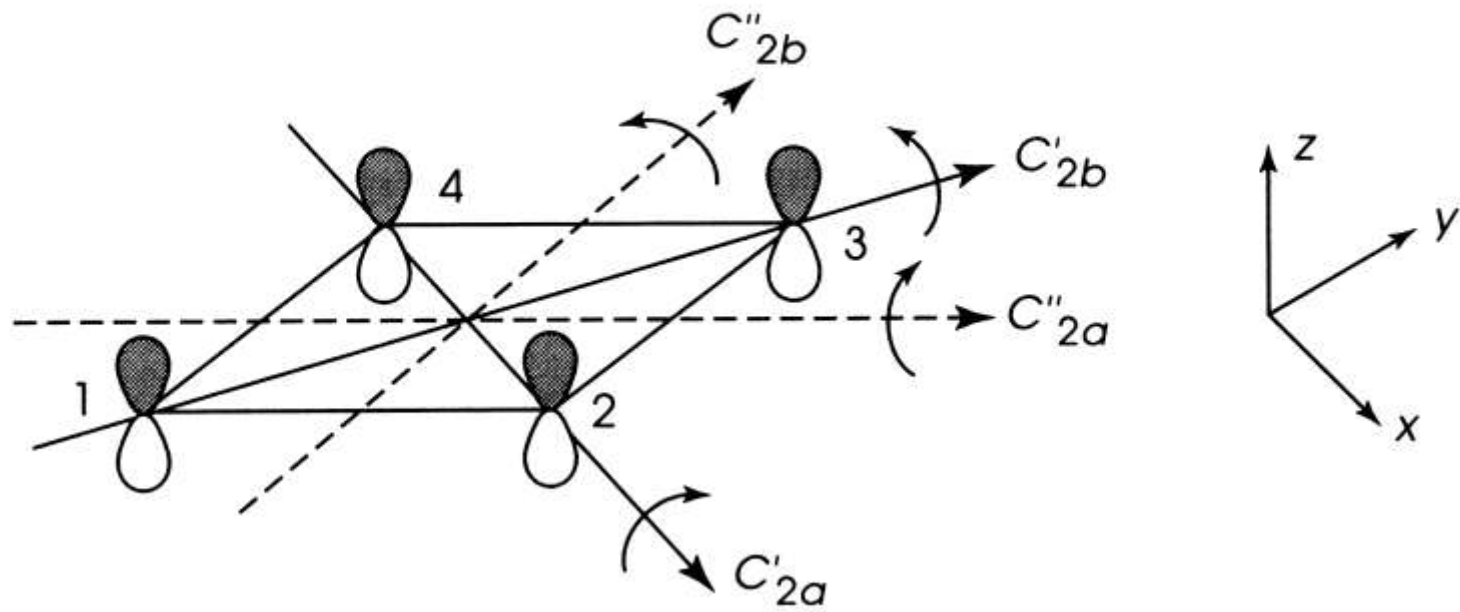
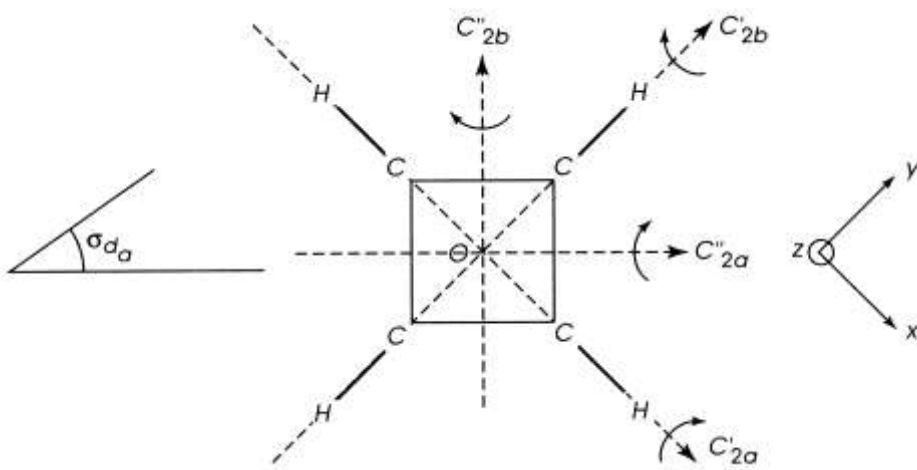
- a δ band out of d_{xy} 's:

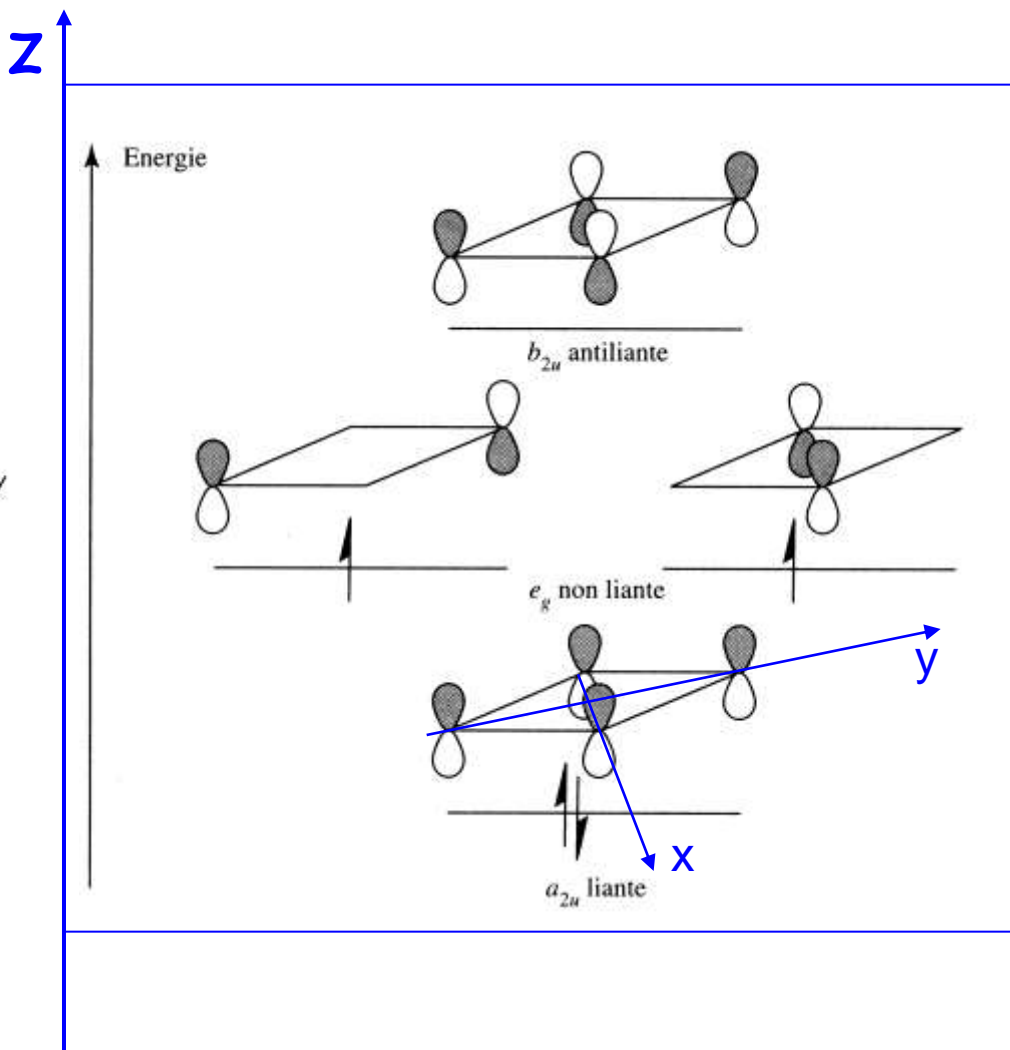
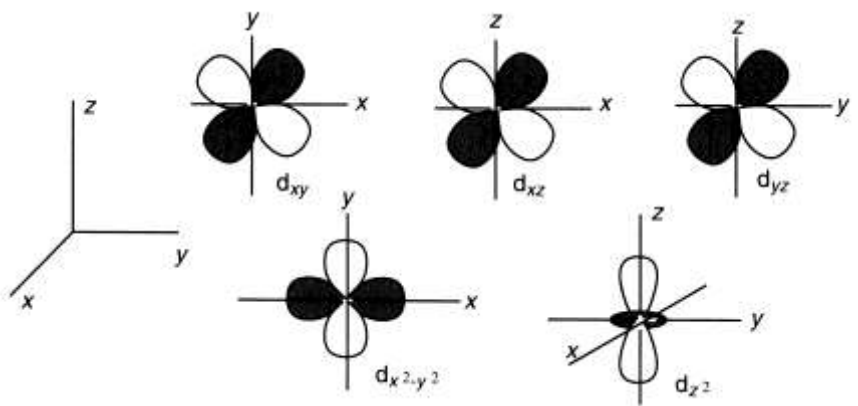
runs up, barely (not quite flat though)

Bloch functions at the zone center ($k = 0$) and the zone edge ($k = \pi/a$)

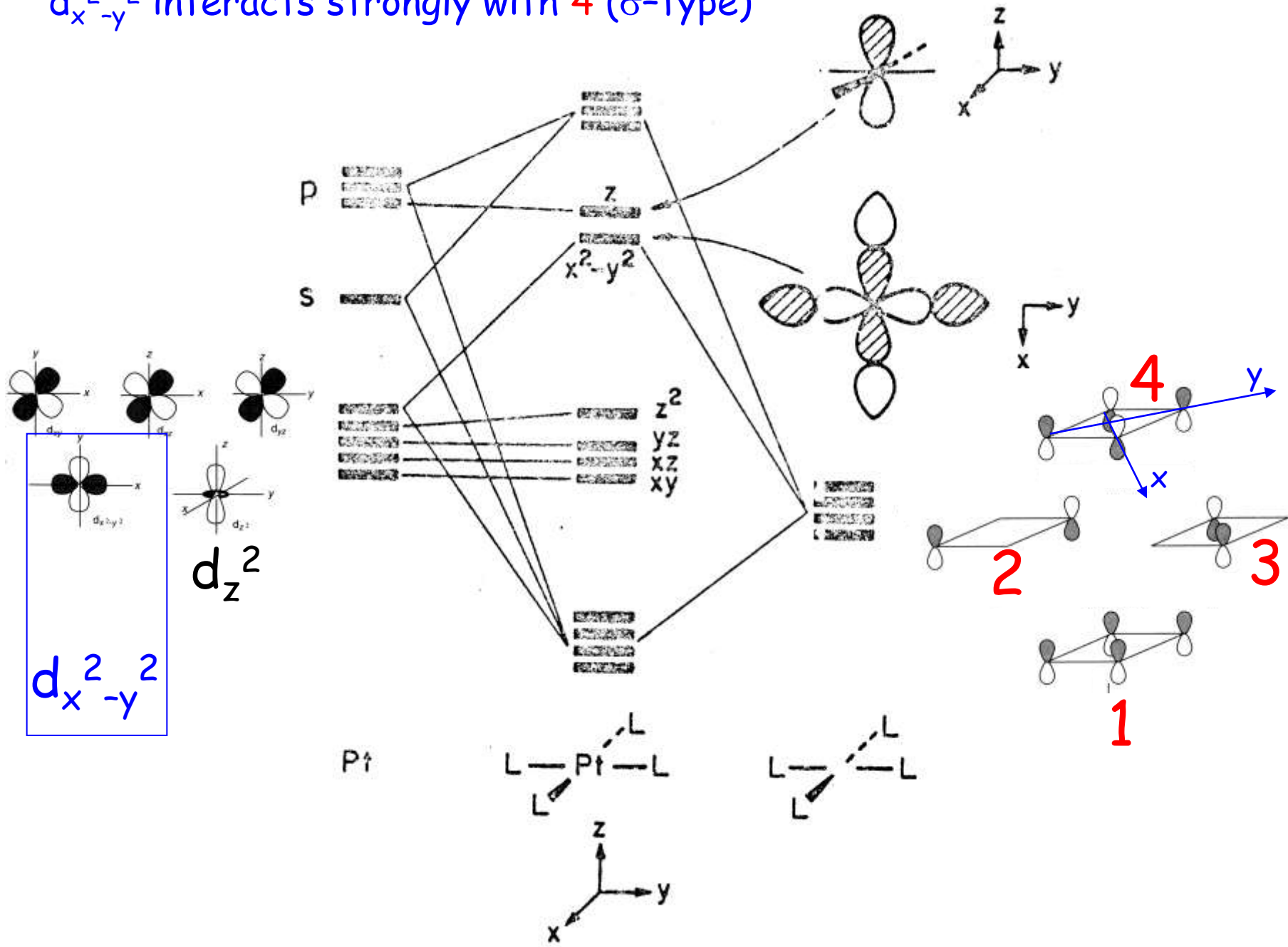


$(2p_z)_i$ orbitals of the 4 carbon atoms ($i = 1, 2, 3, 4$) of cyclobutadiene

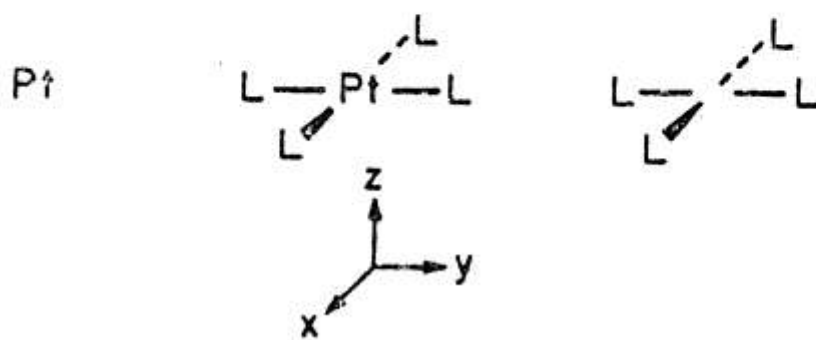
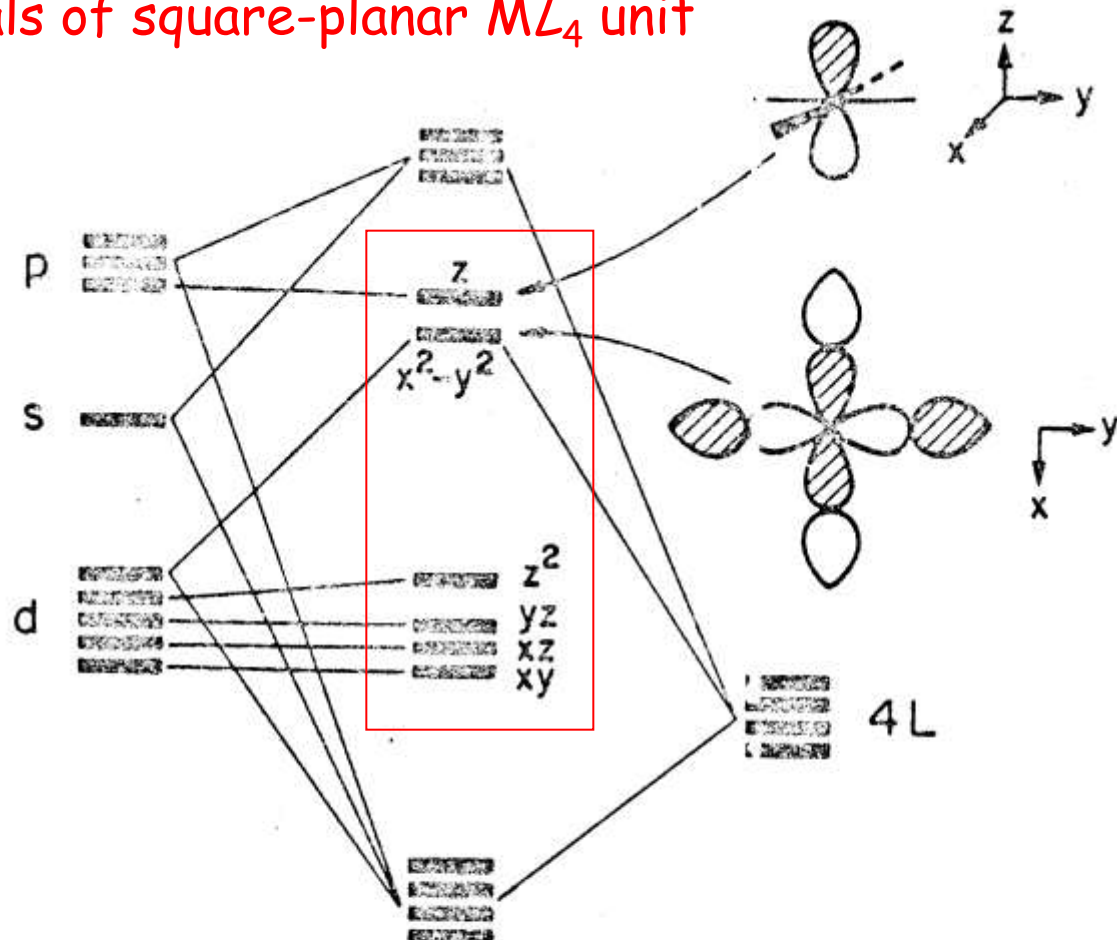


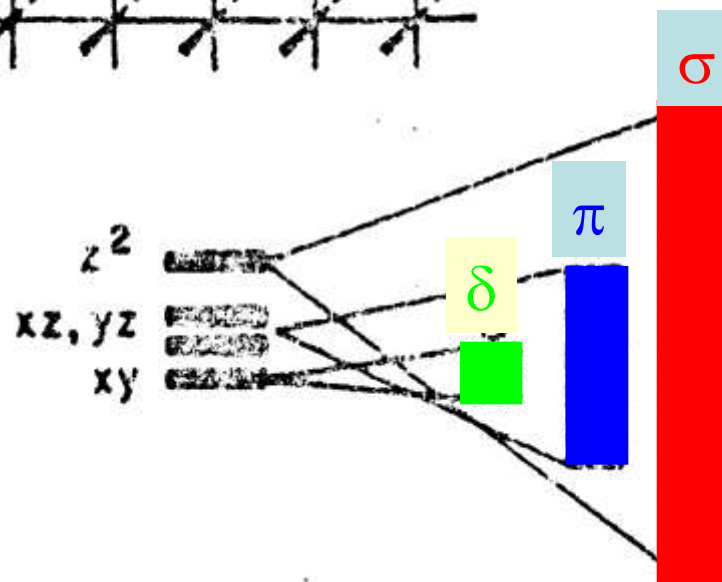
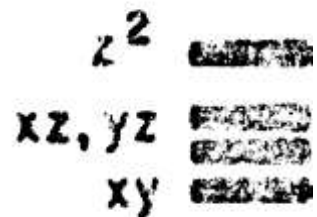
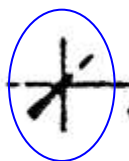
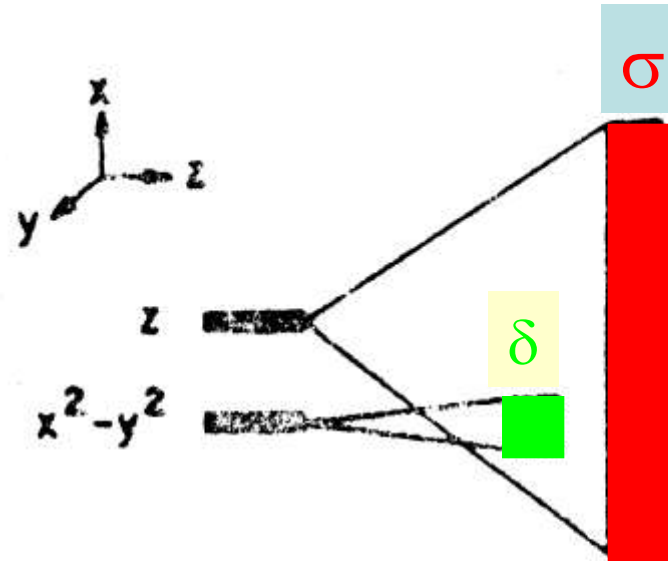


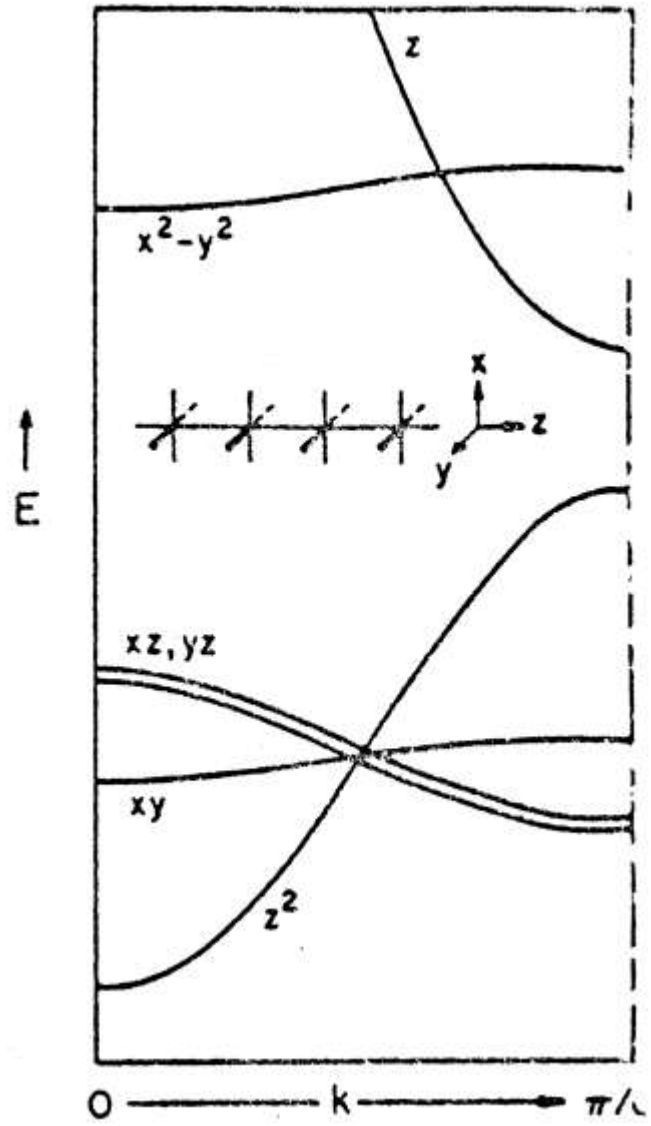
$d_{x^2-y^2}$ interacts strongly with 4 (σ -type)



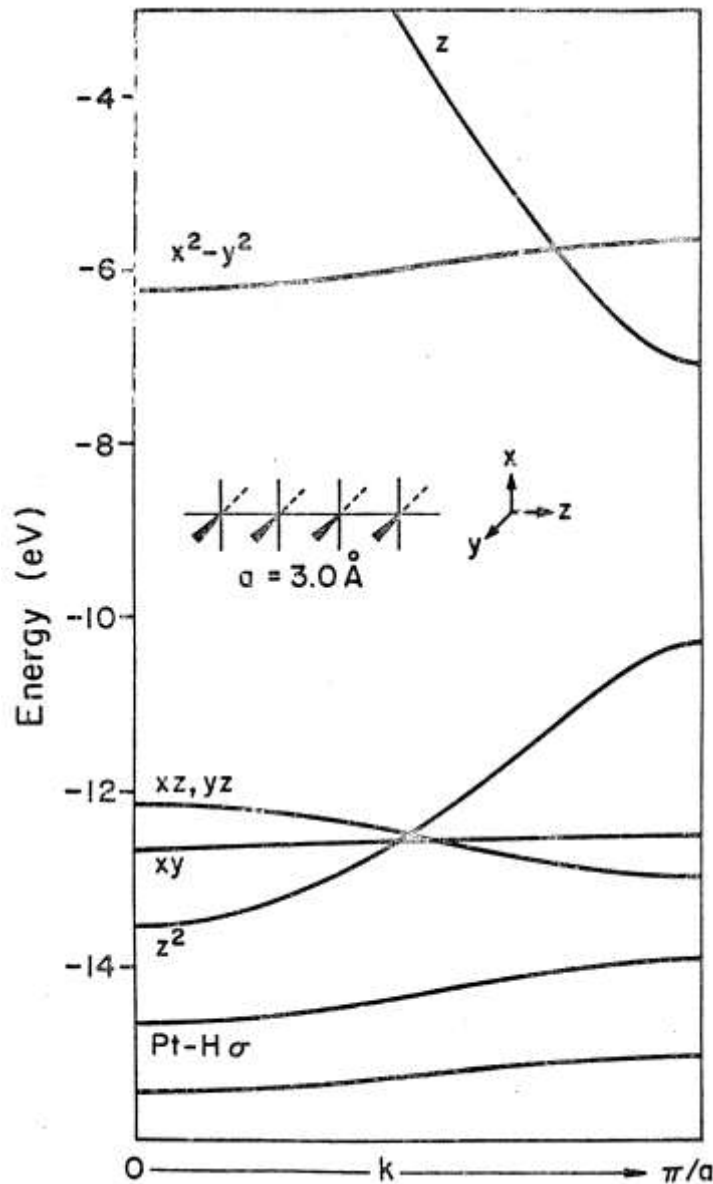
the "d" orbitals of square-planar ML_4 unit







predicted
considerations of band width
and orbital topology



extended Huckel calculation
at Pt-Pt = 3.0 \AA

Pt(II) d⁸

where are the electrons?

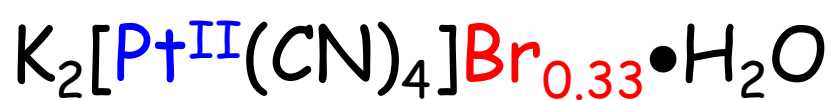
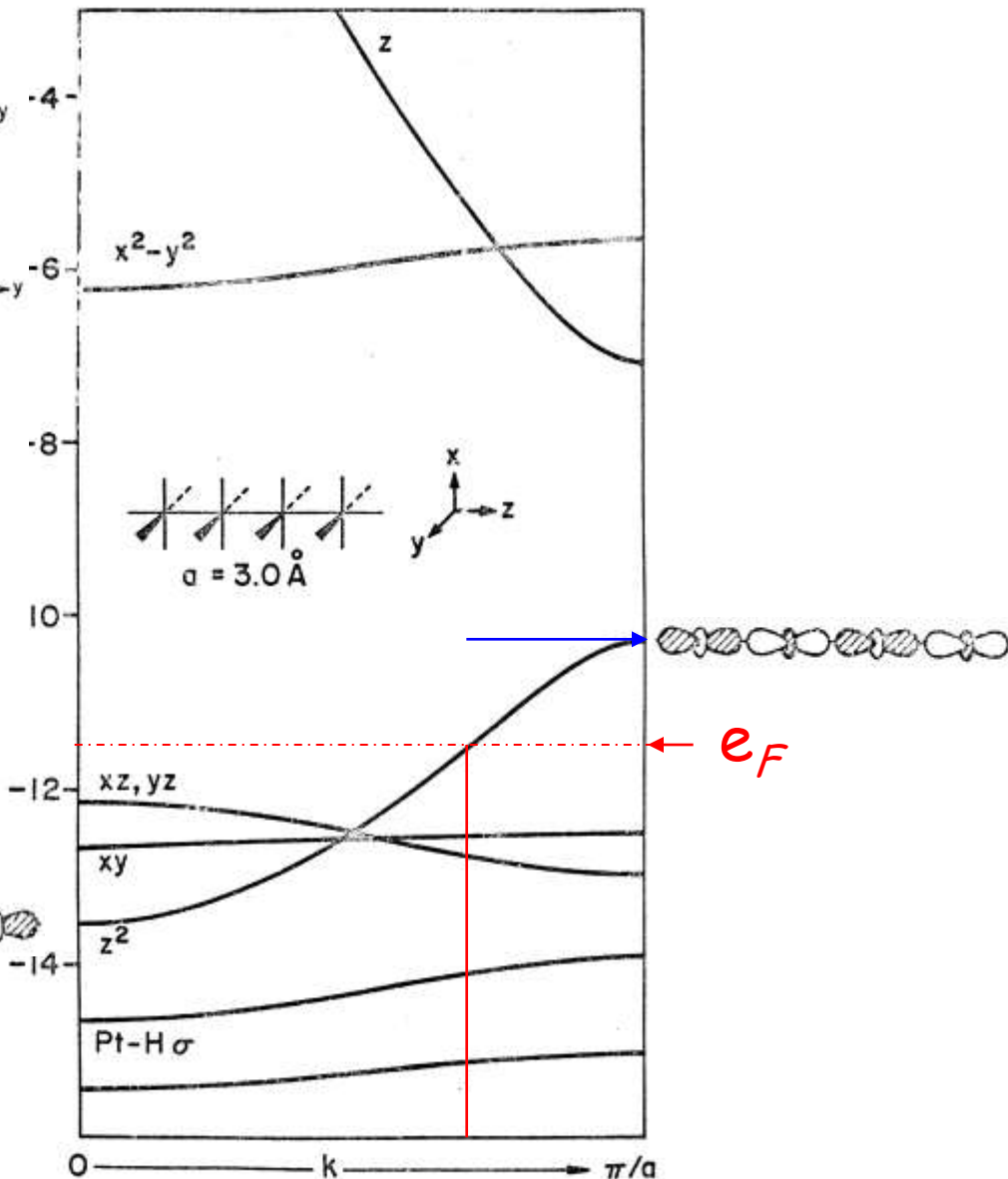
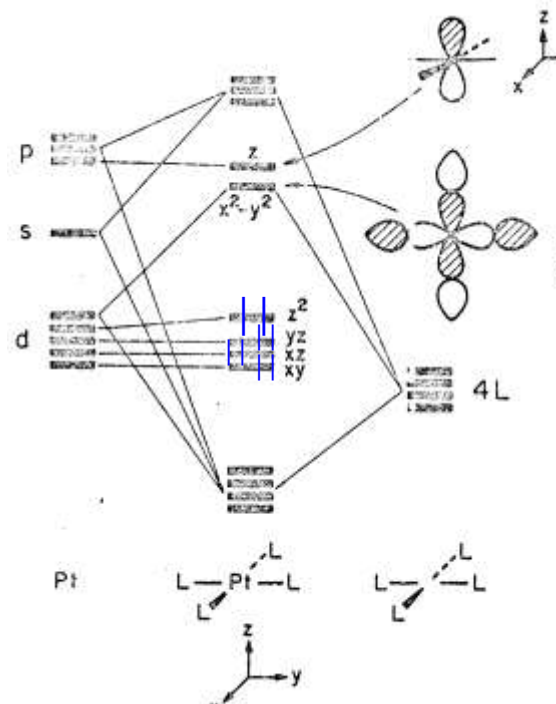


Table 5 Chain-forming tetracyanoplatinate complexes

Complex	Pt valence	Pt-Pt (Å)	Color	Conductivity ^a ($\Omega^{-1} \text{ cm}^{-1}$)
Pt Metal	0	2.775 ^b	Metallic	$\sim 9.4 \times 10^4$
$\text{K}_2[\text{Pt}(\text{CN})_4] \cdot 3\text{H}_2\text{O}$	+2.0	3.48 ^b	White	5×10^{-7}
$\text{K}_2[\text{Pt}(\text{CN})_4]\text{Br}_{0.3} \cdot 3.0\text{H}_2\text{O}$	+2.3	2.88 ^c	Bronze	4-830
$\text{K}_2[\text{Pt}(\text{CN})_4]\text{Cl}_{0.3} \cdot 3.0\text{H}_2\text{O}$	+2.3	2.87 ^d	Bronze	~ 200
$\text{K}_{1.75}[\text{Pt}(\text{CN})_4] \cdot 1.5\text{H}_2\text{O}$	+2.25	2.96 ^e	Bronze	$\sim 70-100$ [see (119)]
$\text{Cs}_2[\text{Pt}(\text{CN})_4](\text{EtHg})_{0.39}$	+2.39	2.83 ^f	Gold	Unknown ^f

^a See (115).

^b See (116).

^c See (117).

^d See (118).

^e See (119).

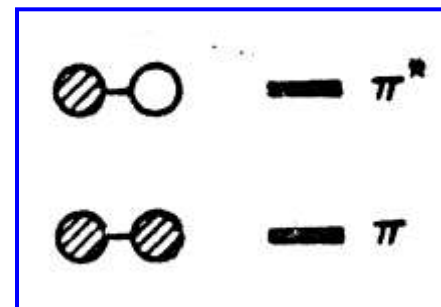
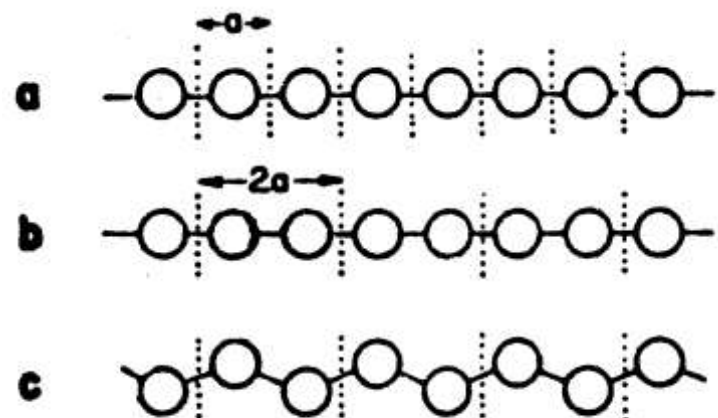
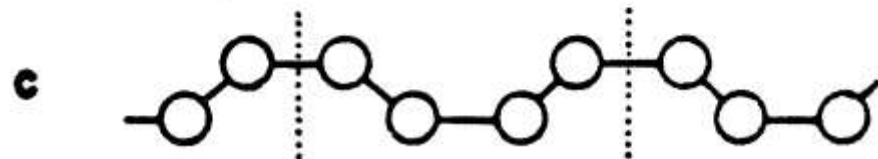
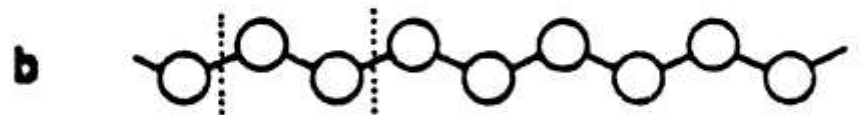
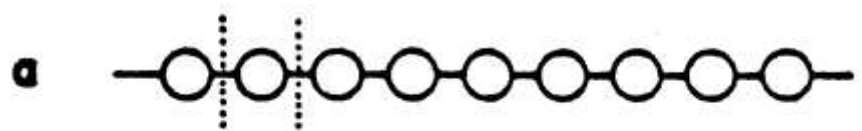
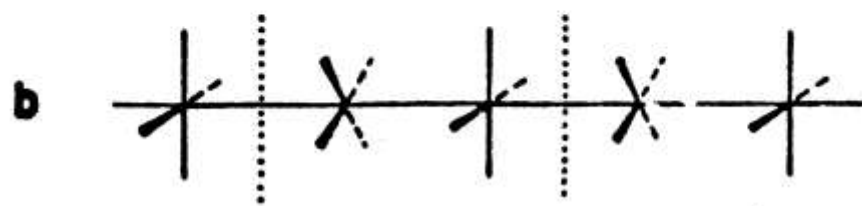
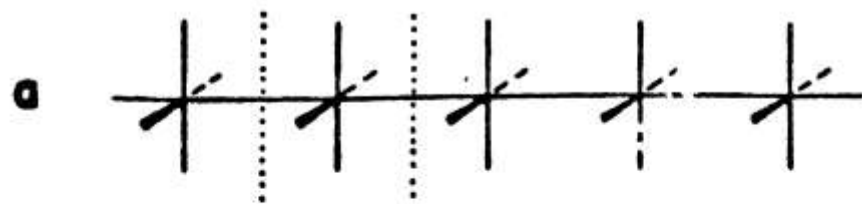
^f See (138).

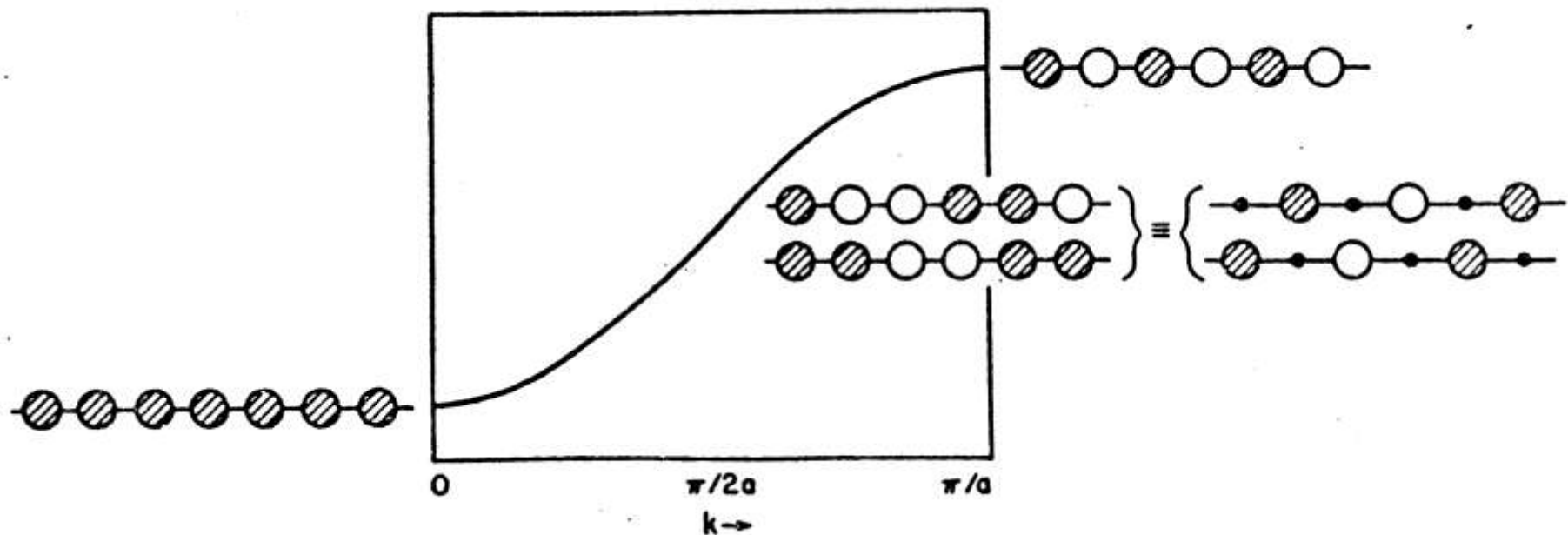
^g See (114).

more than one unit per unit cell :

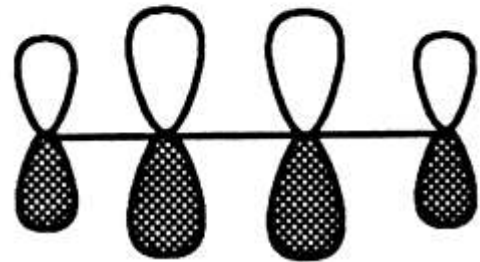
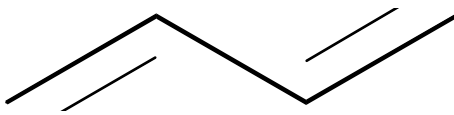
chemists fold bands too !

More than one electronic unit in the unit cell. Folding bands.



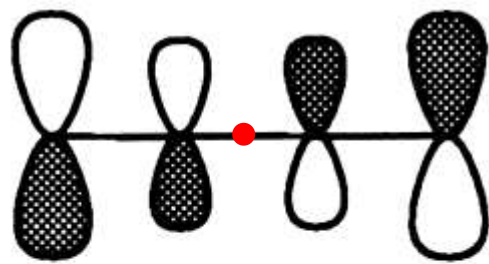
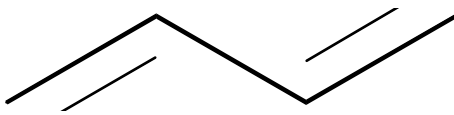


butadiene

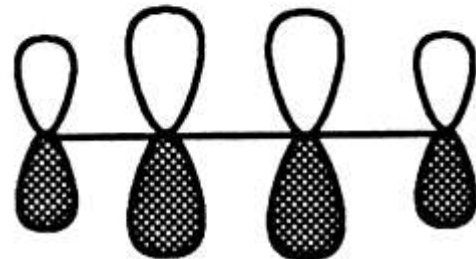


- Ψ_1

butadiene

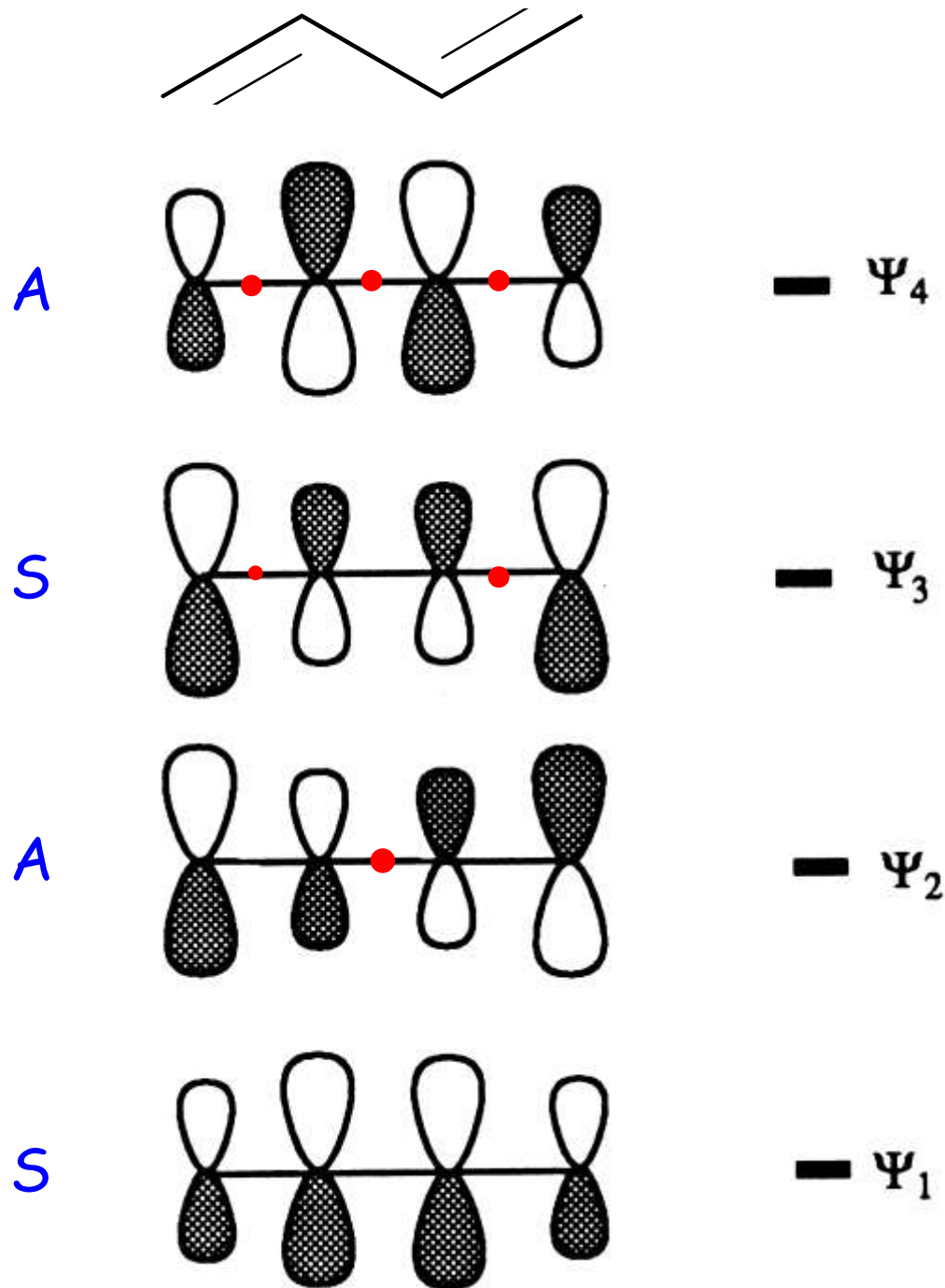


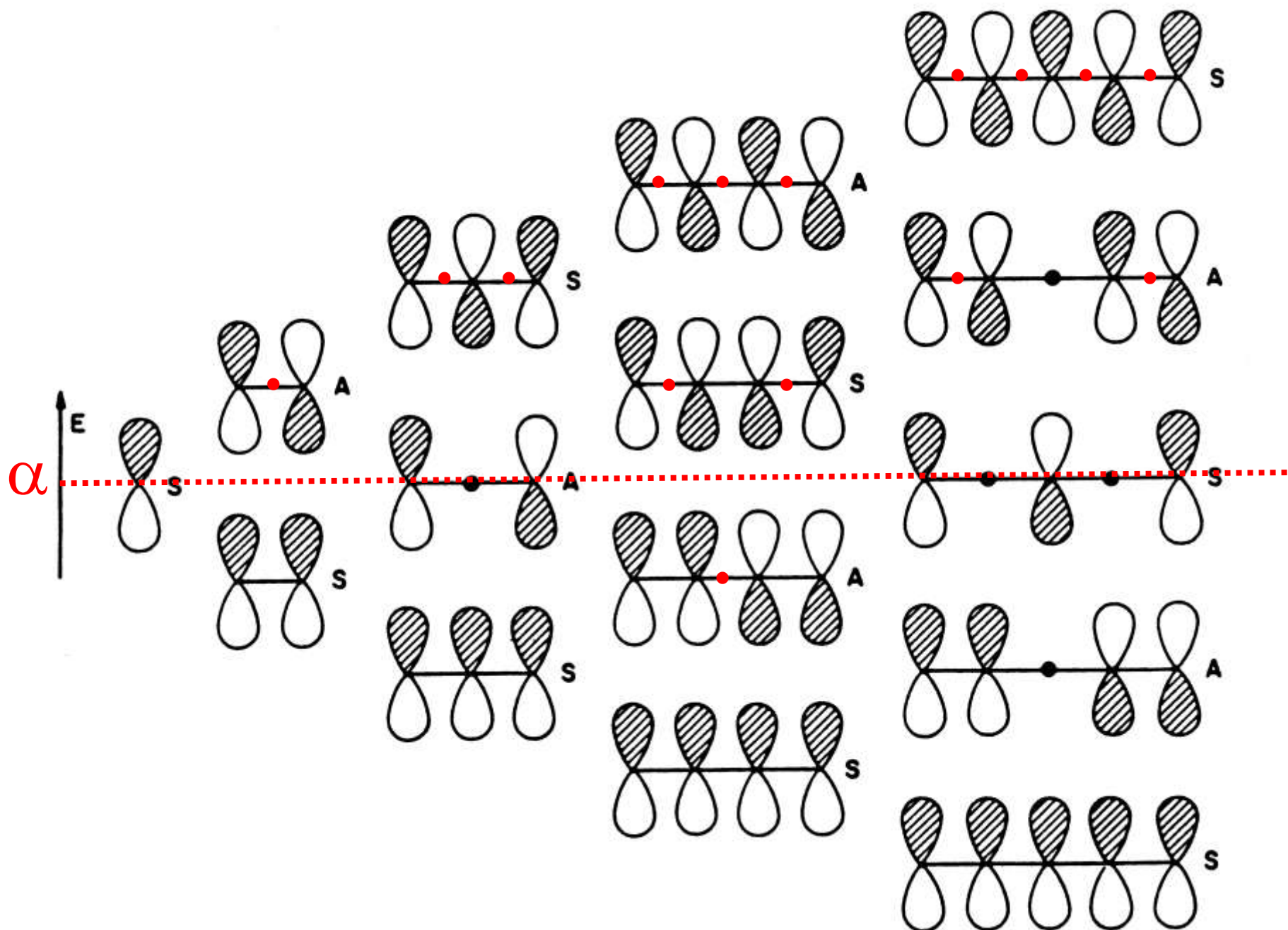
- Ψ_2

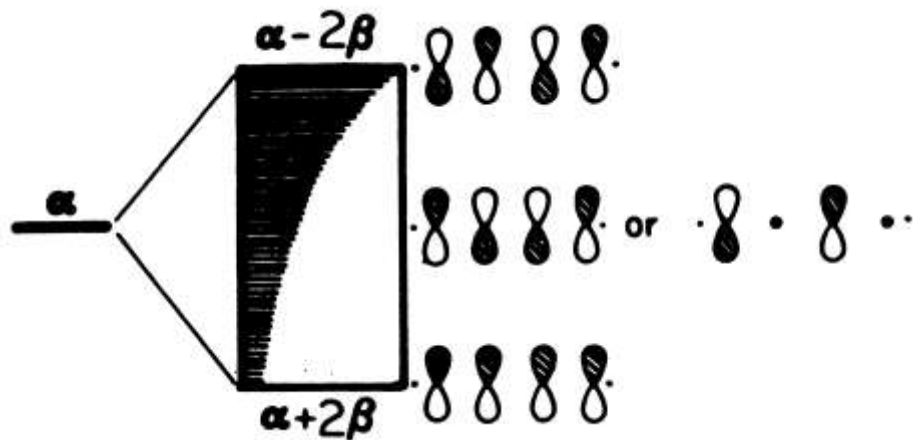
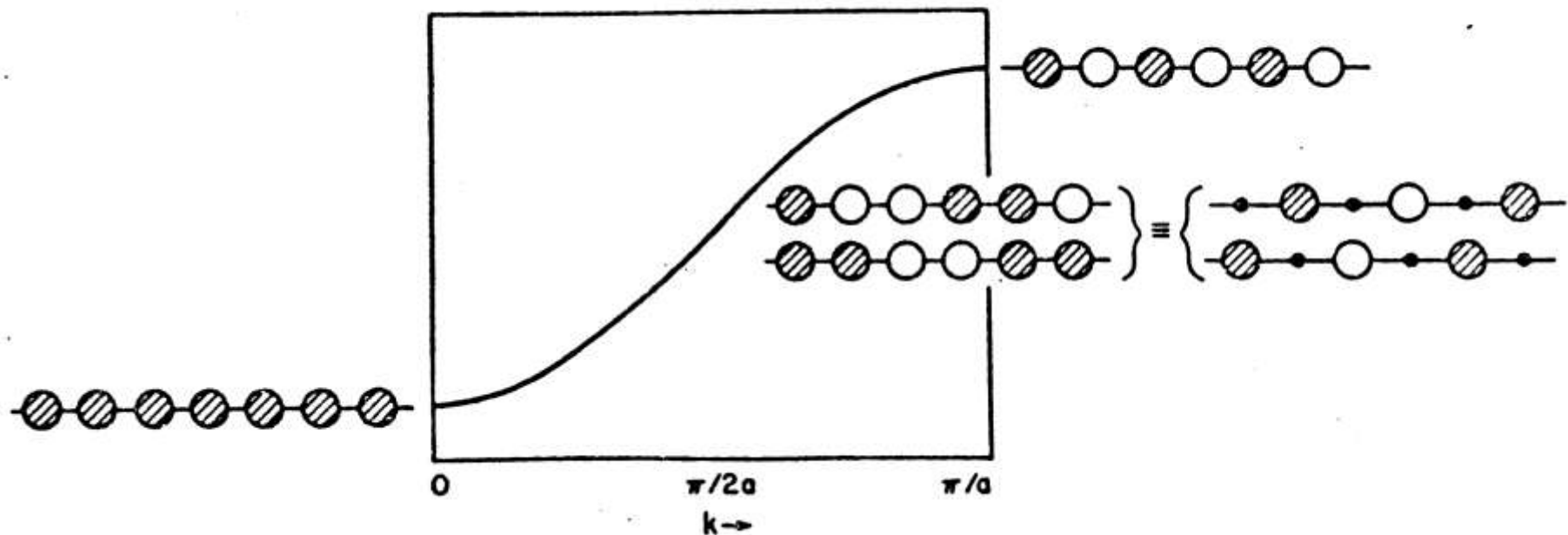


- Ψ_1

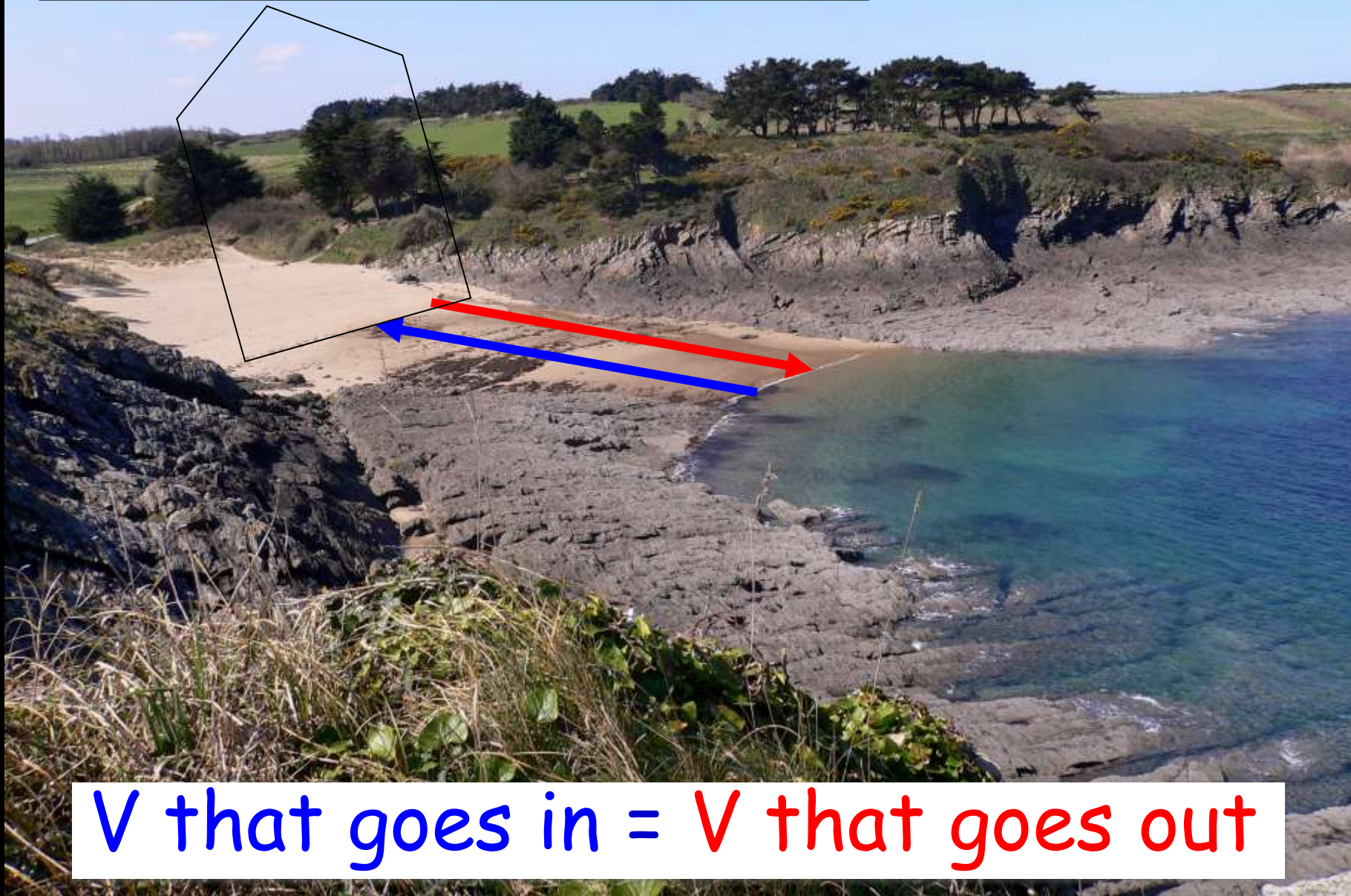
butadiene



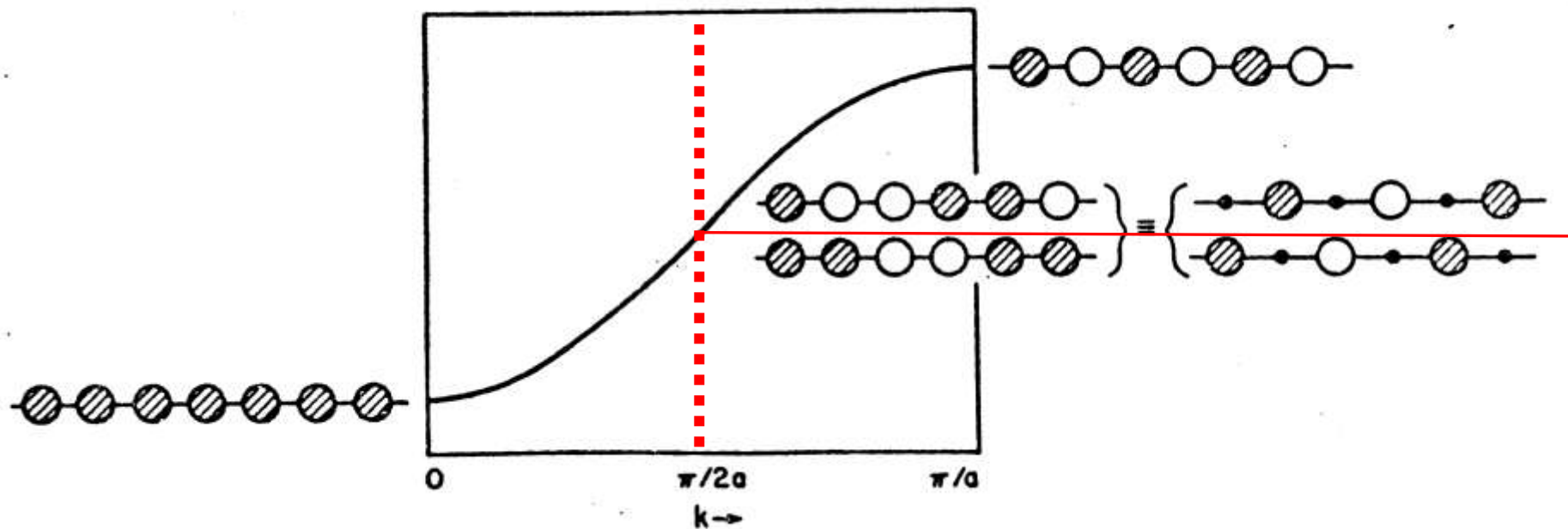




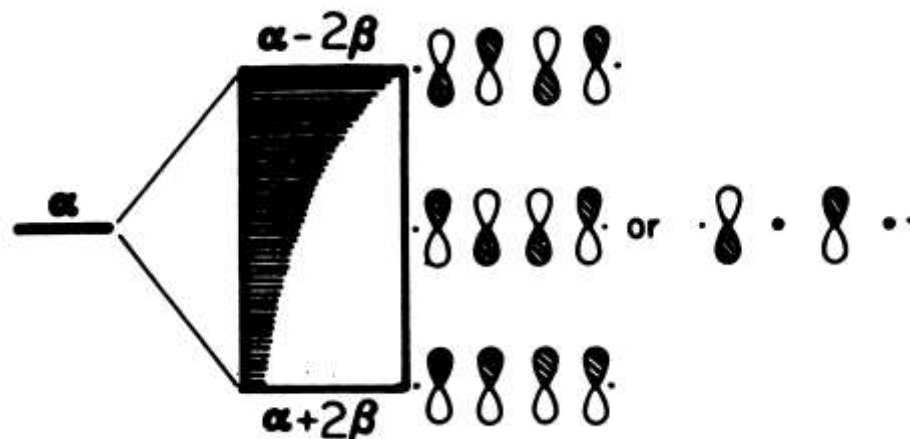
stays still there before going back down (equilibrium)



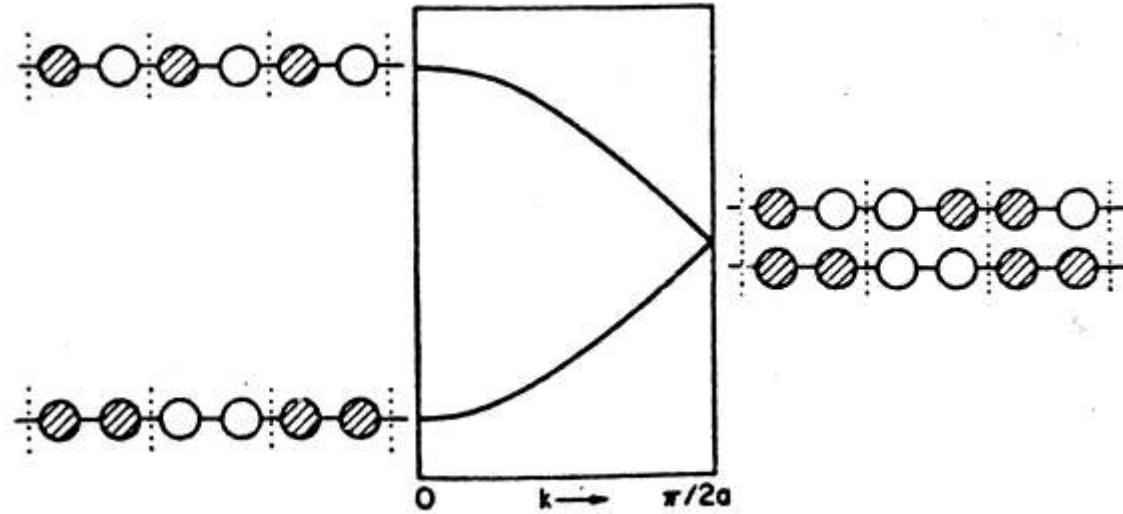
V that goes in = V that goes out

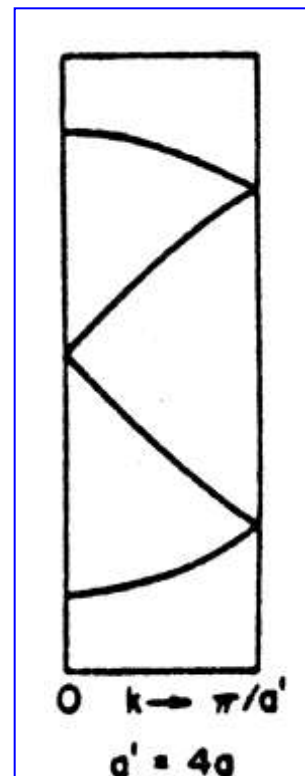
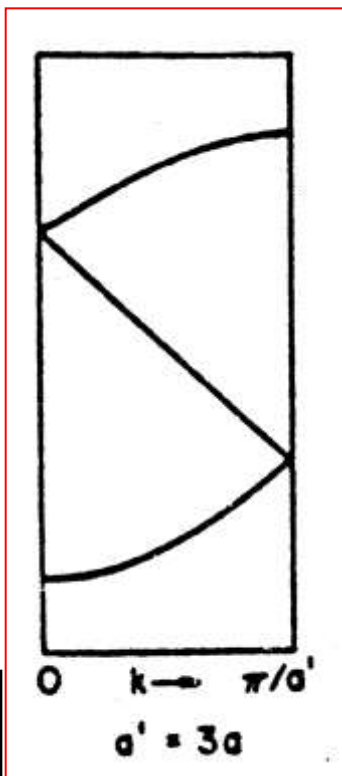
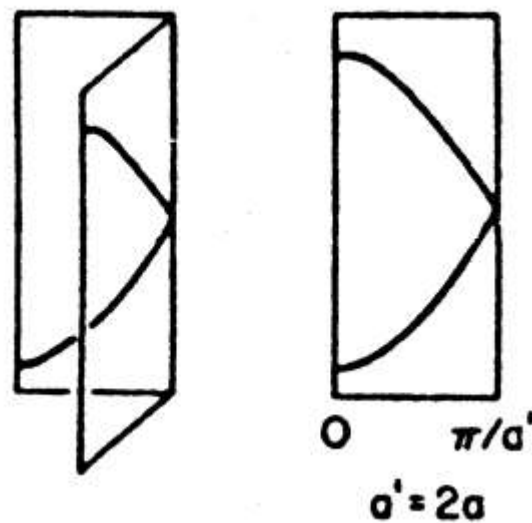
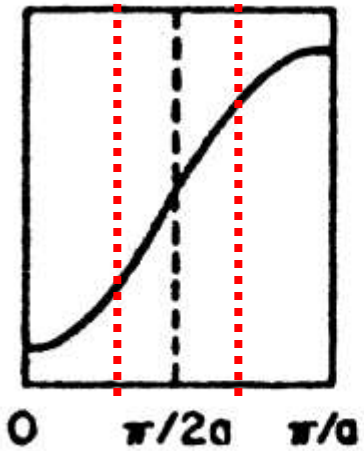


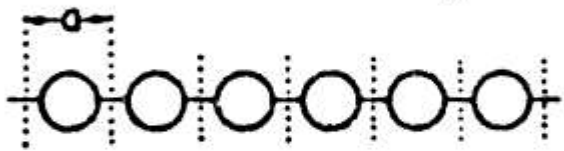
goes through a mid-point in energy where
the net number of bonding states equals that of antibonding states



folding bands

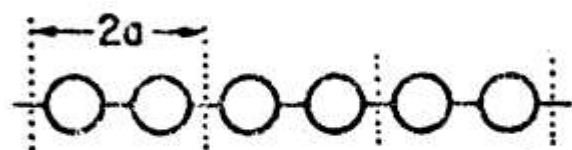
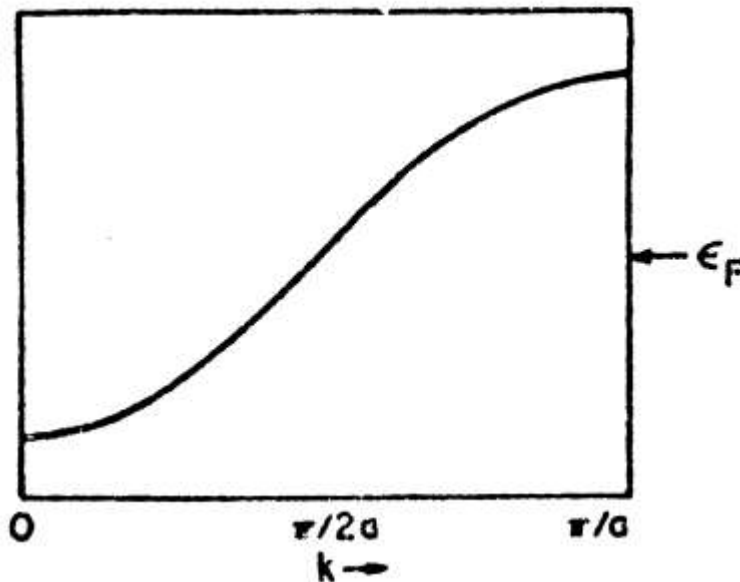




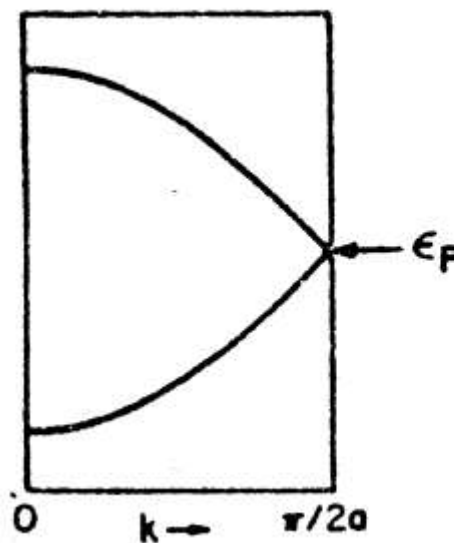


a

43

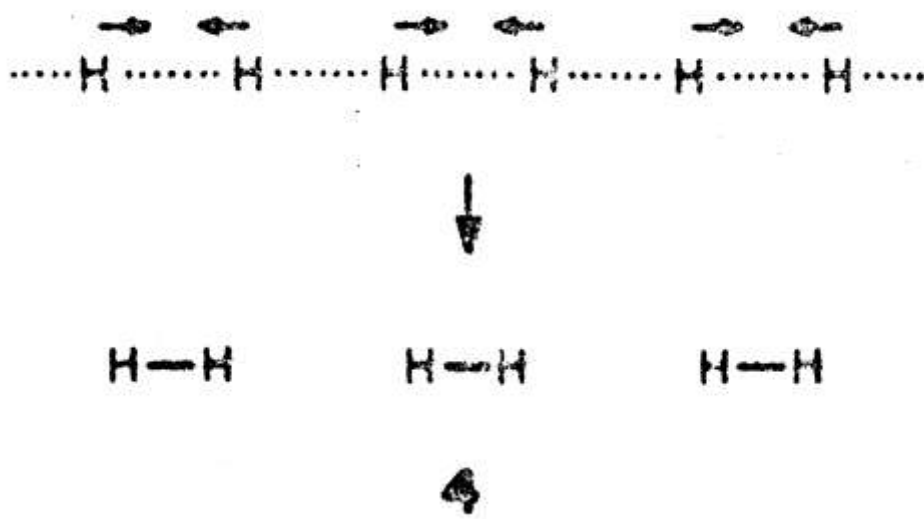


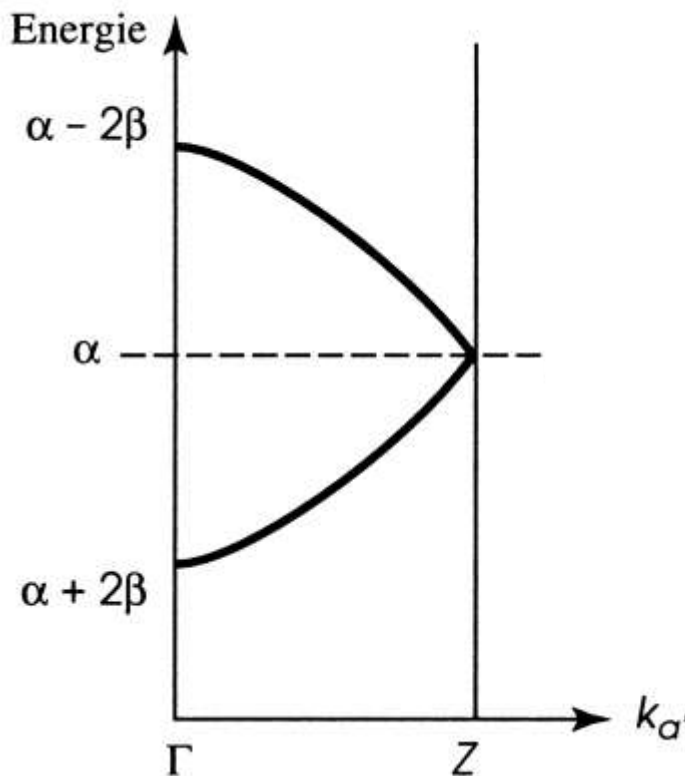
b



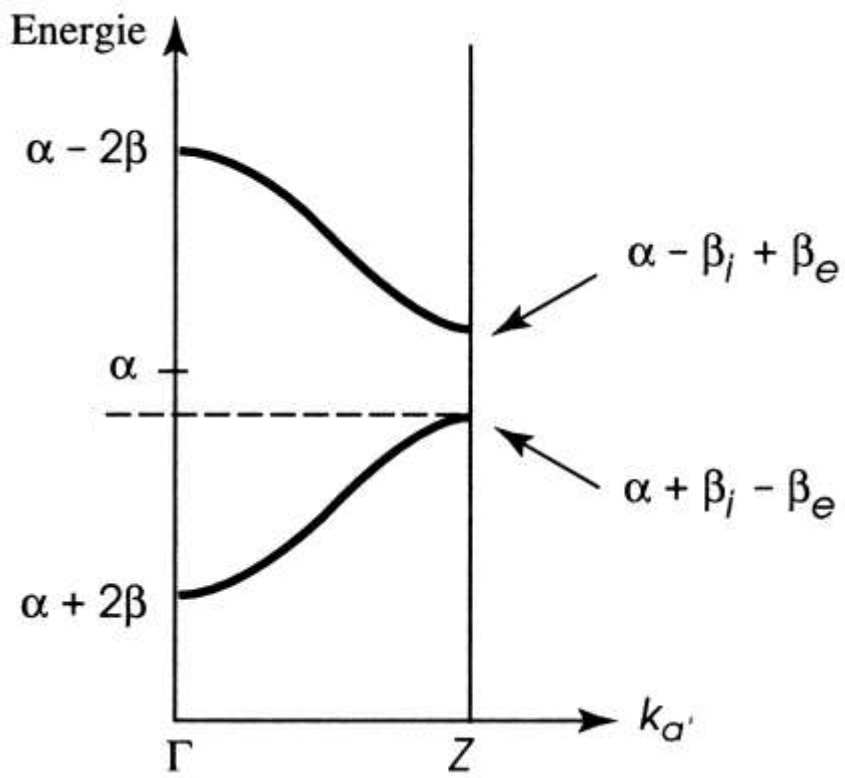
band diagram of a dimerized system. Peierls. electron count. $2k_F$

the chemist's intuitive feeling for what a model chain of hydrogen atoms would do:

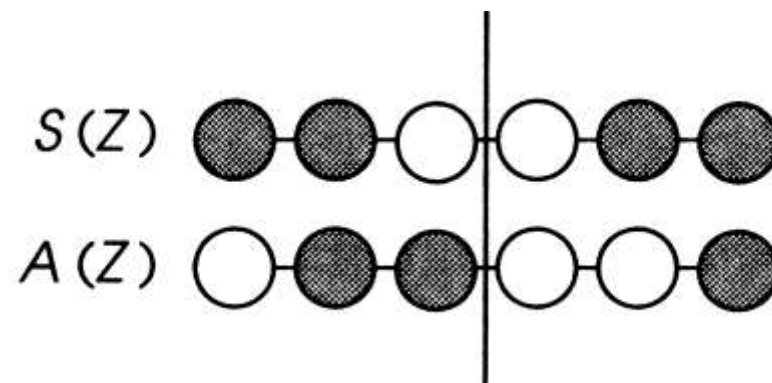




H_n , uniform chain

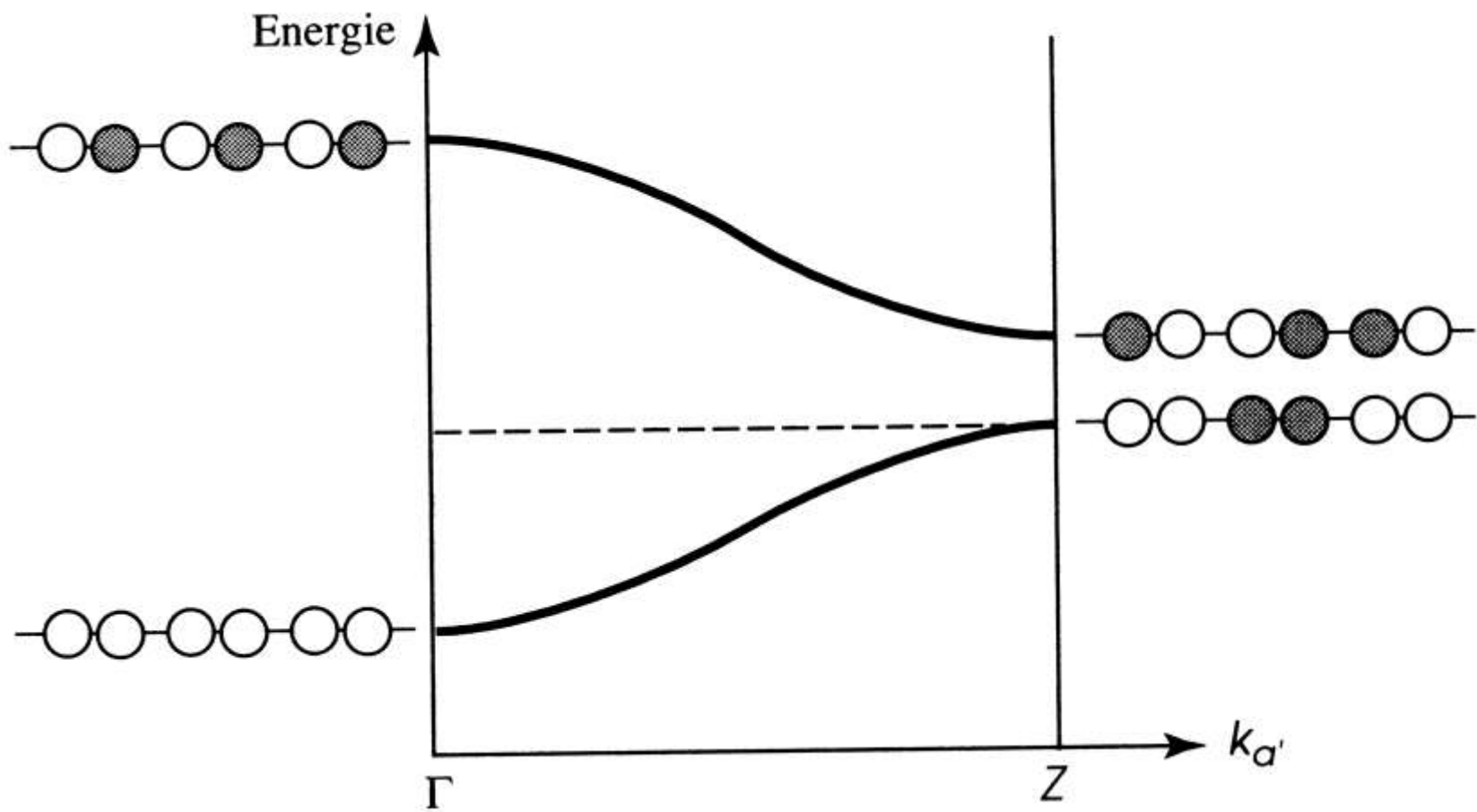


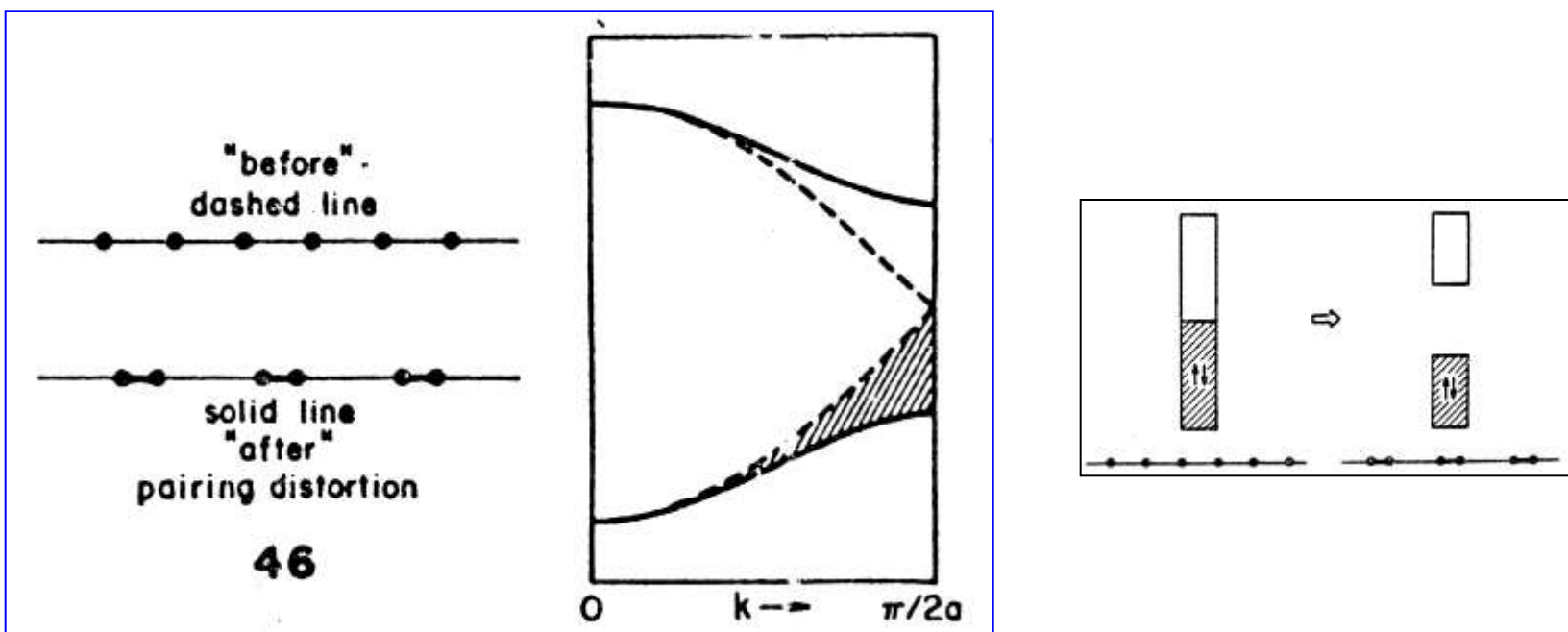
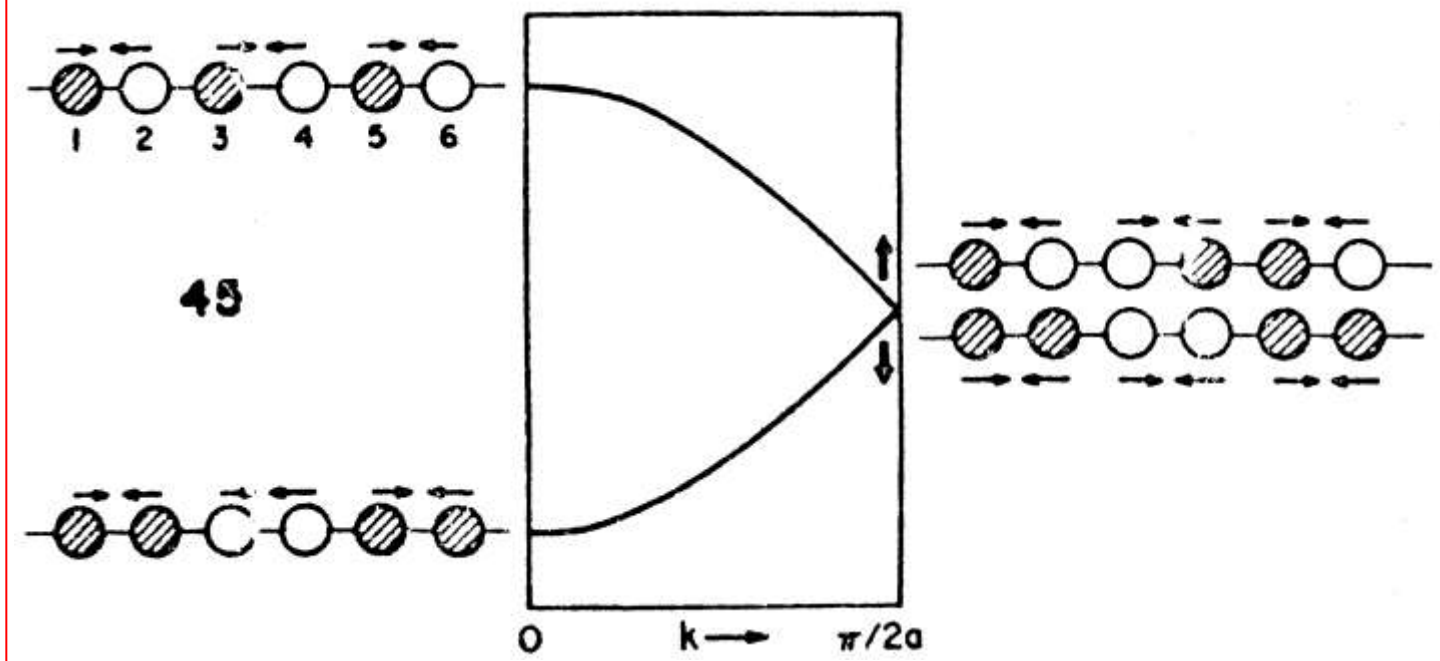
H_n , dimerized chain

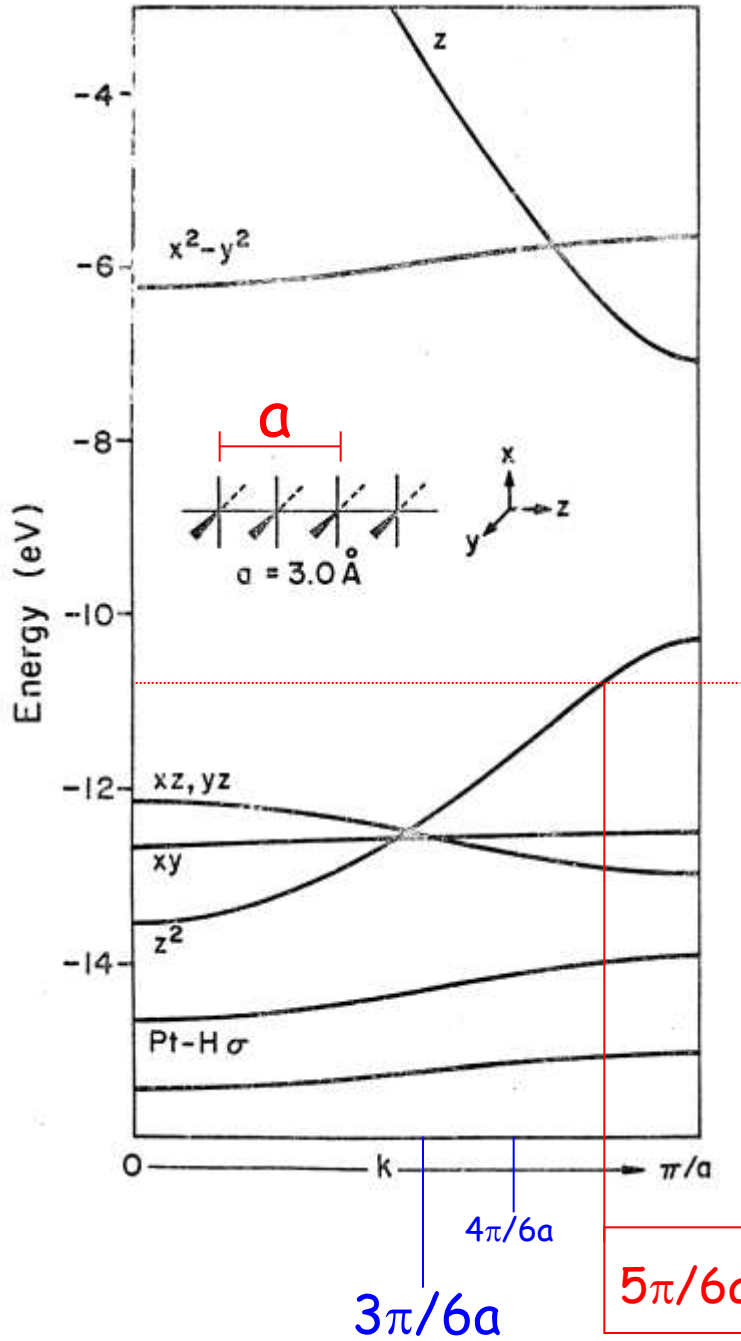


orbitals at the Fermi level for the chain (H_2) $_{n'}$

band diagram of the dimerized system $(H_2)_n$





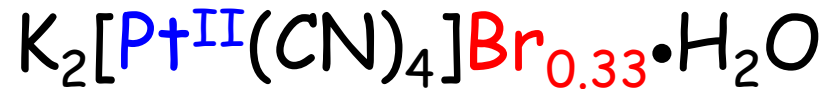


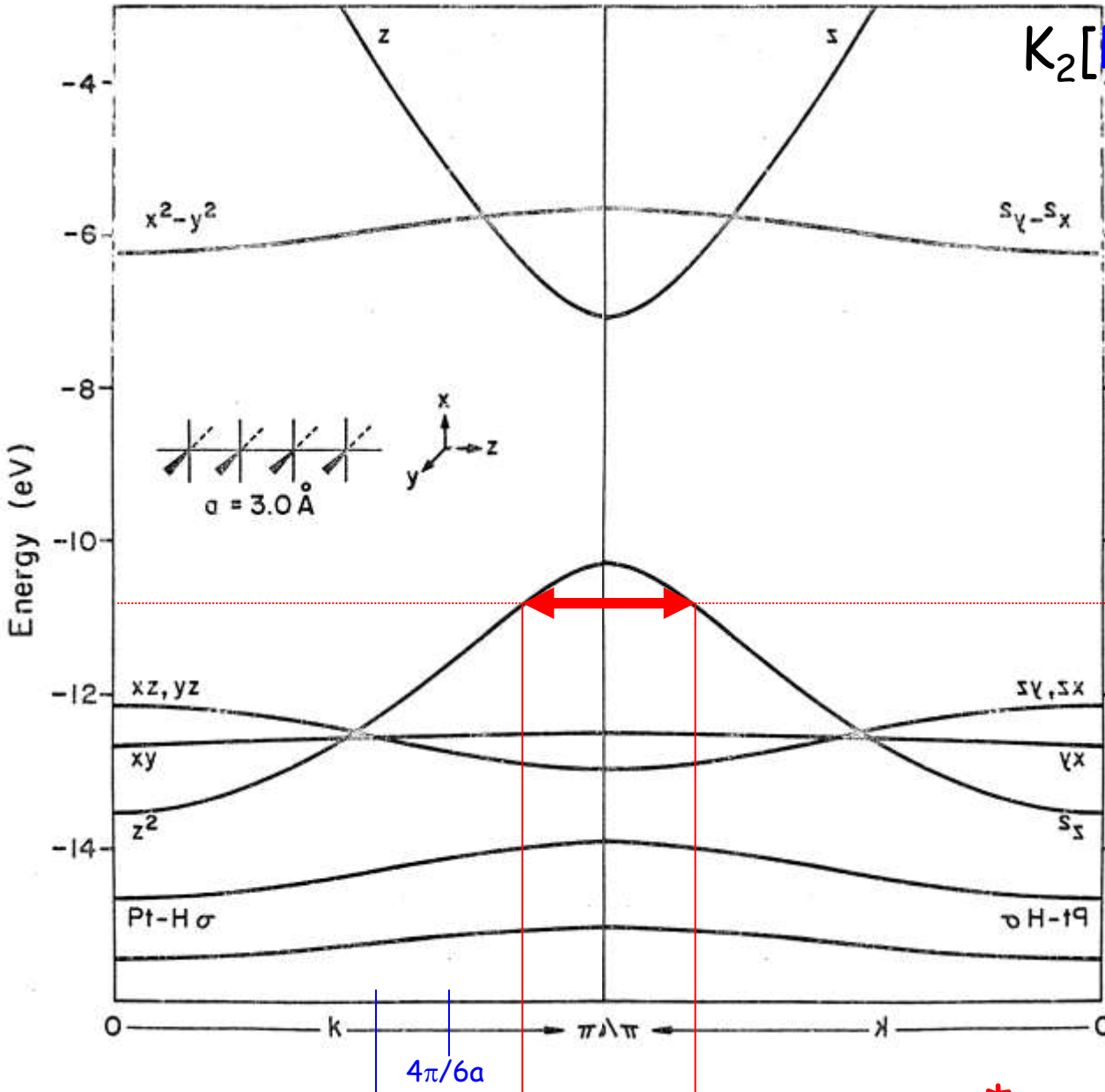
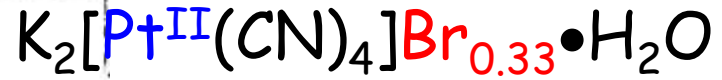
electron count

2 molecules $\text{Pt}(\text{CN})_4$ per unit cell

$$4 - \frac{2}{3} = \frac{10}{3}$$

$$\frac{\frac{2\pi}{a} \times \frac{10}{3}}{4} = 2 \times \frac{5\pi}{6a}$$

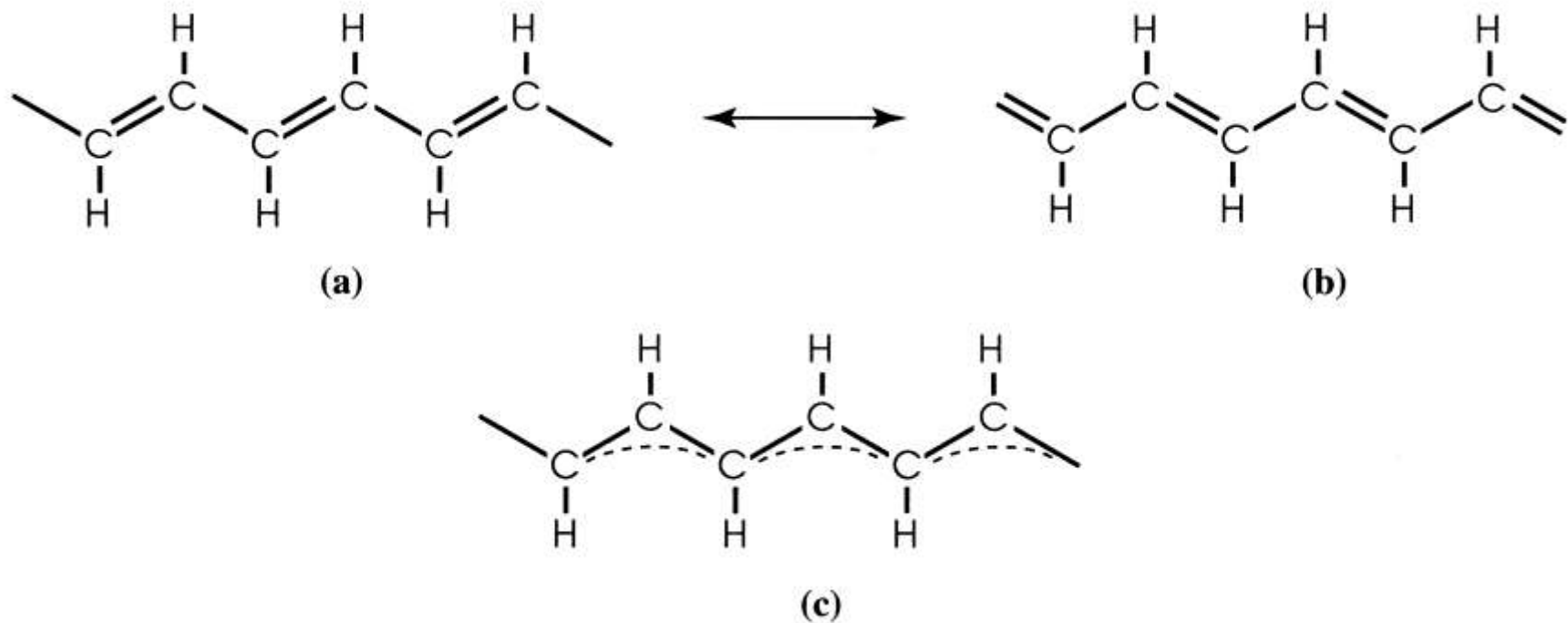


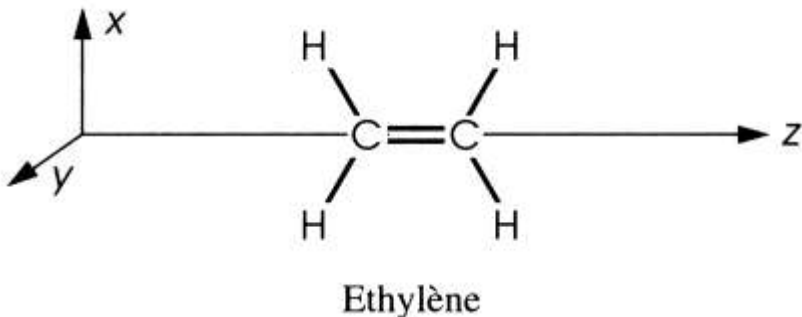


$$2 k_F = \frac{\pi}{3a} = \frac{a^*}{3}$$

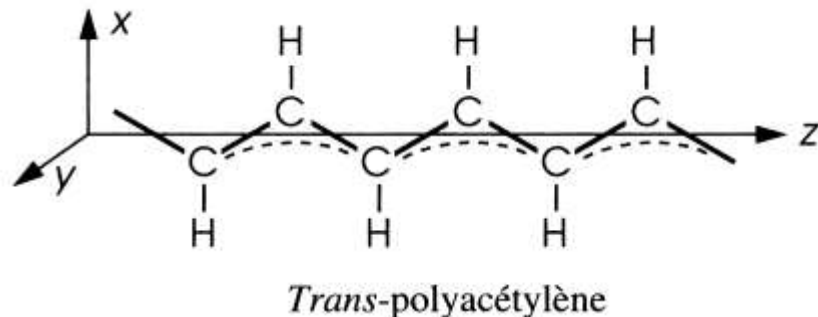
...in the momentum space

2.4 polyacetylene



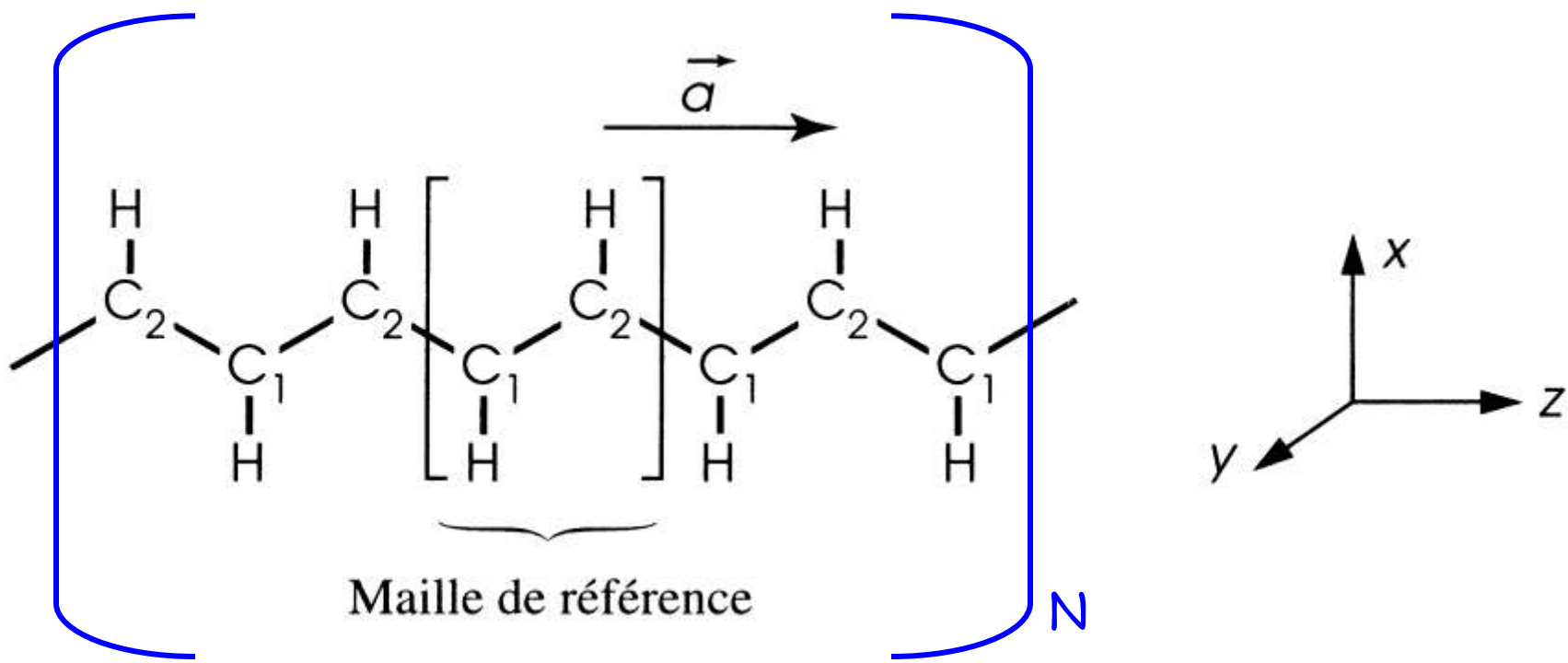


Ethylène



Trans-polyacétylène

Figure 5.3 Système d'axes permettant de décrire l'éthylène et le polyacétylène se trouvant dans le plan xOz .



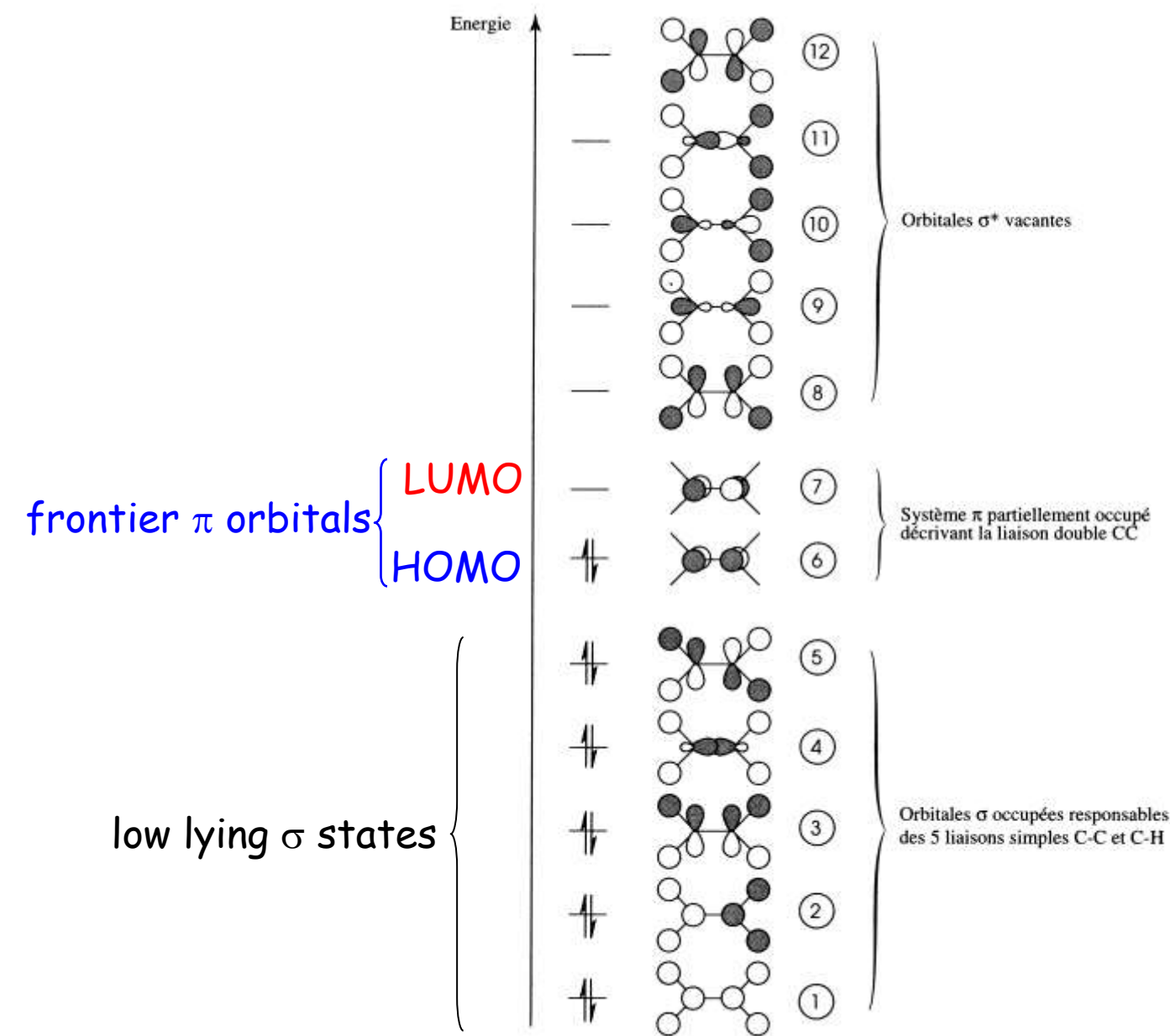


Figure 5.4 Diagramme énergétique des orbitales moléculaires de l'éthylène. Le lecteur désirant avoir plus d'informations à son sujet pourra consulter les références [1] et [2].

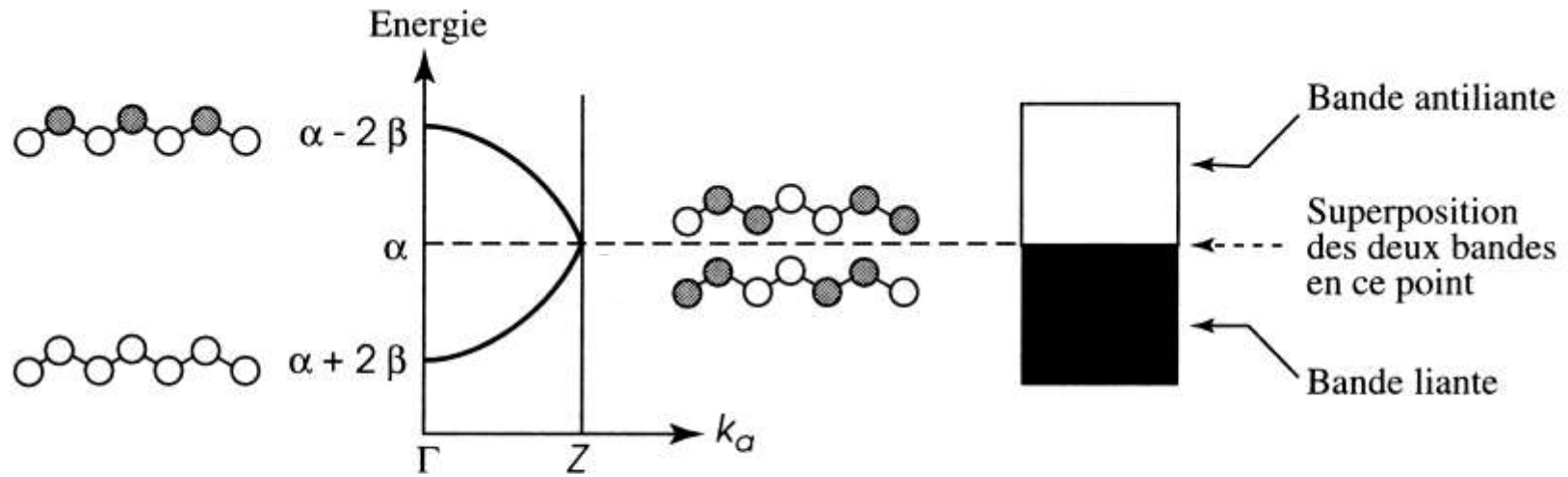
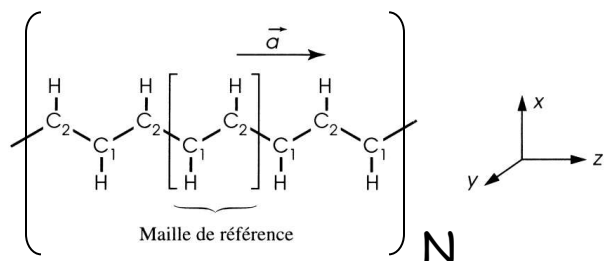
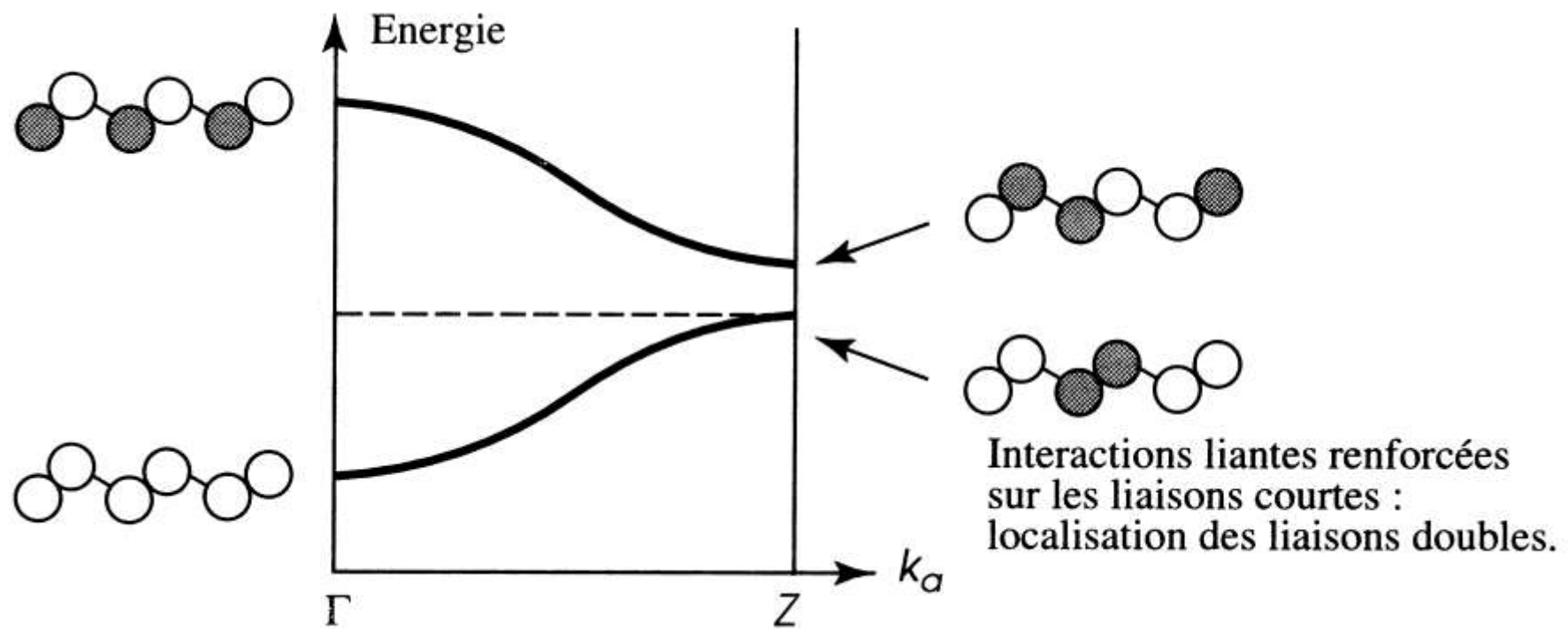
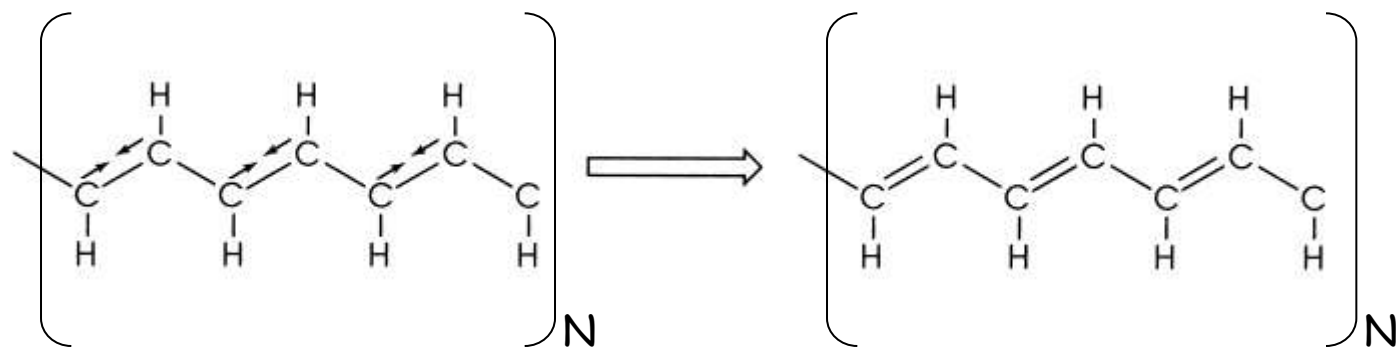
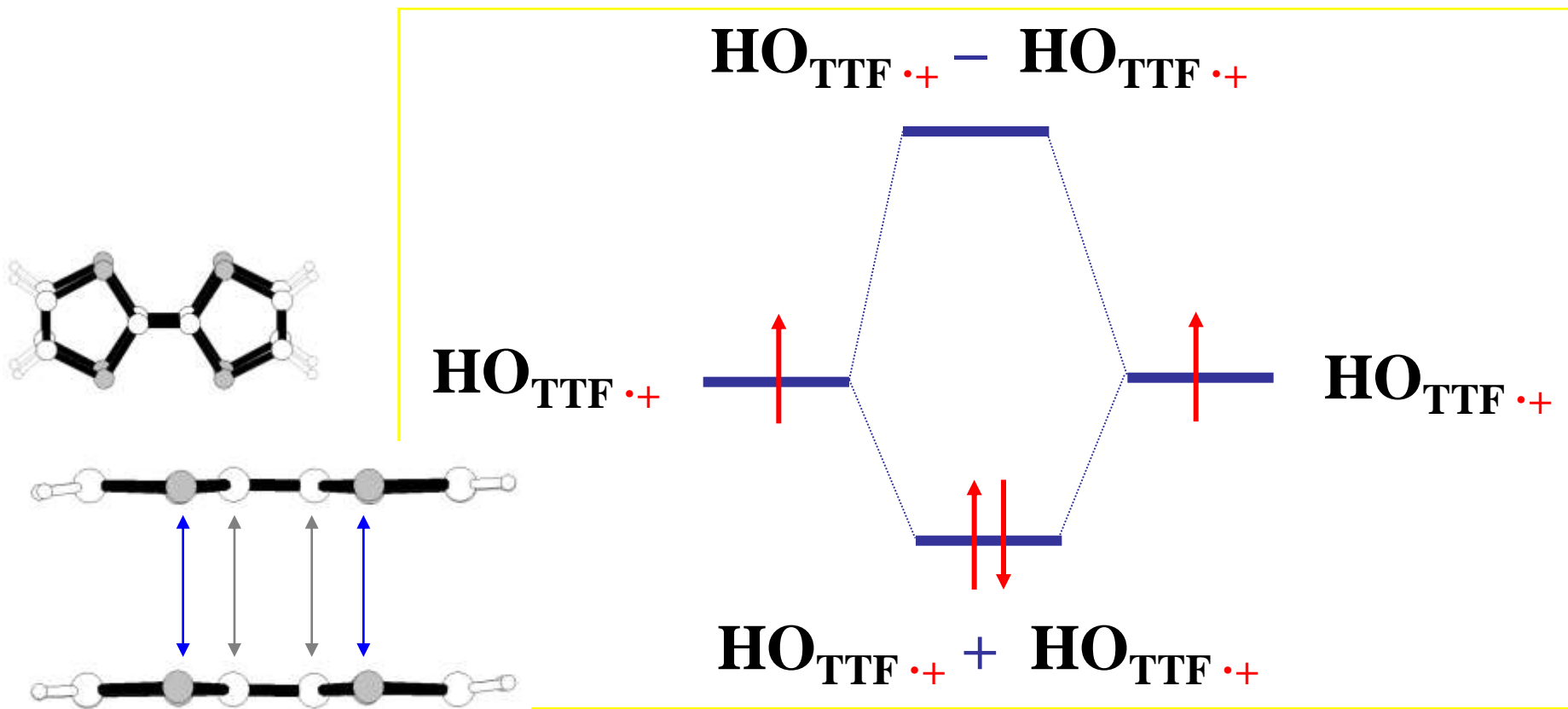


Figure 5.7 Diagramme de bandes à proximité du niveau de Fermi du *trans*-polyacétylène régulier.

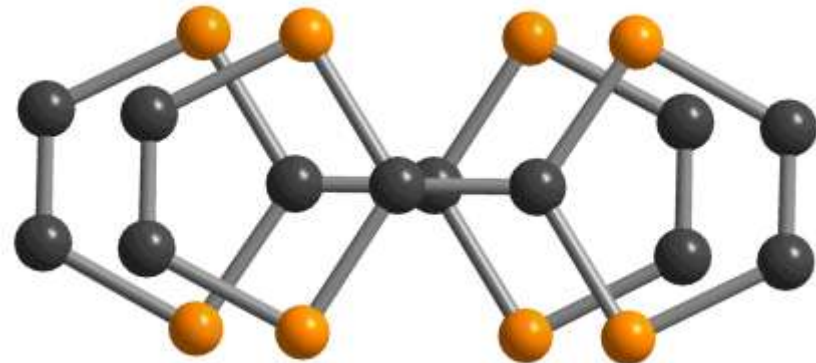


discrete, fully ionic dimers in
[(TTF^{•+})₂][(I₃⁻)₂]



strong bonding: σ type p_π - p_π overlap
eclipsed and diamagnetic

discrete, mixed valence dimer in
 $(\text{TTF})_2^{\cdot+}[\text{Re}_6\text{S}_5\text{Cl}_9^-]$



$\text{HO}_{\text{TTF}}^{\cdot+}$



$\text{HO}_{\text{TTF}}^{\cdot+} - \text{HO}_{\text{TTF}}^{\cdot+}$

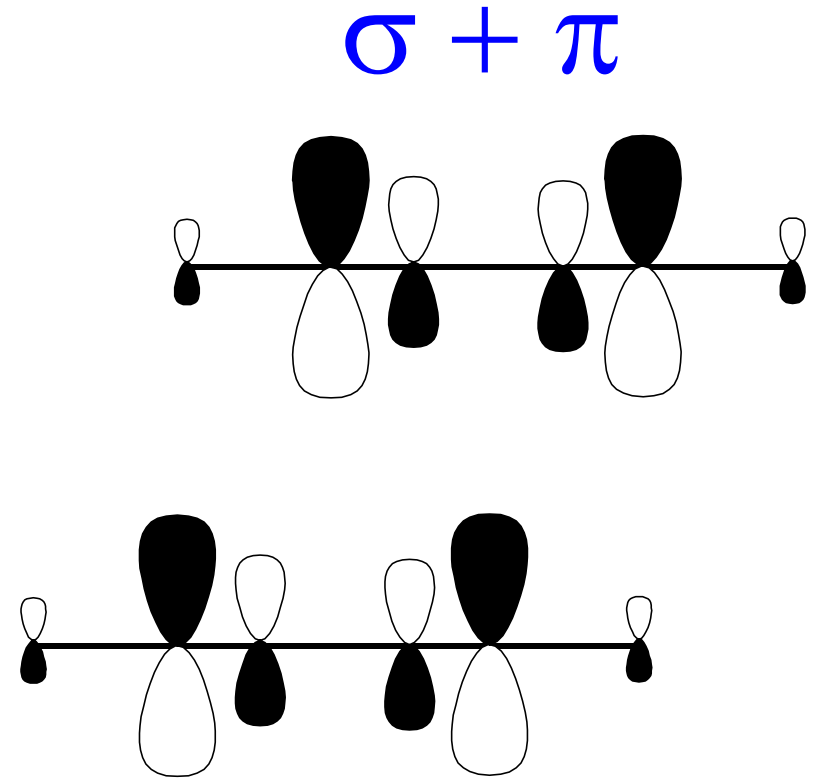
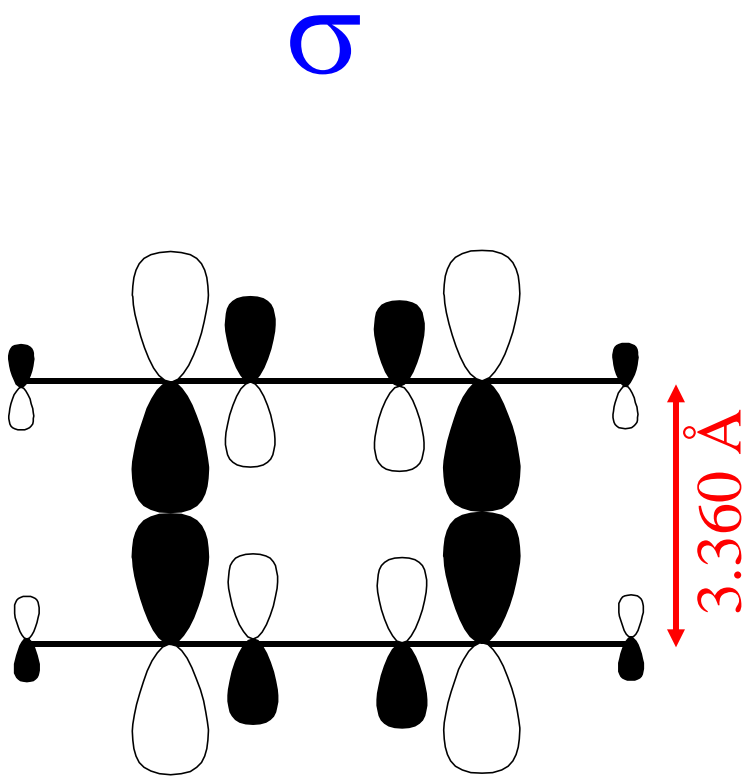


$\text{HO}_{\text{TTF}}^{\cdot+}$

$\text{HO}_{\text{TTF}}^{\cdot+} + \text{HO}_{\text{TTF}}^{\cdot+}$

milder bonding: π type $p_{\pi} - p_{\pi}$ overlap
slipped and paramagnetic

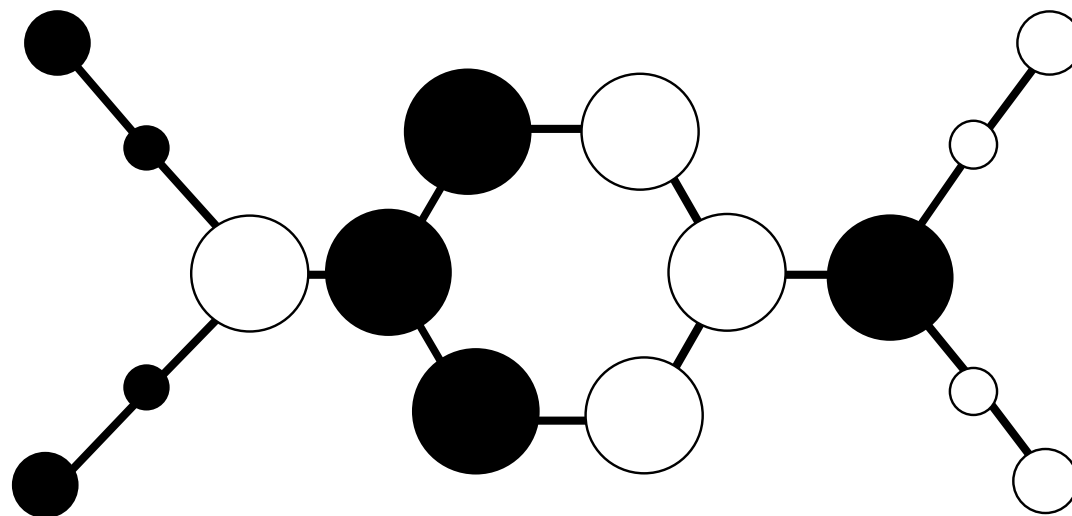
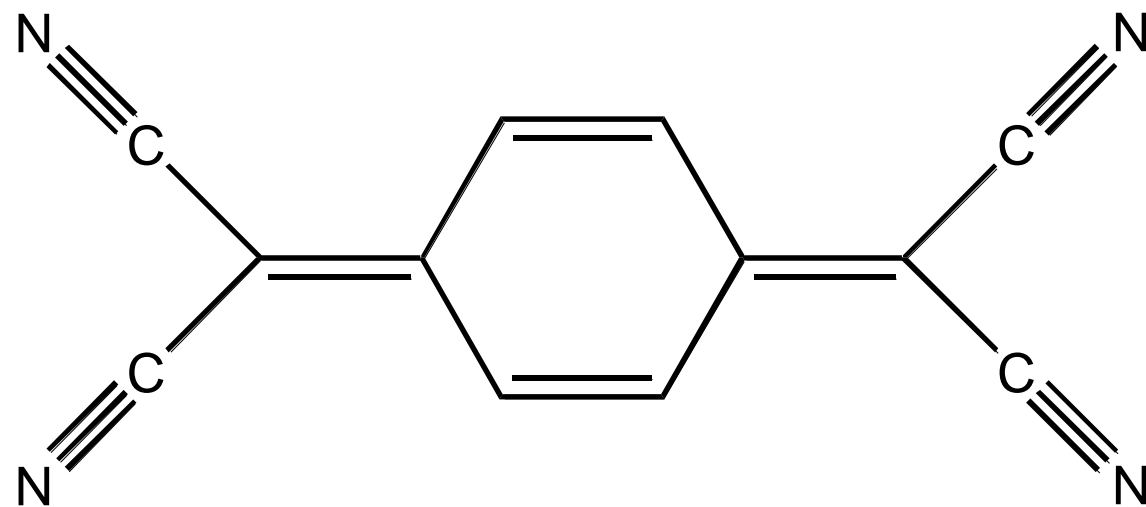
vdW \leftrightarrow $\pi-\pi$ \leftrightarrow recouvrements $p_\pi - p_\pi$ (ρ)



OUTLINE

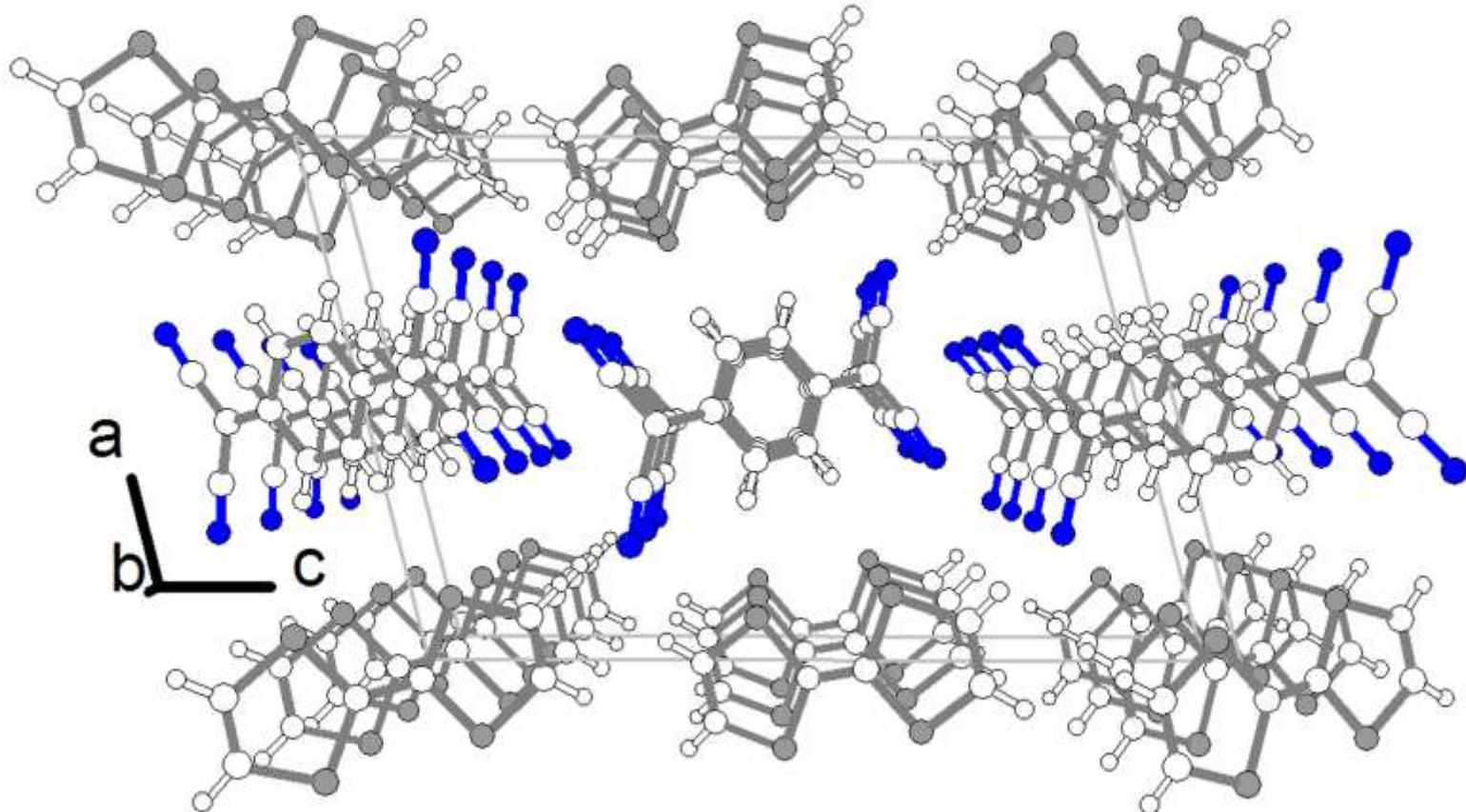
1. electrocrystallization
2. redox chemistry
3. intermolecular interactions, and their redox activation, direct the structure
4. orbitals and band (in one dimension)
5. decipher BS of TTF-TCNQ, Bechgaard salts

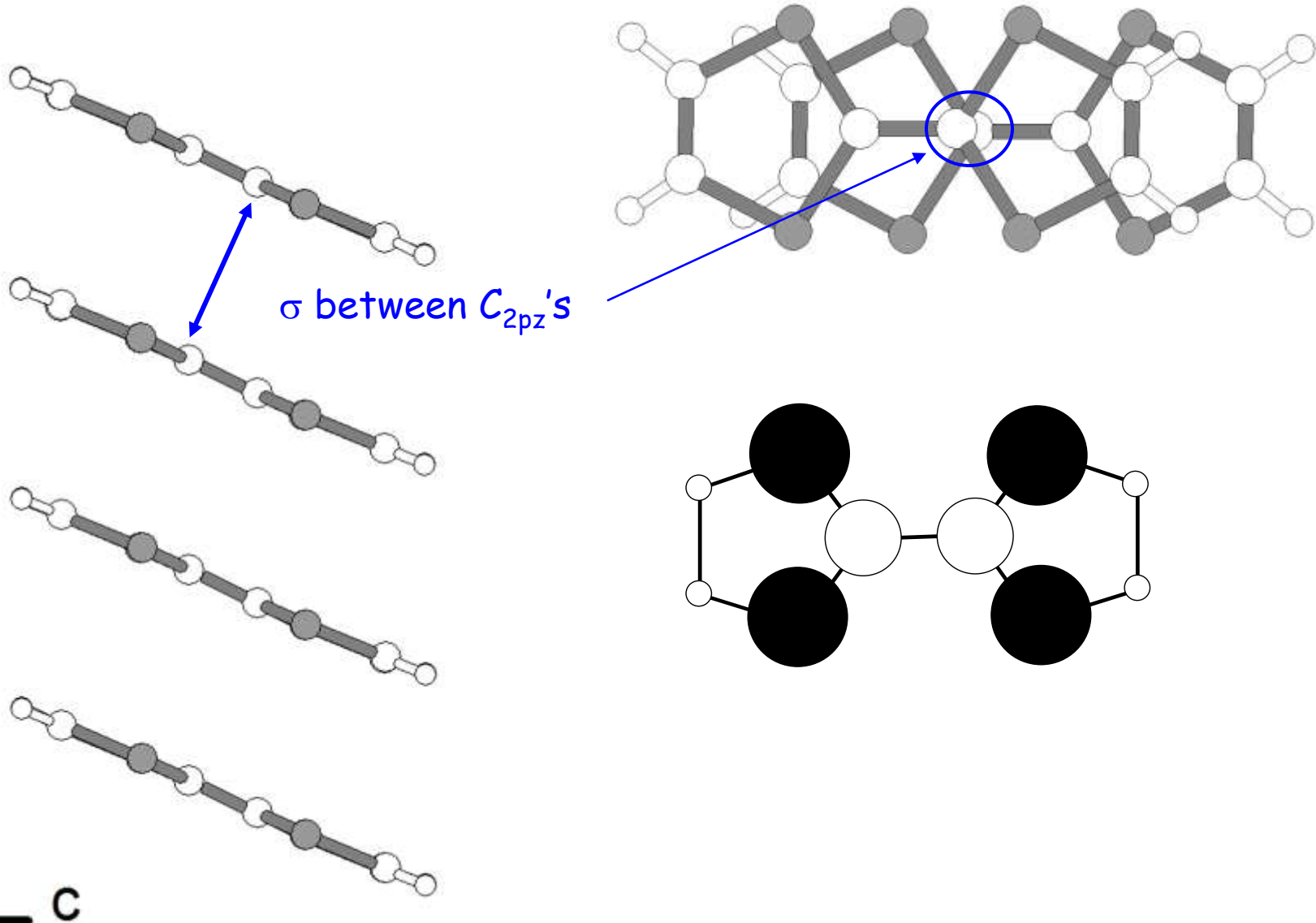
TCNQ

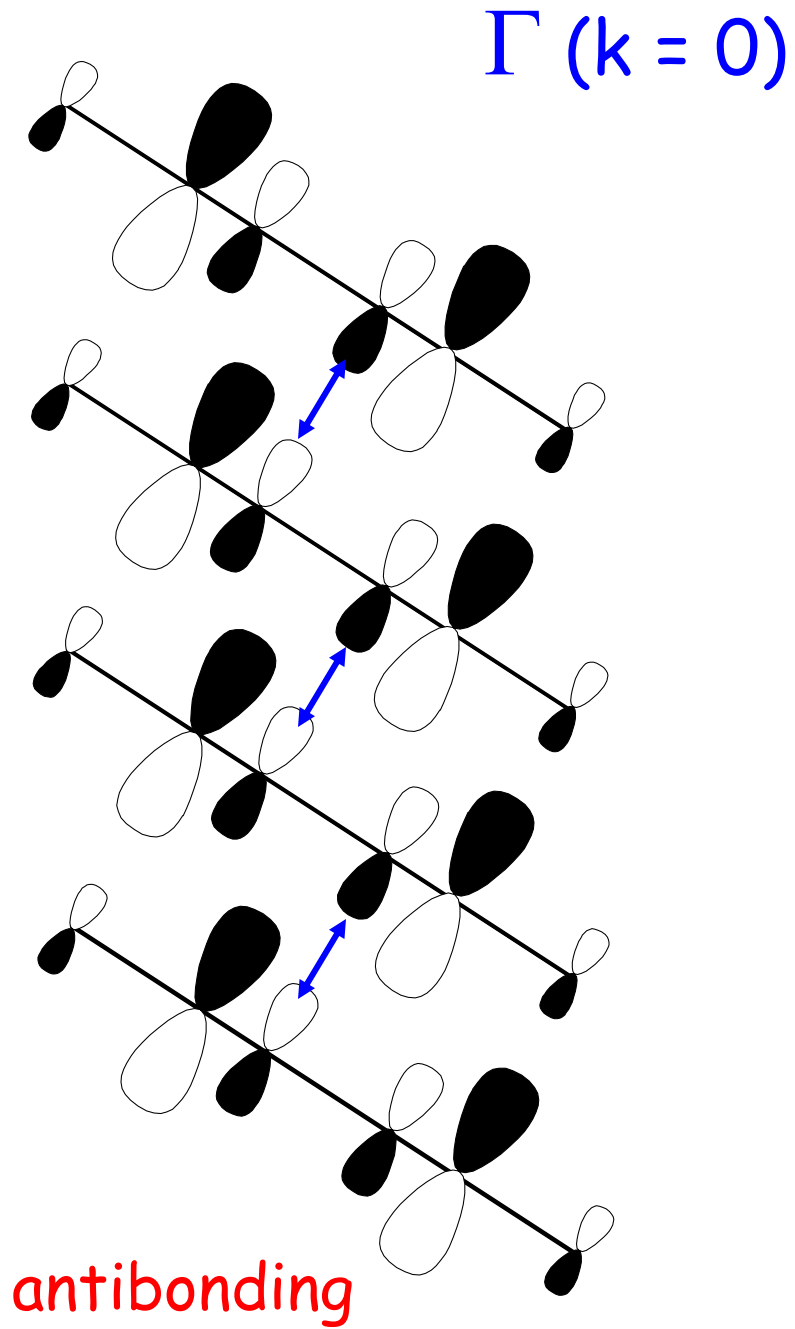
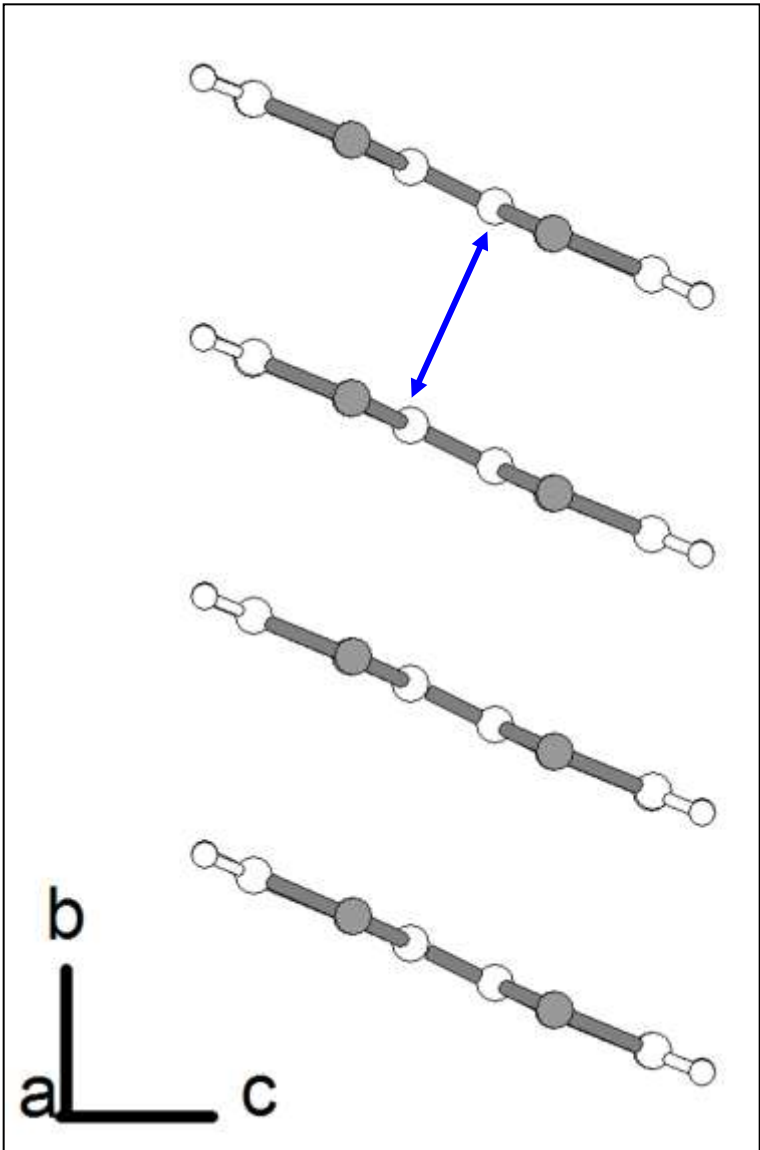


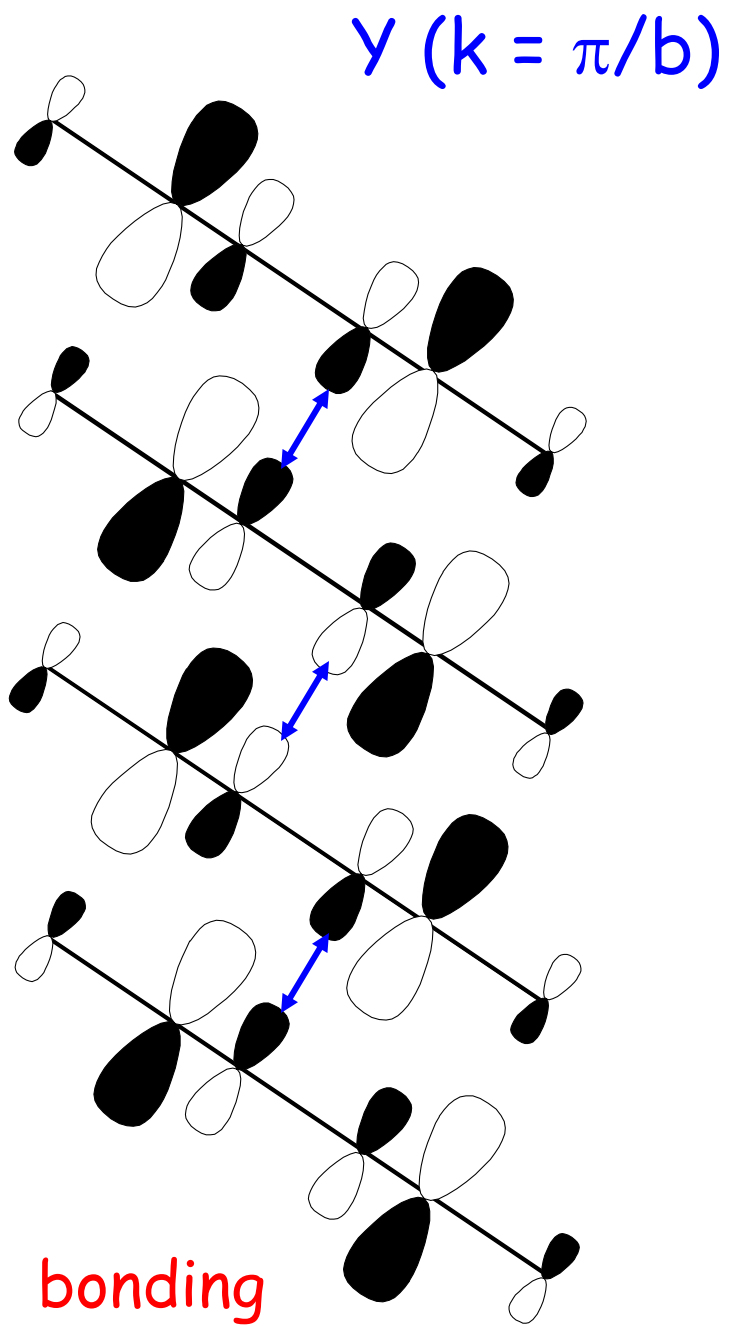
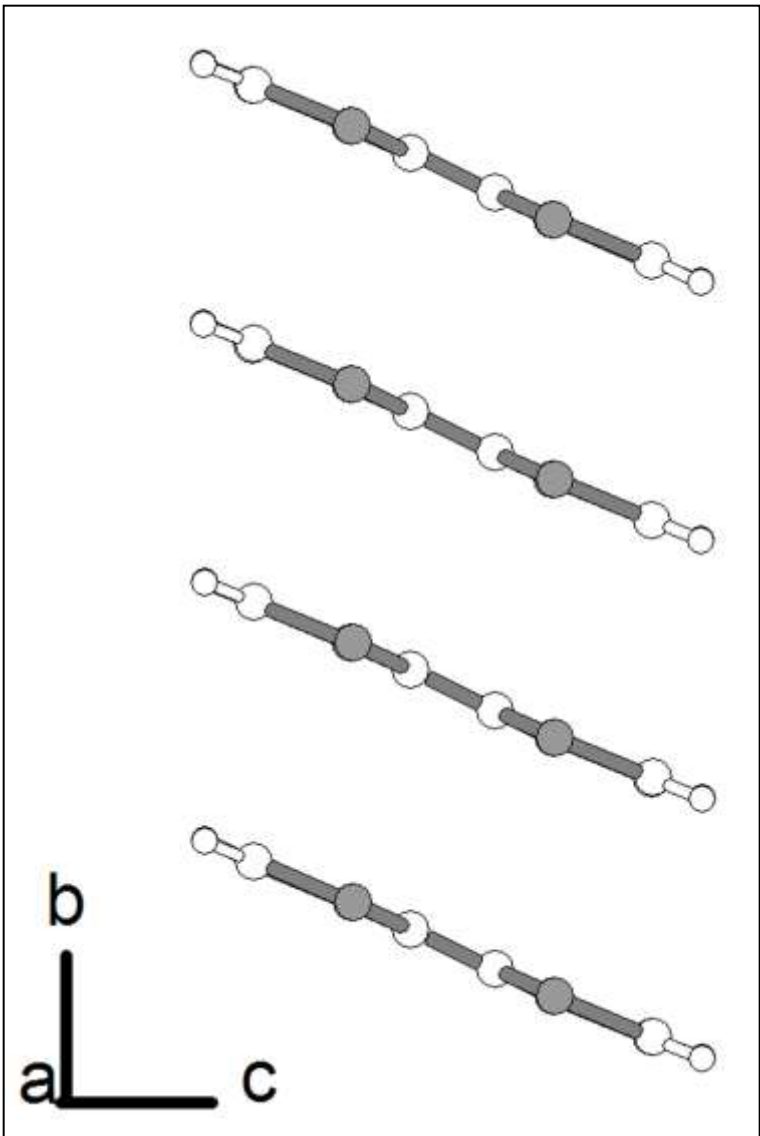
LUMO

TTF-TCNQ

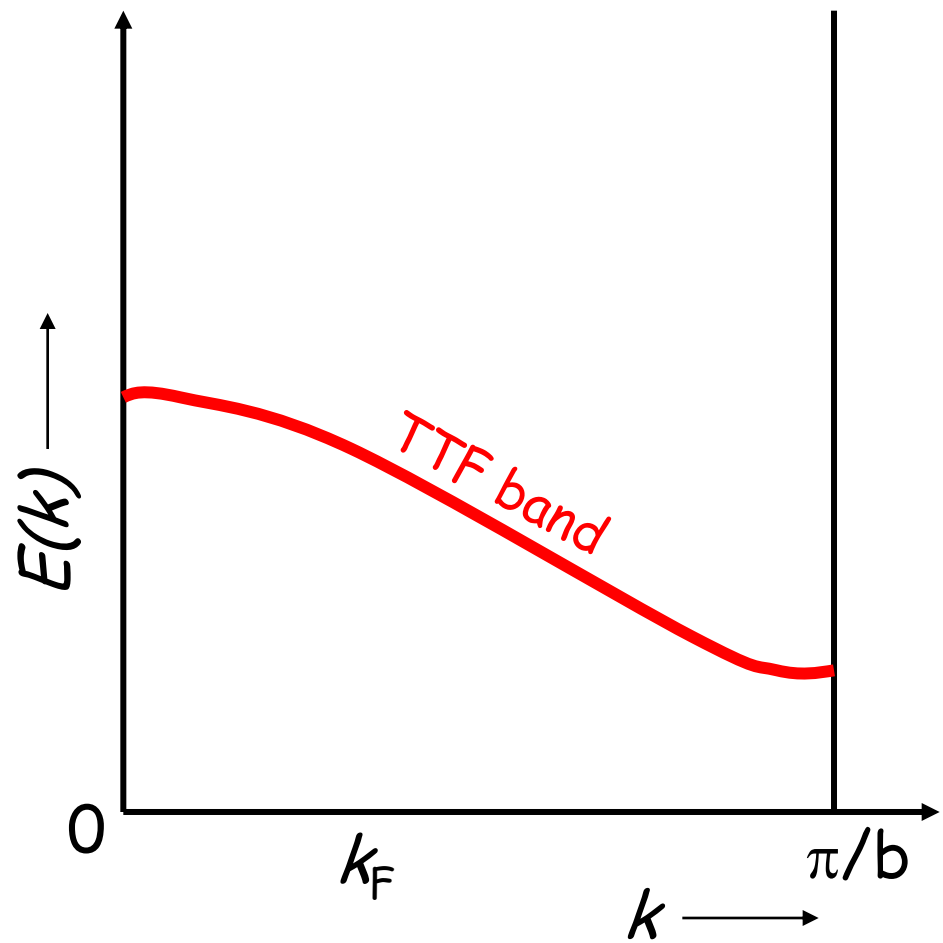
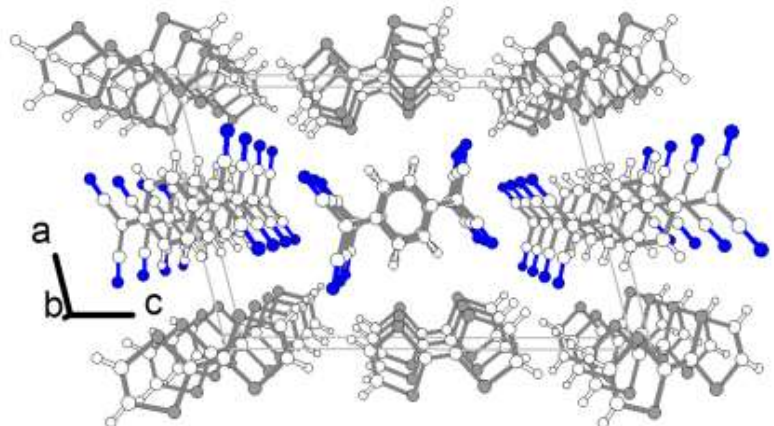


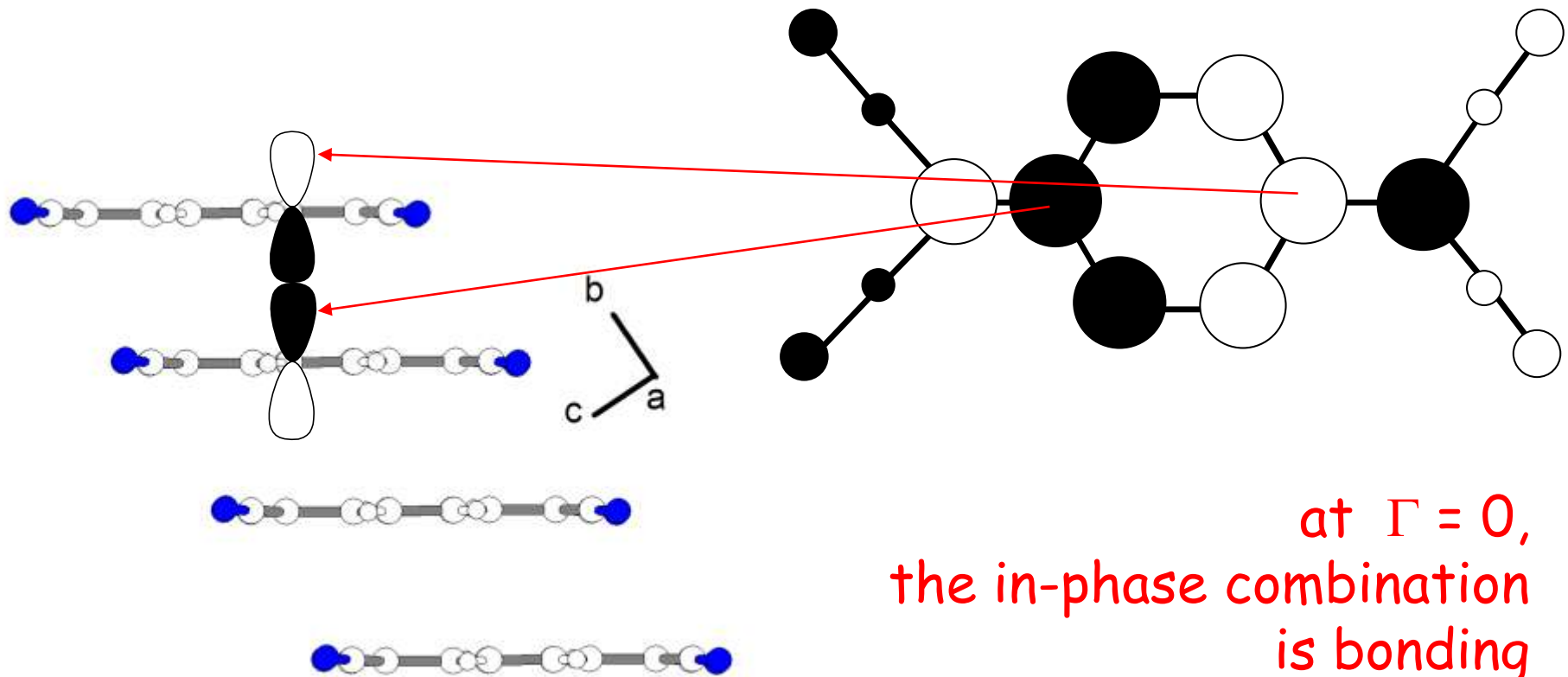
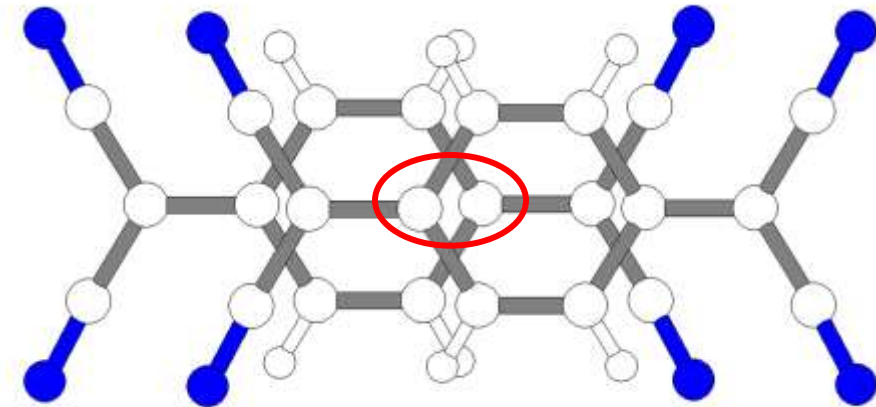






TTF-TCNQ

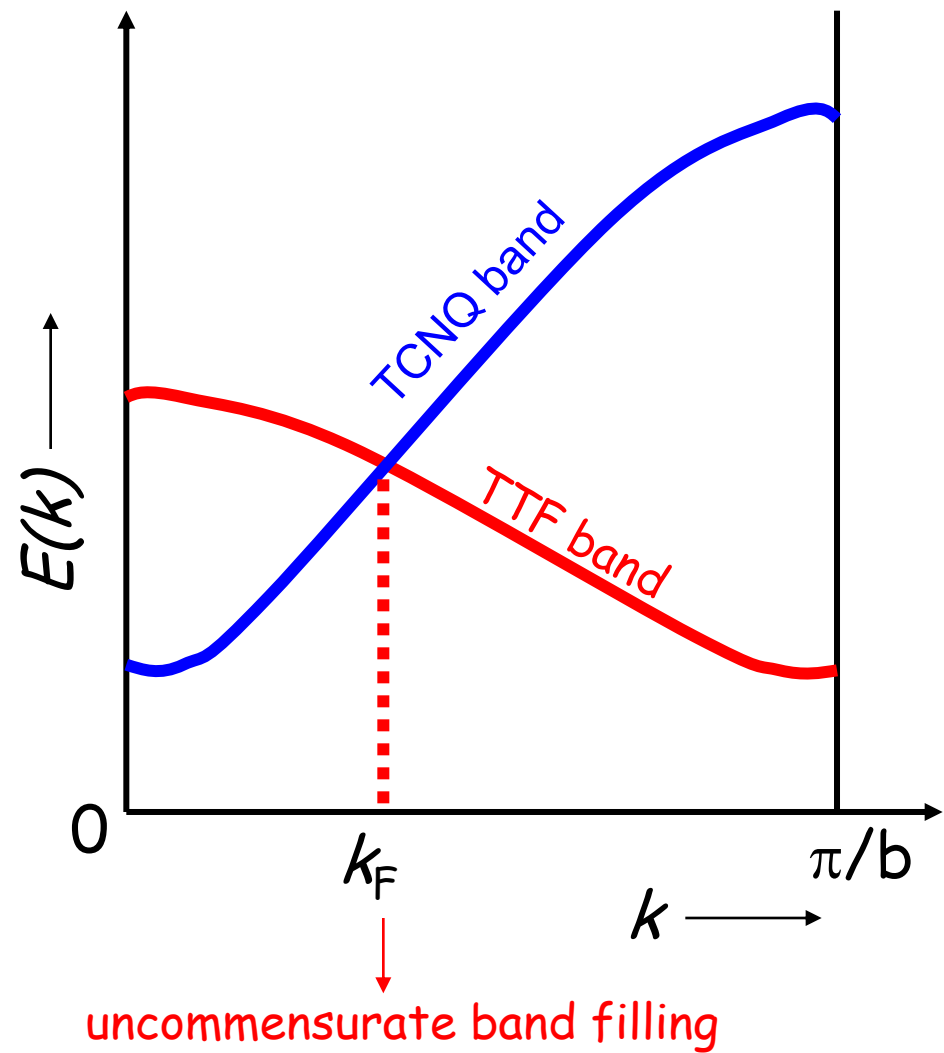
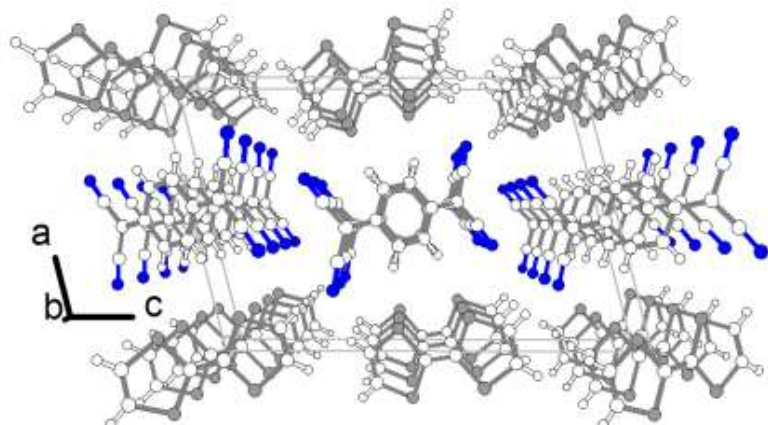


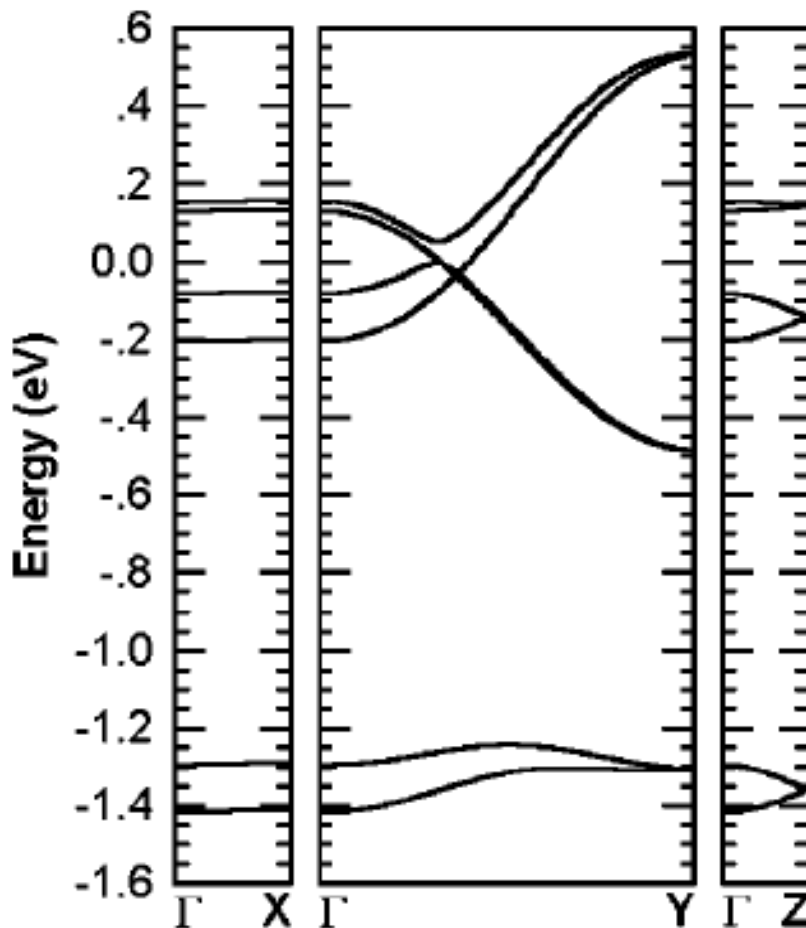


at $\Gamma = 0$,
the in-phase combination
is bonding

TTF-TCNQ

$\rho = 0.59$





recent first principles
BS calculation by
Pablo Ordejón and Enric Canadell
Barcelona

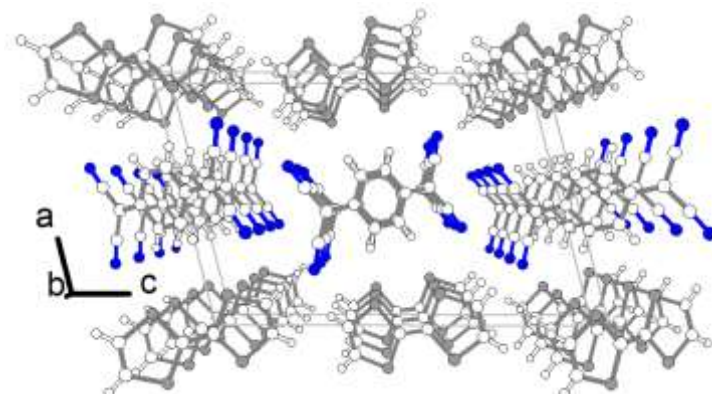
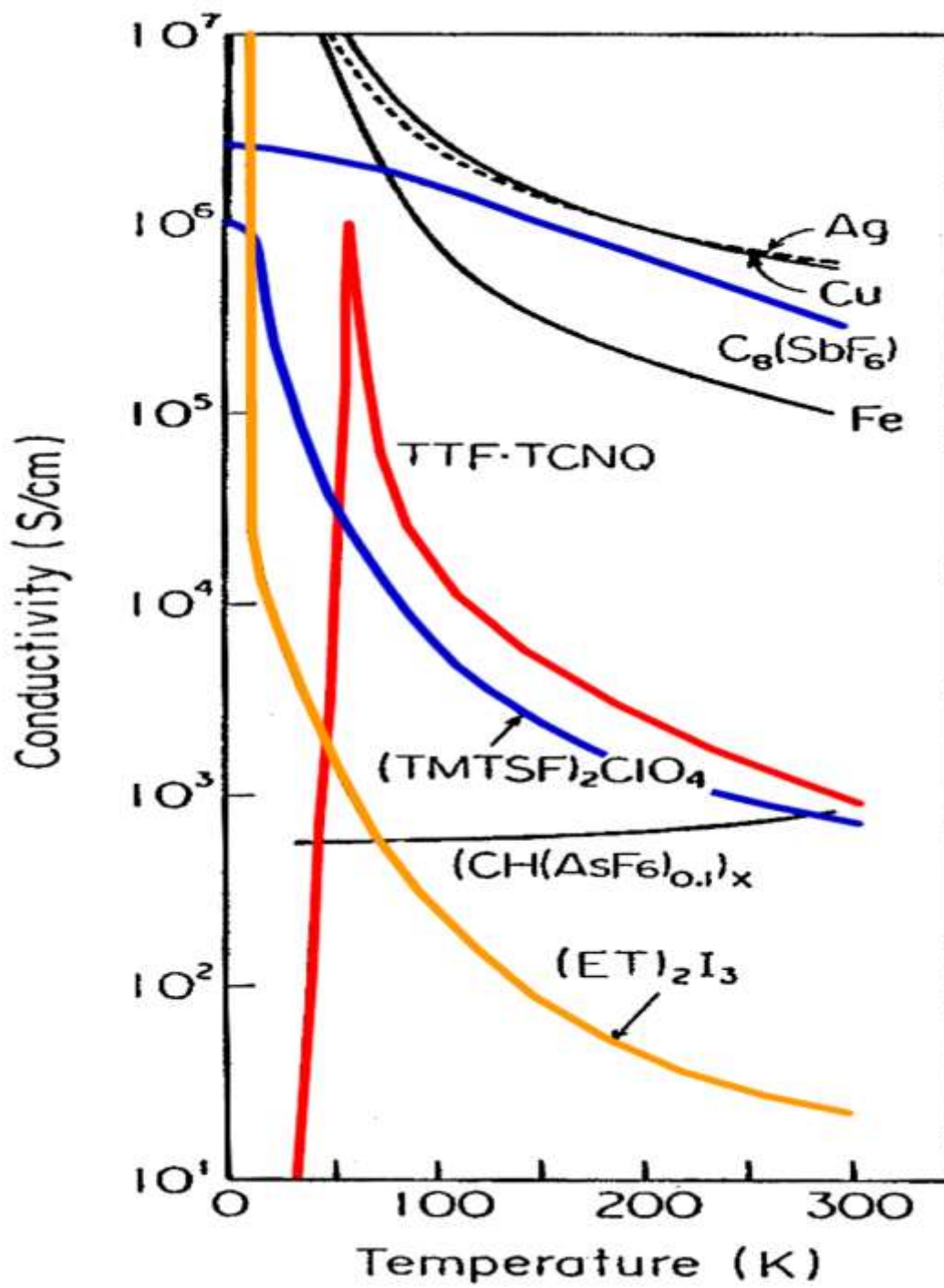
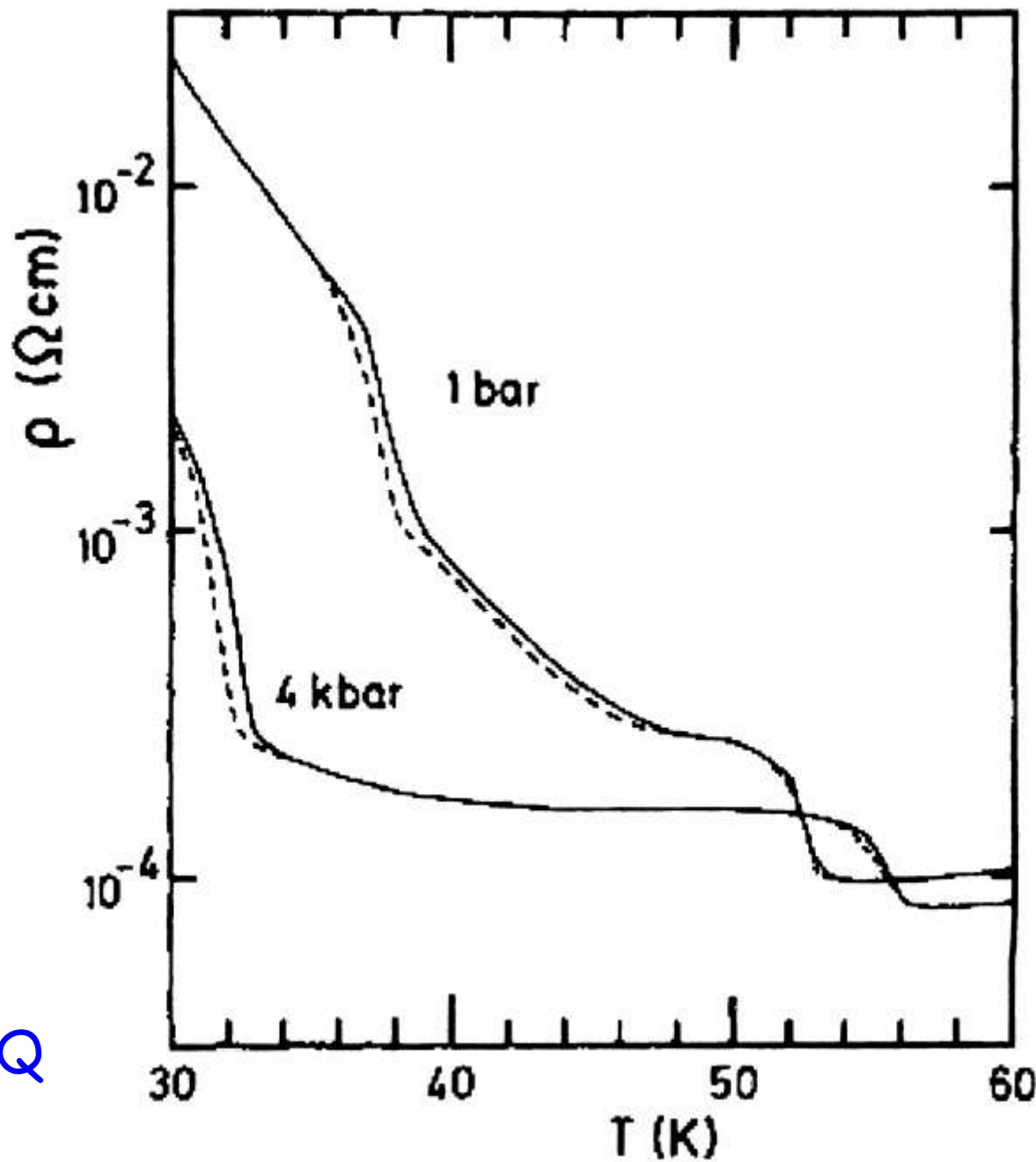


FIG. 2. Band structure near the Fermi level for the room temperature and ambient pressure structure of TTF-TCNQ. $\Gamma = (0,0,0)$, $X = (1/2,0,0)$, $Y = (0,1/2,0)$, and $Z = (0,0,1/2)$ in units of the monoclinic reciprocal lattice vectors. Energy is given relative to the Fermi level.



TTF-TCNQ

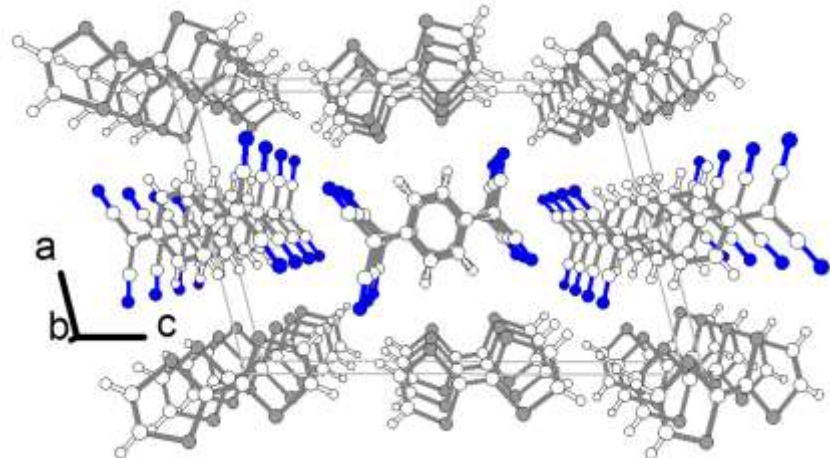


TMTSF-DMTCNQ

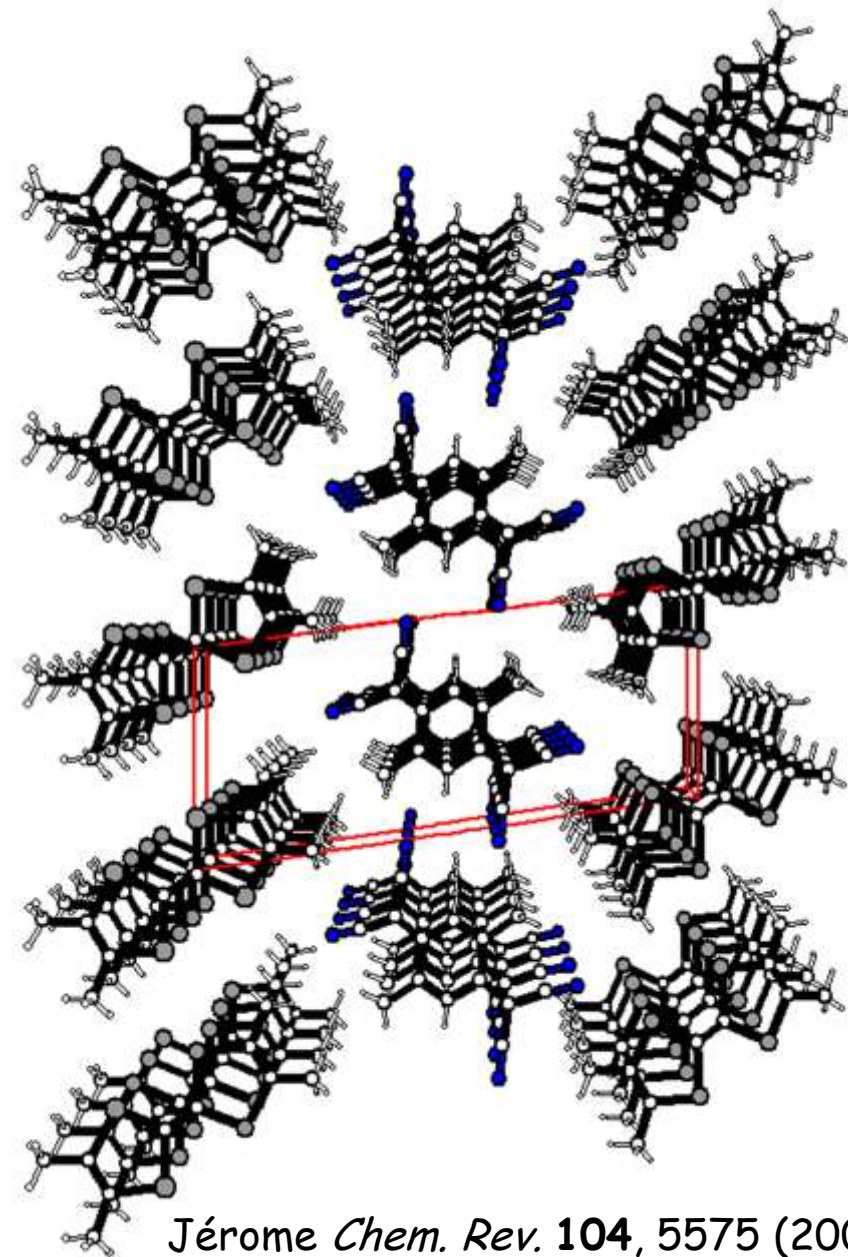
$\rho = 0.5$

!! Peierls transition suppressed at 9 kbars

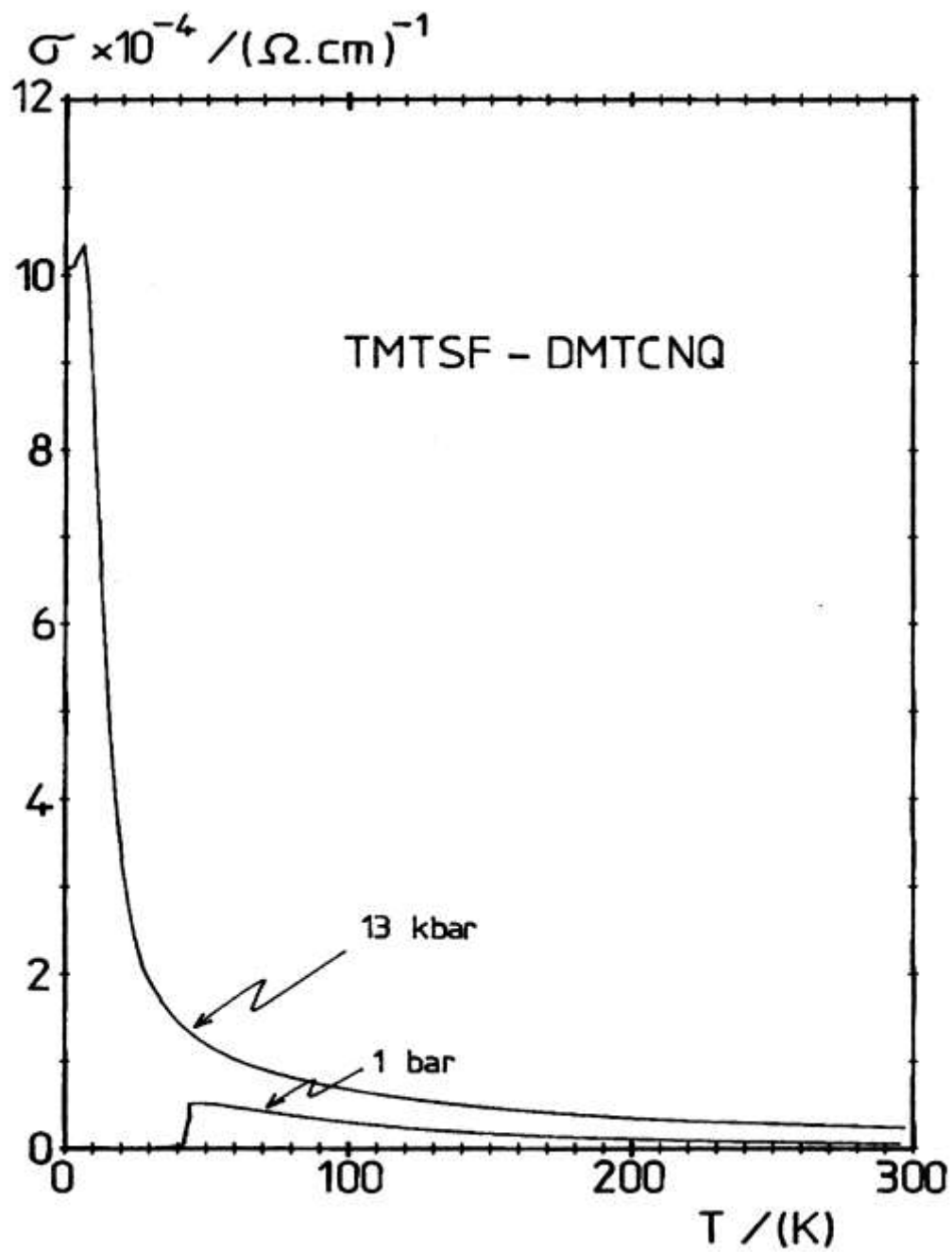
!! Metallic down to liquid helium temperatures under 10 kbars



instead of 0.59 in TTF-TCNQ



Jérôme *Chem. Rev.* 104, 5575 (2004)



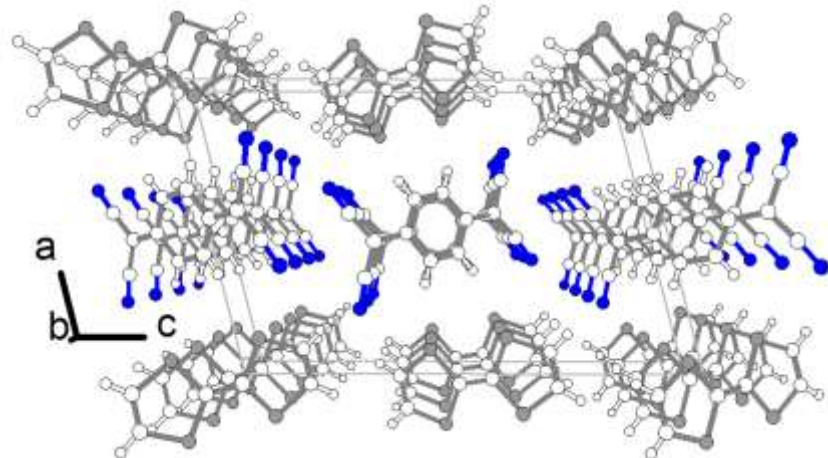
Jérôme
Chem. Rev. 2004, 104
p. 5575

TMTSF-DMTCNQ

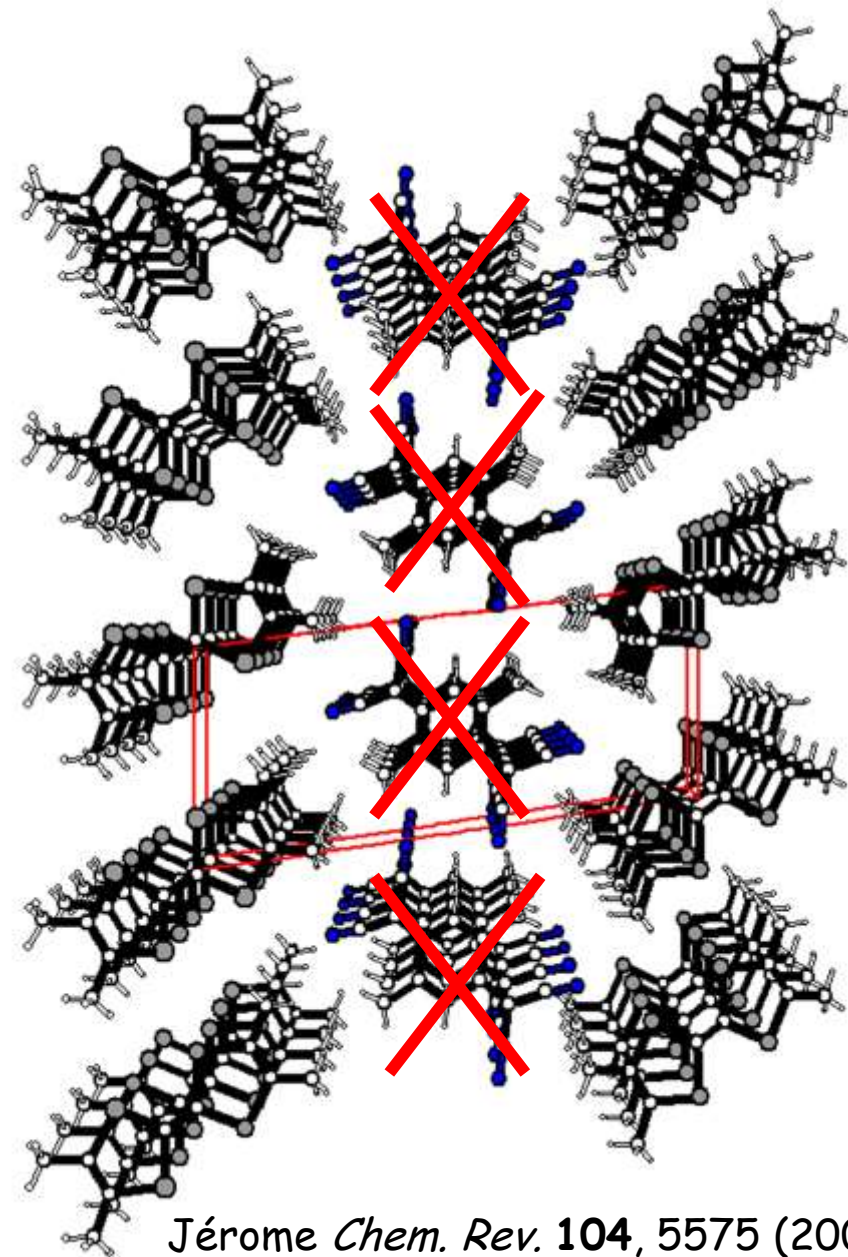
$\rho = 0.5$

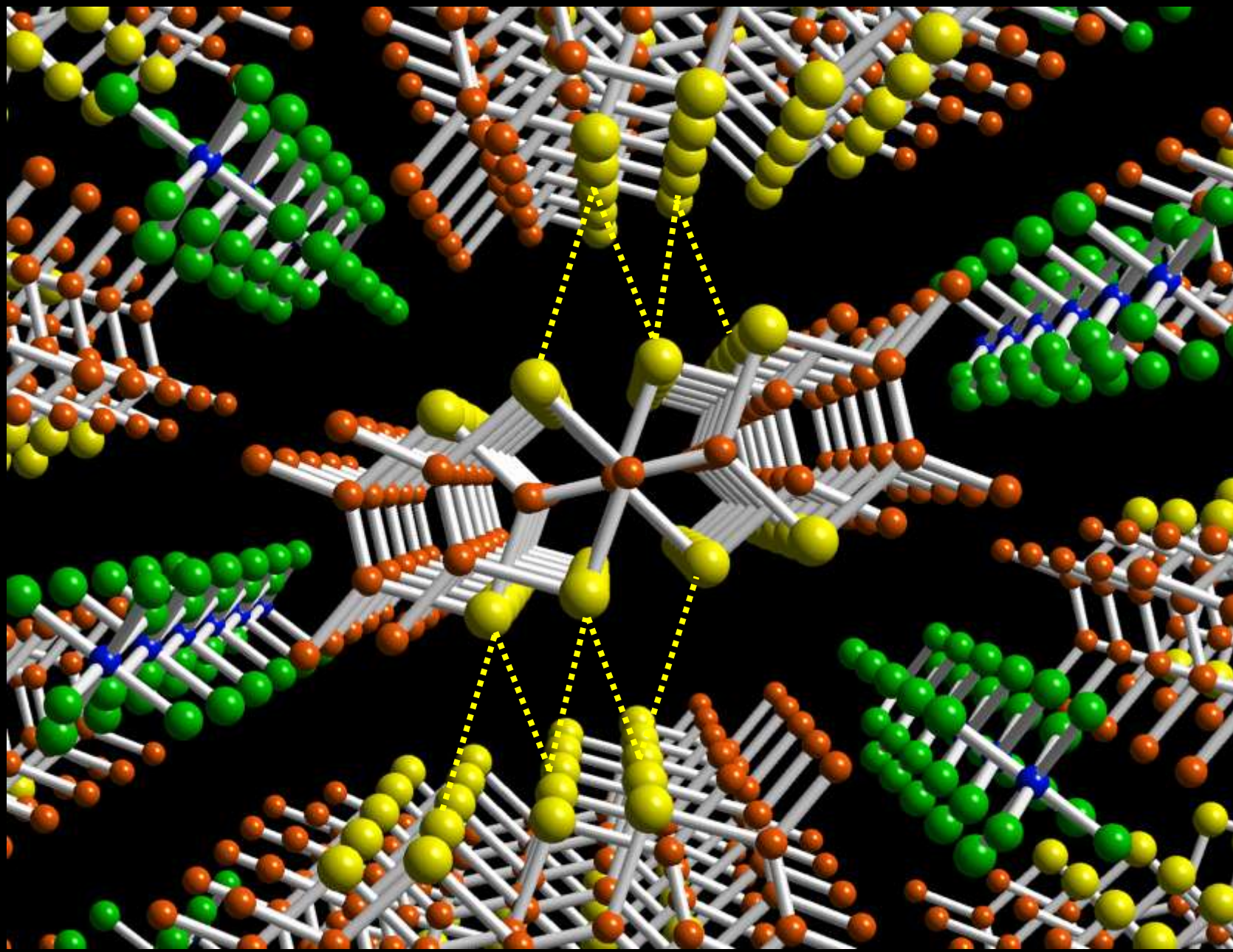
!! Peierls transition suppressed at 9 kbars

!! Metallic down to liquid helium temperatures under 10 kbars

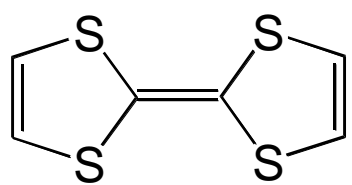
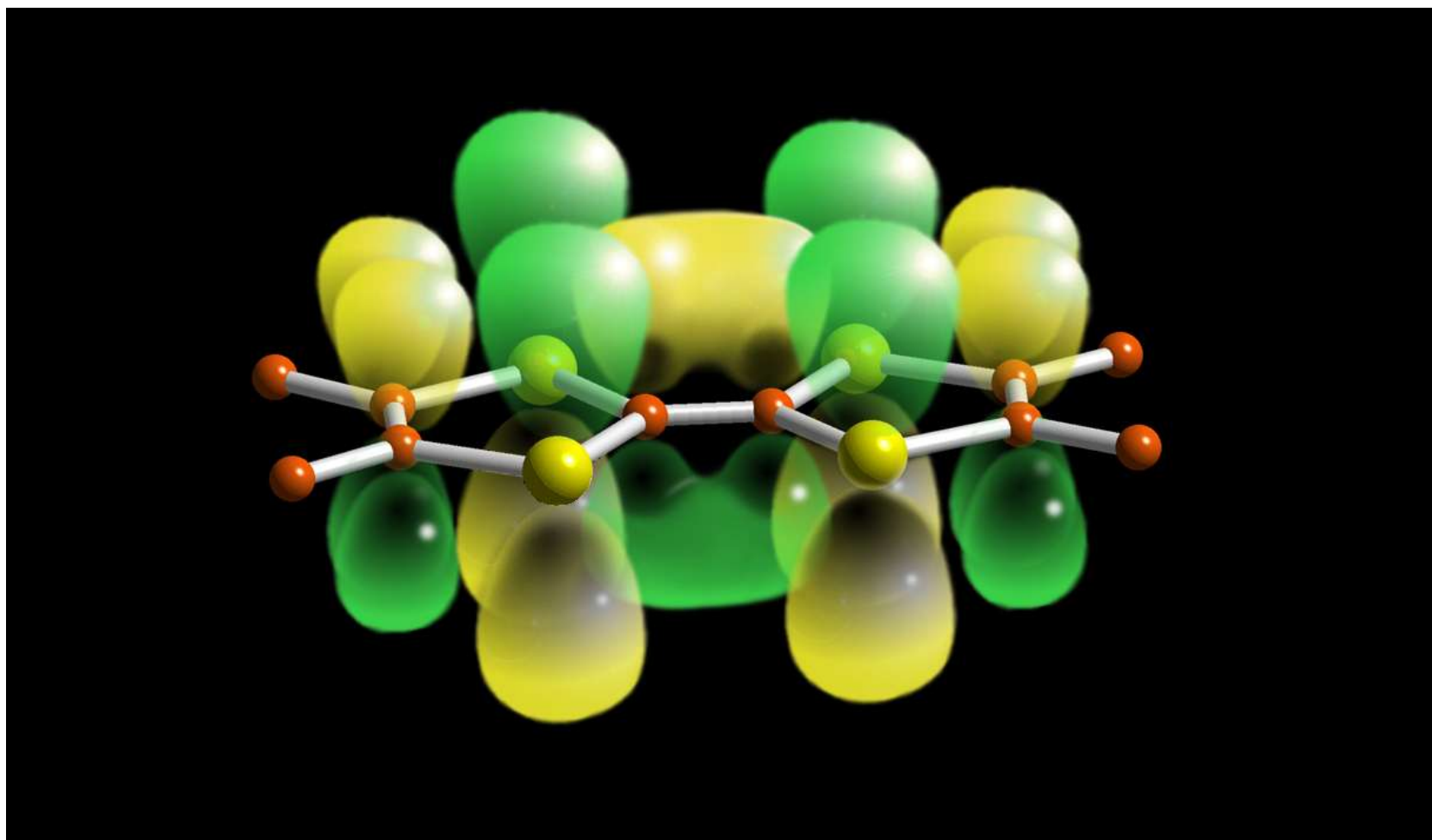


instead of 0.59 in TTF-TCNQ

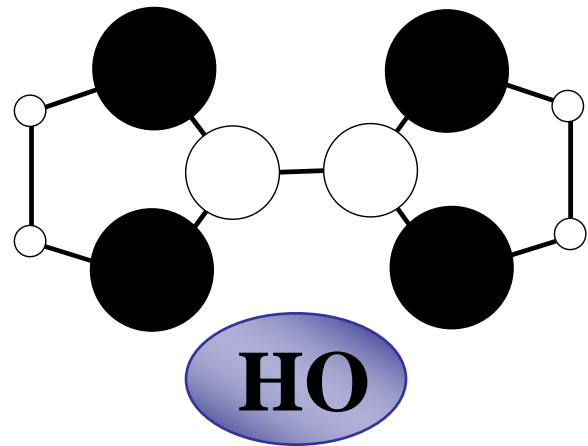




a typical molecular metal: $(\text{TMTSF})_2^{\bullet+}\text{PF}_6^-$

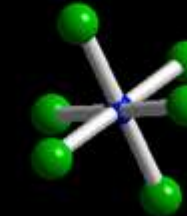
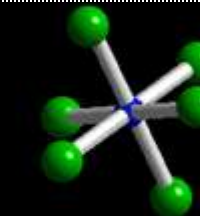
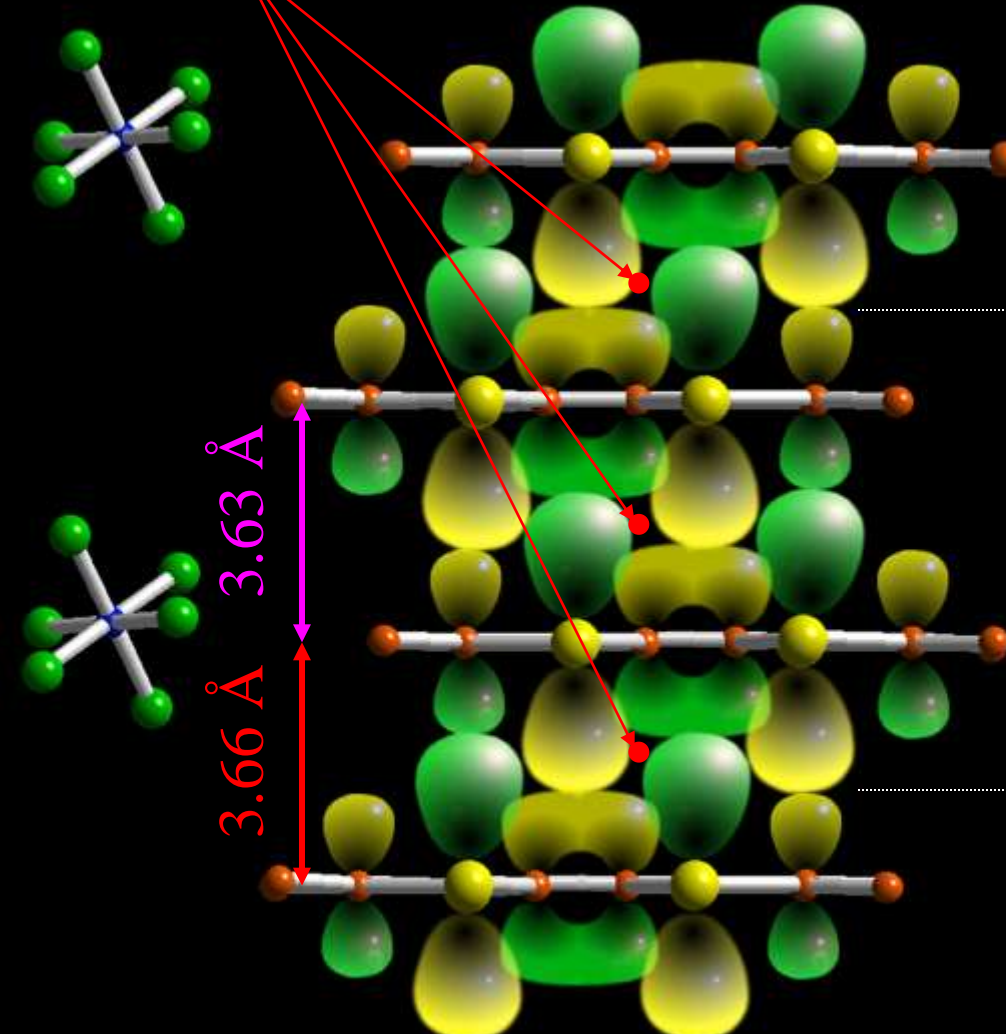


TTF



TMTTF
TMTSF

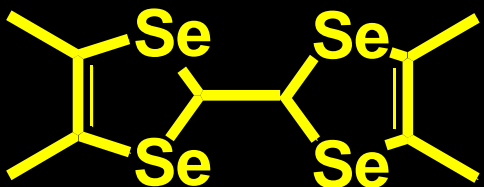
the molecule is symmetric



2 to 1

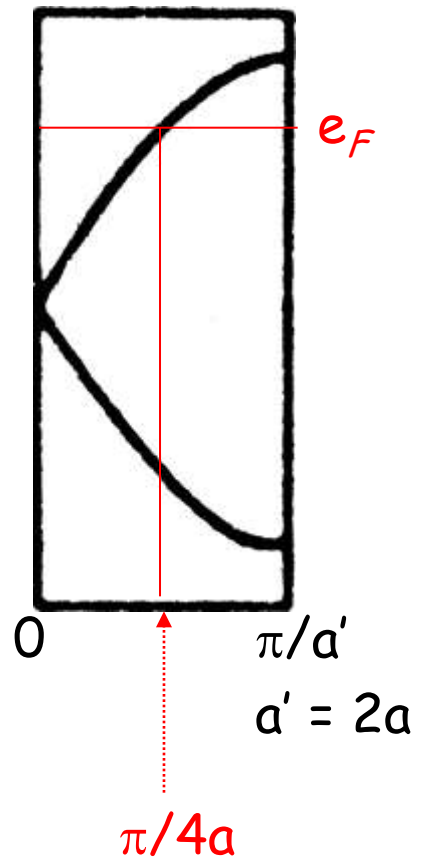
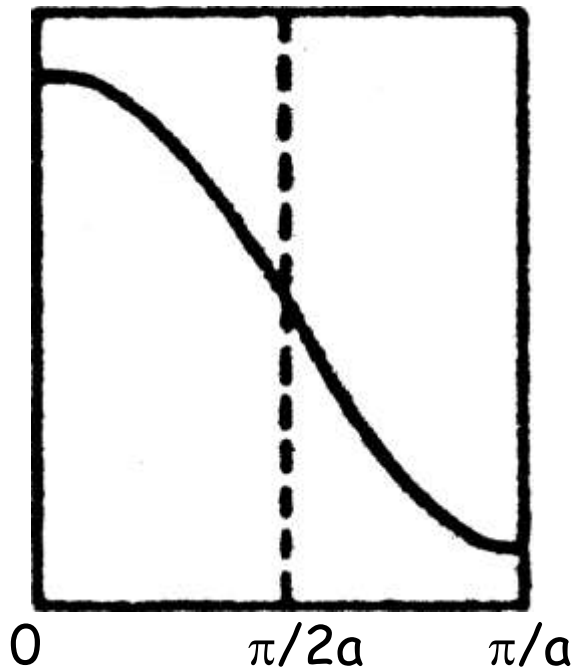
2 molecules per unit in chain along a

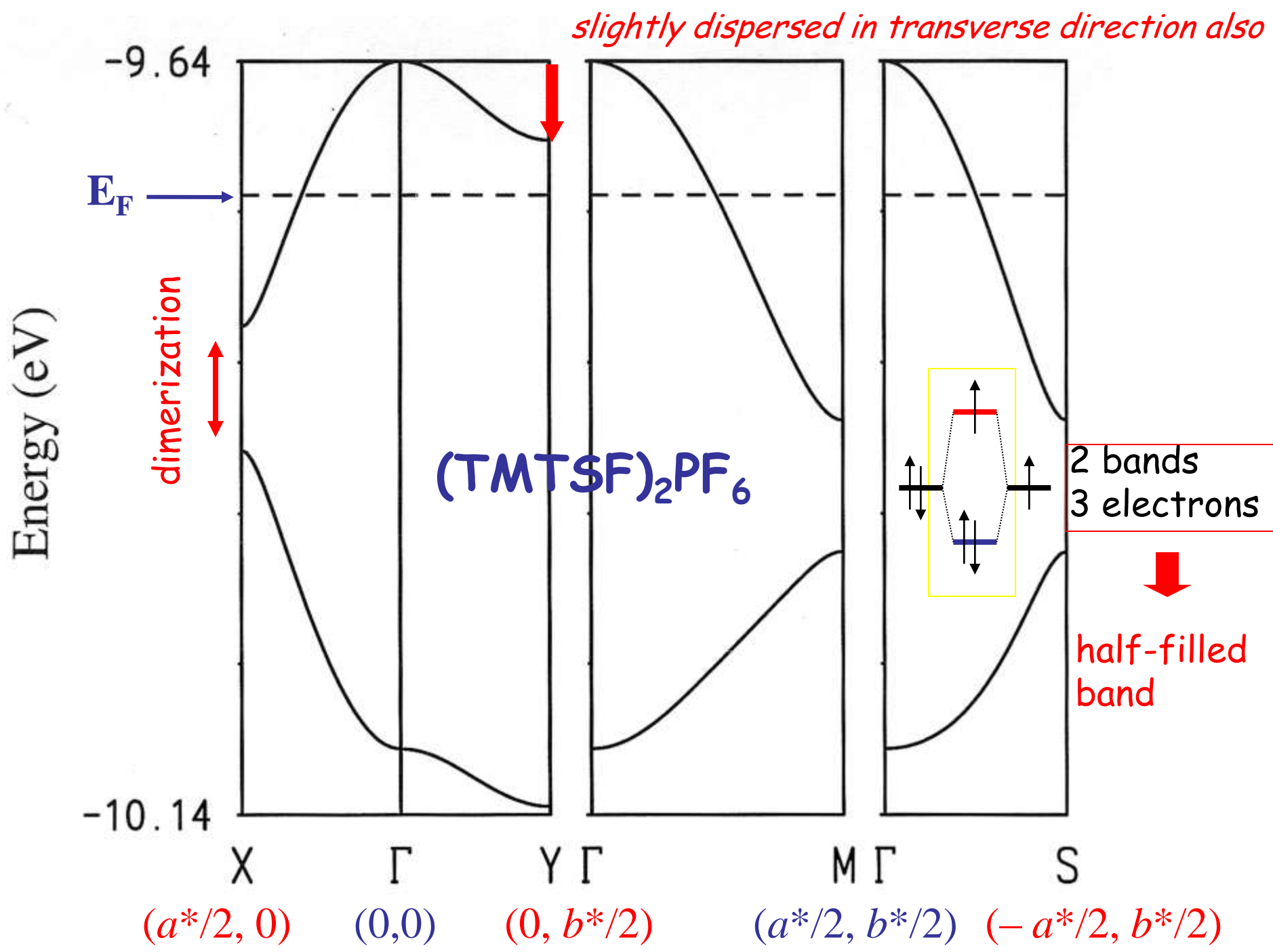
Bechgaard and Fabre salts

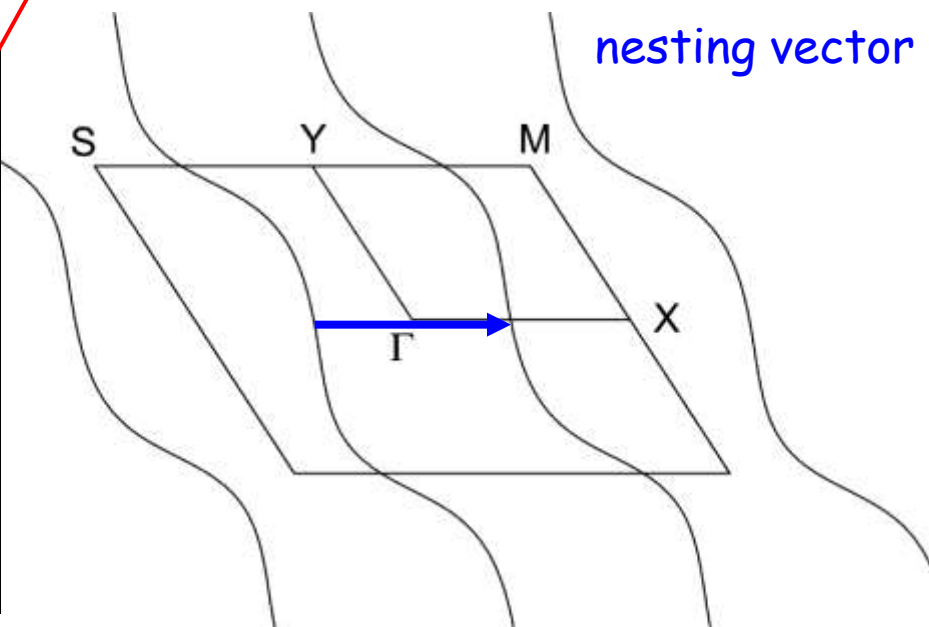
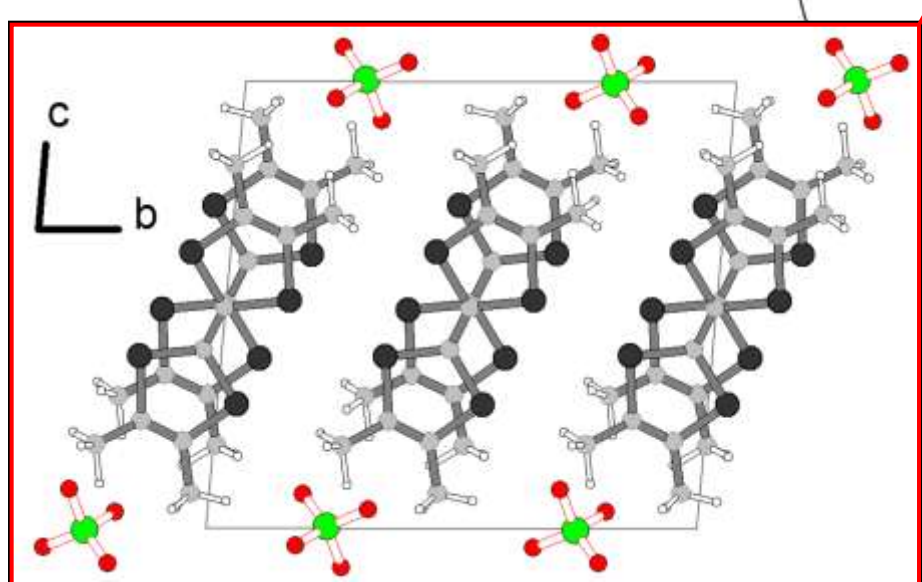
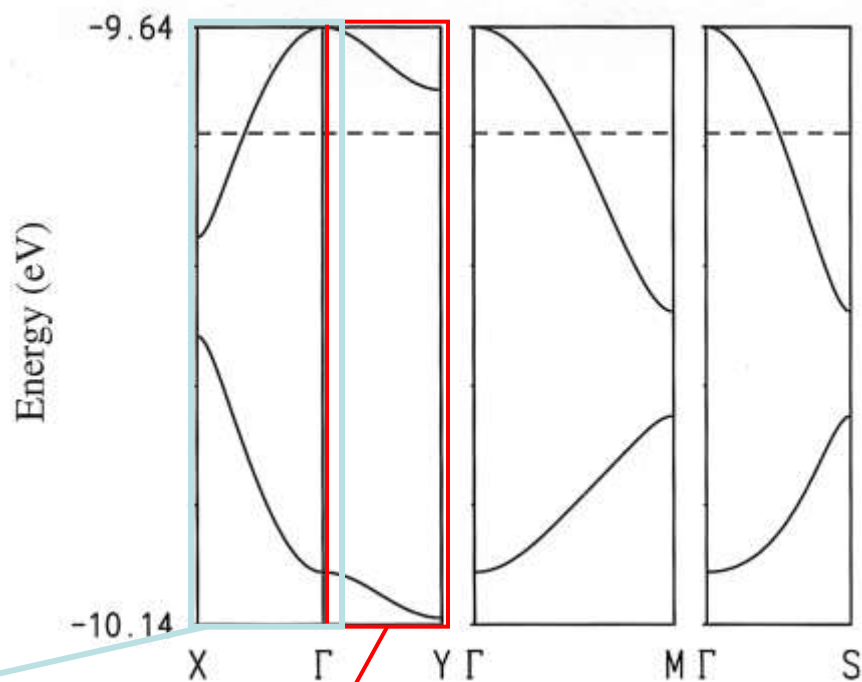
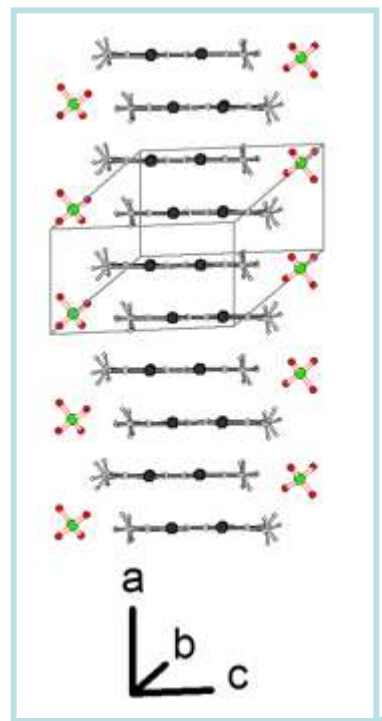


a typical molecular metal: $(\text{TMTSF})_2\text{PF}_6$

$$4 - 1 = 3$$







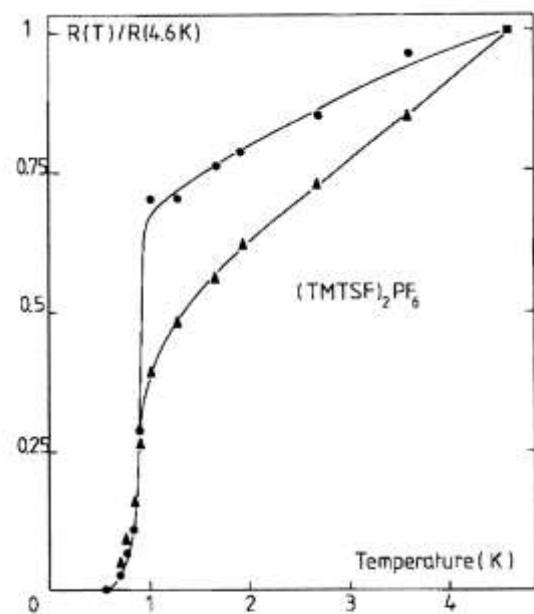


Figure 18. $(TMTSF)_2PF_6$: first observation of organic superconductivity (under a pressure of 9 kbar). (Reprinted with permission from ref 49. Copyright 1980 EDP Sciences.)

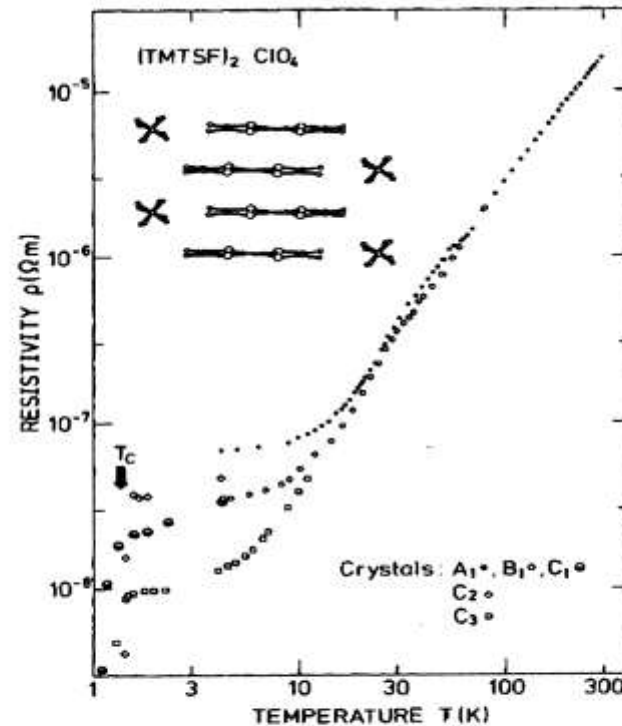
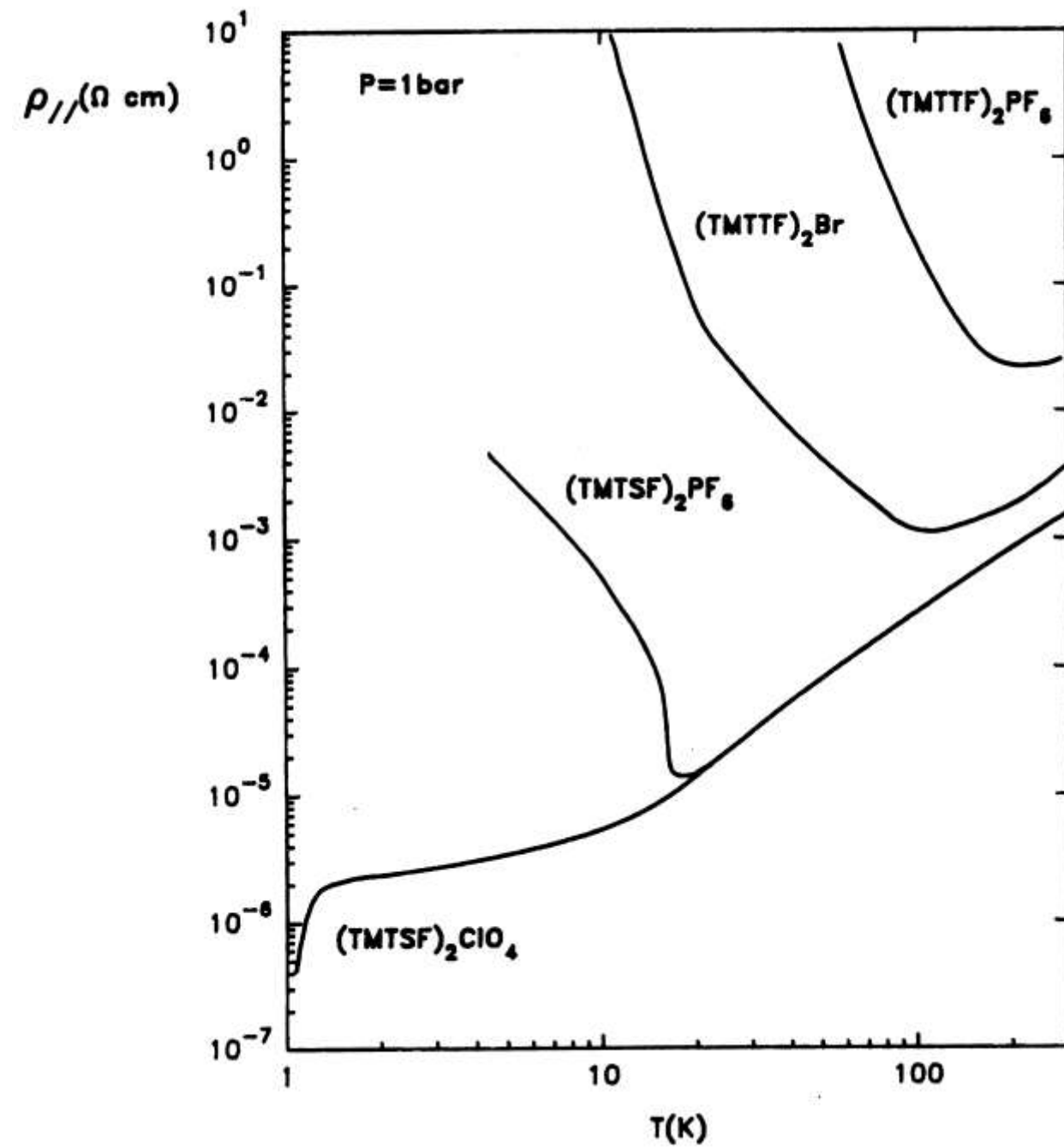
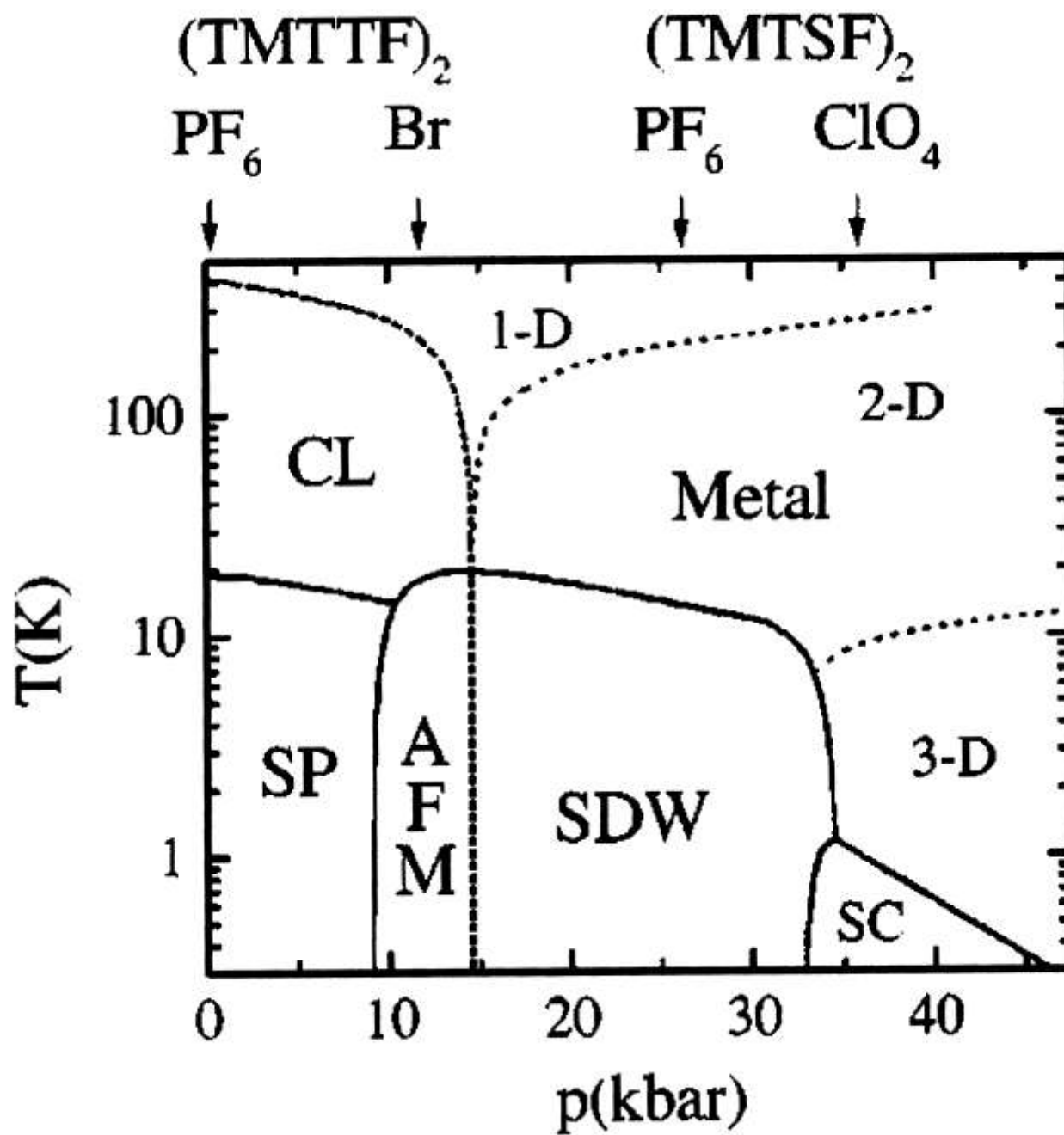


Figure 20. $(TMTSF)_2ClO_4$: first observation of organic superconductivity at ambient pressure. (Reprinted with permission from ref 93. Copyright 1981 American Physical Society.)



Jérôme
Chem. Rev. 2004, 104
p. 5578



OUTLINE

1. electrocrystallization
2. redox chemistry
3. intermolecular interactions, and their redox activation, direct the structure
4. orbitals and band (in one dimension)
5. decipher BS of TTF-TCNQ, Bechgaard salts
6. modify / control electronic structure

Roald Hoffmann

How Chemistry and Physics Meet in the Solid State

Angew. Chem. Int. Ed. Engl. **1987**, *26*, 846-878

Jeremy K. Burdett

Chemical Bonding in Solids

Oxford University Press, 1995

Christophe Iung, Enric Canadell

Description orbitalaire de la structure électronique des solides

1. De la molécule aux composés 1D

Ediscience international, Paris, 1997

Roger Rousseau, Marc Gener, Enric Canadell

Step-by-step construction of the electronic structure of molecular
conductors: Conceptuals aspects and applications

Adv. Funct. Mater. **2004**, *14*, 201

Conceptual Aspects of Structure–Property Correlations and Electronic Instabilities, with Applications to Low-Dimensional Transition-Metal Oxides

ENRIC CANADELL*

Laboratoire de Chimie Théorique, Université de Paris-Sud, 91405 Orsay, France

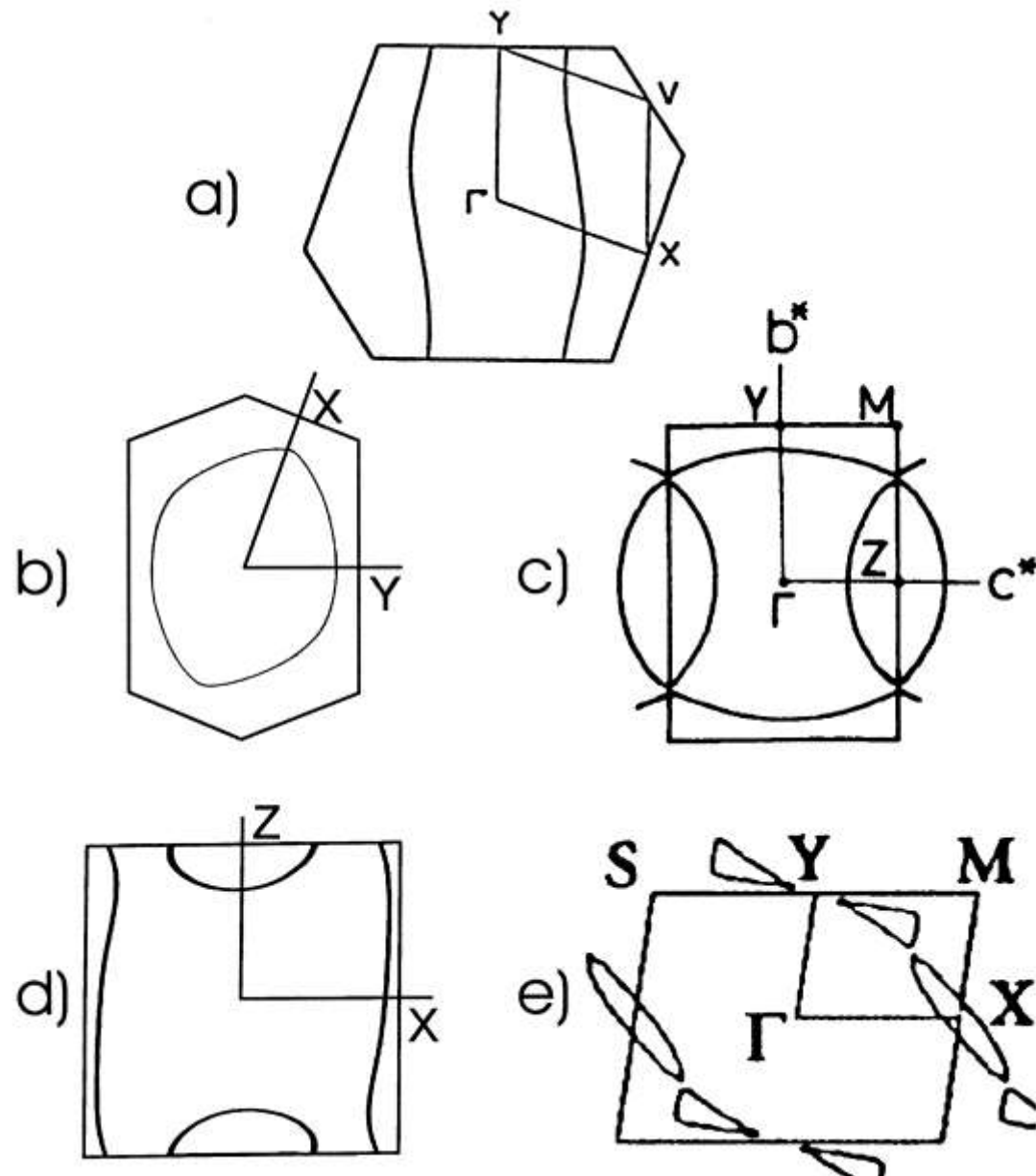
MYUNG-HWAN WHANGBO*

Department of Chemistry, North Carolina State University, Raleigh, North Carolina 27695-8204

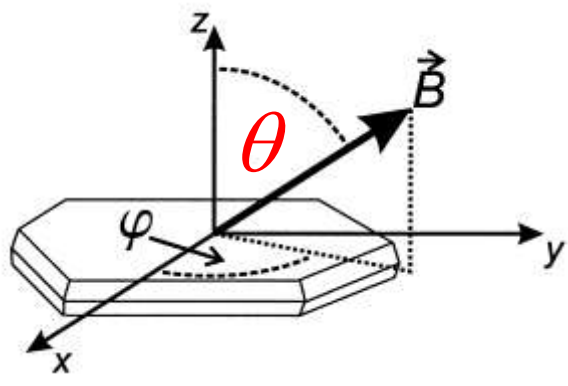
Received November 29, 1990 (Revised Manuscript Received March 14, 1991)

Contents

1. Introduction	966	10. Blue Bronzes	997
2. Electronic Band Structure	967	10.1 Orbital Patterns for the Bottom d-Block Bands	998
2.1 Formation of Energy Band	967	10.2 Interchain Interactions	999
2.2 Orbital Interactions in Solids	968	10.3 Fermi Surfaces and Nesting	1000
2.3 Band Gap and Symmetry Lowering	969	10.4 Interchain Interactions and Nesting in $\text{La}_2\text{Mo}_2\text{O}_7$	1001
2.4 Dispersion Patterns of the t_{2g} -Block Bands	970	11. Magnéli Phase Mo_6O_{23} and Diphosphate Tungsten Bronzes $\text{A}_x(\text{P}_2\text{O}_4)_4(\text{WO}_3)_{4m}$	1002
2.4.1 Corner-Sharing Octahedral Chain	971	11.1 Magnéli Phase Mo_6O_{23}	1002
2.4.2 Edge-Sharing Octahedral Chain	972	11.2 Diphosphate Tungsten Bronzes	1004
3. Vibrational Band Structure	974	12. Lithium Purple Bronze $\text{Li}_{0.9}\text{Mo}_6\text{O}_{17}$, and Other Compounds Containing Zigzag Octahedral Chains as Conducting Paths	1007
3.1 Formation of Energy Band	974	12.1 $\text{Li}_{0.9}\text{Mo}_6\text{O}_{17}$	1007
3.2 Band Gap and Symmetry Lowering	975		
4. Band Structure and Reciprocal Space	976		
4.1 Electronic Structures of Multidimensional	976		

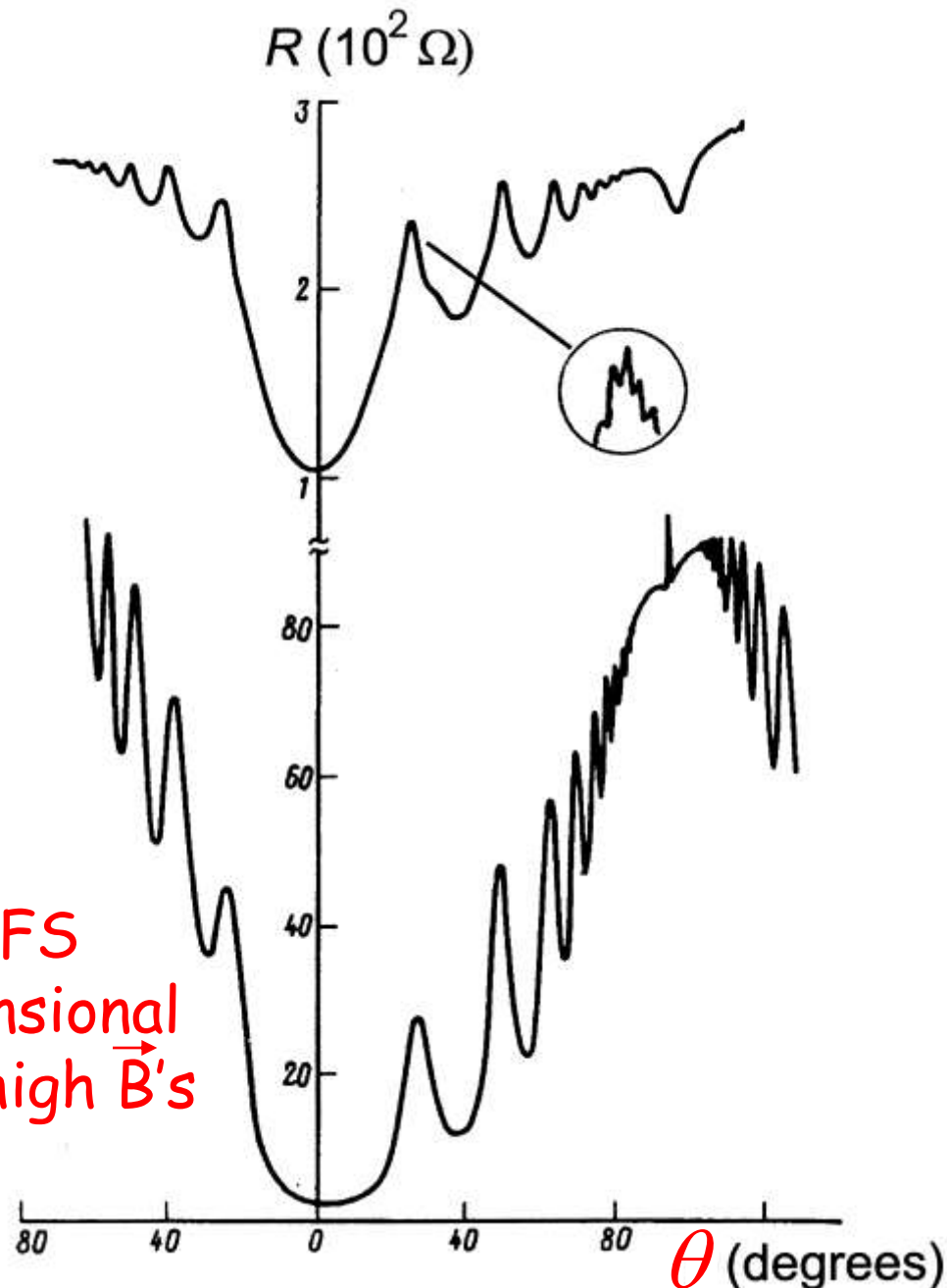


1D / 2D Band Structures and Fermi Surfaces



very pure samples

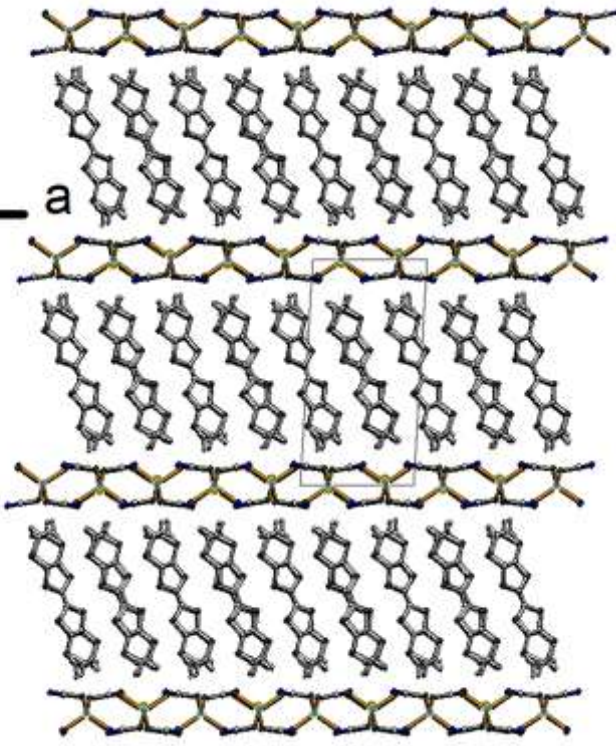
the combination of
very pure samples
and admixtures of 1D/2D FS
makes for a rich low dimensional
physics, especially under high \vec{B} 's



see, Mark V. Kartsovnik *Chem. Rev.* 2004, 104, 5737

a series of 2D metals

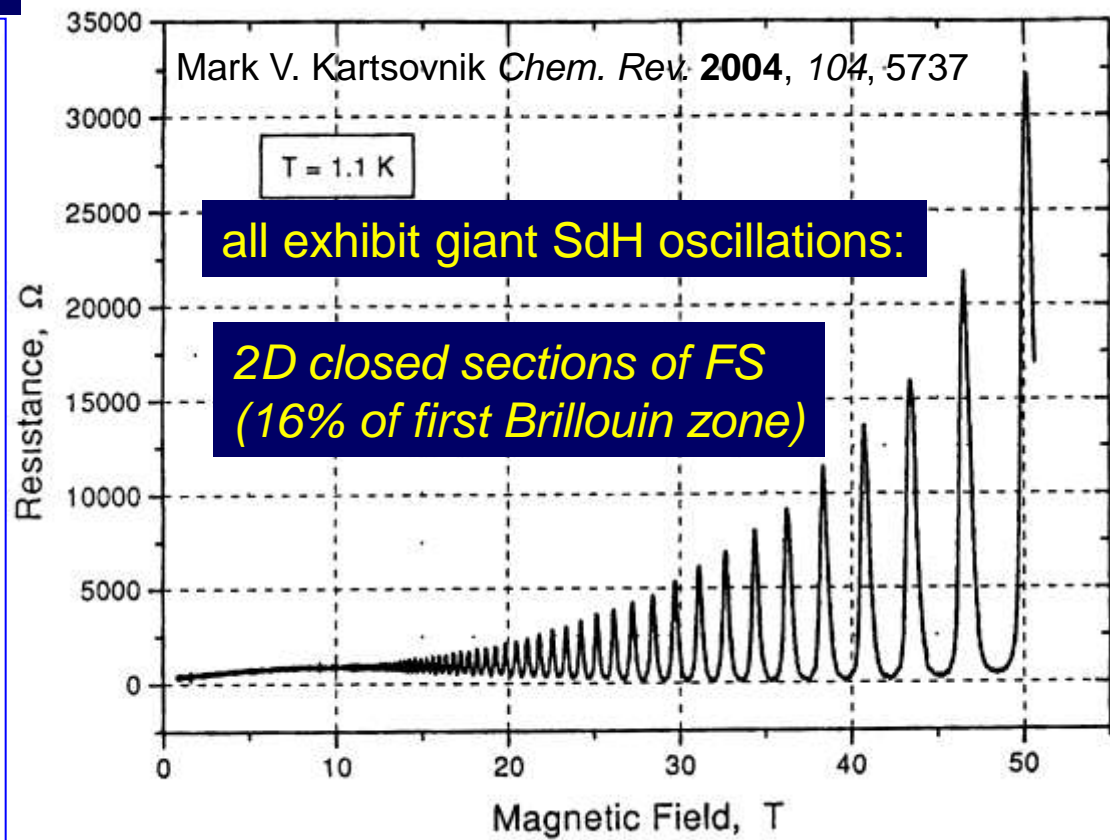
yet with two different types of
charge carriers
with different dimensionality



room temperature
crystal structures,
BS and FS very similar

$\alpha\text{-}(\text{BEDT-TTF})_2[\text{M}^+\text{Hg}^{2+}(\text{QCN}^-)_4]^-$

M = Ti, K, NH₄; Q = S, Se

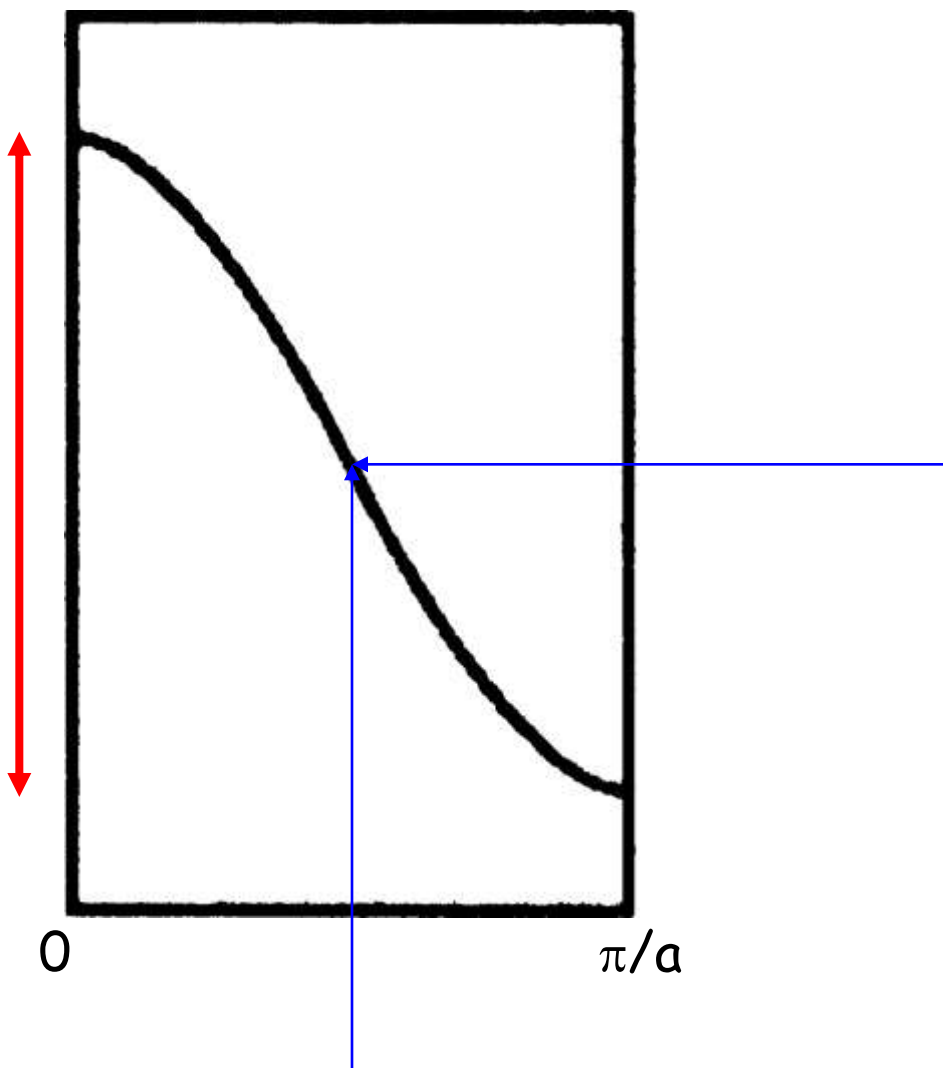


some exhibit a density wave instability:
nested 1D parts of FS

Rousseau, Figueras, Canadell *J. Mol. Struct. (Theochem)* 1998, 424, 135

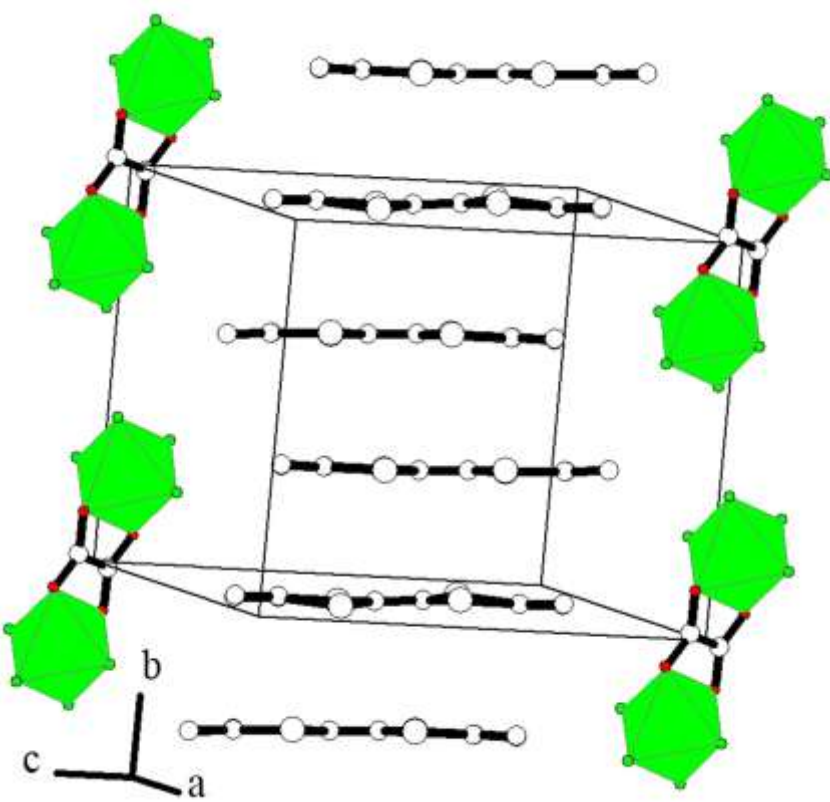
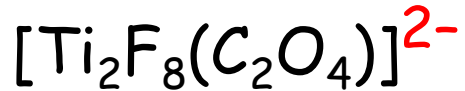
see also *Organic Superconductors* by Ishiguro, Yamaji, Saito Springer-Verlag 1998

modifying the electronic structure

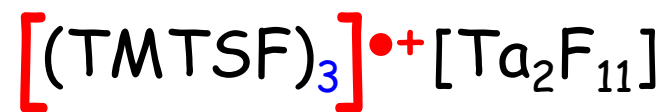
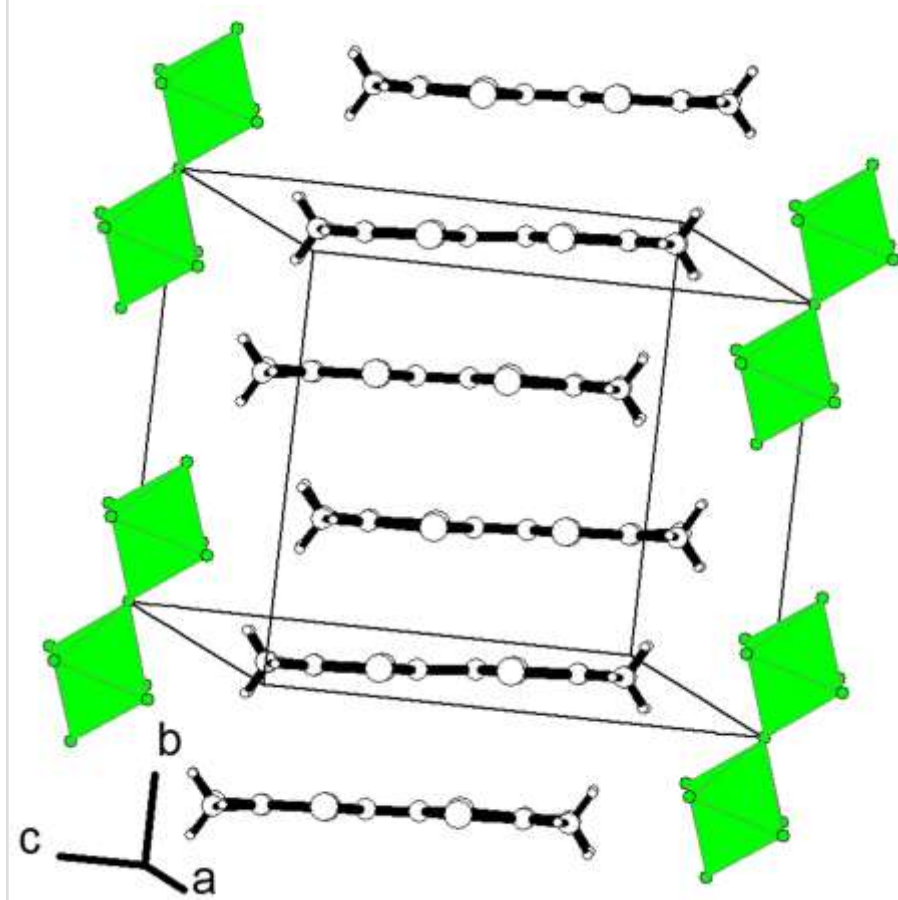
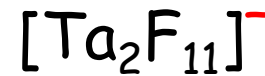


OUTLINE

1. electrocrystallization
2. redox chemistry
3. intermolecular interactions, and their redox activation, direct the structure
4. orbitals and band (in one dimension)
5. decipher BS of TTF-TCNQ, Bechgaard salts
6. modify / control electronic structure
 - 6.1 tune anion charge



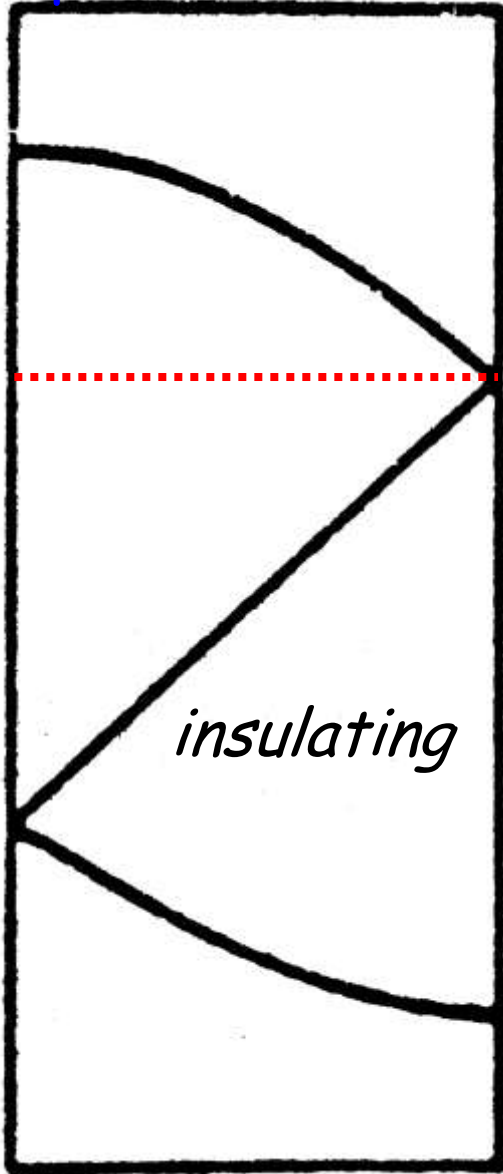
Synth. Met. 1988, 22, 201



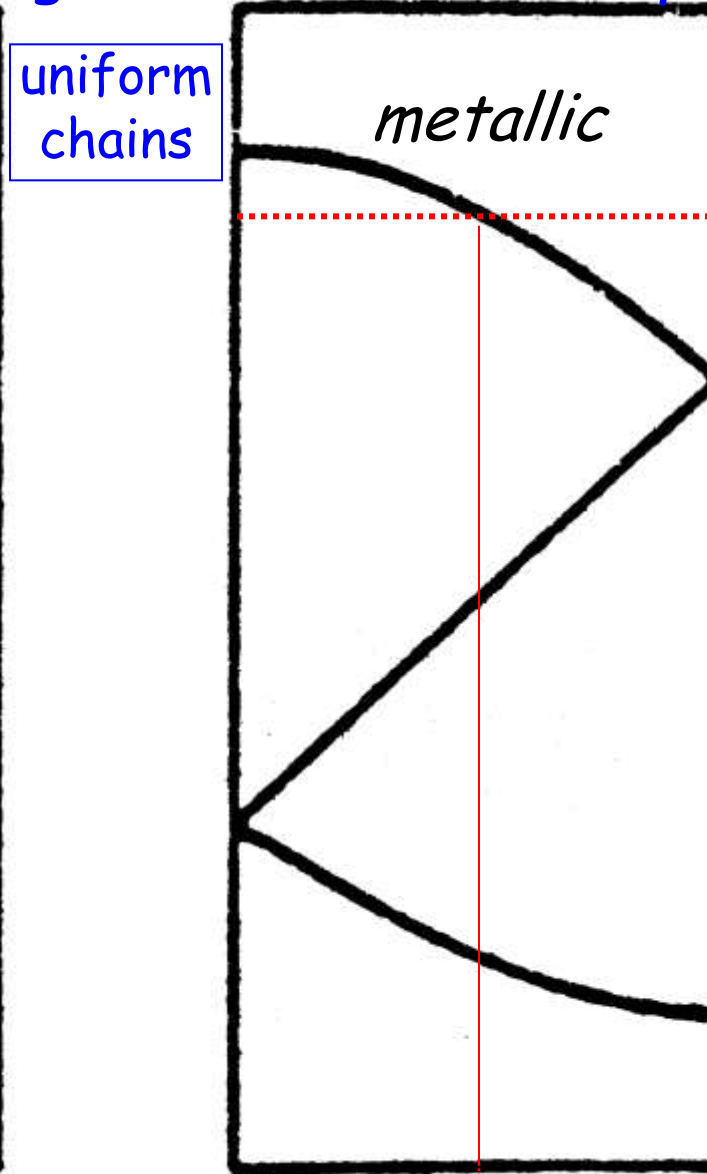
Synth. Met. 1991, 41-43, 1939

predict band diagram and conductivity

6 - 2
i.e.
4 electrons
in
three bands:
highest one
is empty



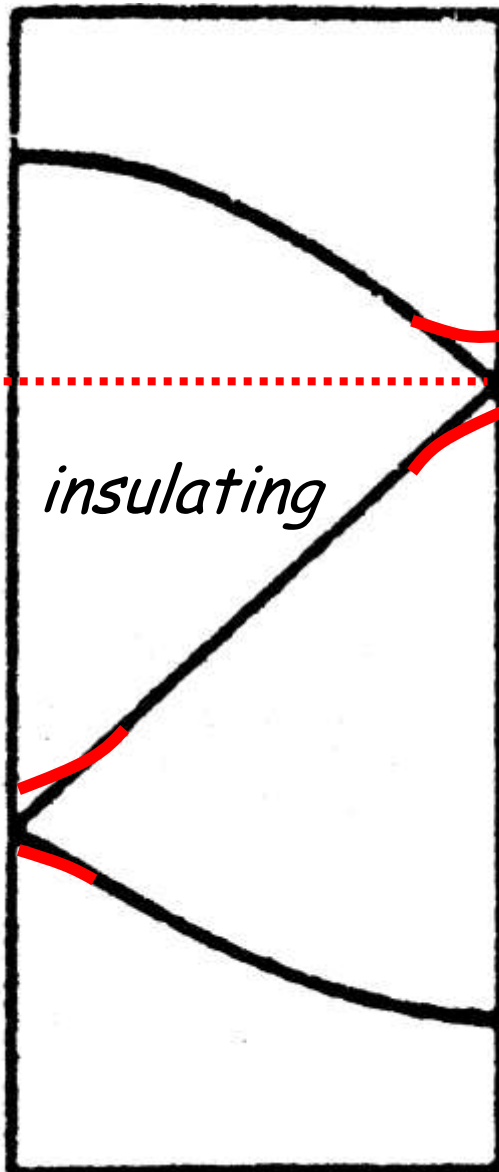
3:1²⁻



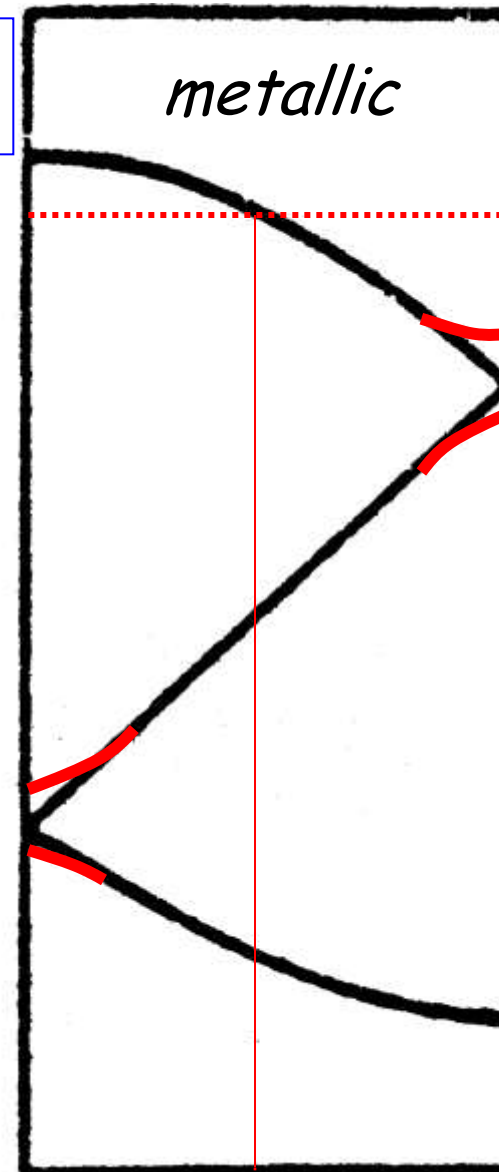
$b' = 3b$

3:1⁻

predict band diagram and conductivity



trimerized
chains



metallic

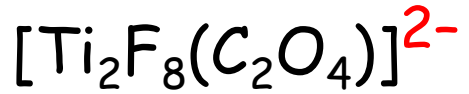
e_F

3:1²⁻

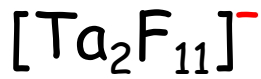
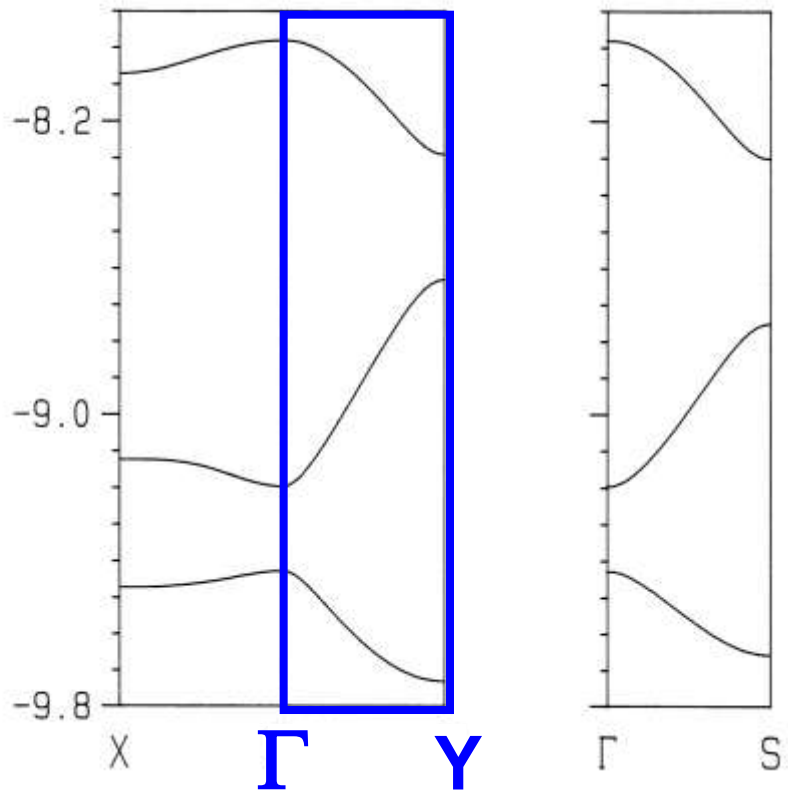
$b' = 3b$

$\pi/6a$

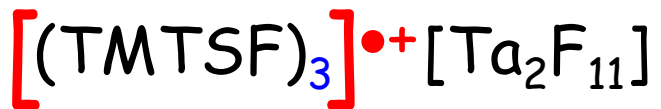
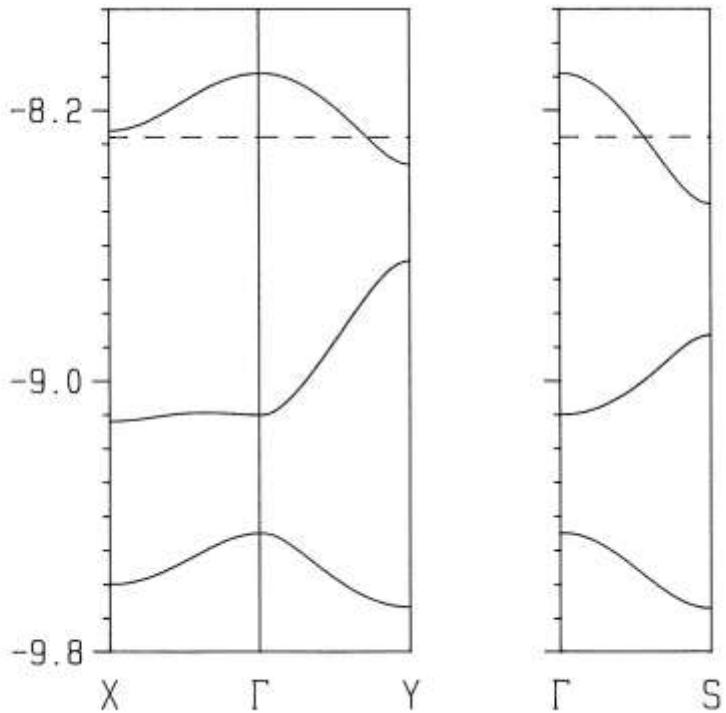
3:1⁻

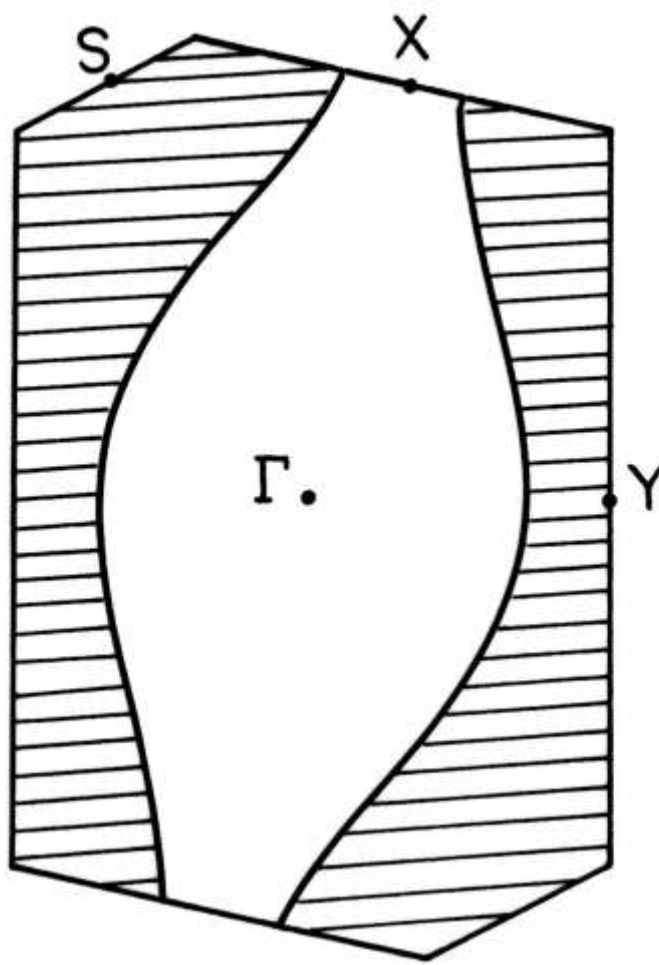
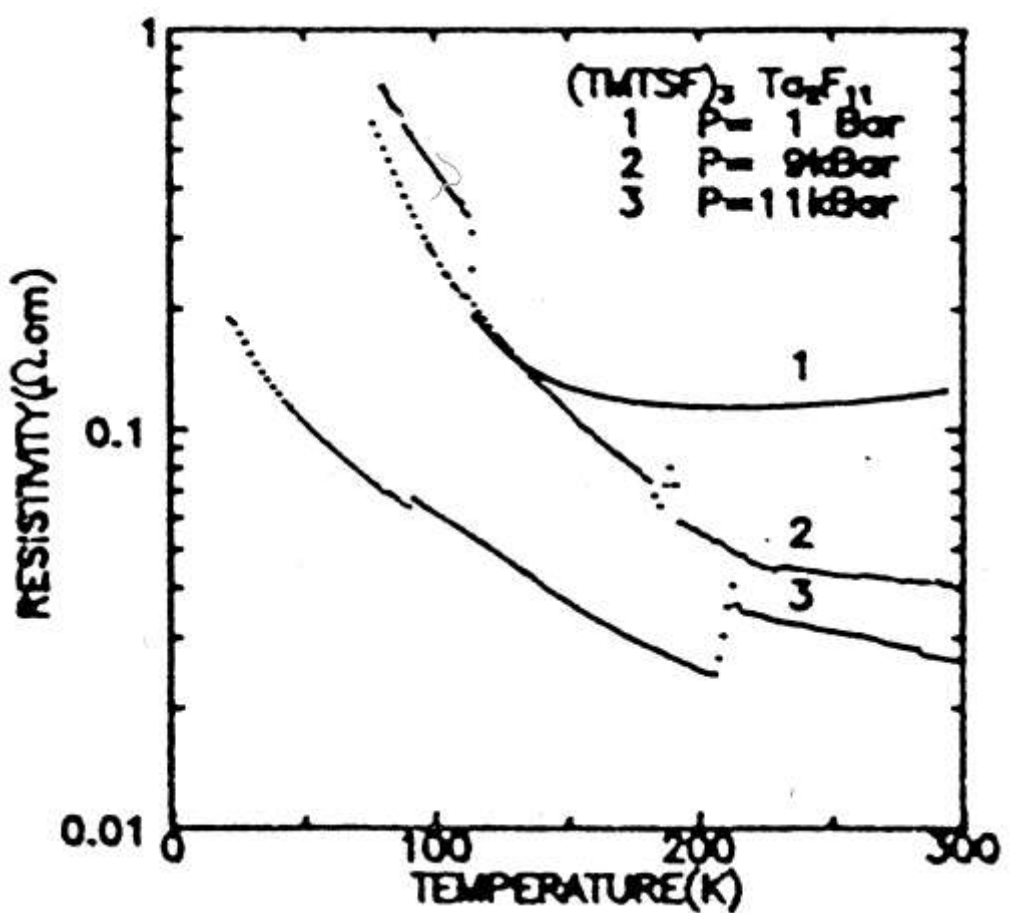


Energy (eV)



Energy (eV)





molecular engineering and band filling

- change the anion charge
- change electron count by tuning the stoichiometry

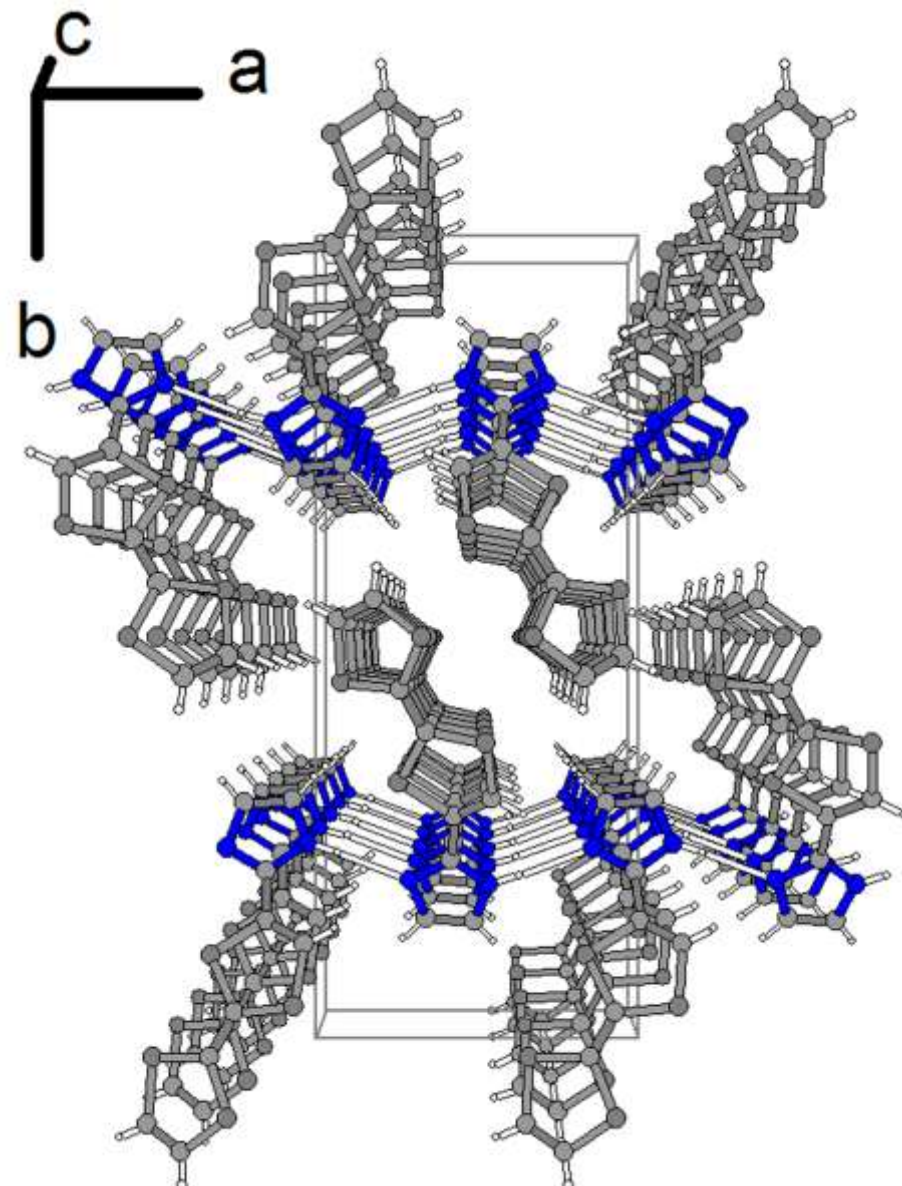
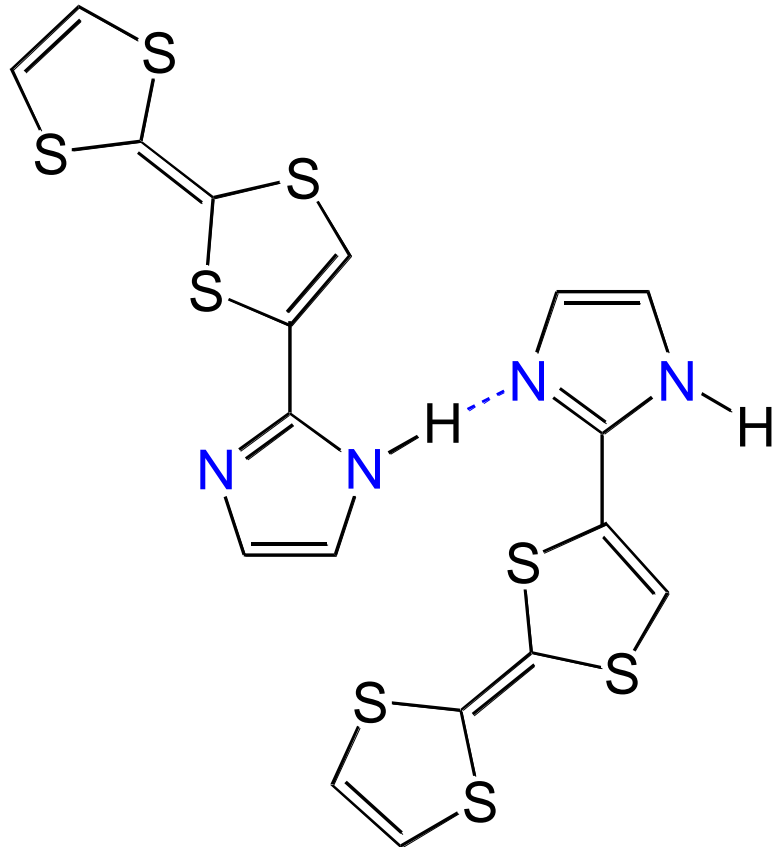
“Modulating the Framework Negative Charge Density in the System
 $\text{BDT-TTP}^{+}/[\text{Re}_6\text{S}_5\text{Cl}_9{}^{1-}]/[\text{Re}_6(\text{S}/\text{Se})_6\text{Cl}_8{}^{2-}]/[\text{Re}_6\text{S}_7\text{Cl}_7{}^{3-}]$: Templating by Isosteric Cluster Anions of Identical Symmetry and Shape, Variations of Incommensurate Band Filling, and Electronic Structure in 2D Metals”

**S. PERRUCHAS, K. BOUBEKEUR, E. CANADELL, Y. MISAKI, P. AUBAN-SENZIER,
C. PASQUIER, P. BATAIL**
J. Am. Chem. Soc. **130**(11), 3335-3348 (2008)

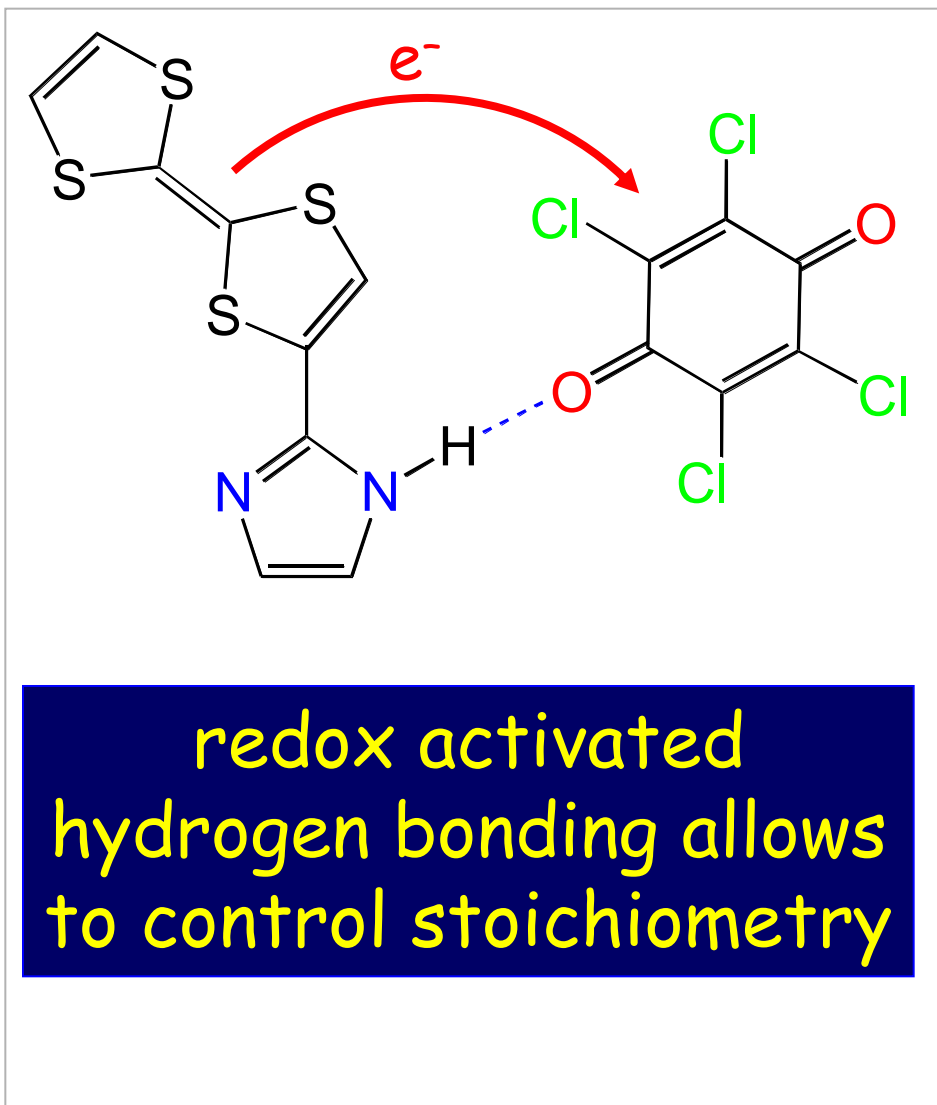
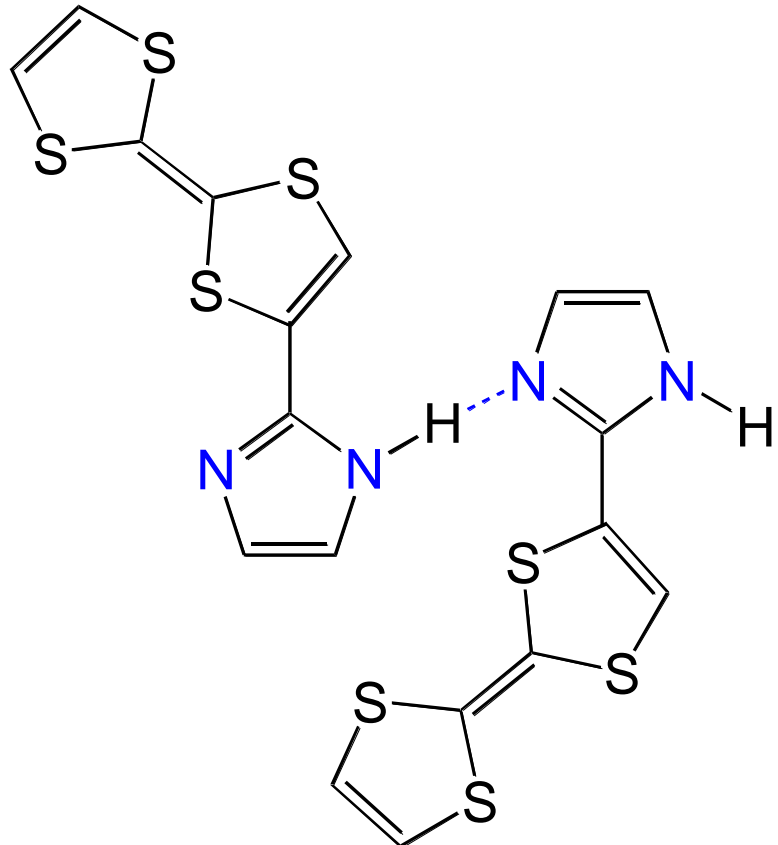
OUTLINE

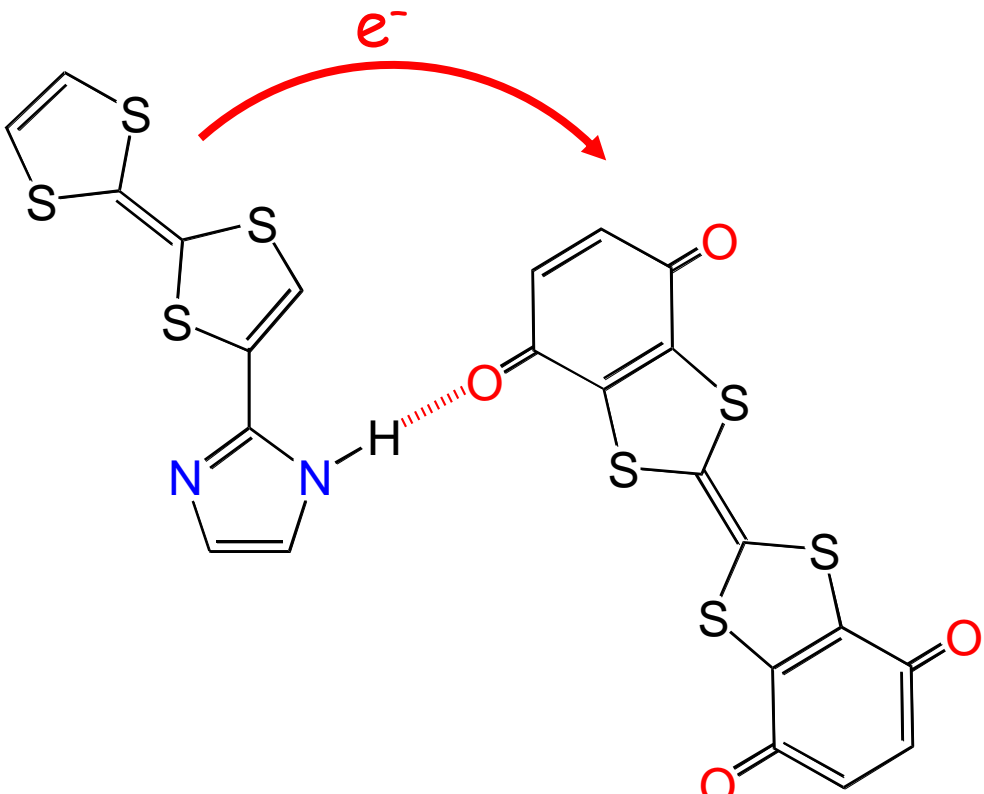
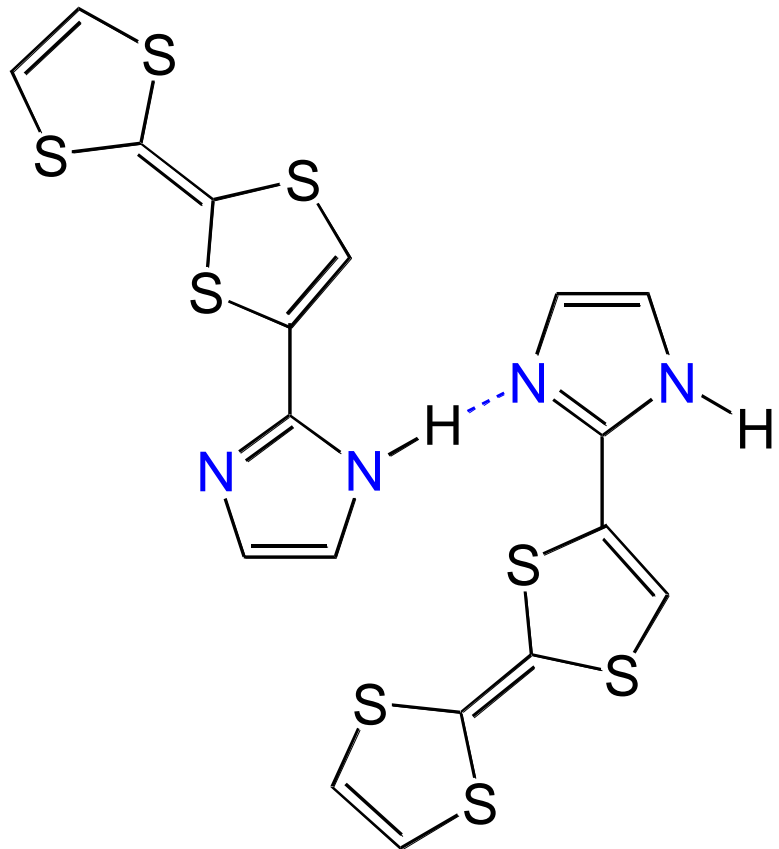
1. electrocrystallization
2. redox chemistry
3. intermolecular interactions, and their redox activation, direct the structure
4. orbitals and band (in one dimension)
5. decipher BS of TTF-TCNQ, Bechgaard salts
6. modify / control electronic structure
 - 6.1 tune anion charge
 - 6.2 tune stoichiometry

Morita-Nakasuji's TTF-imidazole



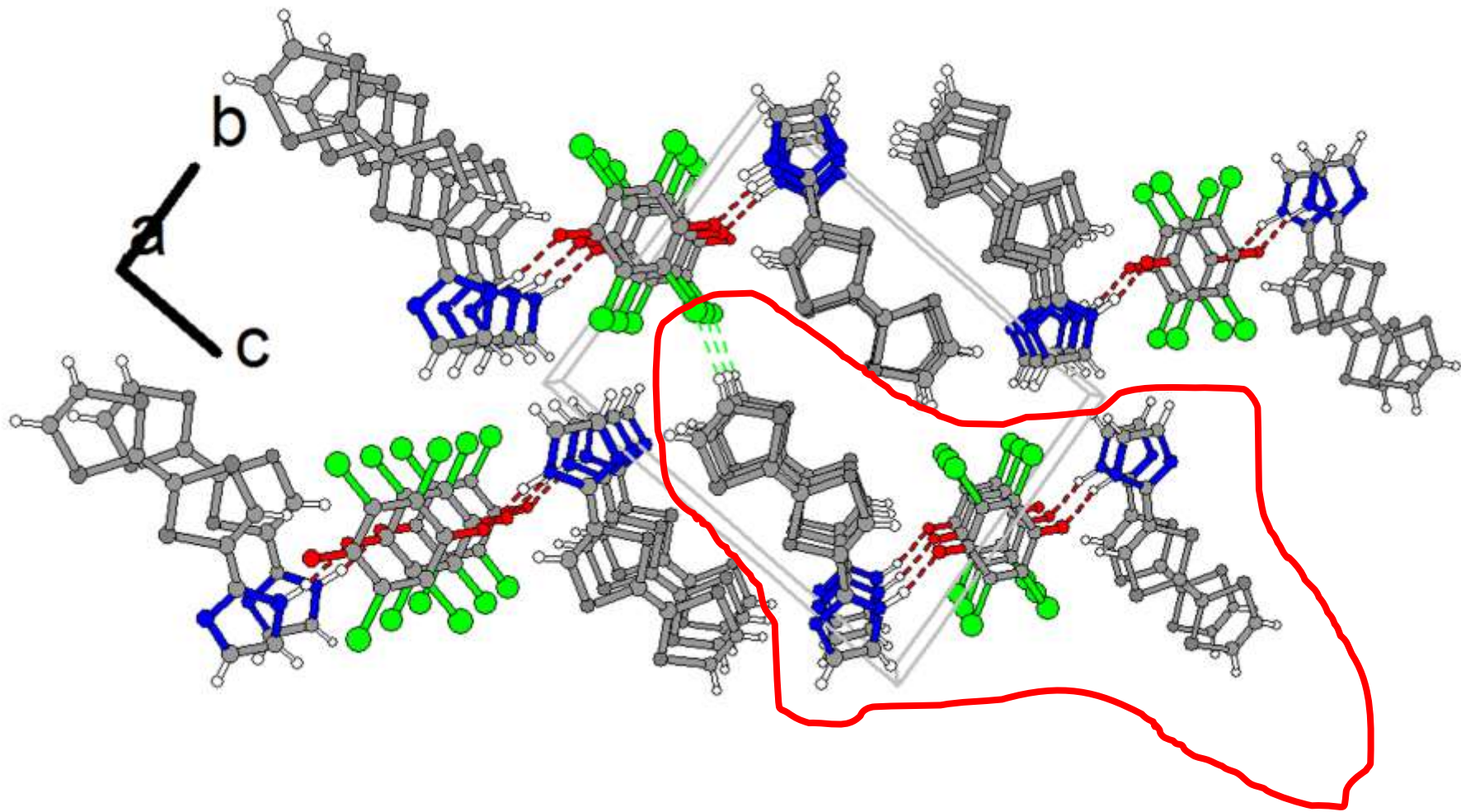
Morita-Nakasuji's TTF-imidazole





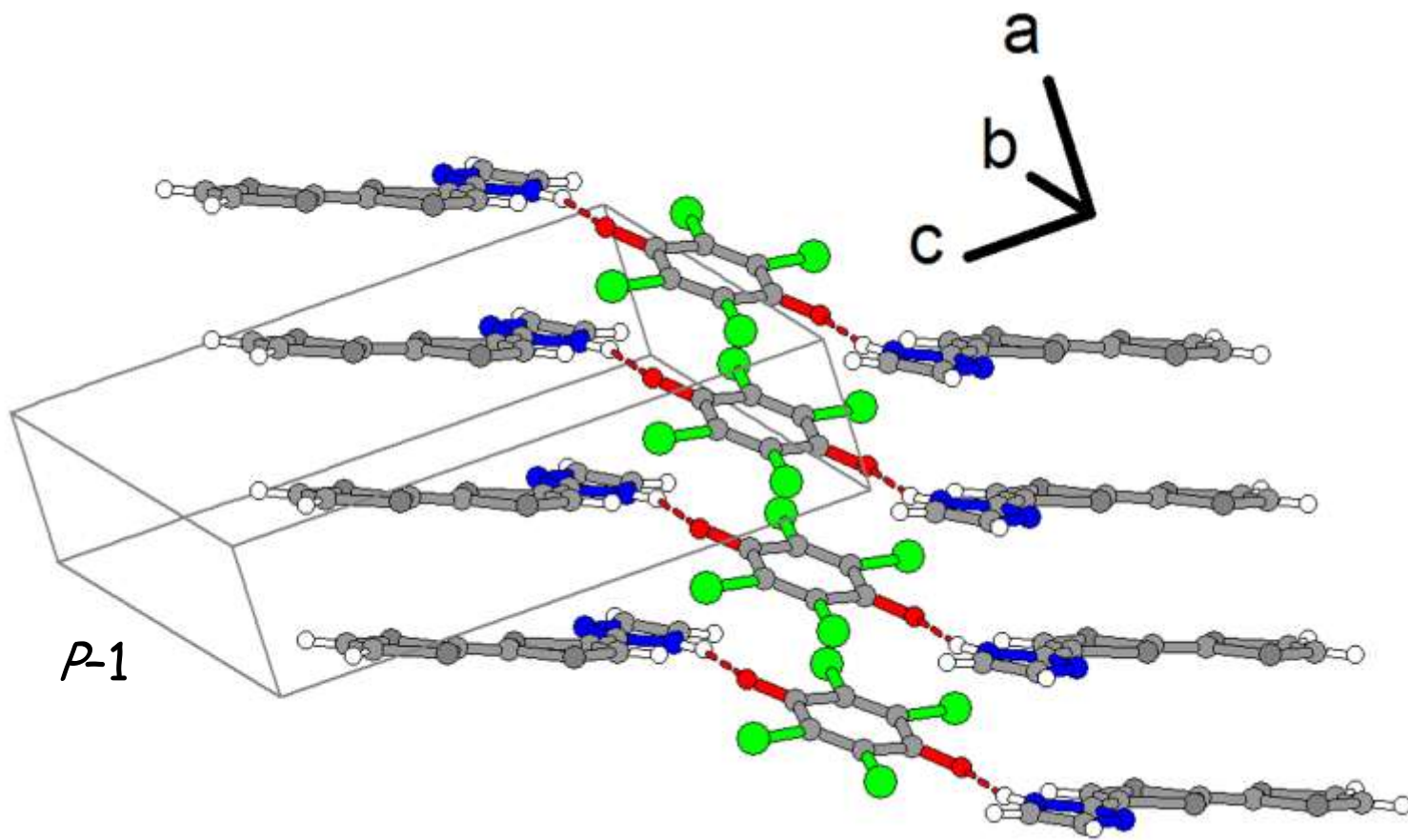
redox activated
hydrogen bonding allows
control of stoichiometry

$(\text{TTF-Im})_2(\text{CHL})$



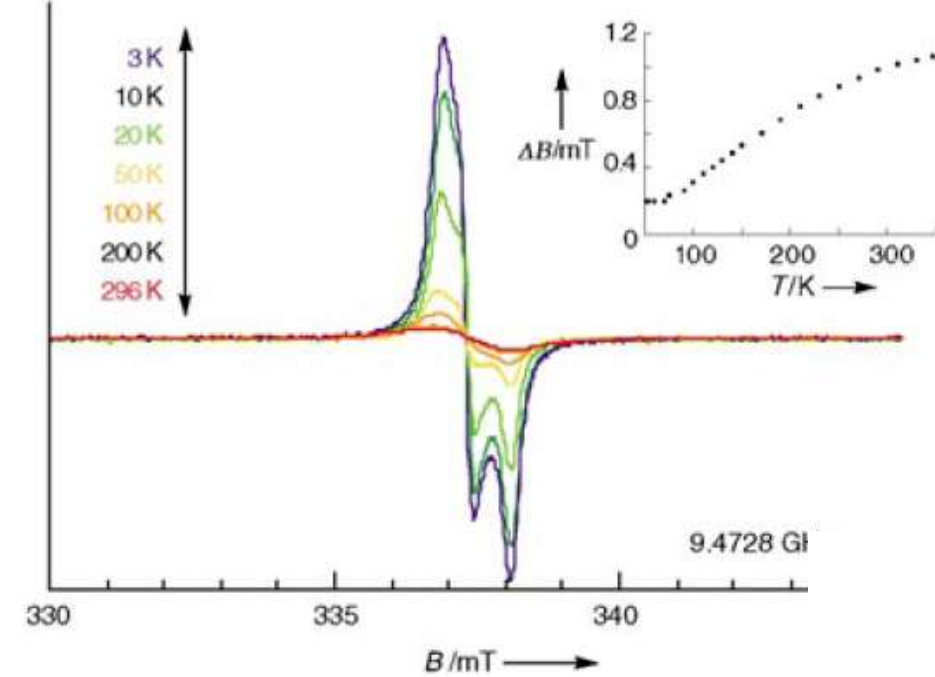
redox activated hydrogen bonding allows control of stoichiometry

$(\text{TTF-Im})_2(\text{CHL})$



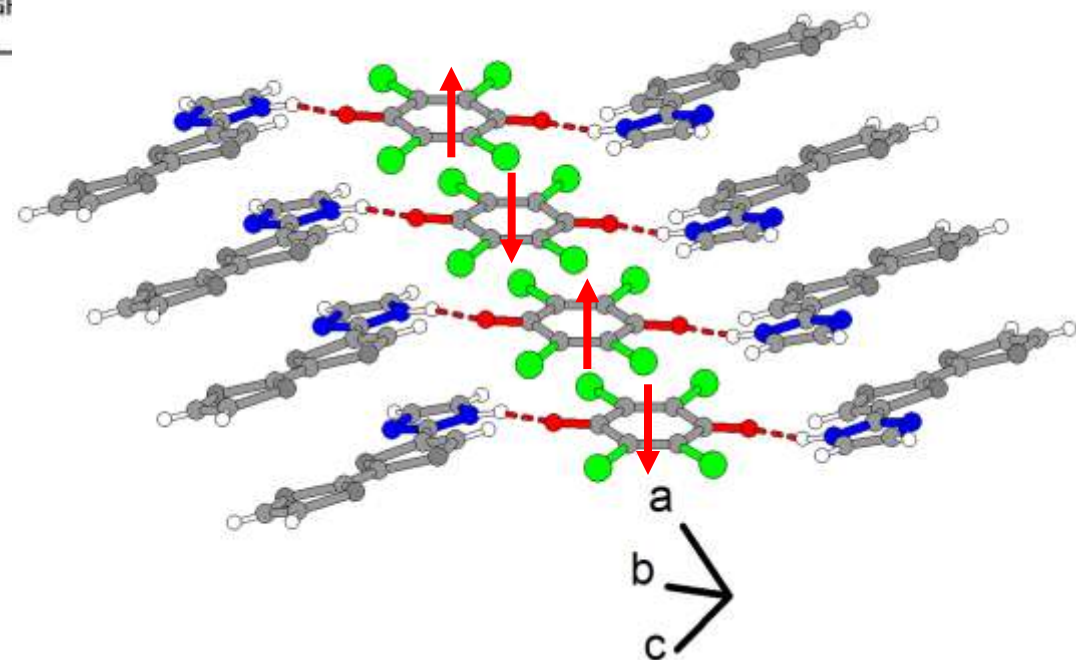
uniform stacks

$(\text{TTF-Im})_2(\text{CHL})$

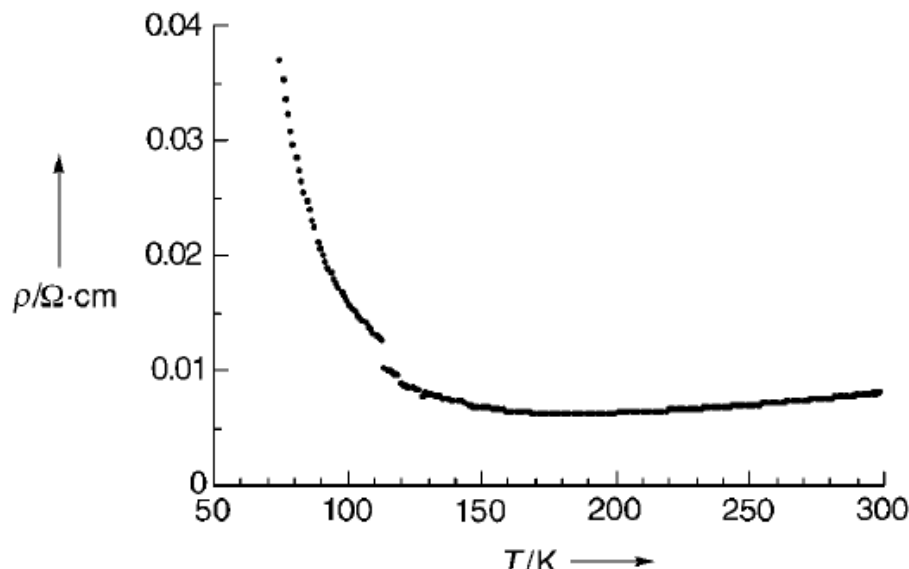


TTF- Im^{+} spin only

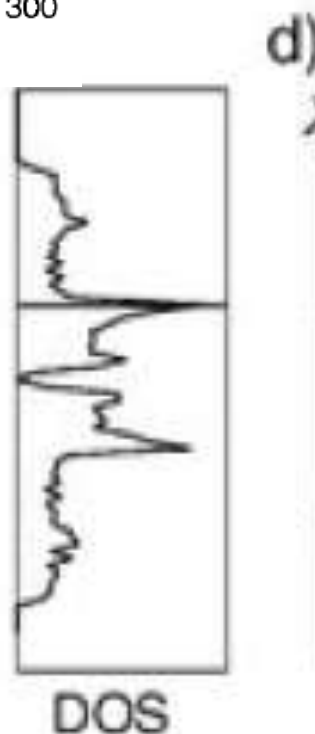
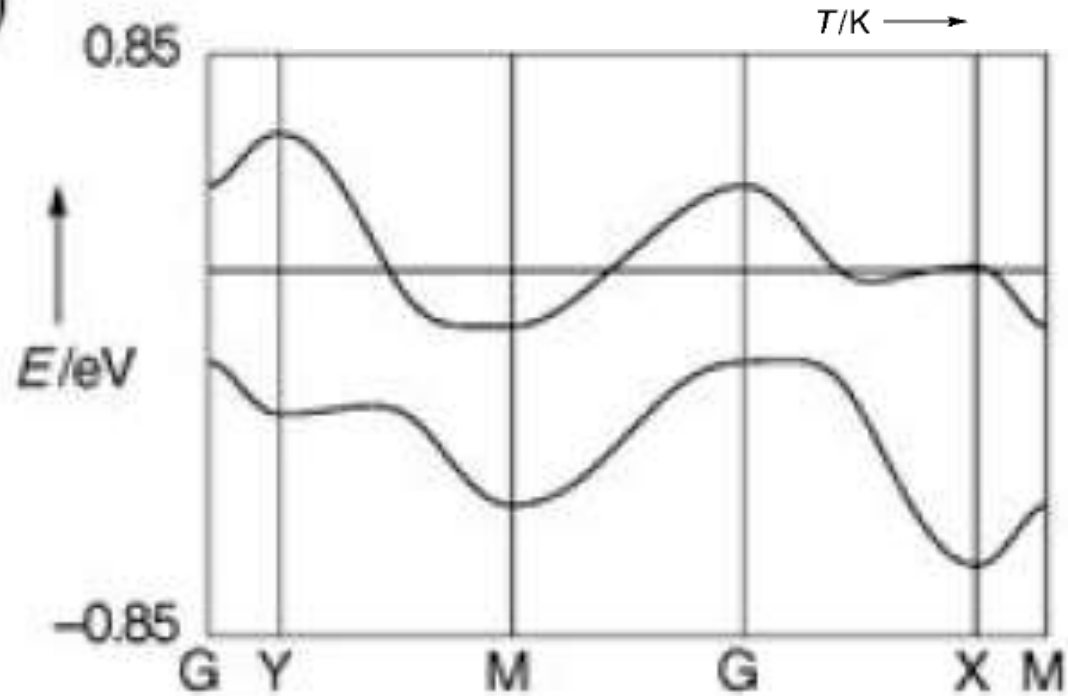
Heisenberg chain of spins on uniform chloranil stacks



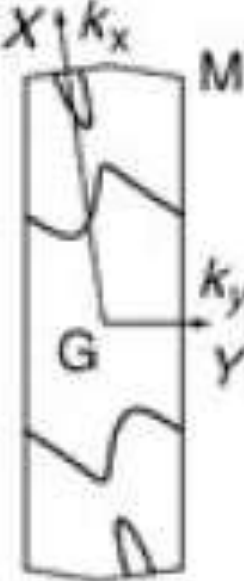
(TTF-**Im**)₂(CHL)



b)



d)



OUTLINE

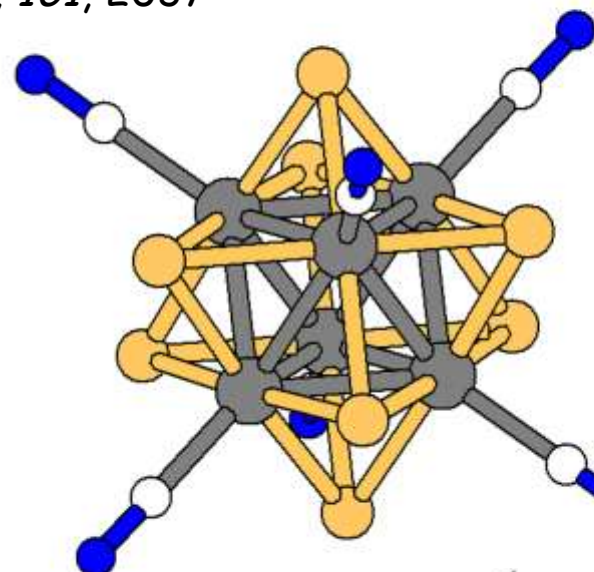
1. electrocrystallization
2. redox chemistry
3. intermolecular interactions, and their redox activation, direct the structure
4. orbitals and band (in one dimension)
5. decipher BS of TTF-TCNQ, Bechgaard salts
6. modify / control electronic structure
 - 6.1 tune anion charge
 - 6.2 tune stoichiometry

EDT-TTF- CONH_2 vs $\text{Re}_6\text{Se}_8(\text{CN})_6]$ ^{4-/3-}

Batail et al.

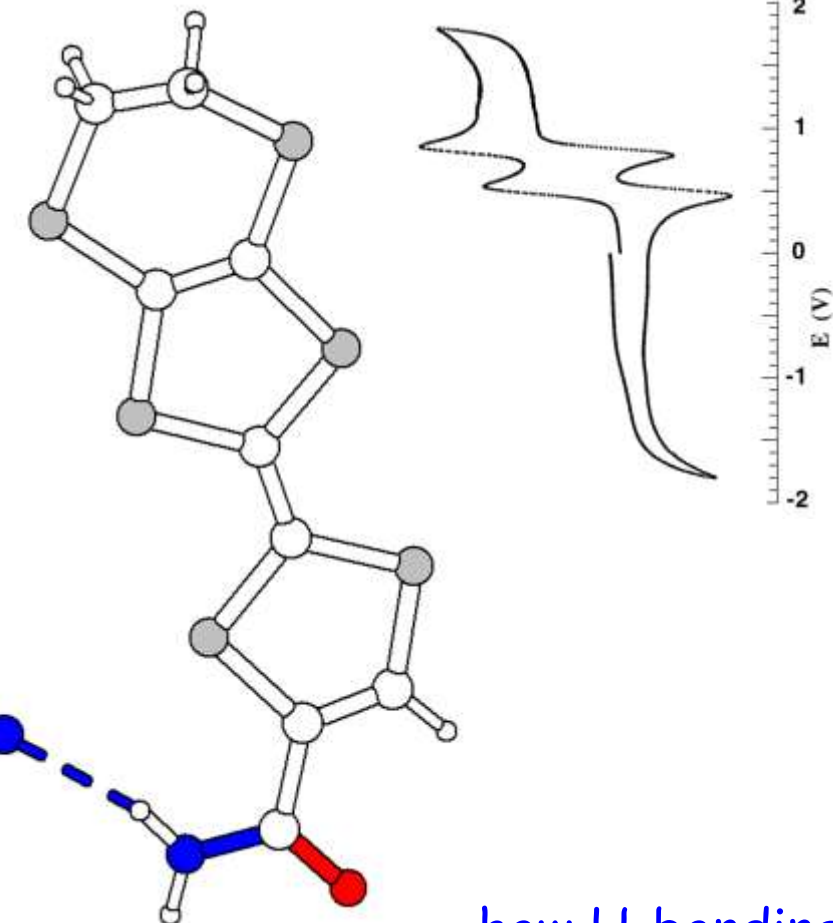
Chem. Rev. 2001, 101, 2037

redox active,
luminescent,
hexanuclear,
molecular
chalcogenide
cluster



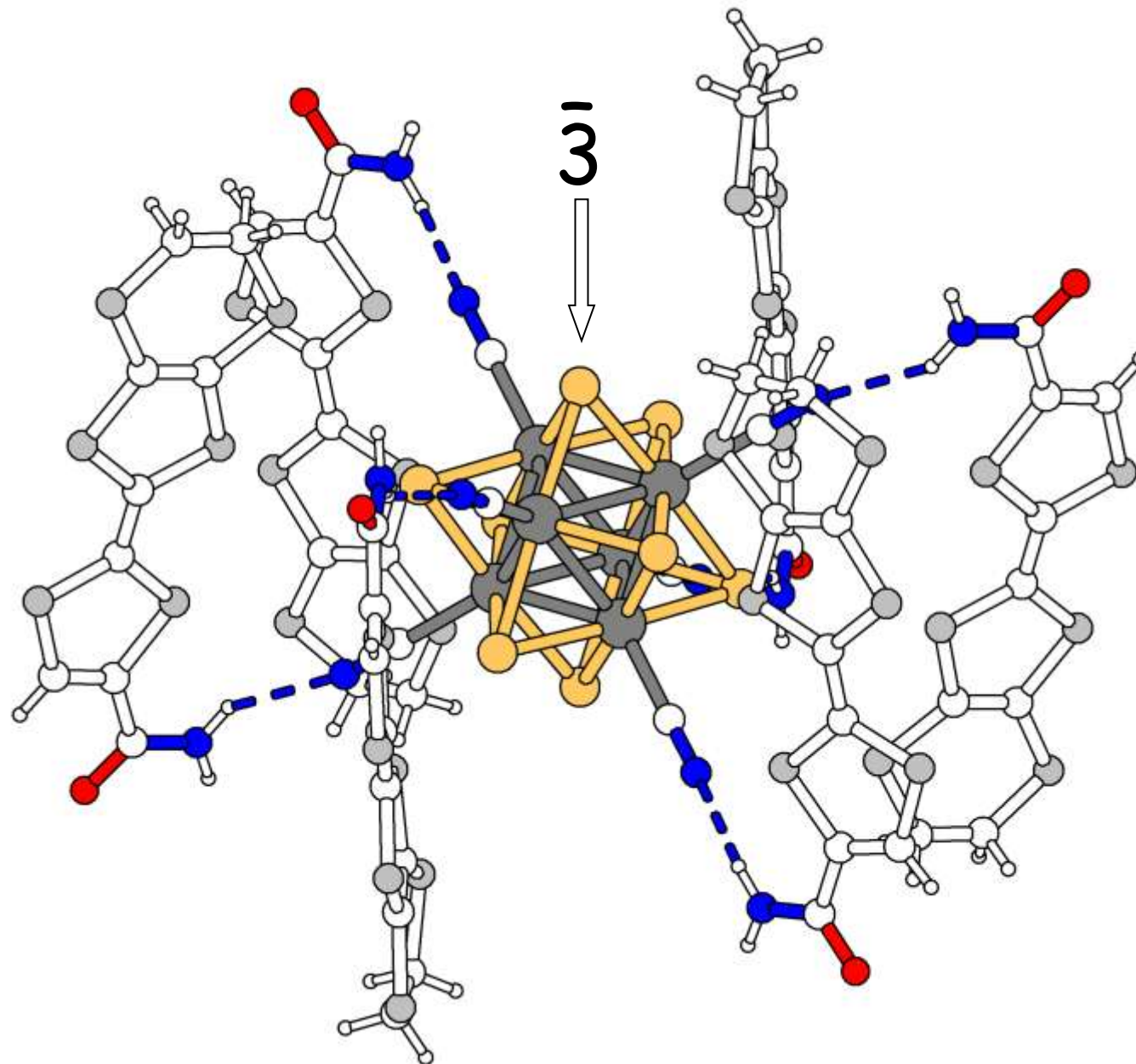
0.3 V/SCE

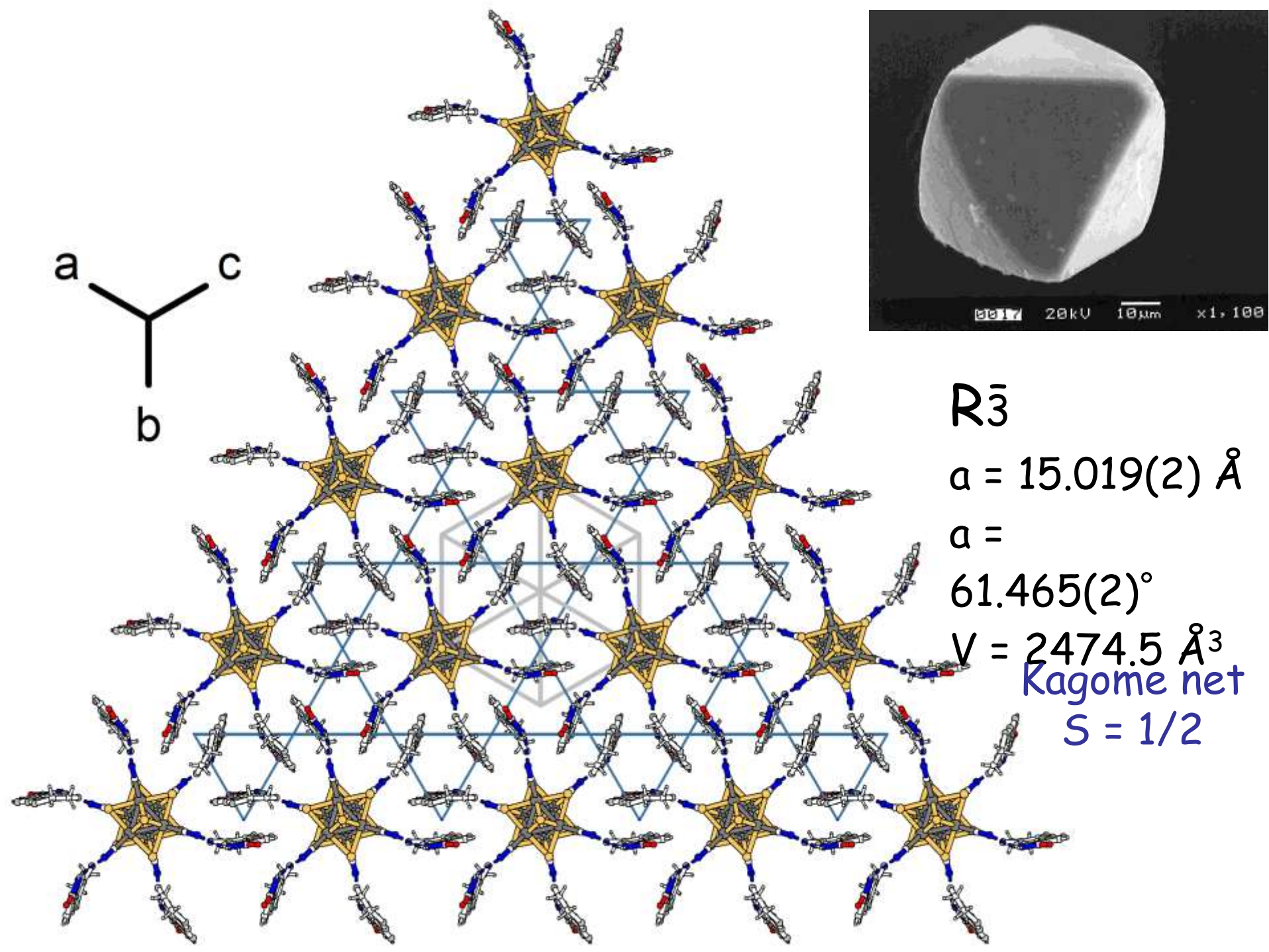
Sasaki, Fedorov et al.
Chem. Lett. 1999, 1121



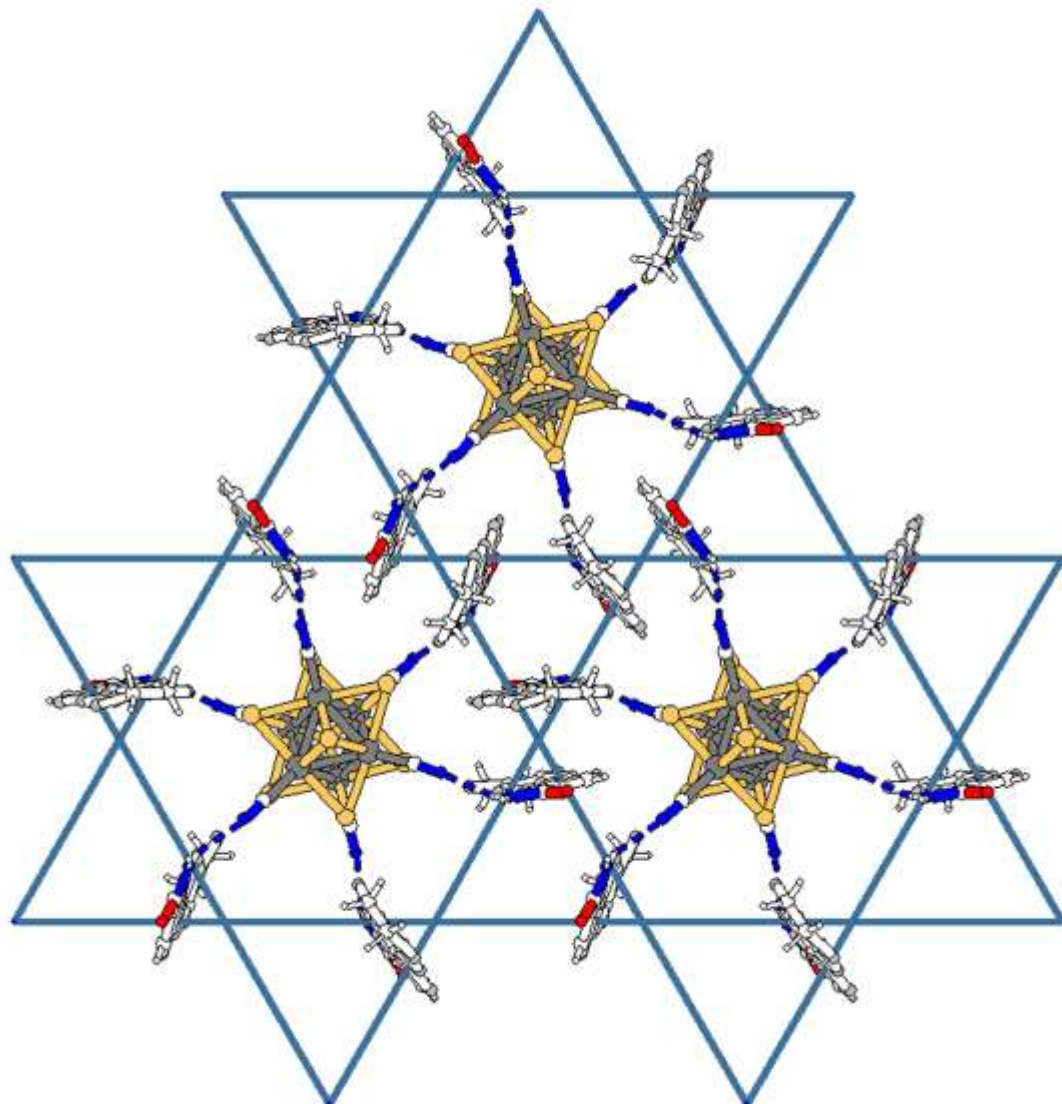
how H-bonding
express octahedral symmetry
of inorganic cluster anion

6 EDT-TTF-CONH₂ + Re₆Se₈(CN)₆]^{4-/3-}





$(EDT-TTF-CONH_2)_6^{(4-p)+} [Re_6Se_8(CN)_6]^{(4-p)-}$

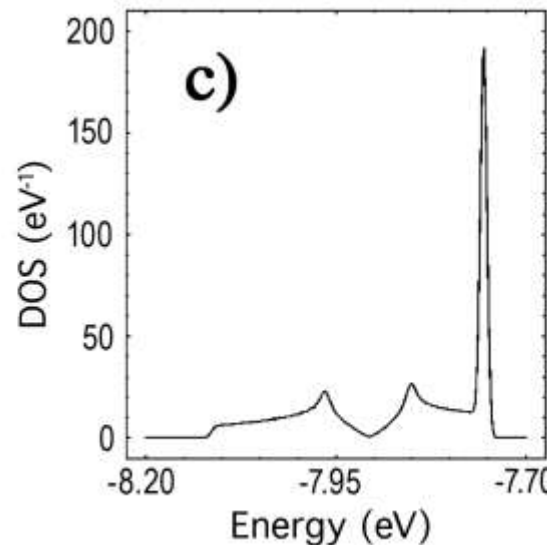


$|\beta|_{\text{HOMO-HOMO}}$

intradimer
0.7062 eV

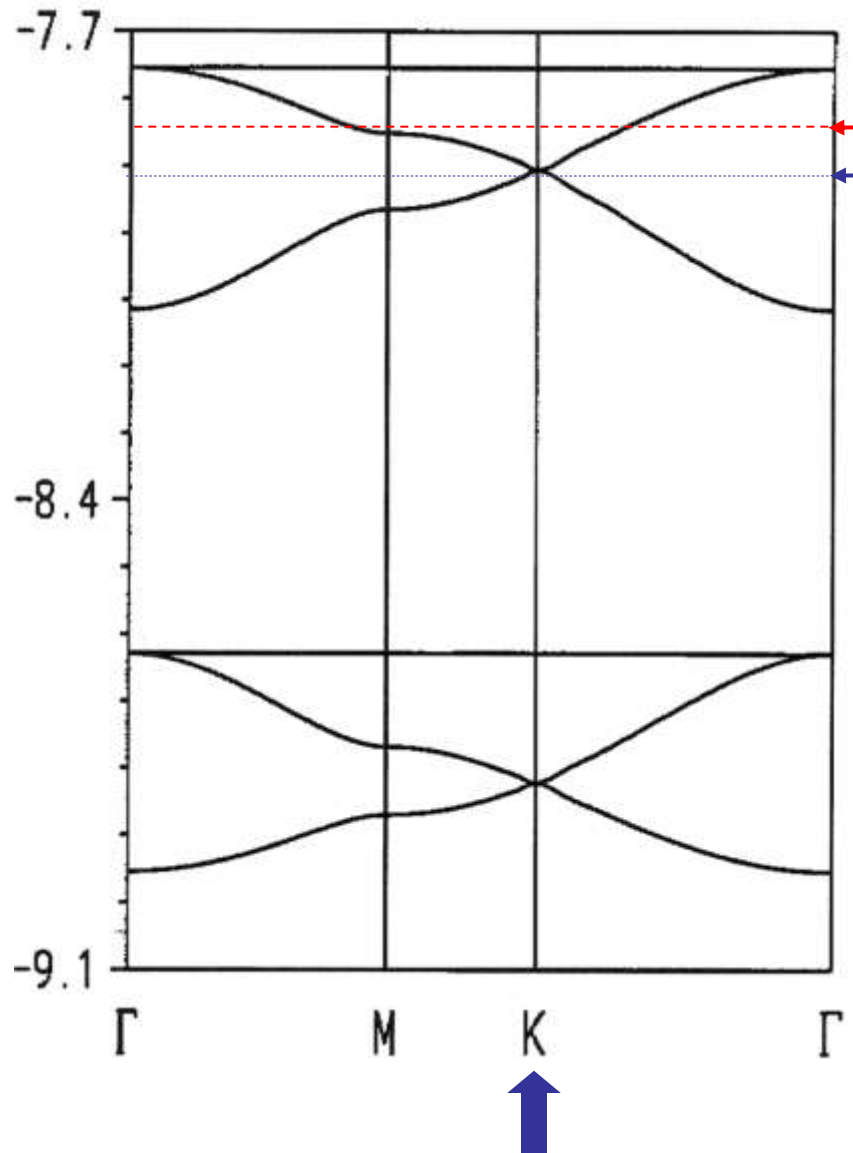
interdimer
0.1375 eV

$(\text{EDT-TTF-CONH}_2)_6^{(4-\rho)+} [\text{Re}_6\text{Se}_8(\text{CN})_6]^{(4-\rho)-}$

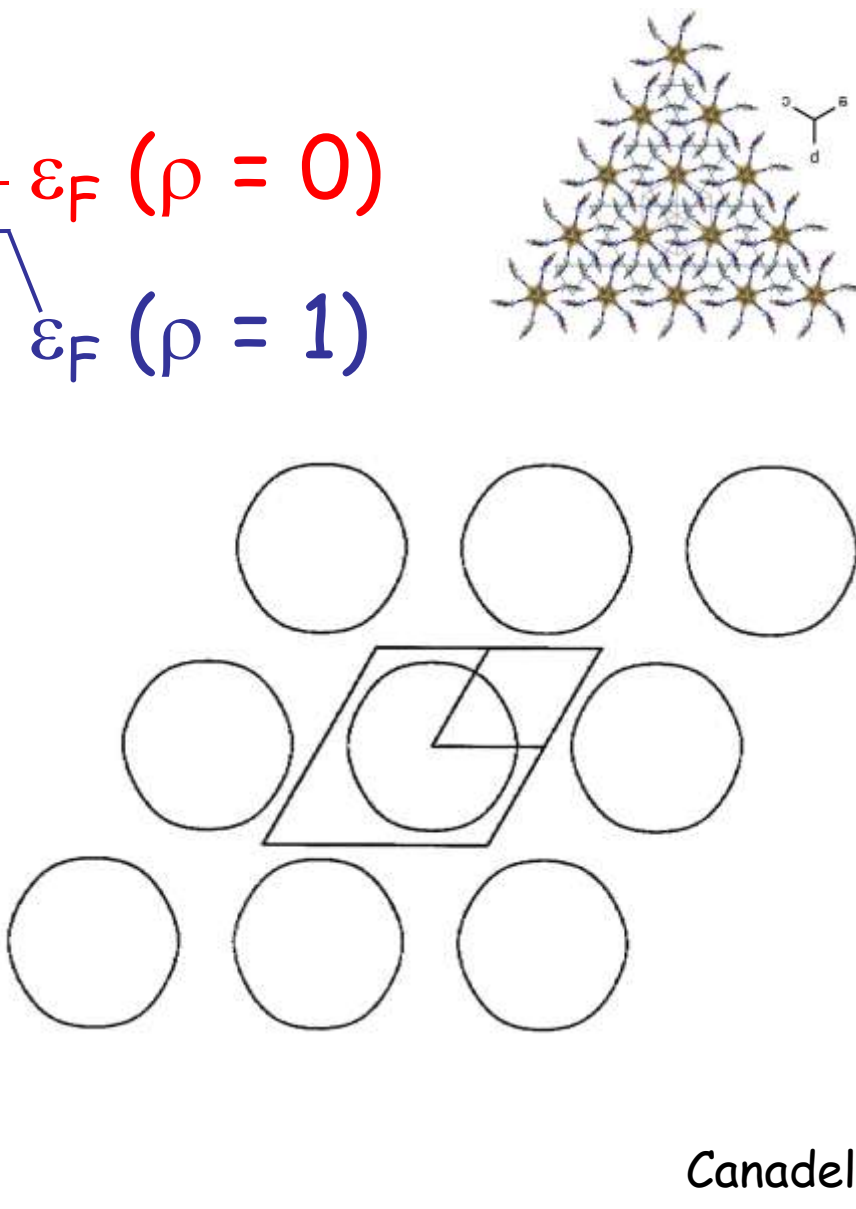


2D

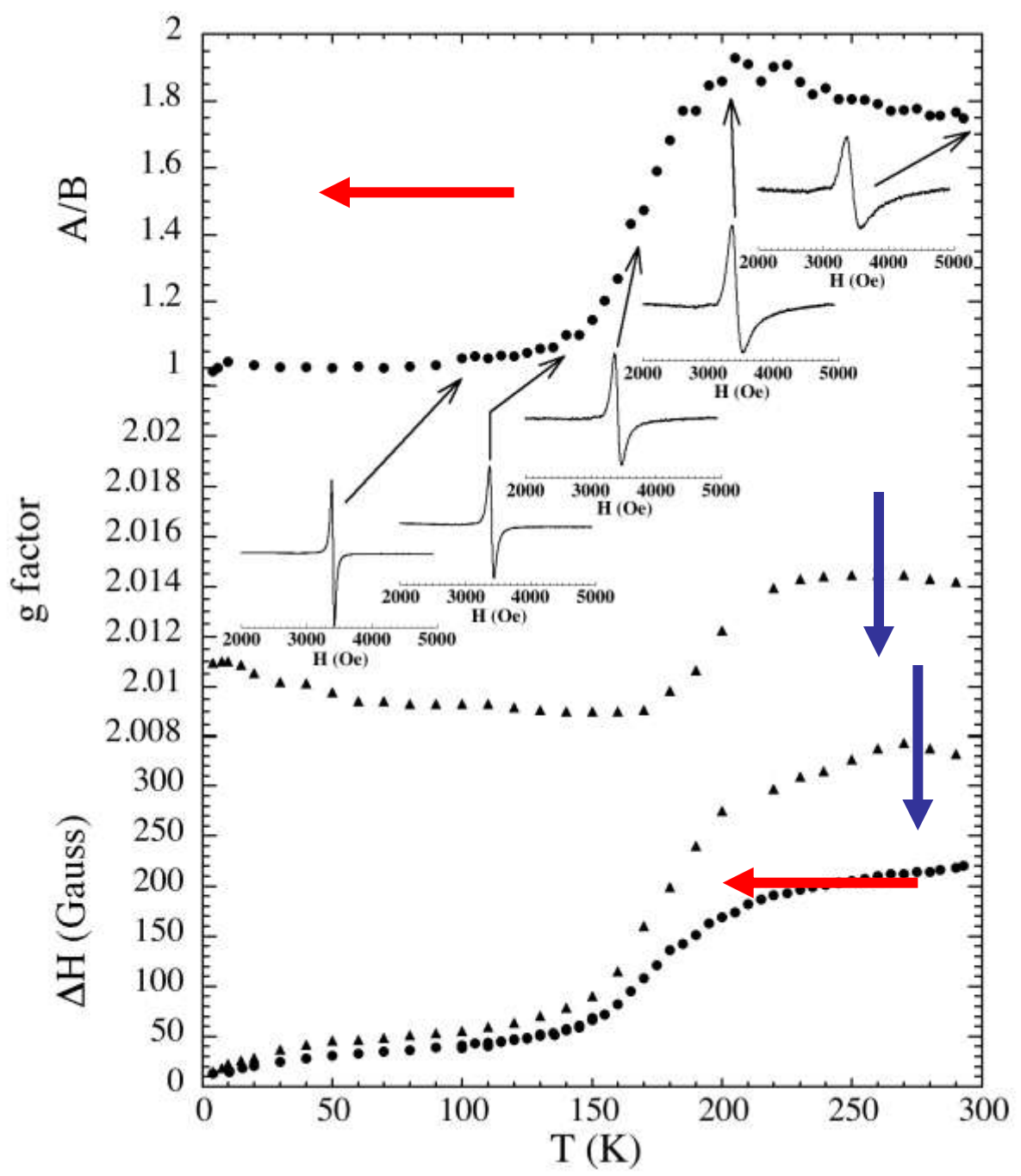
$(\text{EDT-TTF-CONH}_2)_6^{(4-\rho)+} [\text{Re}_6\text{Se}_8(\text{CN})_6]^{(4-\rho)-}$



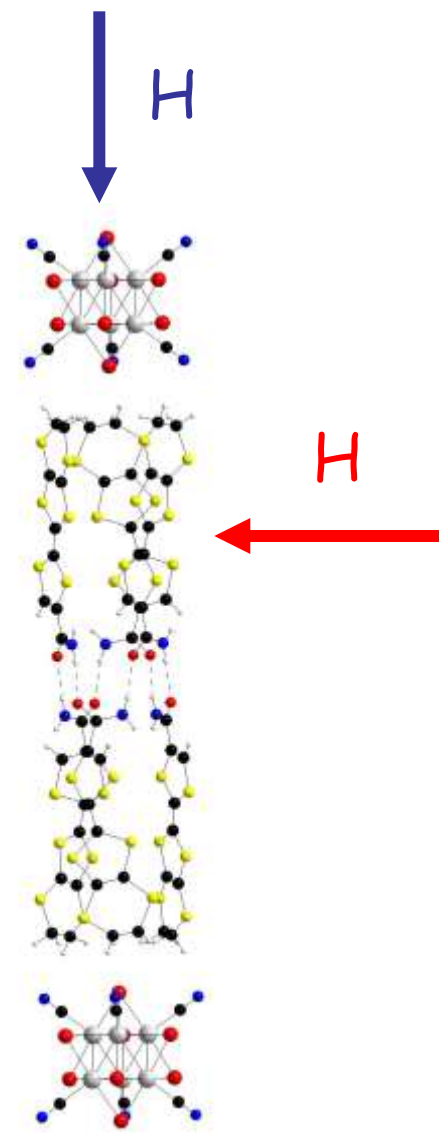
$\epsilon_F (\rho = 0)$
 $\epsilon_F (\rho = 1)$



Canadell



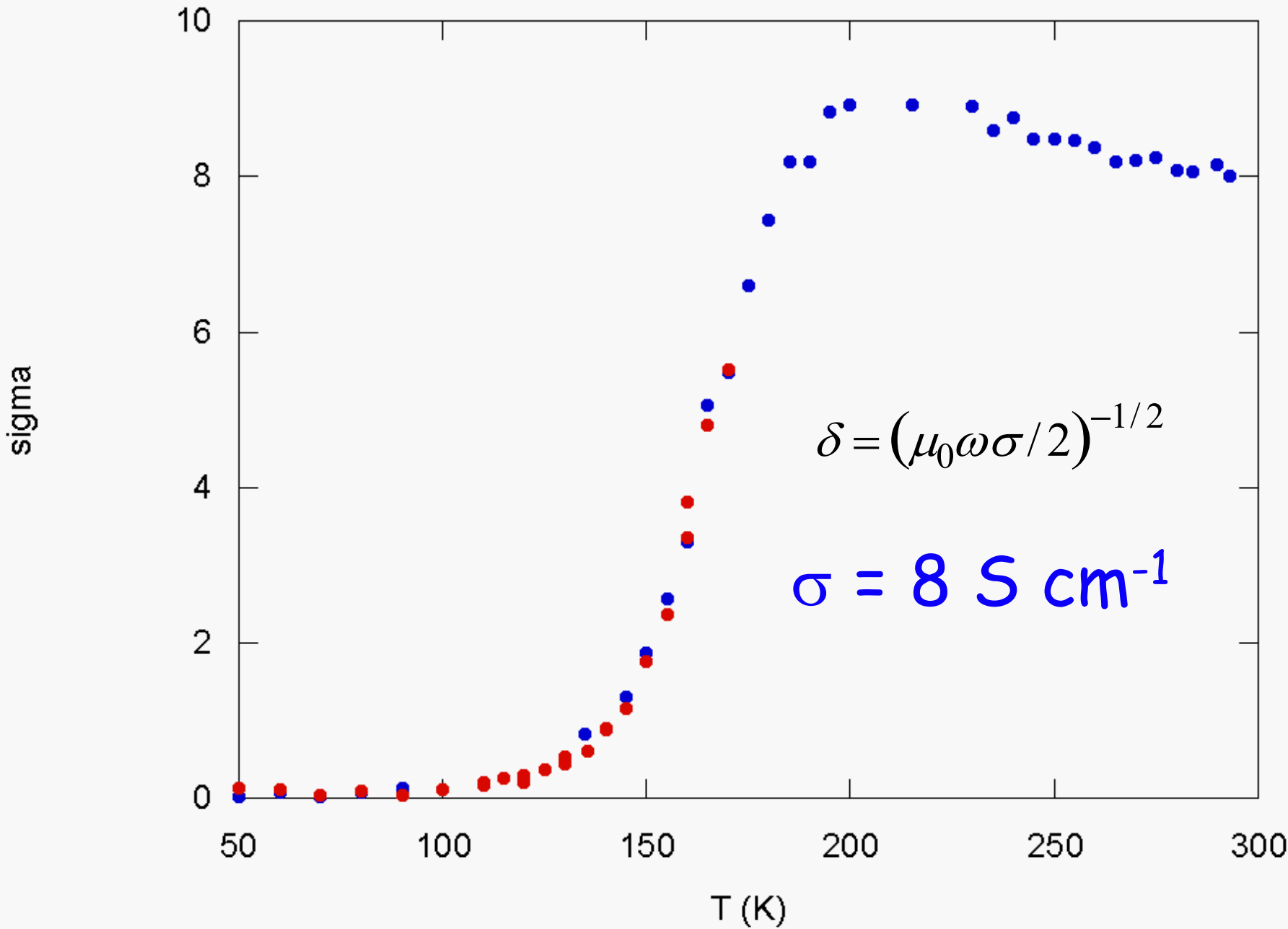
single crystal esr



Coulon, Clérac

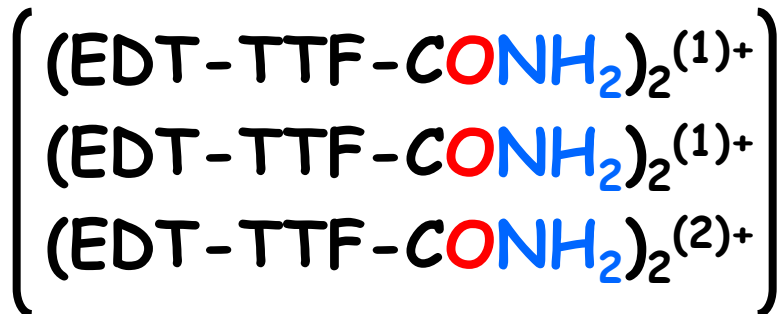
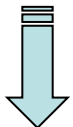
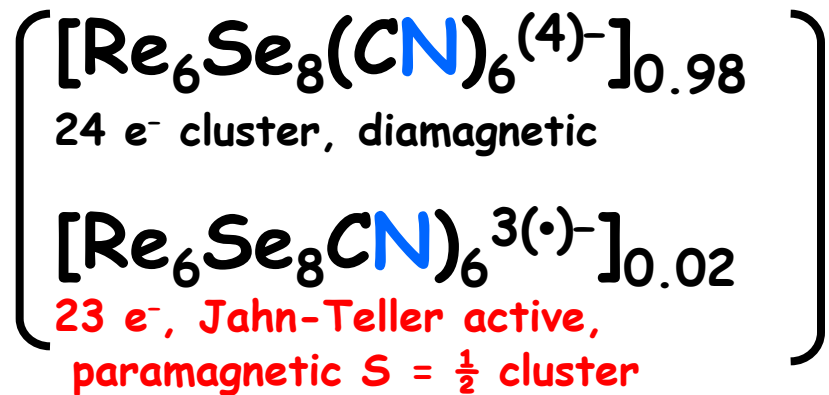
ESR conductivity

Donnees kagome



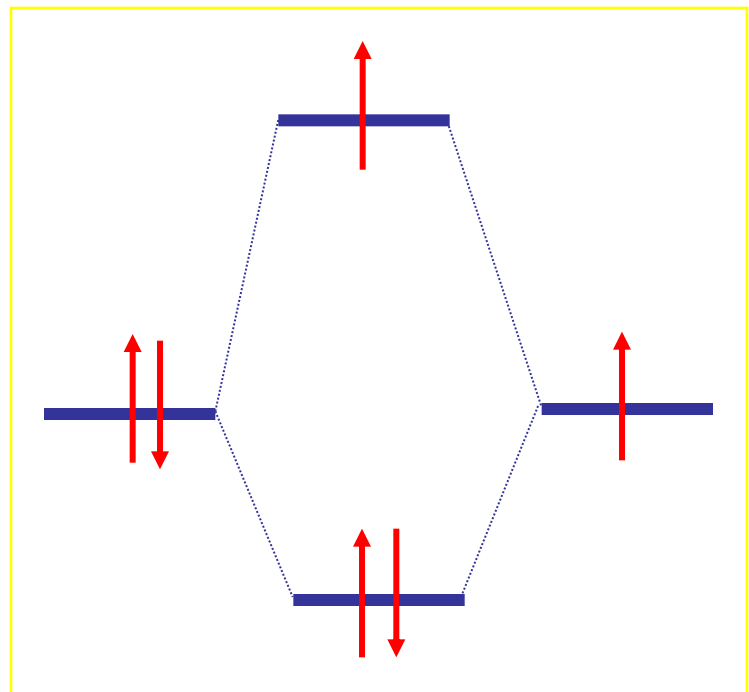
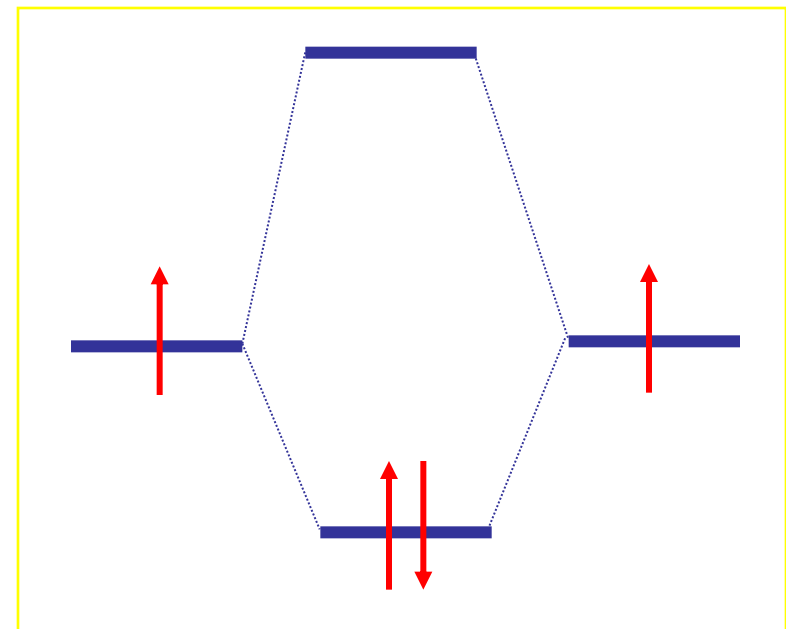
carriers

at room temperature:



below transition

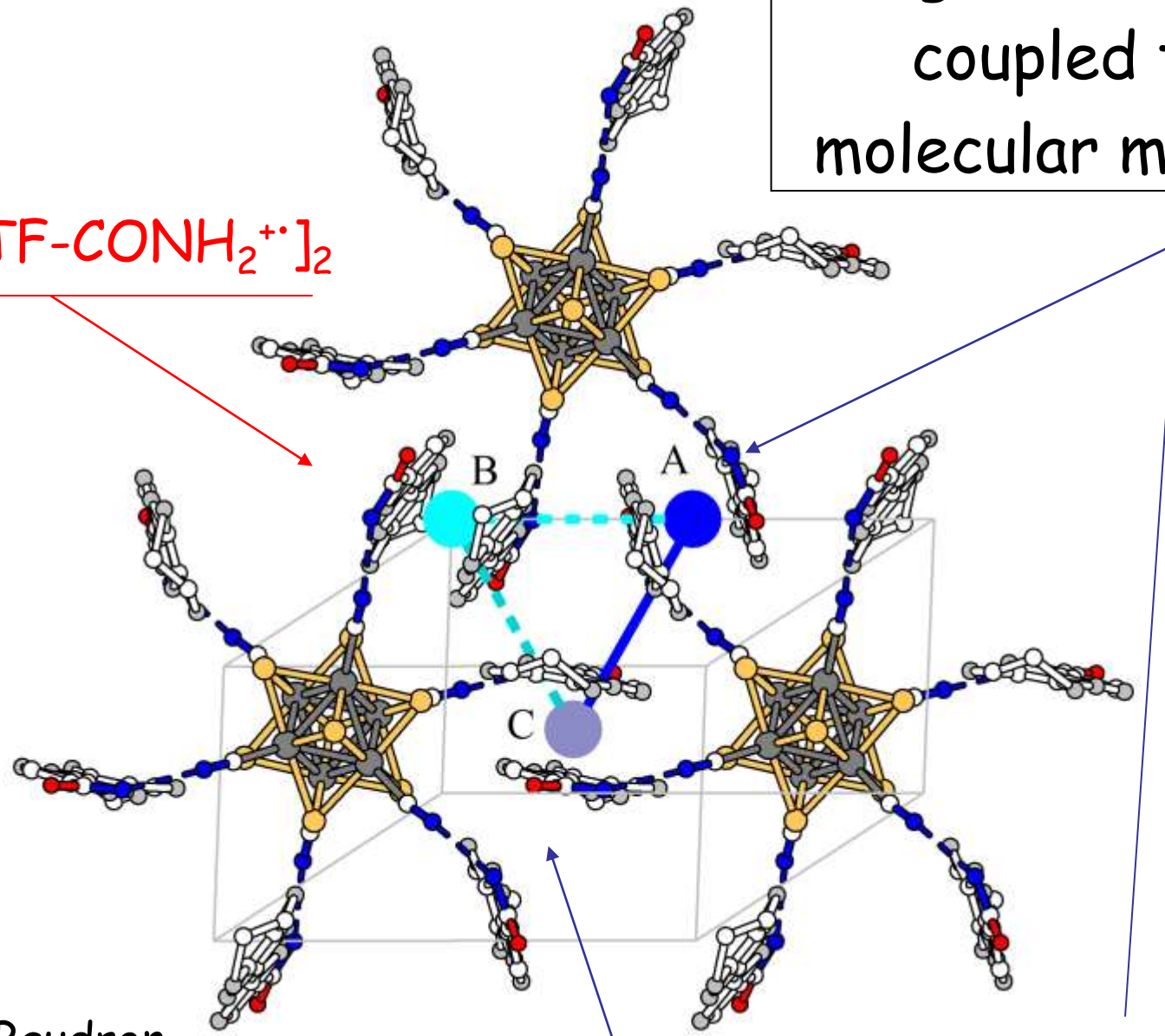
charge disproportionation
charge ordering



triclinic structure @ 100 K

charge localization
coupled to
molecular motion

[EDT-TTF-CONH₂⁺]₂



Stéphane Baudron
Lika Zorina

[EDT-TTF-CONH₂⁺]₂

Mott localization below 200 K

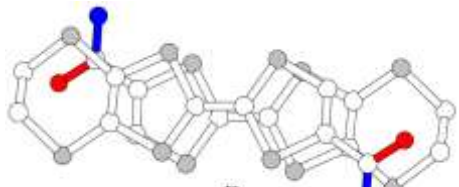
100

300

T(K)

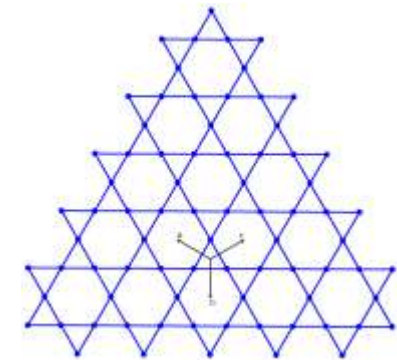
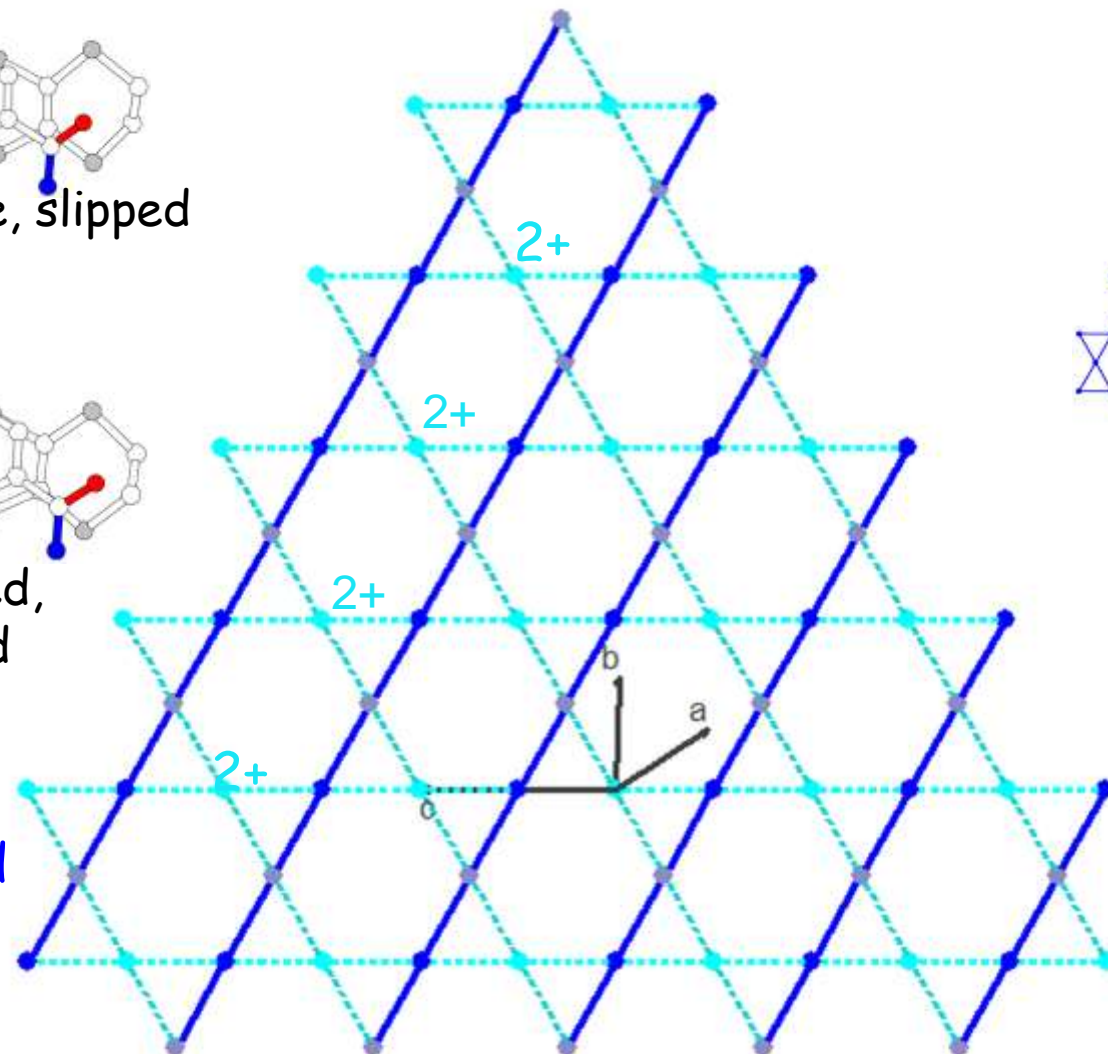


mixed valence, slipped

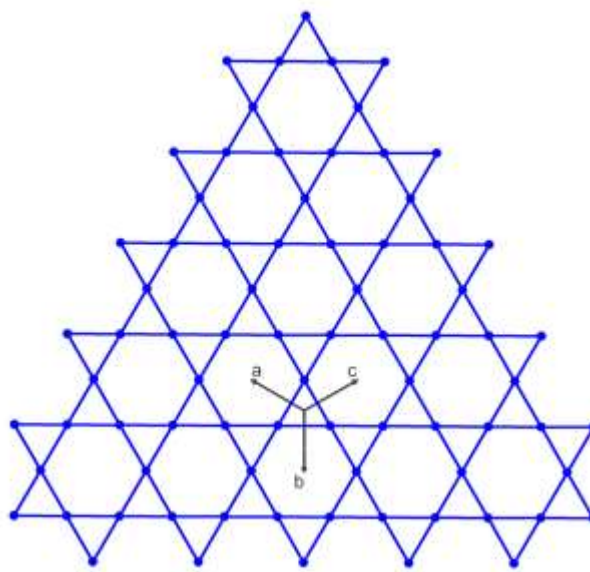


fully oxidized,
more eclipsed

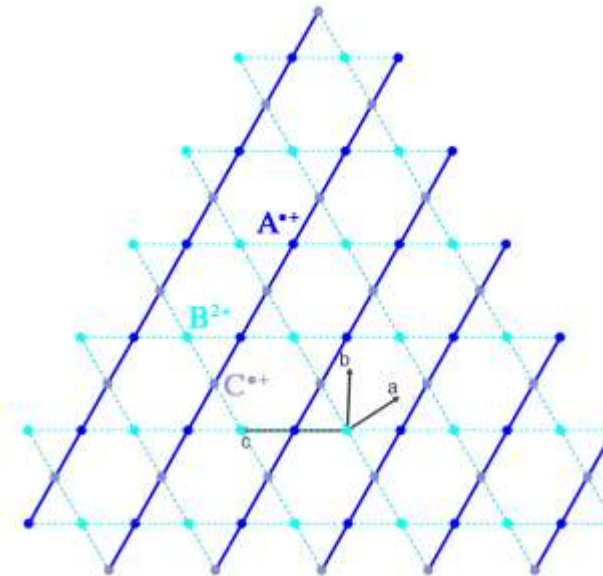
charges
are ordered



Conclusion: Mott localization

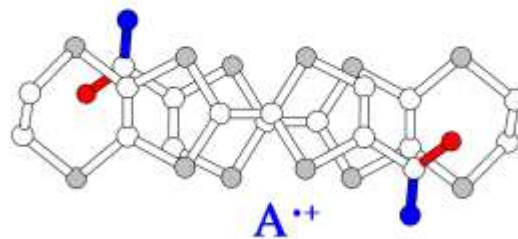


a)

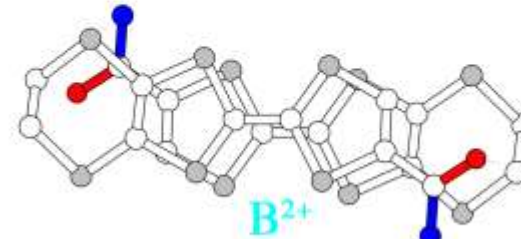


b)

M-I transition coupled to phase transition



c)



d)

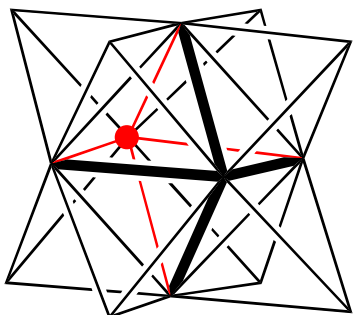
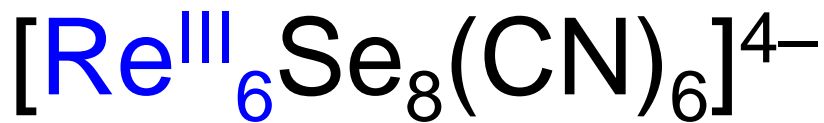
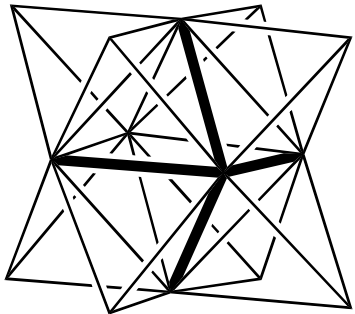
molecular motion (softness of interfacial H-bond interactions)

try and control the property

HOW ?

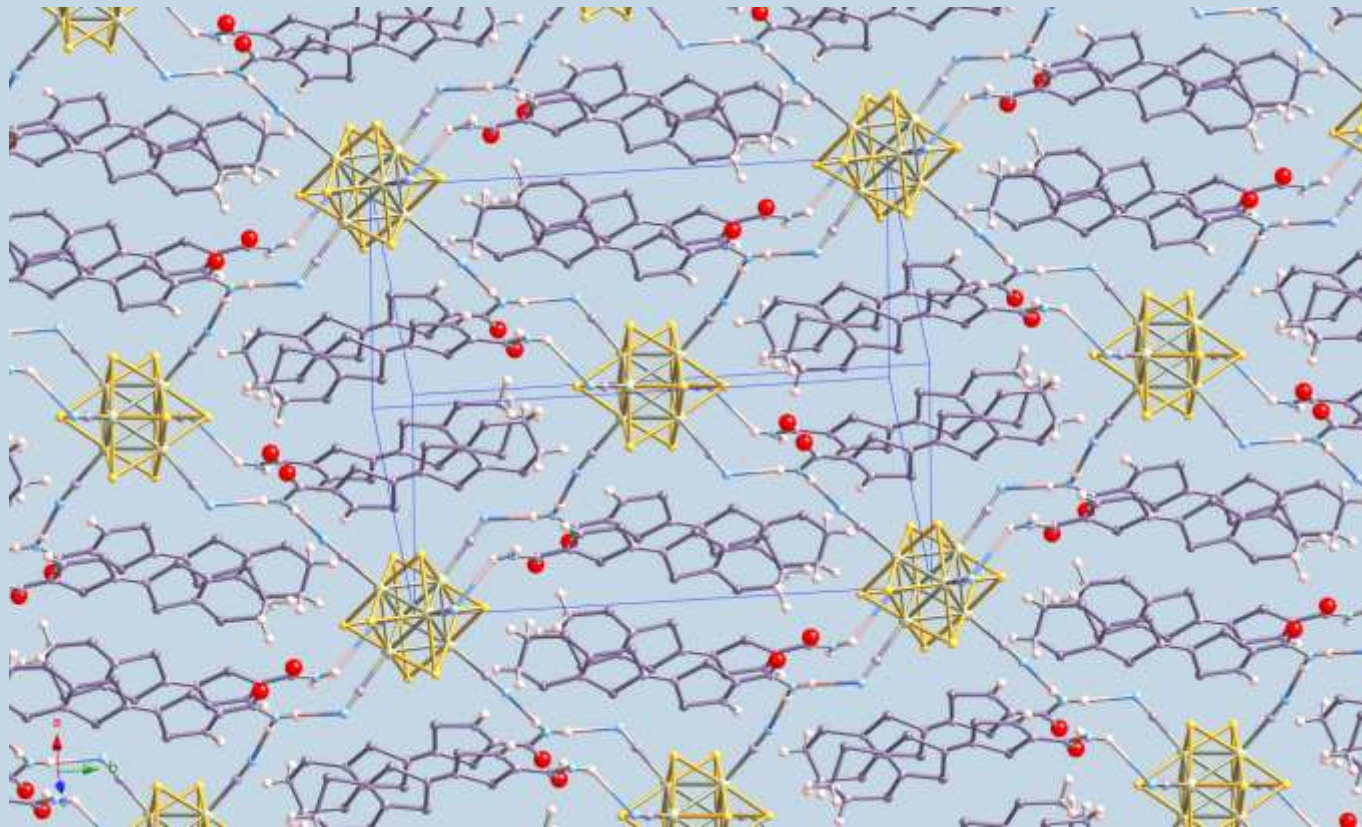
- keeping with Kagome lattice
- change anion charge !

substitute one Re(III) for one Os(IV)



Baudron, Batail + Tulski, Long
France-Berkeley Program 2001-02

$(\text{EDT-TTF-CONH}_2)_4^{(3)+} [\text{Re}_5\text{OsSe}_8(\text{CN})_6]^{(3)-}$



$(\text{EDT-TTF-CONH}_2)_6^{(4)+} [\text{Re}_6\text{Se}_8(\text{CN})_6]^{(4)-}$

OUTLINE

1. electrocrystallization
2. redox chemistry
3. intermolecular interactions, and their redox activation, direct the structure
4. orbitals and band (in one dimension)
5. decipher BS of TTF-TCNQ, Bechgaard salts
6. modify / control electronic structure
 - 6.1 tune anion charge
 - 6.2 tune stoichiometry
 - 6.3 ternary phases by halogen bonding

O-H \cdots O et N-H \cdots O: normal hydrogen bonds

$\text{NH}_4^+ \cdots \text{OH}_2$	19 kcal mole $^{-1}$	0.8 eV
$\text{HO}-\text{H} \cdots \text{Cl}^-$	13.5 kcal mole $^{-1}$	0.6 eV
$\text{HO}-\text{H} \cdots \text{OH}_2$	5 kcal mole $^{-1}$	0.2 eV

CH \cdots X: weaker hydrogen bonds

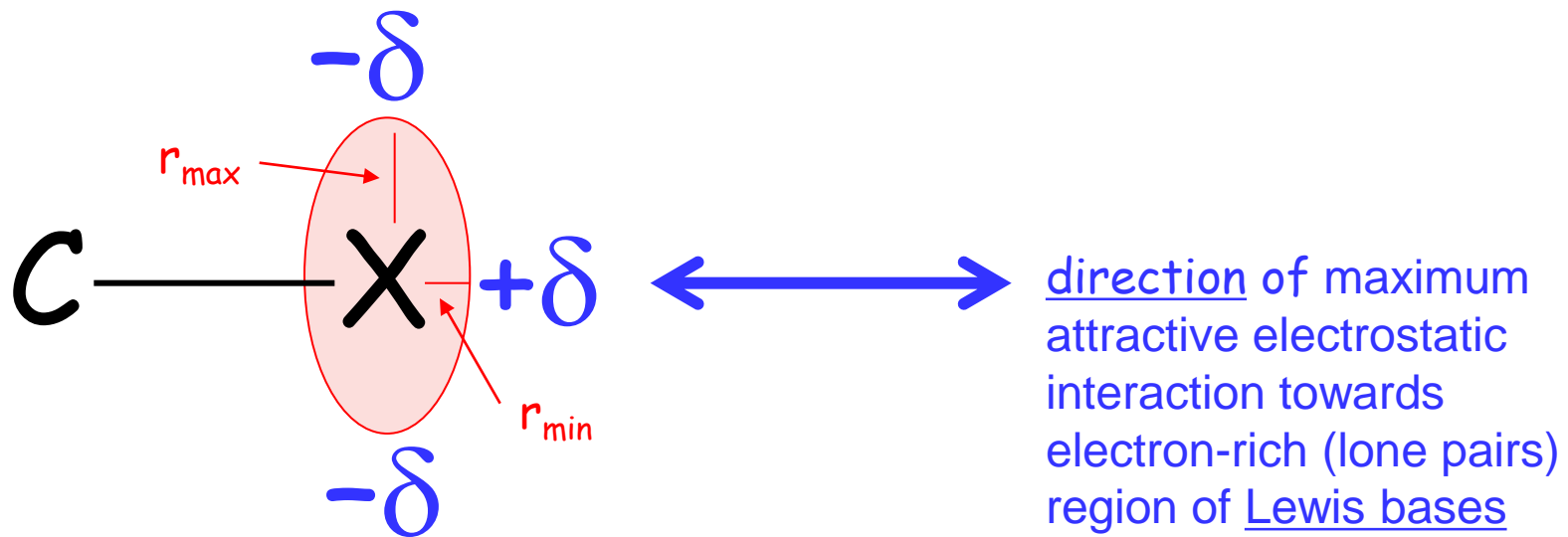
$\text{HC}\equiv\text{C}-\text{H} \cdots \text{OH}_2$	2.2 kcal mole $^{-1}$	0.1 eV
$\text{H}_2\text{C}=\text{C}-\text{H} \cdots \text{OH}_2$	1 kcal mole $^{-1}$	0.04 eV

halogen bonds: comparable to normal hydrogen bonds

$\text{C}-\text{Cl} \cdots \text{N}\equiv\text{C}$	2.4 kcal mole $^{-1}$	0.1 eV
$\text{CF}_3-\text{I} \cdots \text{NH}_3$	6 kcal mole $^{-1}$	0.3 eV

$$1 \text{ kcal mole}^{-1} = 4.33641146 \times 10^{-2} \text{ eV}$$

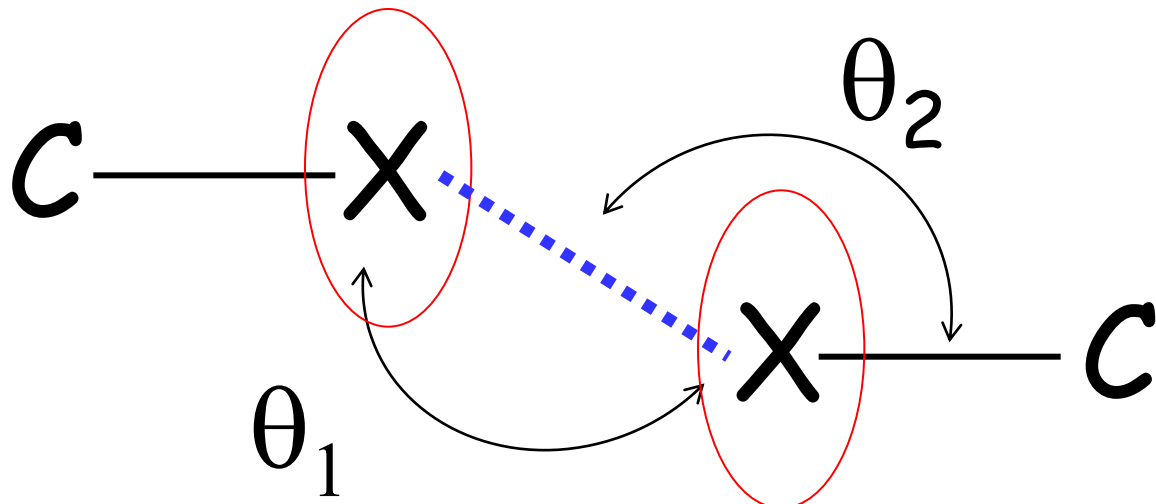
halogen bonding in the solid state: as strong and even more directional than hydrogen bonding



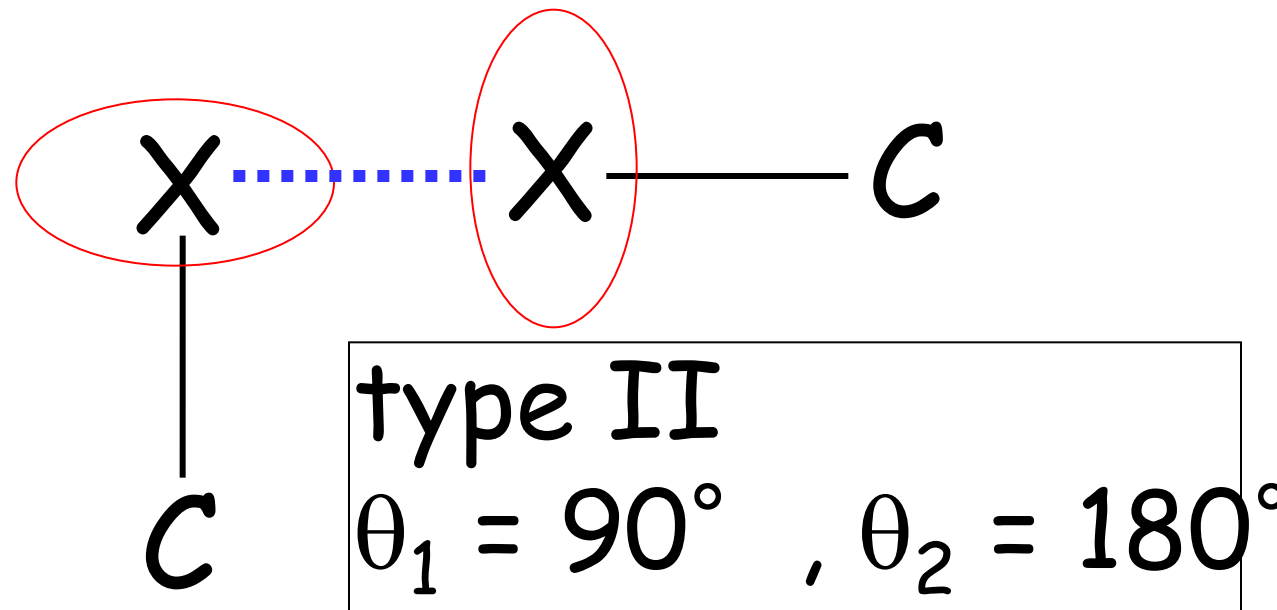
polar flattening

$-O-$, $C=O$
 $-S-$, $C=S$
 sp^3 and sp^2 amines (pyridine)
 $N\equiv C-$ groups
 $I>Br>Cl$

halogen bonding in the solid state: as strong and even more directional than hydrogen bonds



type I
 $\theta_1 = \theta_2$

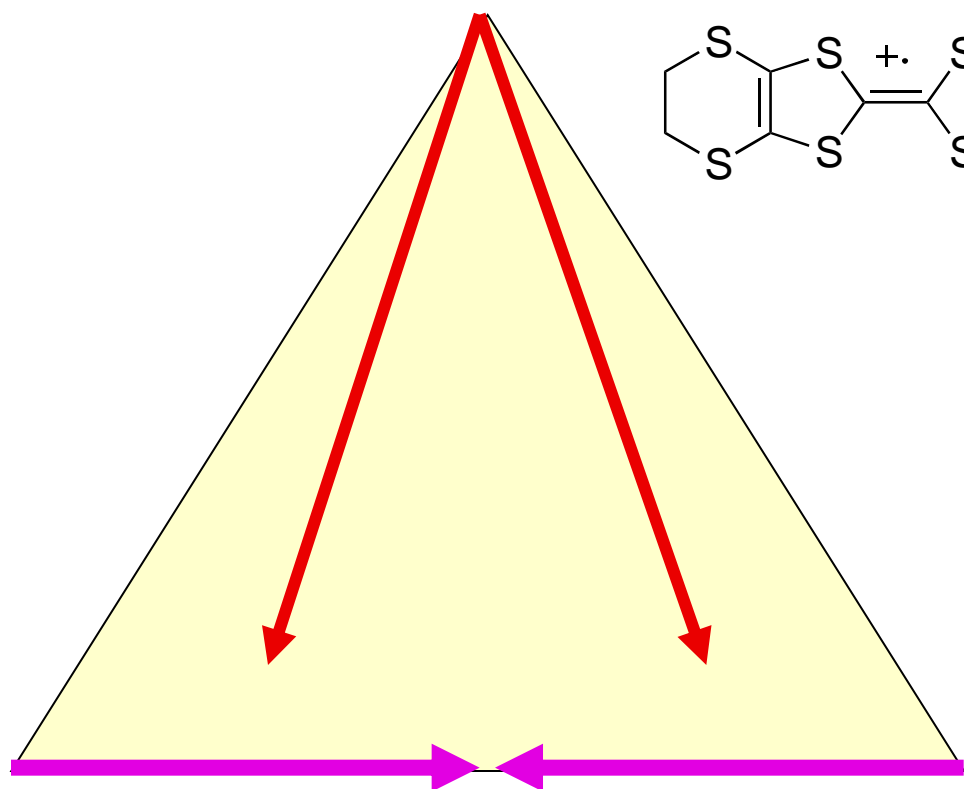
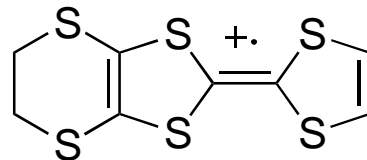


type II
 $\theta_1 = 90^\circ, \theta_2 = 180^\circ$

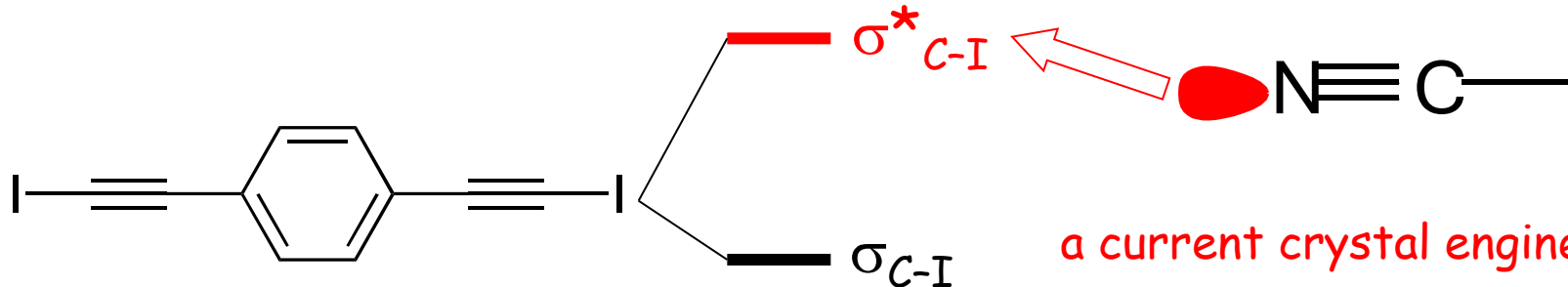
Desiraju et al.
JACS, 111, 8725 (1989)

Fourmigué, Batail
Chem. Rev. 104, (2004)

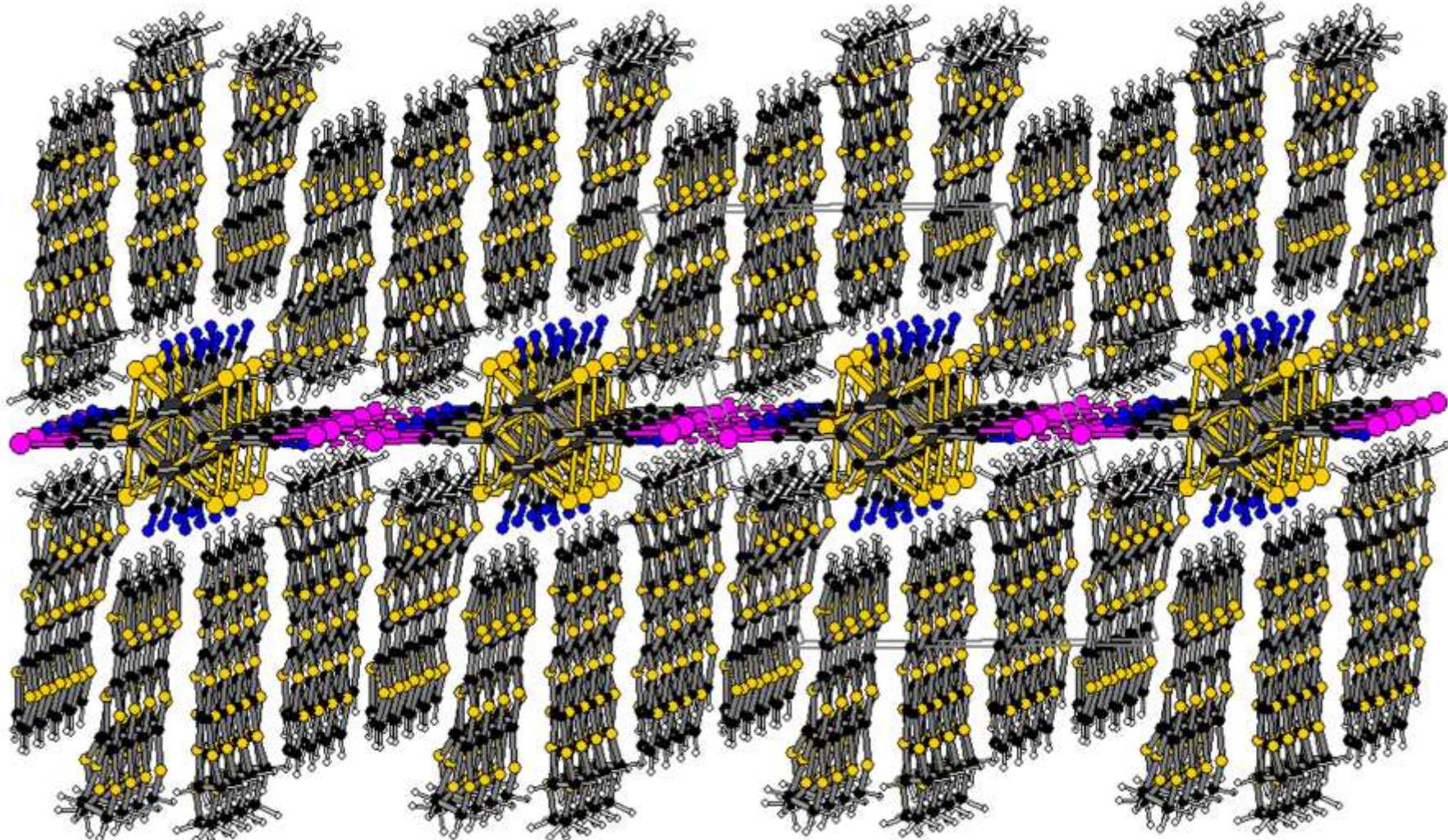
EDT-TTF^{•+}



also probing the extend of a covalent component to halogen bonding:



a current crystal engineering issue



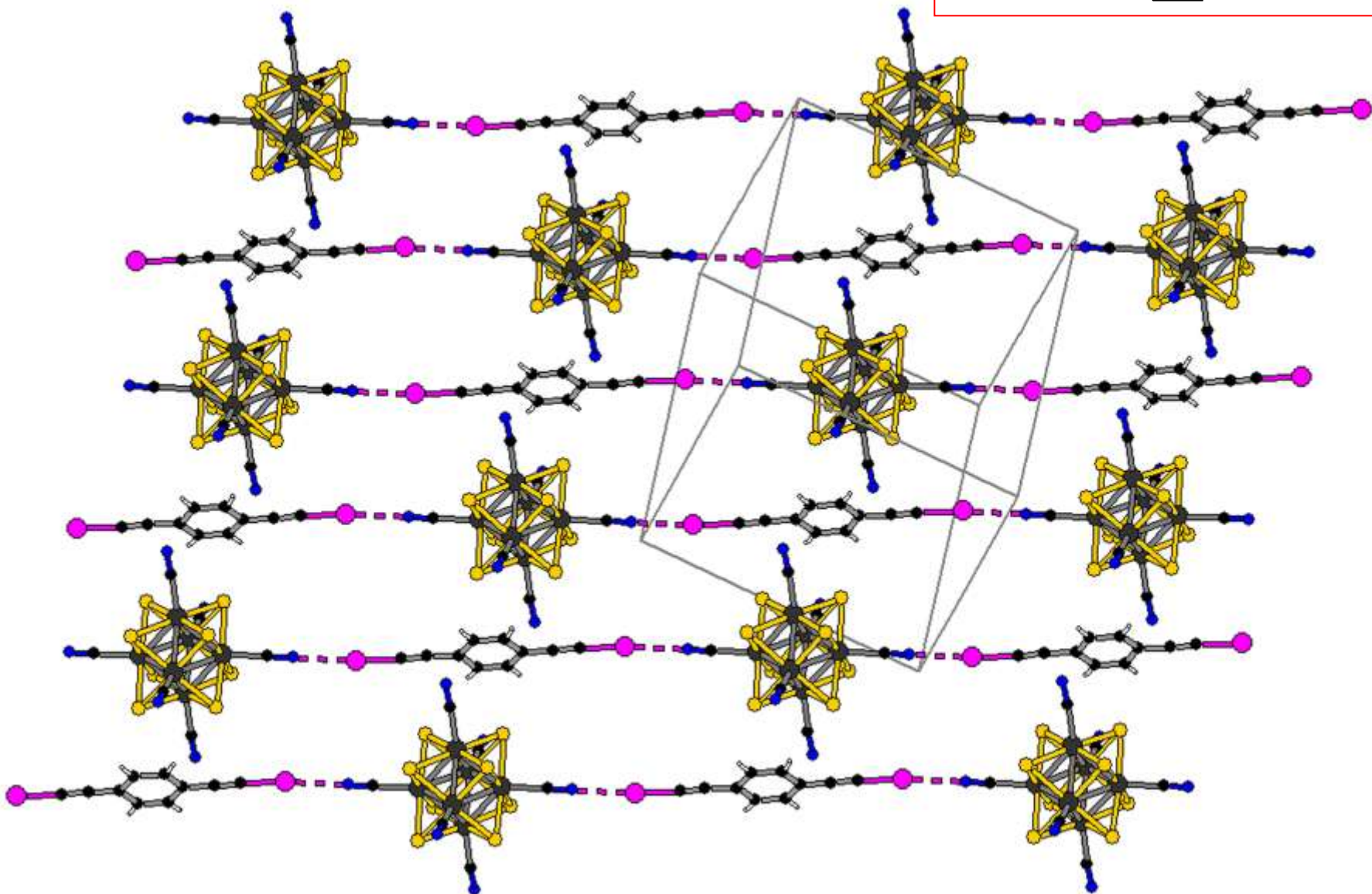
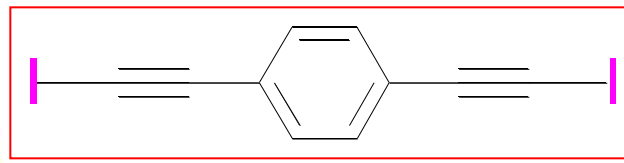
Anne-Lise Barrès

8:1:1

n:2:1

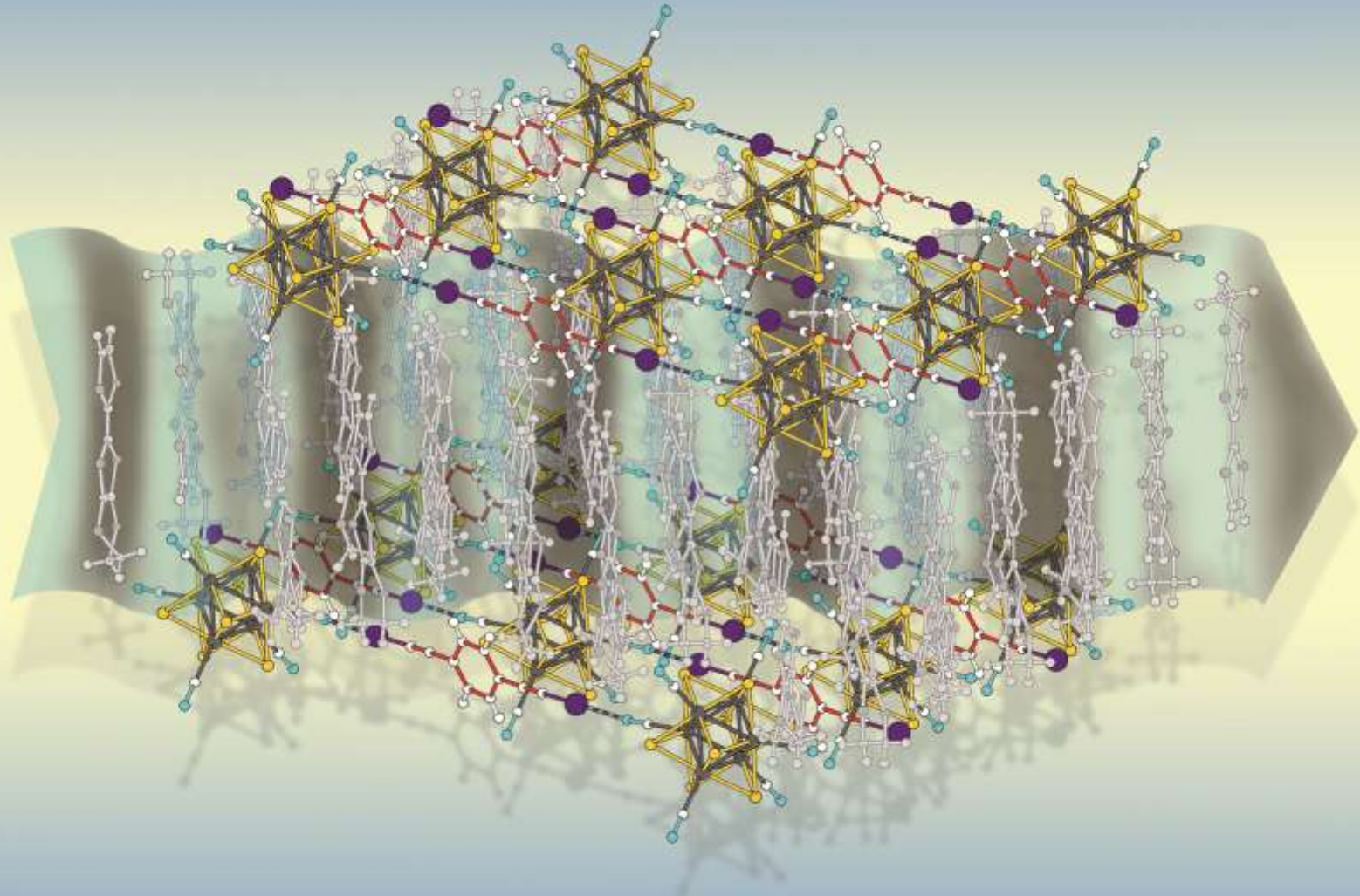
n:3:1

halogen-bonded co-polymer



$(\text{EDT-TTF})_8(p\text{-BIB}) \bullet [\text{Re}_6\text{Se}_8(\text{CN})_6]$

$(EDT-TTF)_8 \bullet (p\text{-}BIB) \bullet [Re_6Se_8(CN)_6]$

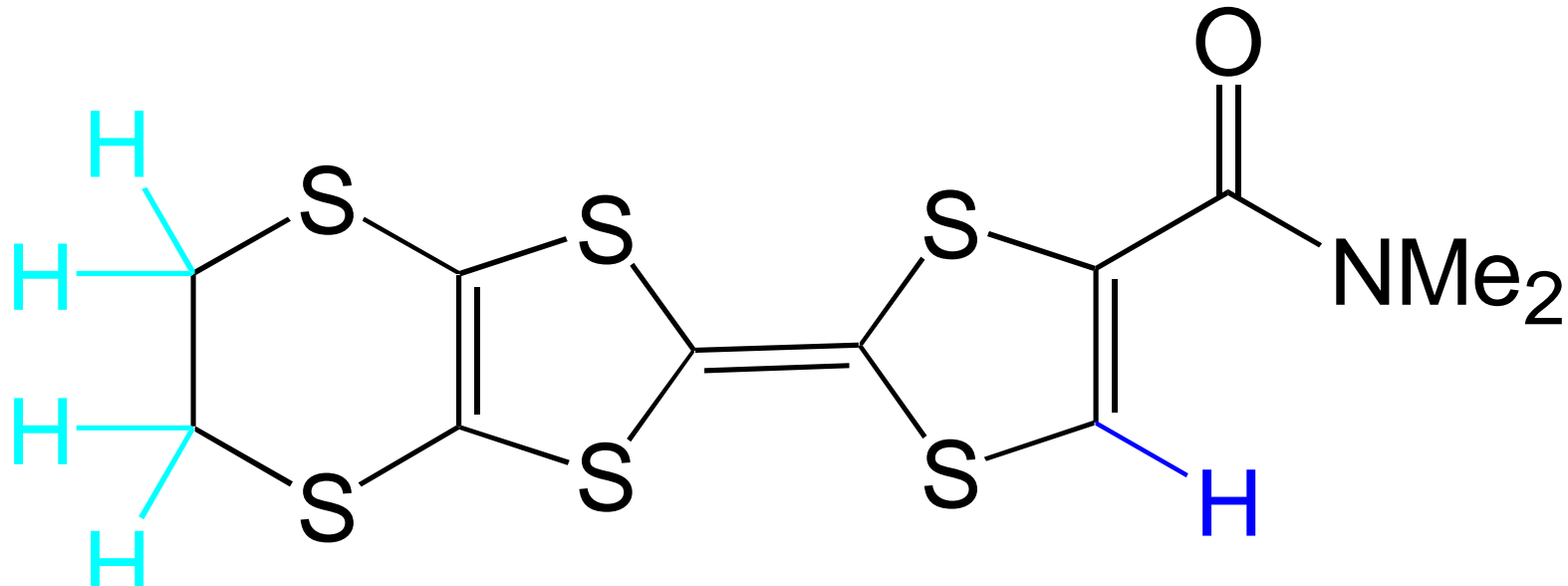


OUTLINE

1. electrocrystallization
2. redox chemistry
3. intermolecular interactions, and their redox activation, direct the structure
4. orbitals and band (in one dimension)
5. decipher BS of TTF-TCNQ, Bechgaard salts
6. modify / control electronic structure
 - 6.1 tune stoichiometry
 - 6.2 tune anion charge
 - 6.3 ternary phases by halogen bonding
 - 6.4 $[H^+]/[\text{hole}]$ mixed valence
 - 6.5 chemical pressure

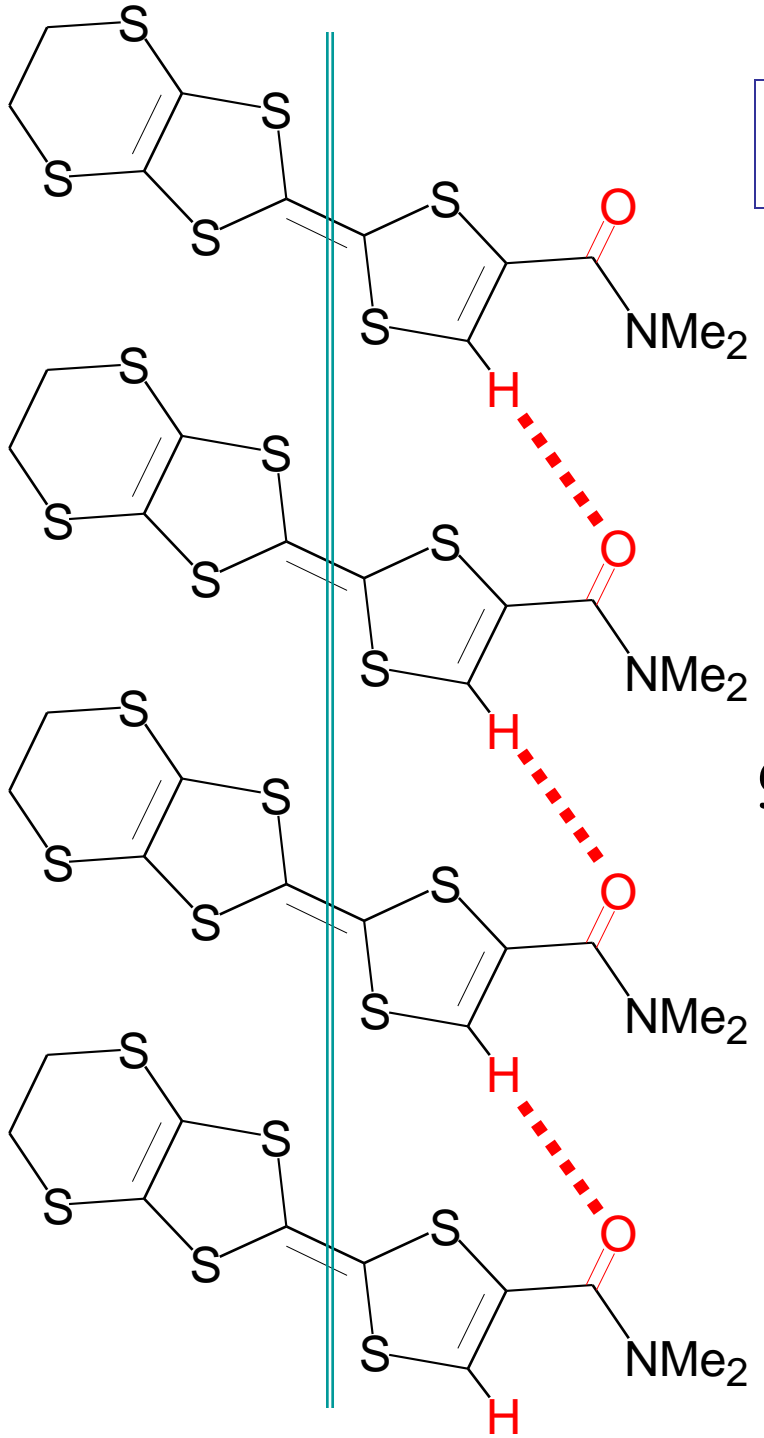
$\delta-(\text{EDT-TTF-CONMe}_2)_2X$, $X = \text{AsF}_6^-$, Br^-

genuine 3/4-filled band Mott insulators



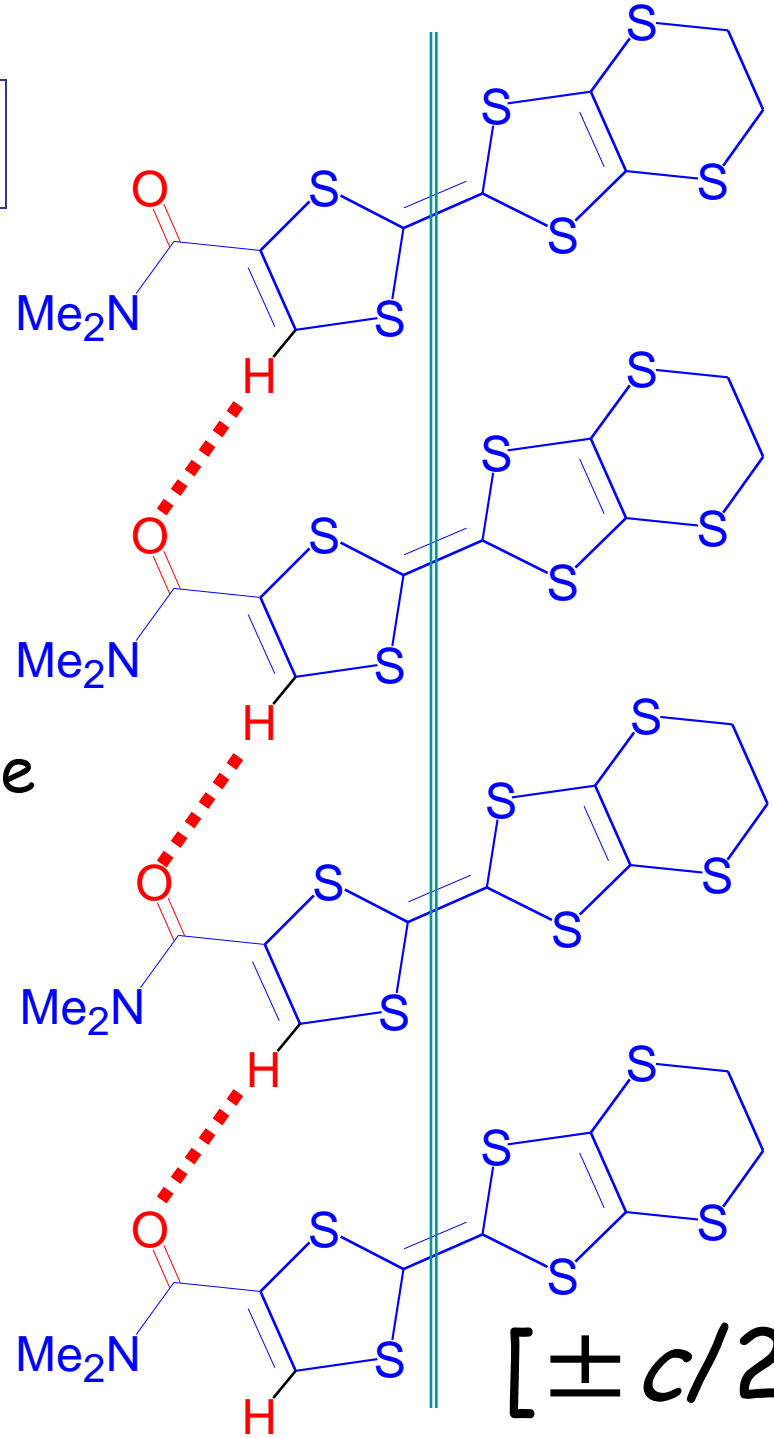
C_1 symmetry

K. HEUZÉ, M. FOURMIGUÉ, P. BATAIL, C. COULON, R. CLÉRAC, E. CANADELL,
P. AUBAN-SENZIER, S. RAVY, D. JÉROME
Adv. Mater. 15, 1251-1254 (2003)

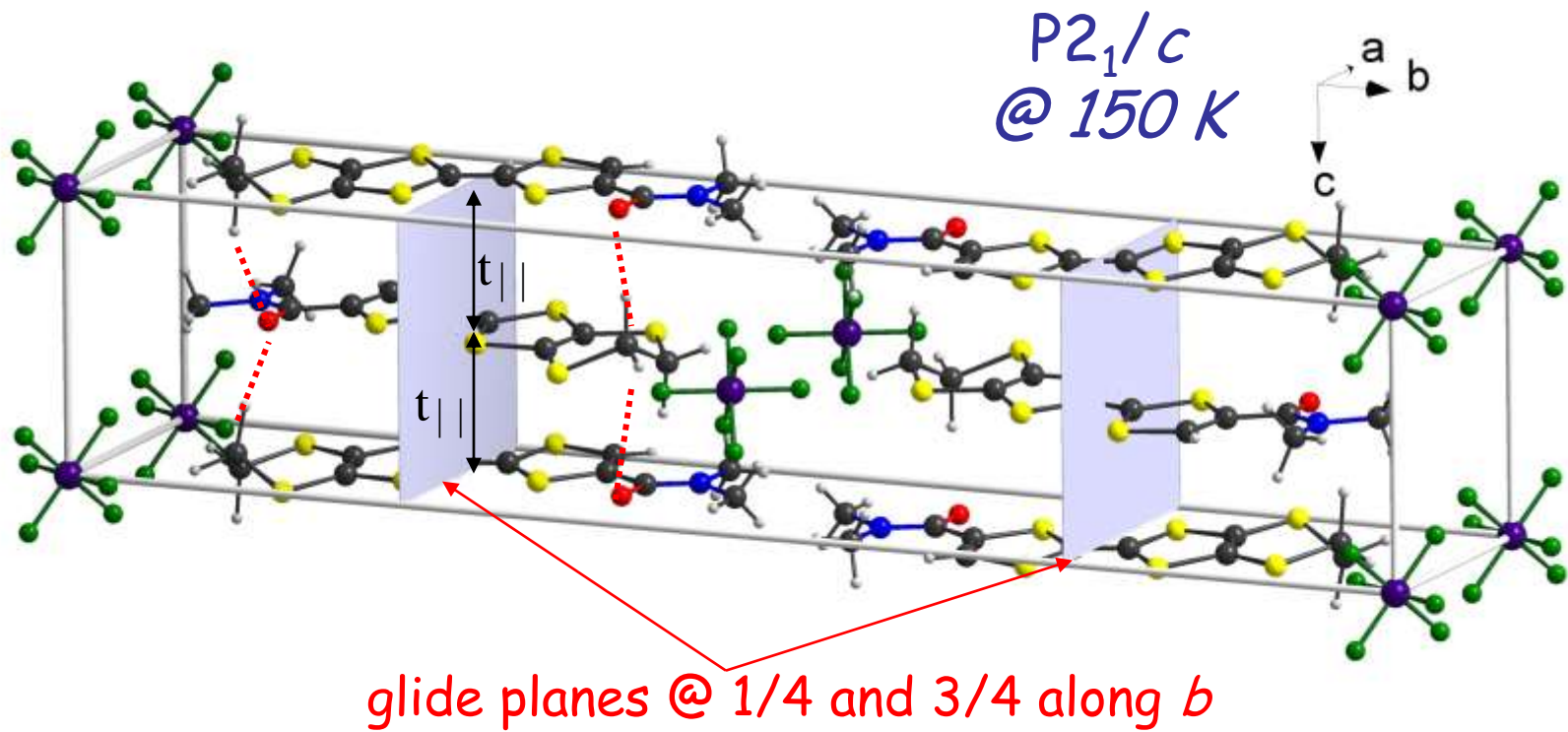


P2₁/c

apply
glide plane



glide plane imposed by the C_1 Molecular Symmetry



glide plane imposes stack uniformity

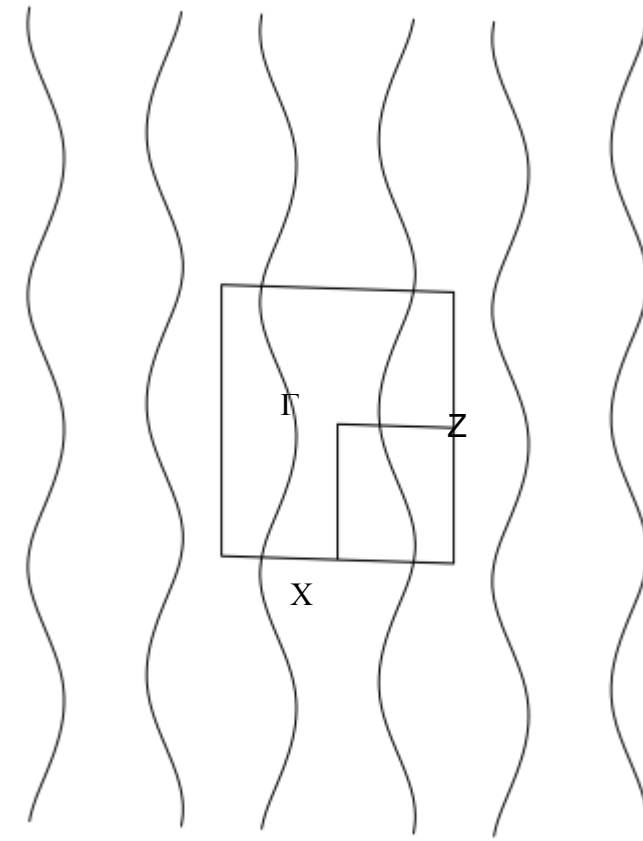
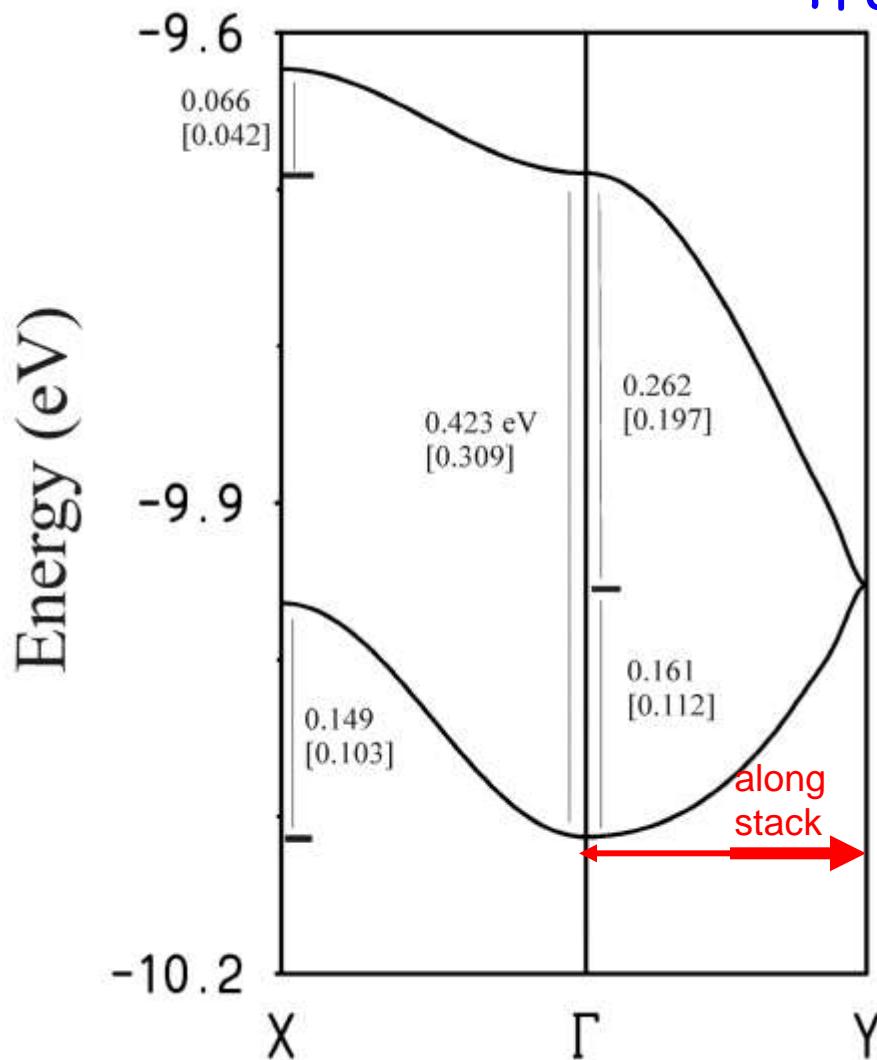
non dimerized, 2 molecules, 1 hole per unit along chain:

band is $\frac{1}{4}$ -filled with holes

$t_{||} = + 71 \text{ meV}$ despite criss-cross overlap:

band structure and Fermi surface: a sizeable t_{\perp}

Transfer integrals Br^- vs $[\text{AsF}_6^-]$

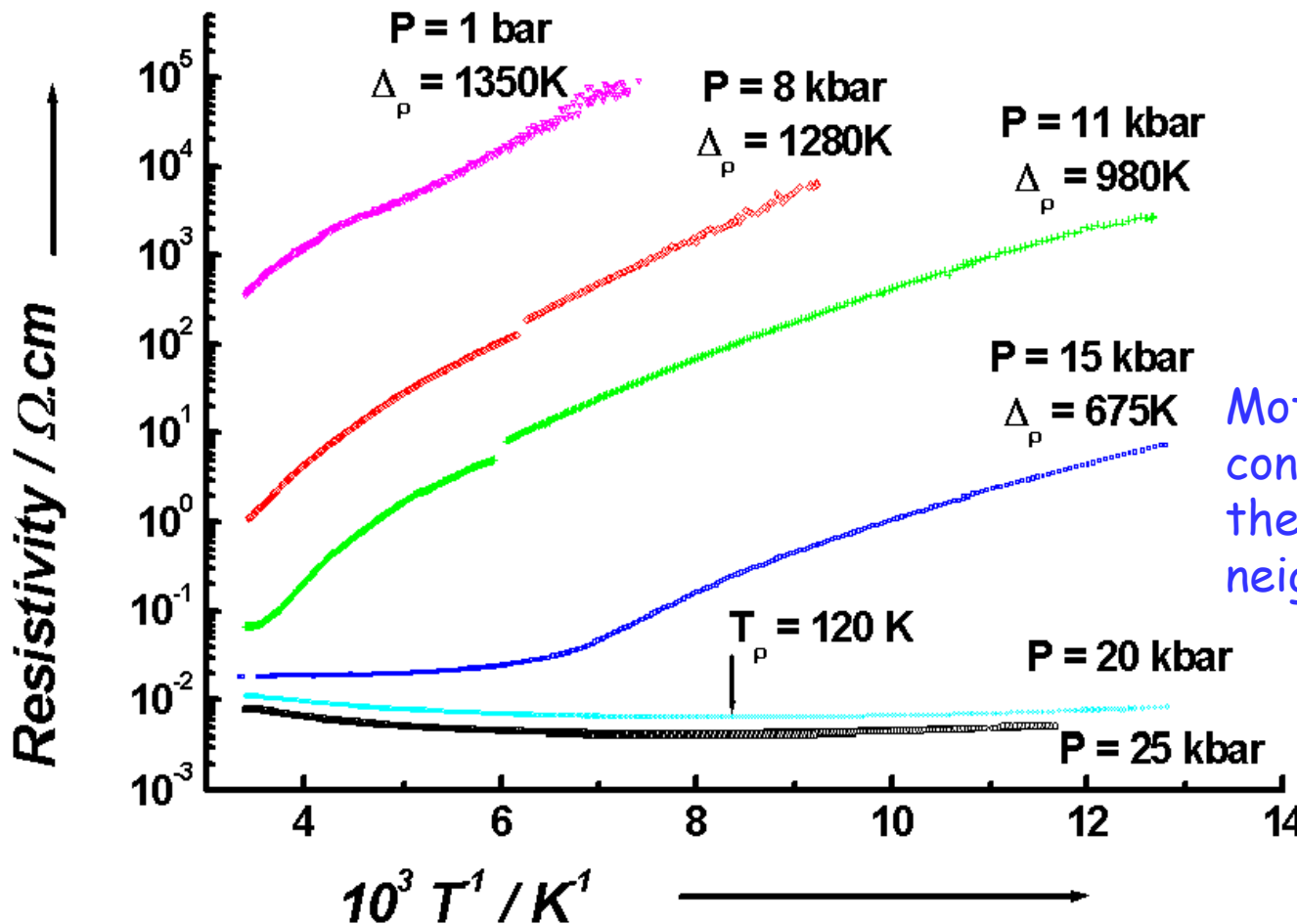


total bandwidth is 0.31 eV for AsF_6^- : very similar to $(\text{TMTTF})_2\text{Br}$
which, however, has a small dimerization gap of 0.027 eV

Enric Canadell

Mott insulator!!:

the underlying mechanism for fermions localization
can only come from the quarter-filling umklapp



AsF_6^-

Mott gap mostly
controlled by
the on-site and nearest
neighbor interactions

Auban-Senzier
Jérôme

decrease Mott gap by applying chemical pressure:

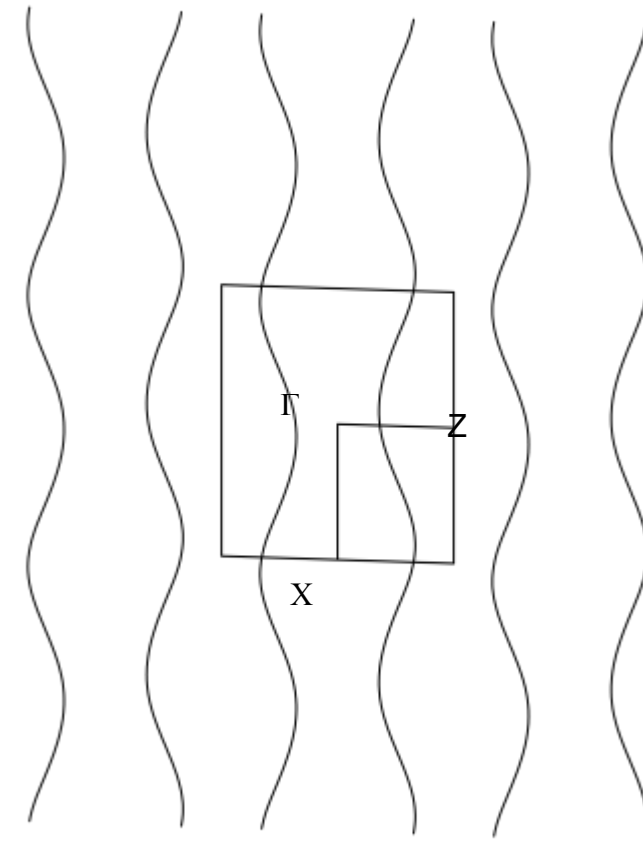
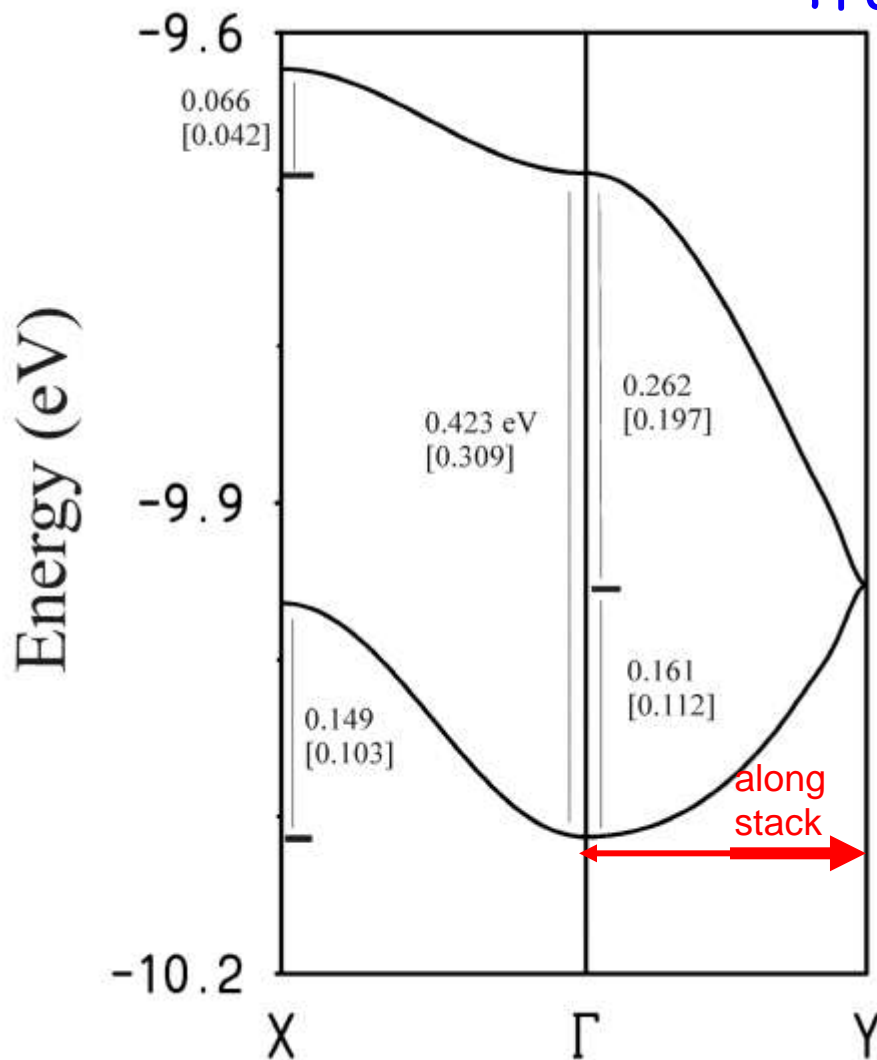
$$V (\text{AsF}_6^-) = V (\text{Br}^-) + 76 \text{ \AA}^3$$

	X = Br ⁻	X = AsF ₆ ⁻		
Temperature / K	150	295	100	150 295
a / Å	6.480(1)	6.5049(9)	6.422(1)	6.4459(8) 6.4622(3)
b / Å	6.9762(9)	7.1097(4)	7.0157(8)	7.0618(9) 7.2419(4)
c / Å	32.671(9)	32.691(3)	35.465(5)	35.562(4) 35.557(2)
α / °	90	90	90	90 90
β / °	90	90	90	90 90
γ / °	92.45(2)	90	92.26(1)	91.73(1) 90
V / Å ³	1475.6(5)	1511.9(3)	1596.6(3)	1618.0(3) 1664.0(2)

7 kbar

band structure and Fermi surface: a sizeable t_{\perp}

Transfer integrals Br^- vs $[\text{AsF}_6^-]$



total bandwidth is 0.31 eV for AsF_6^- : very similar to $(\text{TMTTF})_2\text{Br}$
which, however, has a small dimerization gap of 0.027 eV

Enric Canadell

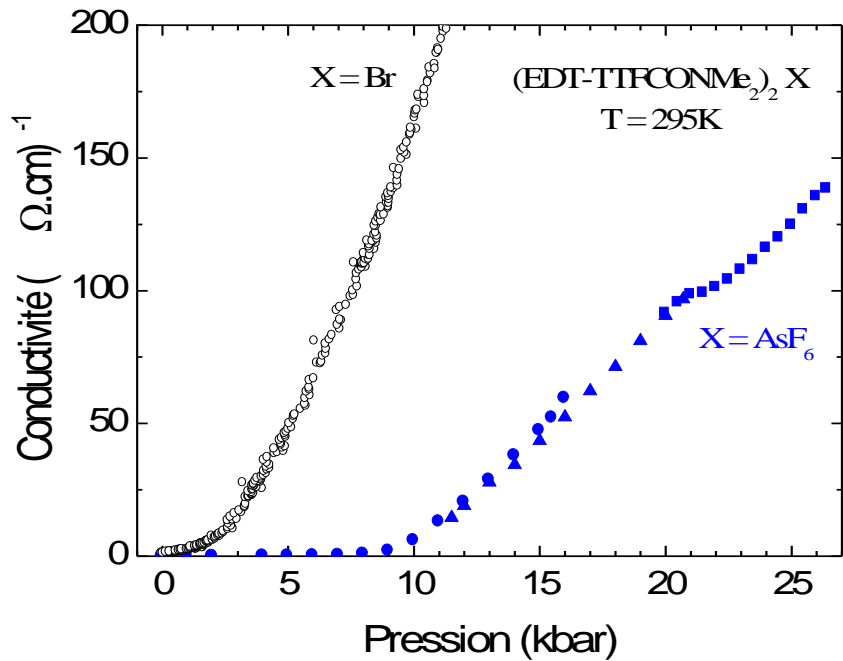
Table 4. Main parameters of the calculated band structure for δ -(EDT-TTF-CONMe₂)₂Br at room temperature (RT) and 150 K, and δ -(EDT-TTF-CONMe₂)₂AsF₆ at 100 K.

	W _c , meV	W _a , meV	W _{a'} , meV
δ -(EDT-TTF-CONMe ₂) ₂ Br at RT	371	84	194
δ -(EDT-TTF-CONMe ₂) ₂ Br at 150 K	423	66	149
δ -(EDT-TTF-CONMe ₂) ₂ AsF ₆ at 100 K	309	42	103

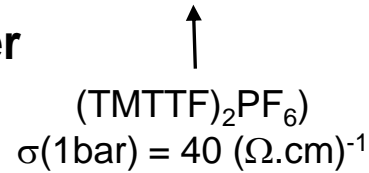
(EDT-TTF-CONMe₂)₂X

$X = \text{AsF}_6$ $\sigma(1\text{bar}) = 0.03$
 $(\Omega \cdot \text{cm})^{-1}$

$X = \text{Br}$ $\sigma(1\text{bar}) = 1 (\Omega \cdot \text{cm})^{-1}$

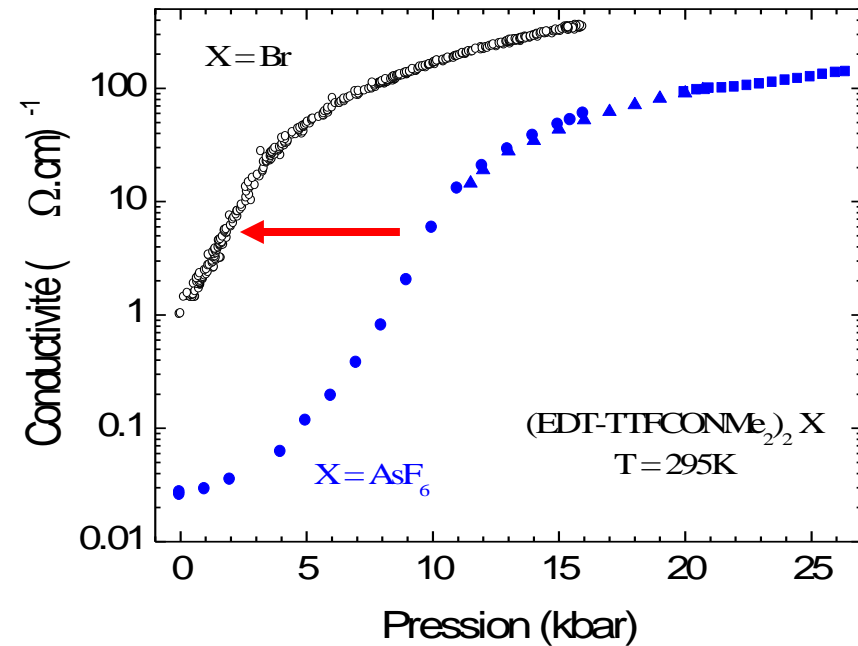


P. Auban-Senzier
C. Pasquier
D. Jérôme



Transport sous pression : $\sigma_c(P)$ à T ambiante

forte augmentation de $\sigma(P)$ à basse pression (régime localisé)
puis dépendance linéaire (idem $(\text{TM})_2\text{X}$) (régime métallique)
à partir de $X = \text{AsF}_6$: **décalage de 7 kbar / $X = \text{Br}$**
et de 15 kbar / $(\text{TMTTF})_2\text{PF}_6$

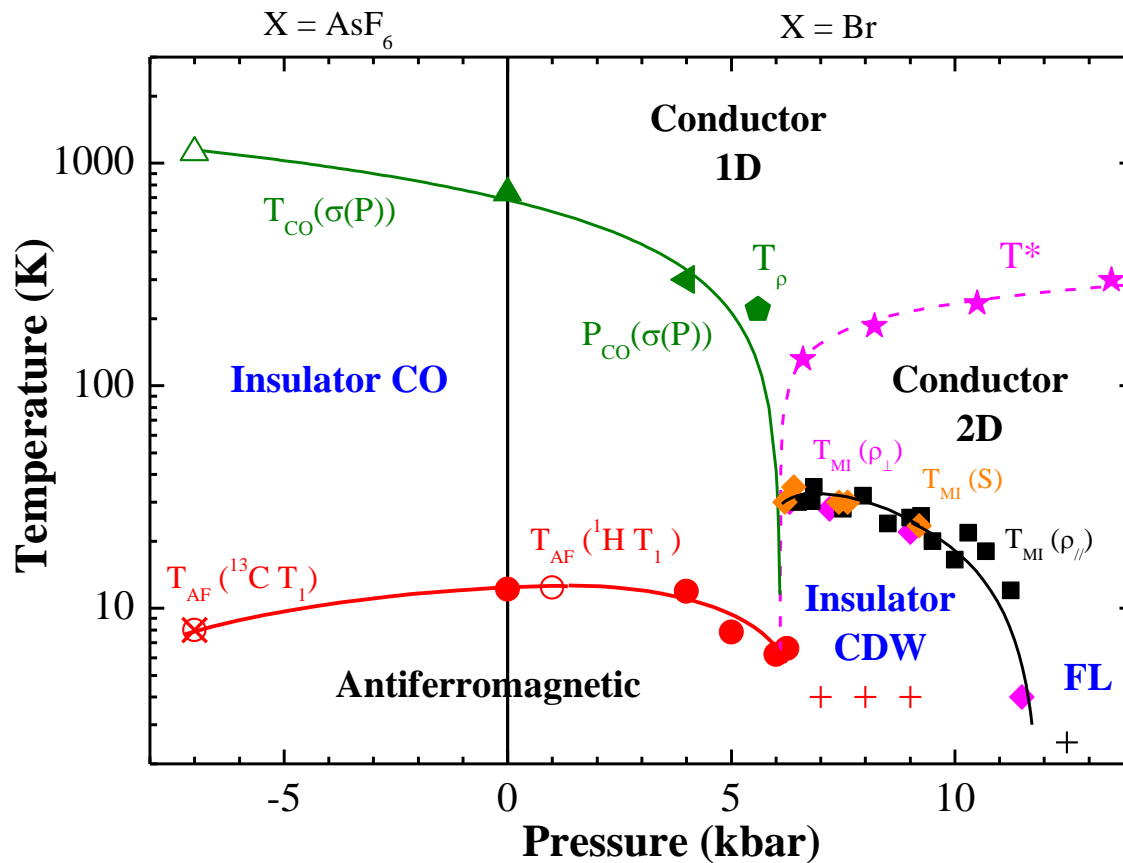


$\text{AsF}_6 \rightarrow \text{Br}^- = -7 \text{ kbar}$

Q-1D $\frac{1}{4}$ filled systems

NON-DIMERIZED

$(EDT-TTF-CONMe_2)_2X$, $X=AsF_6, Br$



$$\Delta_{dim} = 0$$

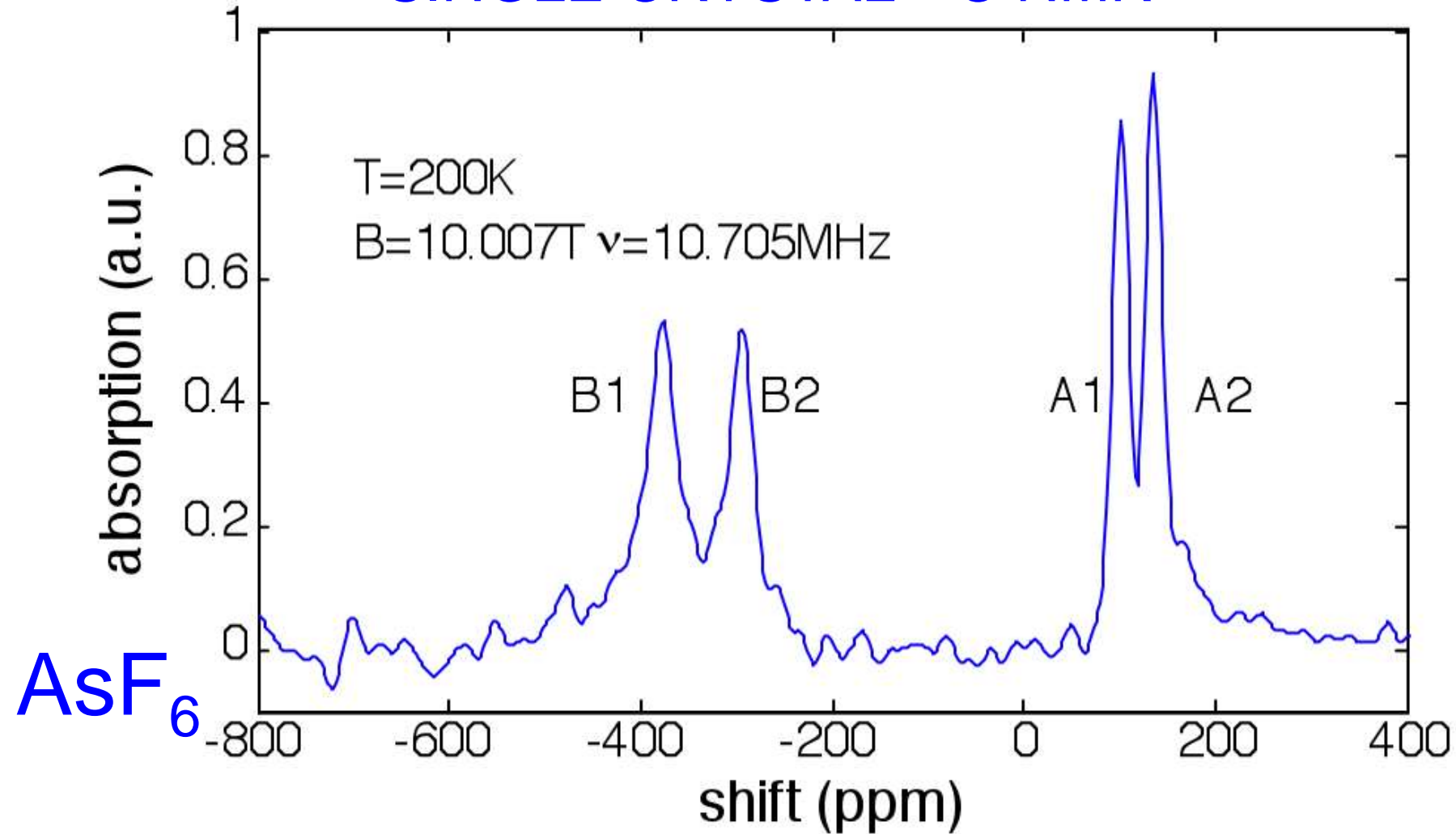
CO with AF ground state, no SP, no SDW, no SC

CO / AF \rightarrow CDW \rightarrow FL

"Phase diagram of quarter-filled band organic salts, $[EDT-TTF-CONMe_2]_2 X$, $X = AsF_6$ and Br "

P. AUBAN-SENZIER, C. R. PASQUIER, D. JEROME, S. SUH, S. E. BROWN, C. MEZIERE, P. BATAIL
 Phys. Rev. Lett. 102, 257001 (2009)

SINGLE CRYSTAL ^{13}C NMR

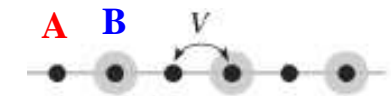
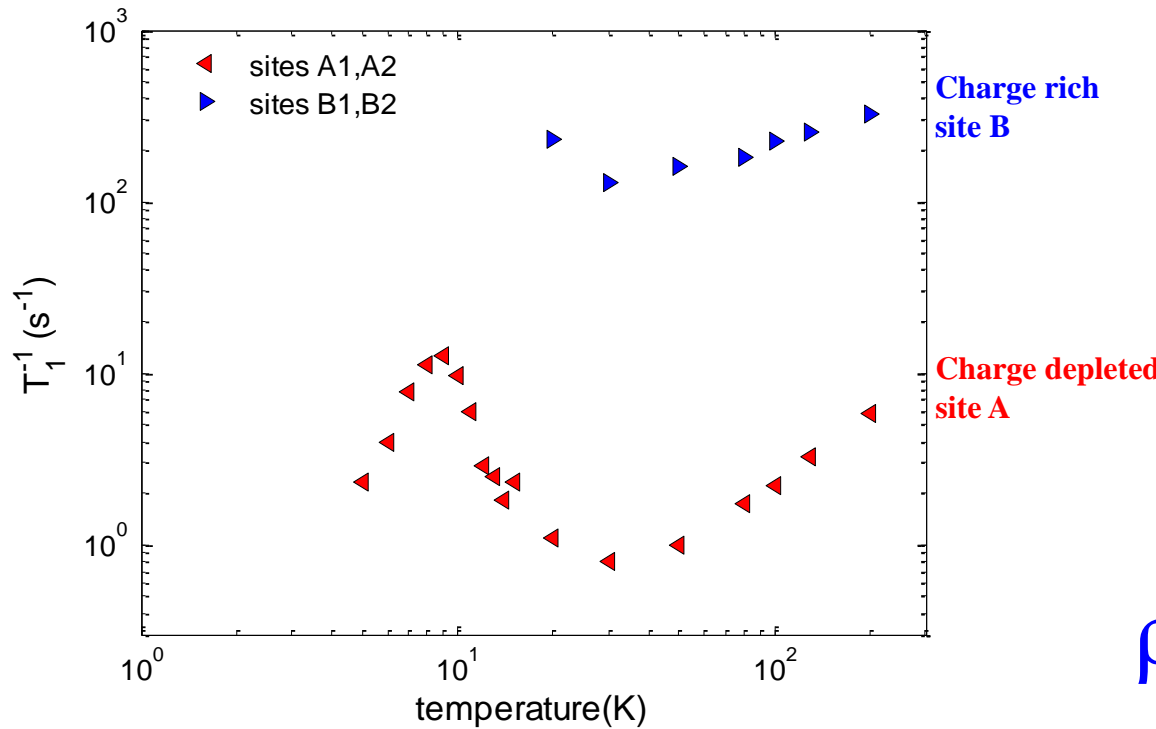


^{13}C NMR Spectrum recorded at $T = 200\text{ K}$ and applied field $B = 10.007\text{ T}$.
For arbitrary orientations, there are four non-equivalent sites (labelled A1, A2, B1, B2)

Steve Suh, Stuart E. Brown, UCLA

AsF_6

$^{13}\text{C} T_1^{-1}$ (T)



$$\rho_B / \rho_A = 9 / 1$$

$$T_1^{-1}(B) / T_1^{-1}(A) = (\rho_B / \rho_A)^2$$

large and T independent charge ratio $r_B / r_A = 9 / 1 \quad 10 < T < 200\text{K}$

Charge ratio $\approx 3 / 1$ in
(DI-DCNQI)₂Ag, K.Hiraki, K. Kanoda., *PRL* 80, 4737 (1998)
(TMTTF)₂AsF₆, F. Zamborszky et al., *PRB* 66, 081103(R) (2002)

full refinement and analysis of symmetry of
3D CO structure
based on single crystal synchrotron X-ray data

identify

an anti-phase, static modulation wave of Br⁻ atoms,
in synchronicity with on-site localization of holes

Leokadiya Zorina, Sergey Simonov, Cécile Mézière, Enric Canadell, Steve Suh, Stuart E. Brown, Pierre Fertey, Pascale Foury-Leykleian, Jean-Paul Pouget, Patrick Batail *J. Mater. Chem.* 19, 6980-6994 (2009)

REFINED WIGNER STRUCTURES



T. Kakiuchi, Y. Wakabayashi, H. Sawa, T. Itou, K. Kanoda, *Phys. Rev. Lett.*, 2007, **98**, 066402.



T. Kakiuchi, Y. Wakabayashi, H. Sawa, T. Takahashi, T. Nakamura, *J. Phys. Soc. Jpn.*, 2007, **76**, 113702.



S. Aoyagi, K. Kato, A. Ota, H. Yamochi, G. Saito, H. Suematsu, M. Sakata, M. Takata, *Angew. Chem. Int. Ed.*, 2004, **43**, 3670.



M. Watanabe, Y. Noda, Y. Nogami, H. Mori, *J. Phys. Soc. Jpn.*, 2004, **73**, 921.

PAUL ATTFIELD's WORK ON CO IN INORGANICS

powder neutron diffraction studies on half-doped manganites
 $(\text{Pr}_{0.5}\text{Ca}_{0.5}\text{MnO}_3, \text{TbBaMn}_2\text{O}_6, \text{YBaMn}_2\text{O}_6)$
and magnetite (Fe_3O_4)

J. P. Attfield, *Solid St. Sc.*, 2006, **8**, 861-867

R. J. Goff, J. P. Wright, J. P. Attfield, P. G. Radaelli,
J. Phys. Cond. Mat., 2005, **17**, 7633-7642

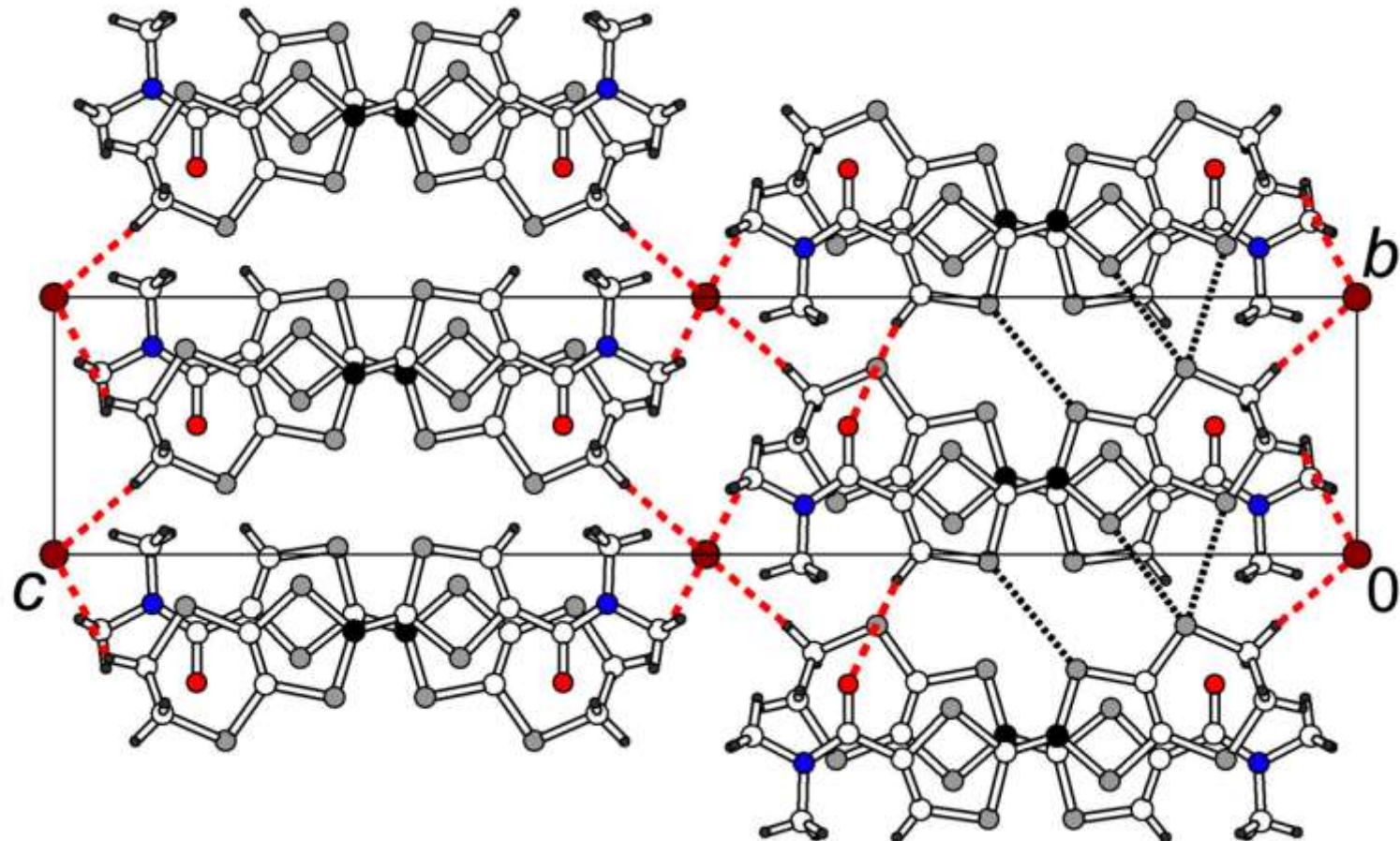
R. J. Goff, J. P. Attfield, *Phys. Rev. B*, 2004, **70**, 140404

J. P. Wright, J. P. Attfield, P. G. Radaelli,
Phys. Rev. Lett., 2001, **87**, 266401

Br

— Pmna at 300 K for averaged structure

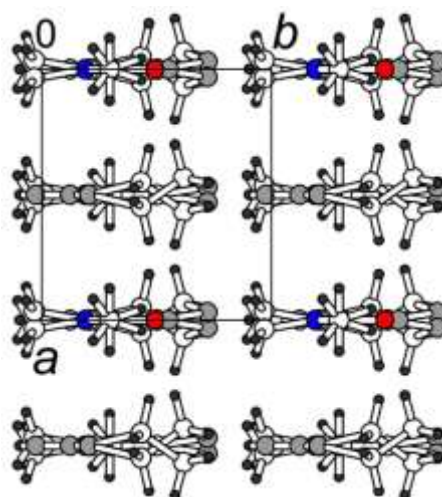
one independent molecule in asymmetric unit



do NOT allow for charge ordering

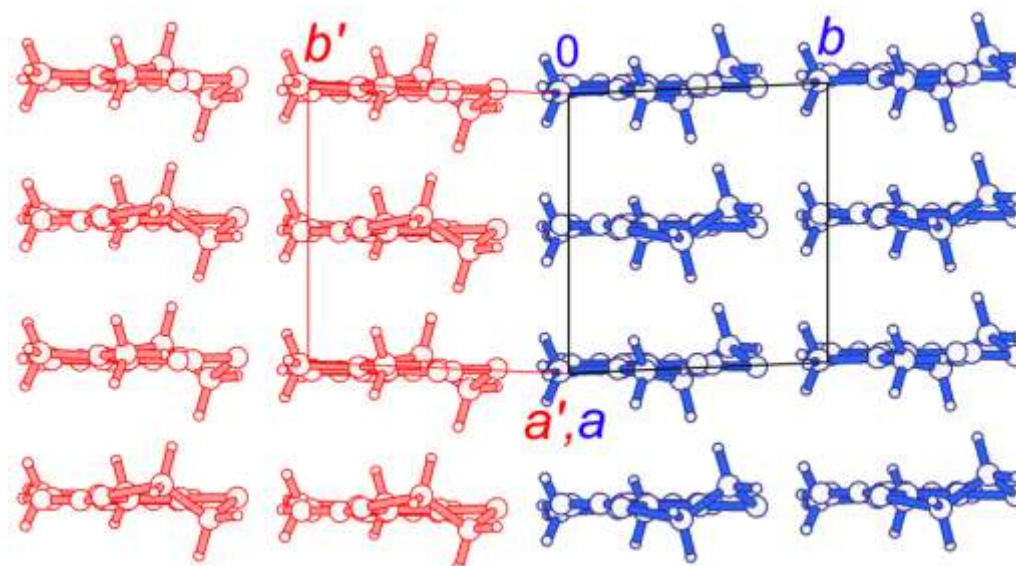
twinned monoclinic structure below 190 K

$Pmna$



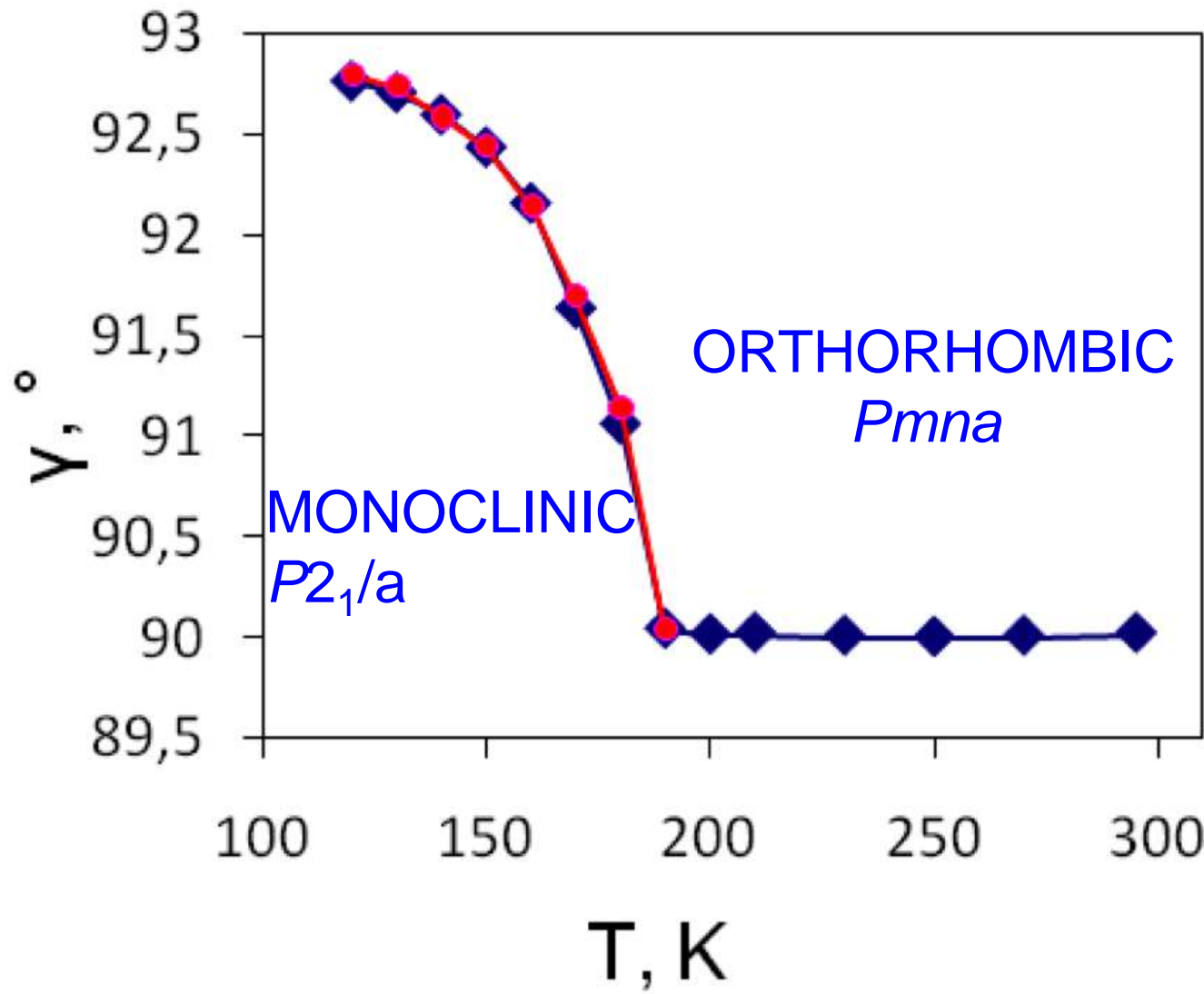
Lika Zorina

$P2_1/a$



keeps with local two-fold axial symmetry about a

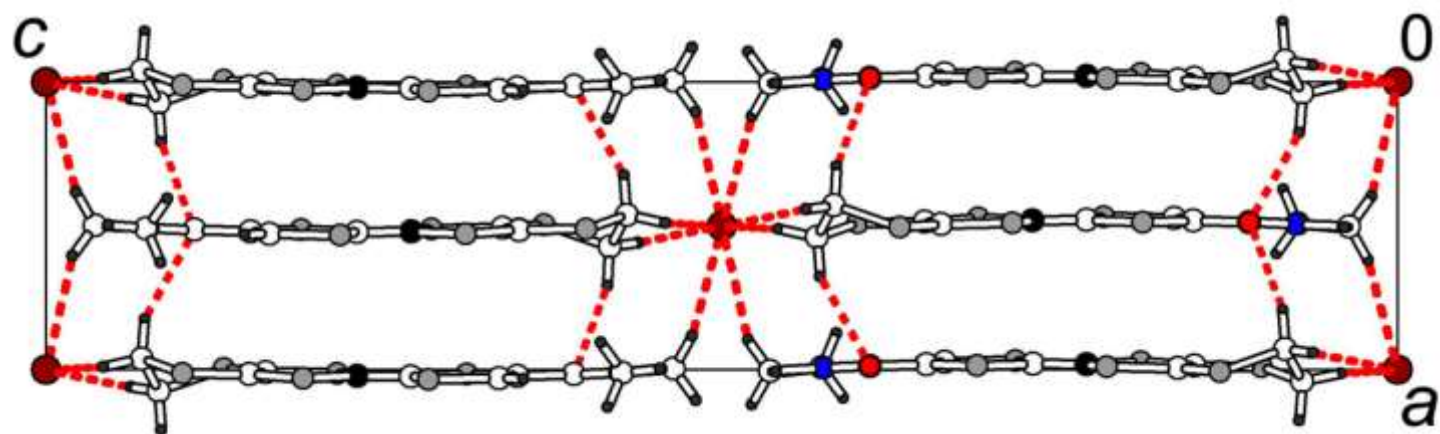
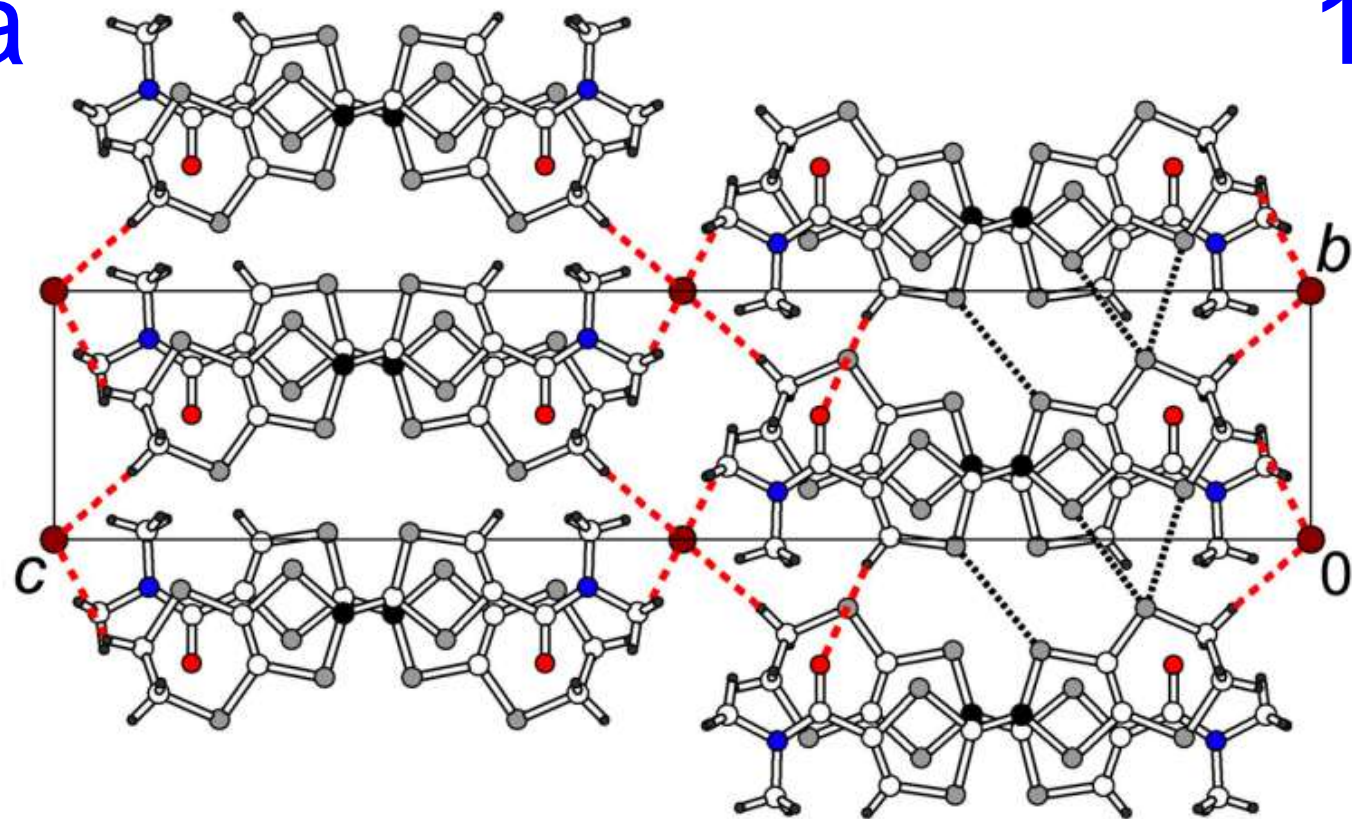
Br



Change in the γ lattice angle across the structural phase transition.
Blue rhombuses and red circles below the transition are data points for
the two different twin domains in the monoclinic phase.

$P2_1/a$

150 K



Bruker 4-circle
CCD, Angers

Synchrotron
SOLEIL

Pmna, 2

?, 4

collected 18647 42335

independent 2333 12895

R_1 [$\text{I} > 2\sigma(\text{I})$] 0.0331 0.0521

a large collection of systematic absences reflections
to work with in orthorhombic symmetry

Table 5. Number of systematic absence exceptions* in the orthorhombic double unit cell of δ - $(\text{EDT-TTF-CONMe}_2)_2\text{Br}$ at room temperature.

	$a = 7.1126(5) \text{ \AA}$		$b = 13.0250(7) \text{ \AA}$ (double axis)		$c = 32.759(1) \text{ \AA}$			
	$b \perp x$	$2_1 \parallel x$	$n \perp y$	$2_1 \parallel y$	$a \perp z$	$b \perp z$	$n \perp z$	$2_1 \parallel z$
N**	6678	31	2549	79	1017	1097	828	217
$N, I > 3\sigma(I)$	231	4	60	0	17	24	17	6
$\langle I/\sigma(I) \rangle$	0.7	1.2	0.6	0.3	0.5	0.5	0.4	0.6
Absence conditions	$0kl:$ $k=2n+1$	$h00:$ $h=2n+1$	$hol:$ $h+l=2n+1$	$0k0:$ $k=2n+1$	$hk0:$ $h=2n+1$	$hk0:$ $k=2n+1$	$hk0:$ $h+k=2n+1$	$00l:$ $l=2n+1$

(*) Only possible symmetry elements (i.e. with low $\langle I/\sigma(I) \rangle$ ratio) are listed in the table.

(**) N is the number of reflections satisfying the absence conditions.

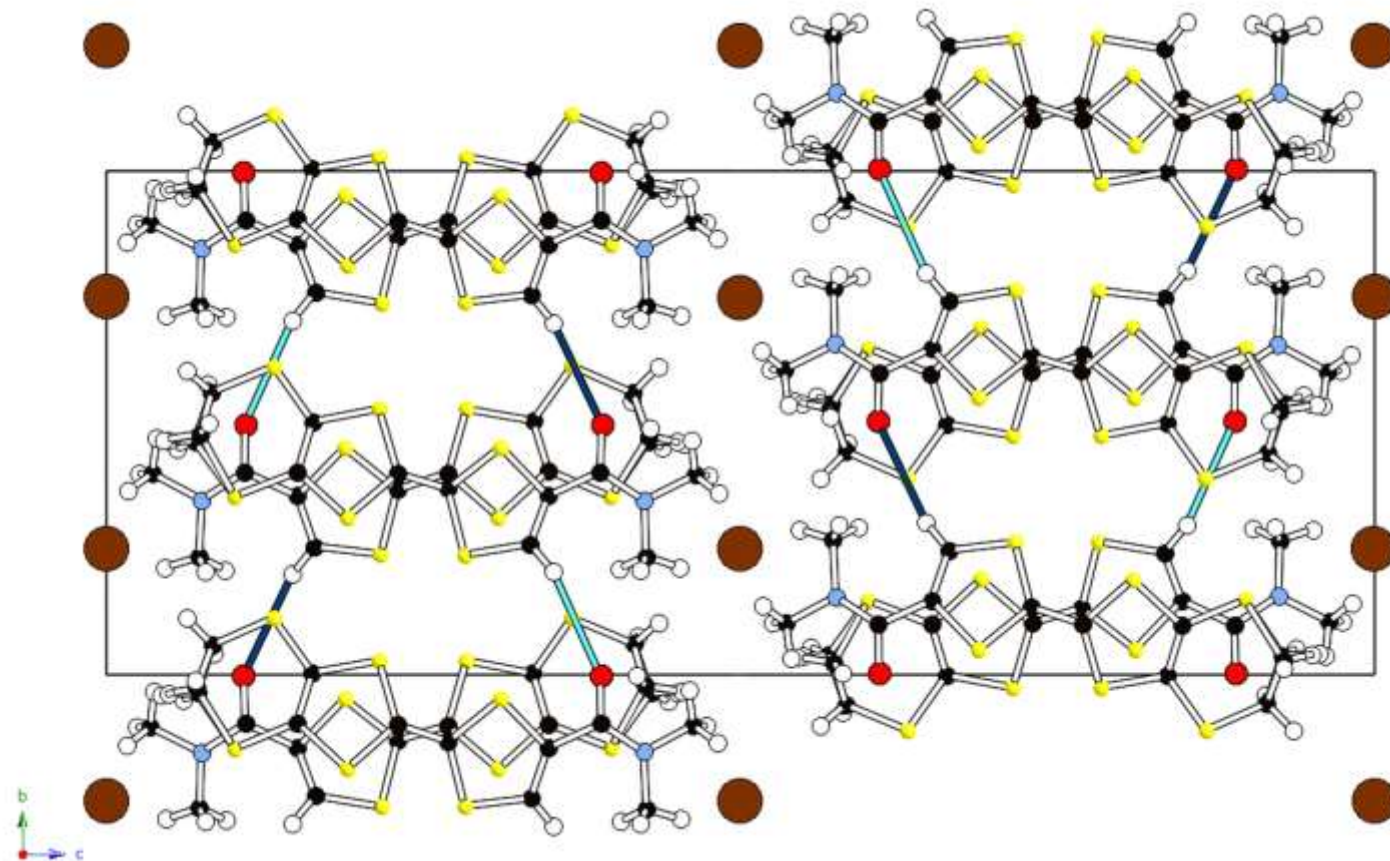
analysis of synchrotron data

compatible with
 $Pmnn, P2nn, P22_12_1$

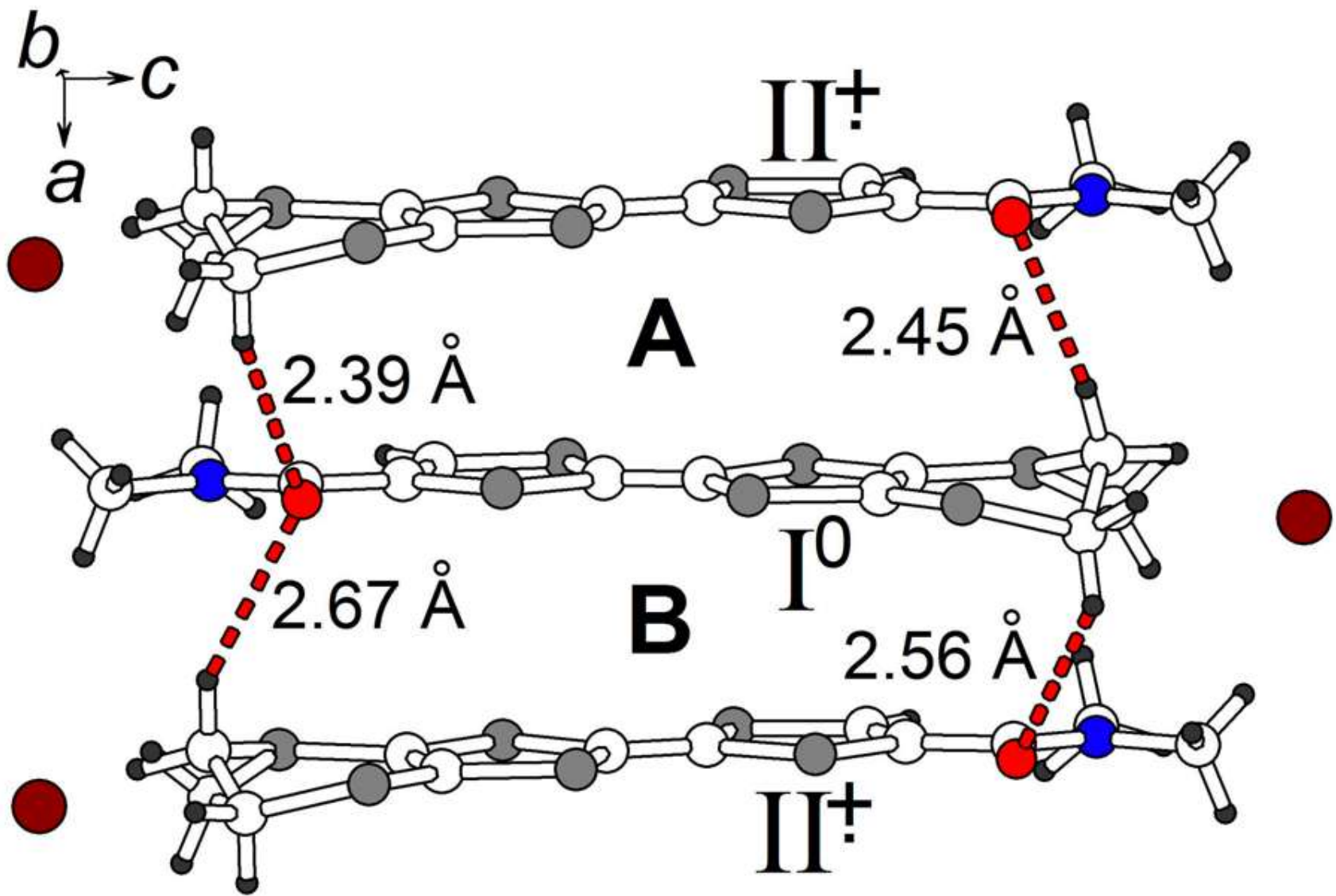
P2nn

two independent molecules in asymmetric unit

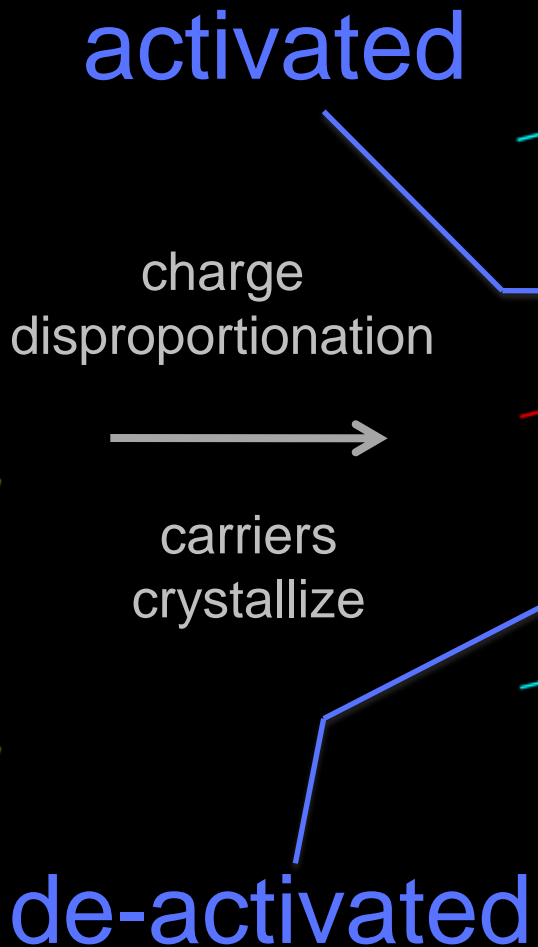
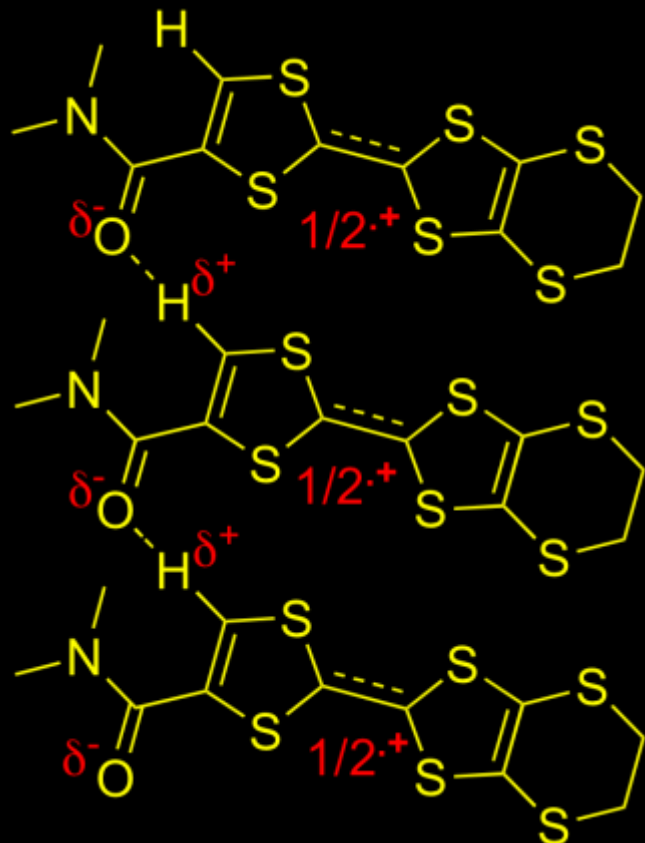
2b



in agreement with CO



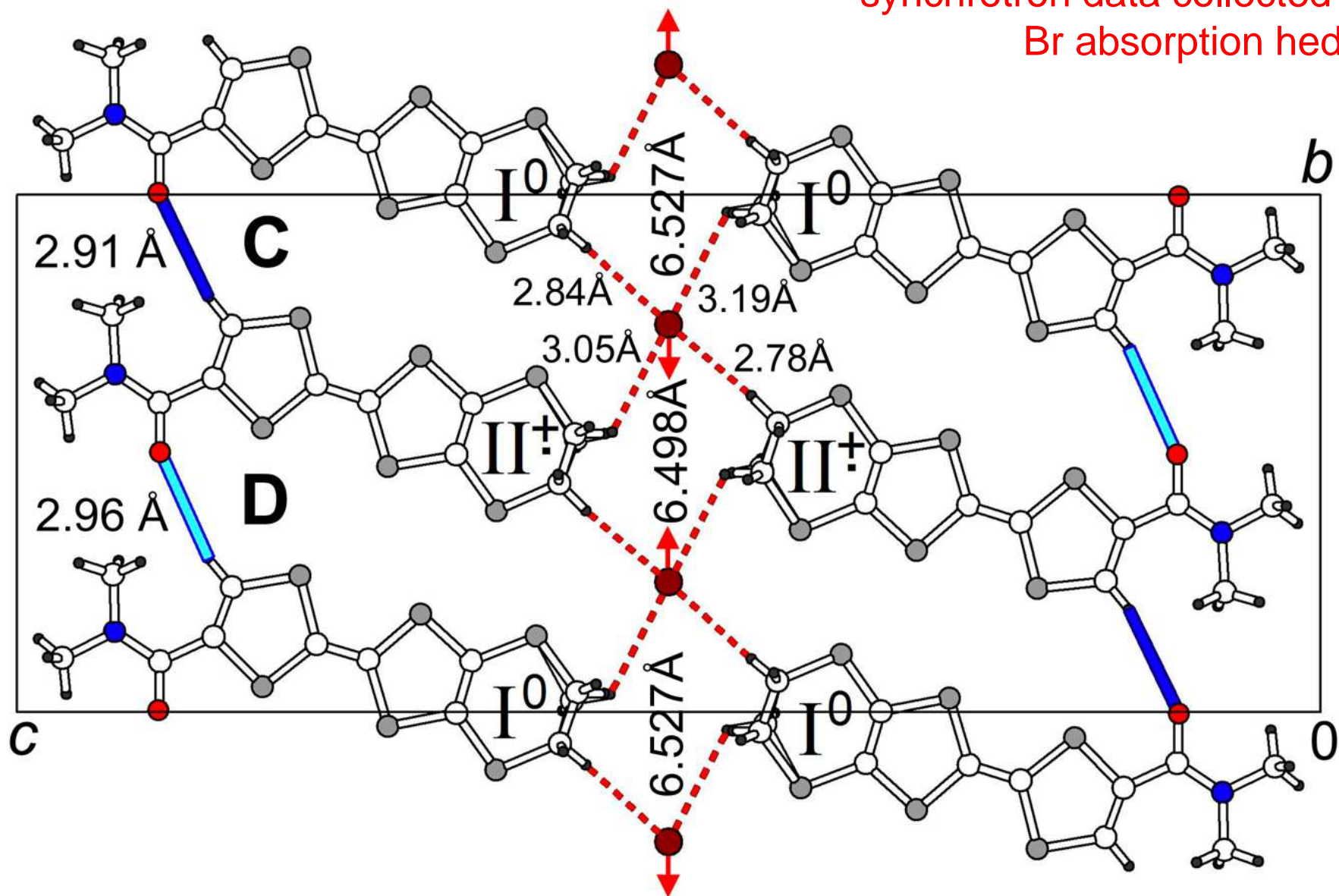
activation of large collections of CH...O hydrogen bonds
in synchronicity with CO:



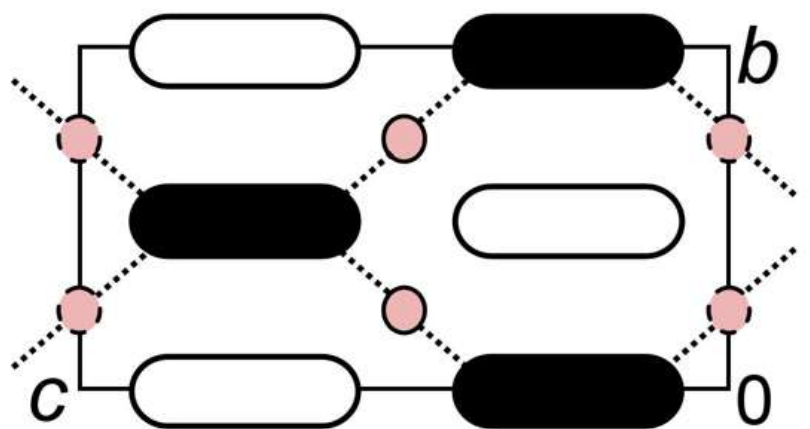
Wigner structure
Mott insulator

- concerted mechanism
- long range electrostatic modulation

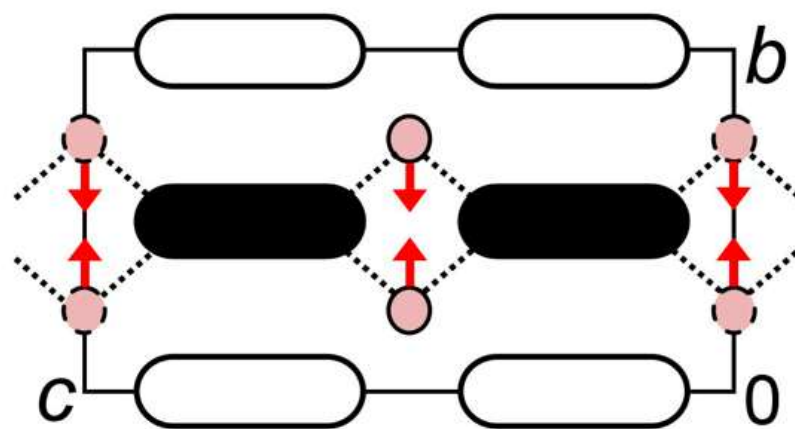
synchrotron data collected at
Br absorption hedge



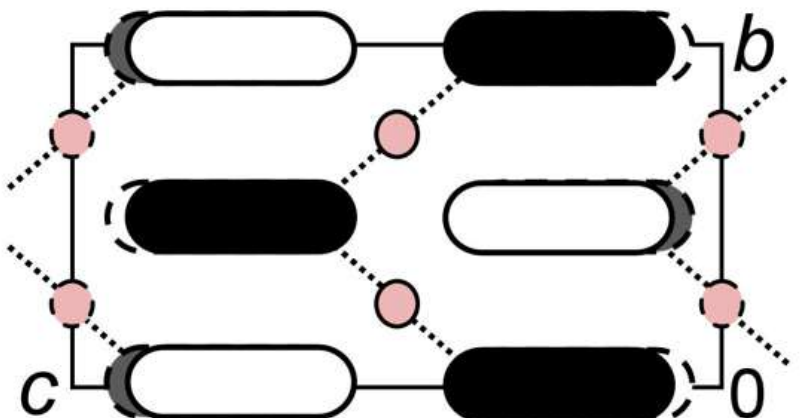
modulation of Br^- displacements



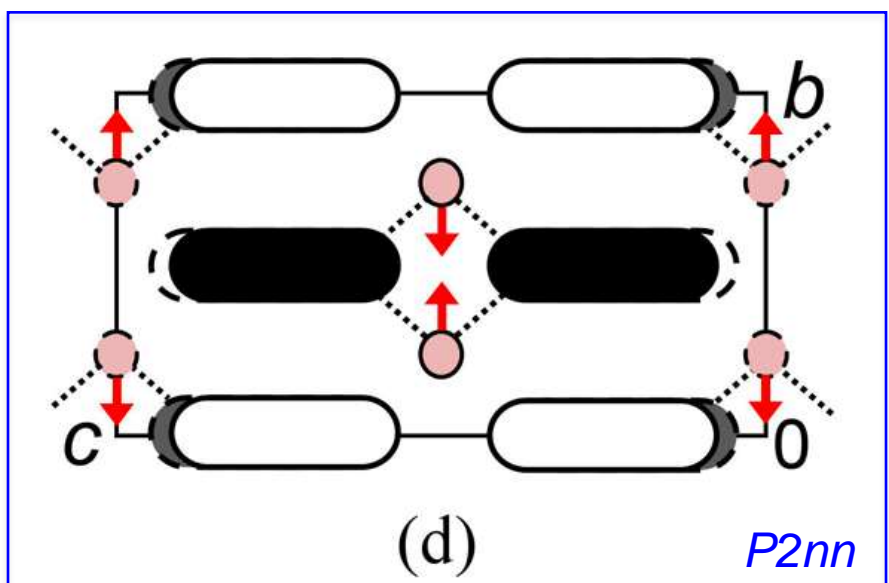
(a)



(b)

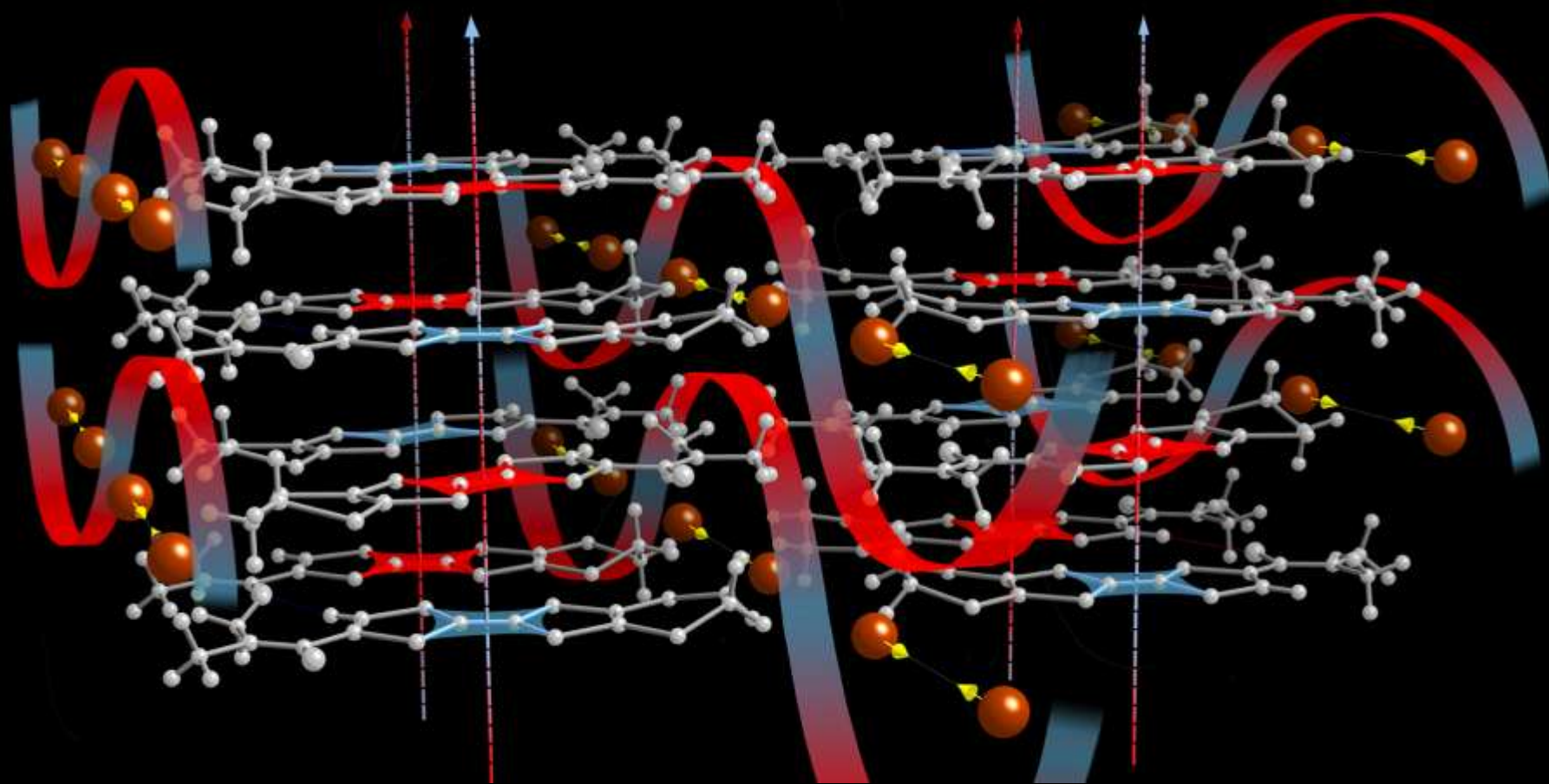


(c)



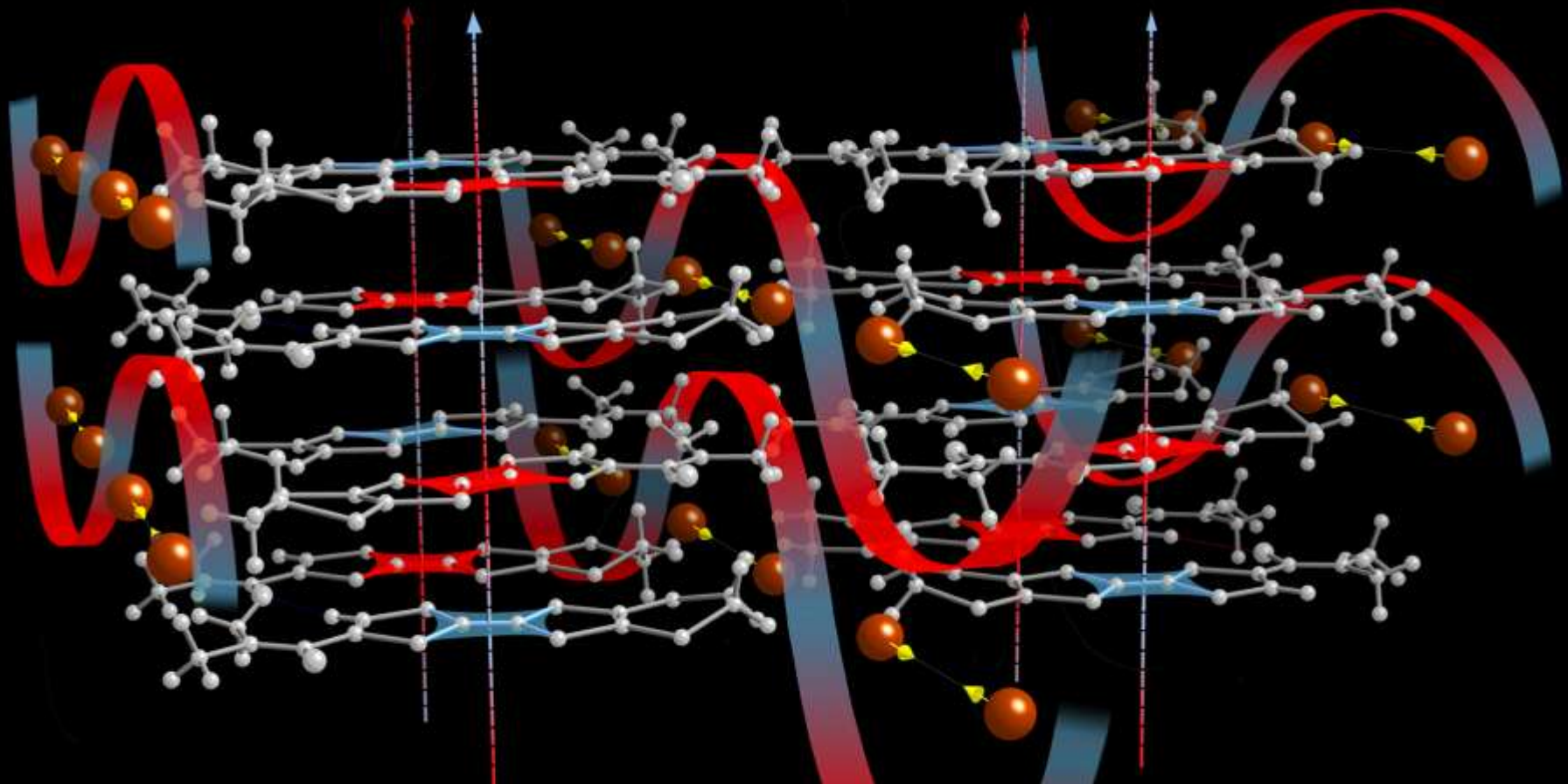
anti-phase modulation

3D charge ordered structure



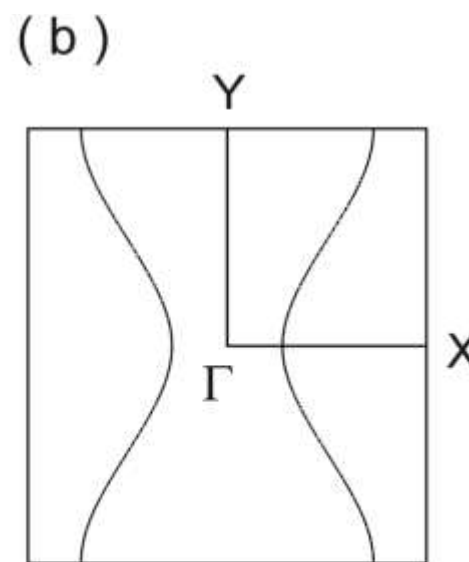
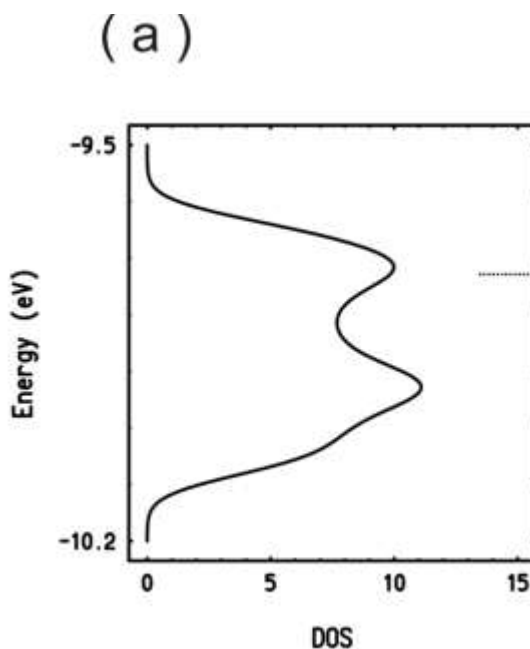
$P2nn$

compatible with ferroelectricity

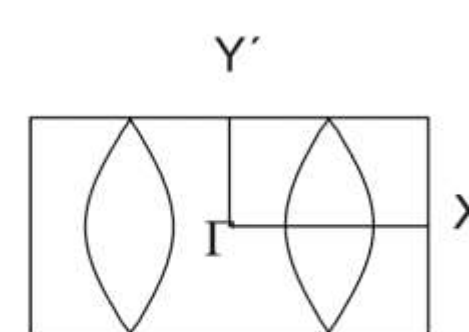
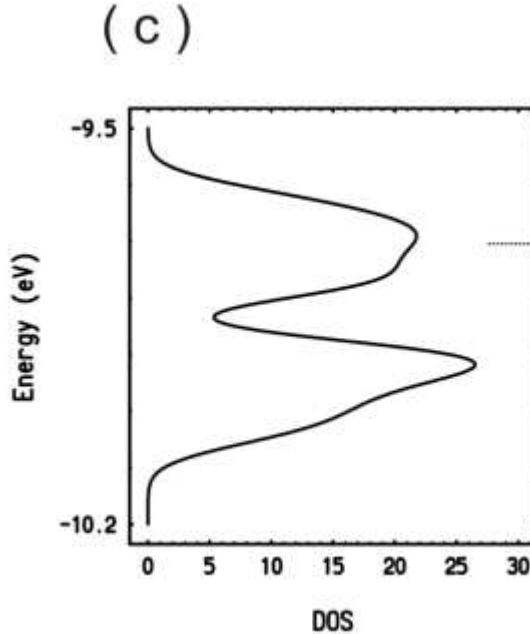


Br⁻ static modulation wave

Pmna



P2nn



despite the occurrence of CO,
stacks appear to remain
essentially uniform

Résumé

chimie et physique des interactions intermoléculaires faibles à l'unisson dans les conducteurs moléculaires en basse dimension